In Vitro and *In Vivo* Models to Assess the Mechanism of Lapatinib-Induced Diarrhoea

A Thesis Submitted for the Degree of Doctor of Philosophy by

Wan Nor I'zzah Wan Mohamad Zain

Discipline of Medicine,
School of Medicine, Faculty of Health Sciences,
The University of Adelaide, Australia

December 2016

This thesis is dedicated to my loving husband, Yasser and my precious children, Ammar and Yasmin for all their loves, supports and sacrifices.

Declaration

"I certify that this work contains no material which has been accepted for the award of any other degree or diploma in my name, in any university or other tertiary institution and, to the best of my knowledge and belief, contains no material previously published or written by another person, except where due reference has been made in the text. In addition, I certify that no part of this work will, in the future, be used in a submission in my name, for any other degree or diploma in any university or other tertiary institution without the prior approval of the University of Adelaide and where applicable, any partner institution responsible for the joint-award of this degree."

I give consent to this copy of my thesis, when deposited in the University Library, being made available for loan and photocopying, subject to the provisions of the Copyright Act 1968.

I also give permission for the digital version of my thesis.

……..

Wan Nor I'zzah Wan Mohamad Zain

December 2016

Table of Contents

Contents

Chapter 1 ..... **1**

Introduction **1**

1.1 Background of study 1

1.2 ErbB1 3

1.2.1 ErbB1 properties 3

1.2.2 Location of expression and normal functions 5

1.2.3 Post-translational regulation 6

1.2.4 Transcriptional regulation 7

1.2.5 Role in cancer 9

1.3 Mechanism of action of ErbB1 targeted drugs 10

1.3.1 mAbs 11

1.3.2 Single target TKIs 13

1.3.3 Dual target TKIs 14

1.3.4 Multitarget TKIs 17

1.4 ErbB1 role in gastrointestinal tract 24

1.5 Diarrhoea associated with ErbB1 targeted therapies 29

1.5.1 Mechanisms of diarrhoea in ErbB1 targeted therapies 30

1.5.2 Incidence of diarrhoea in ErbB1 targeted therapies 32

1.5.3 Management of diarrhoea in ErbB1 targeted therapies 38

1.6 Role of ErbB1 in diarrhoea mechanisms 40

1.7 Other factors of ErbB1 inhibitor-induced diarrhoea 47

1.8 Conclusion 48

1.9 Research question, hypothesis and aims of study 48

Chapter 2 ..... **50**

General methods **50**

2.1 Cell lines, chemicals and reagents 50
2.2 Cell culture 51
2.3 XTT cell proliferation assay 51
2.4 RNA isolation 52
2.4.1 Cell lines 52
2.4.2 Animal tissues 53
2.5 Reverse transcription 54
2.6 Primer design 54
2.7 Real-time Polymerase Chain Reaction (PCR) 55
2.8 Calculation of relative expression of genes 56
2.9 Preparation of tumour inoculum 56
2.10 Histological examination 57
2.11 Measurement of villus height and crypt depth in jejunum and colon 57
2.12 Immunohistochemistry staining for caspase-3 and Ki-67 58
2.13 Statistical analysis 60
Chapter 3 61
Cytotoxic effect of lapatinib on rat breast tumour (Walker 256) and rat jejunum (IEC-6) cell lines and assessment of ErbB1 and ErbB2 expression 61
3.1 Introduction 61
3.2 Materials and Methods 64
3.2.1 Chemicals and reagents 64
3.2.2 Cell harvesting 65
3.2.3 Cytotoxicity assays 66
3.2.4 Fluorescence activated cell sorting (FACS) analysis 67
3.2.5 Real-time PCR 68
3.2.6 Immunofluorescence staining of total ErbB1 and ErbB2 & phosphorylated ErbB1 and ErbB2 (pErbB1 and pErbB2) 69
3.2.7 Statistical analysis 70

3.3 Results 70
3.3.1 Cytotoxic effect of lapatinib on Walker 256 and IEC-6 70
3.3.2 Mechanism of cell death induced by lapatinib 76
3.3.3 ErbB1 and ErbB2 mRNA expression 81
3.3.4 Detection of total and phosphorylated ErbB1 and ErbB2 proteins 83
3.4 Discussion 109
3.5 Conclusion 114
3.6 Acknowledgements 115
Chapter 4 116
Development of a Walker 256 tumour-bearing rat model to study the effects of lapatinib on the intestine 116
4.1 Introduction 116
4.2 Materials and Methods 118
4.2.1 Animals 118
4.2.2 Walker 256 tumour rat model 118
4.2.3 Blood analysis 120
4.2.4 Histological examination 120
4.2.5 Measurement of villus height and crypt depth in colon and jejunum 120
4.2.6 Immunohistochemistry of caspase-3 and Ki-67 121
4.2.7 Real-time PCR 121
4.2.8 Statistical analysis 121
4.3 Results 121
4.3.1 Body weight 121
4.3.2 Tumour growth 122
4.3.3 Blood analysis 124
4.3.4 Histological analysis 143
4.3.5 Measurement of villus height and crypt depth in jejunum and colon 147
4.3.6 Detection of apoptosis (caspase-3) and proliferation (Ki-67) 151

4.3.7 ErbB1 and ErbB2 mRNA expression in tumour tissue 165
4.4 Discussion 166
4.5 Conclusion 172
Chapter 5 173
Investigating lapatinib-induced diarrhoea in a tumour-bearing rat model 173
5.1 Introduction 173
5.2 Materials and Methods 174
5.2.1 Animals 174
5.2.2 Drug 175
5.2.3 Lapatinib-induced diarrhoea in a tumour-bearing rat model 175
5.2.4 Diarrhoea assessment 176
5.2.5 Histological assessment 177
5.2.6 Measurement of villus height and crypt depth 177
5.2.7 Immunohistochemistry staining 177
5.2.8 Tumour mitotic index 180
5.2.9 Statistical analysis 180
5.3 Results 180
5.3.1 Body weight 180
5.3.2 Tumour growth 184
5.3.3 Tumour weight 185
5.3.4 Tumour mitotic index 186
5.3.5 Organ weight 187
5.3.6 Diarrhoea assessment 189
5.3.7 Histological analysis 190
5.3.8 Measurement of villus height and crypt depth in jejunum and colon 191
5.3.9 Caspase-3 and Ki-67 protein detection in jejunum and colon 192
5.3.10 Total and phosphorylated ErbB1 and ErbB2 protein detection in jejunum and colon 196

5.4 Discussion 200
5.5 Conclusion 206
Chapter 6 207
Effect of lapatinib on T84 colonic epithelial monolayer integrity 207
6.1 Introduction 207
6.2 Materials and methods 210
6.2.1 Cell culture 210
6.2.2 Chemicals 210
6.2.3 XTT cell proliferation assay 211
6.2.4 Effect of lapatinib on cell permeability 211
6.2.5 Effect of lapatinib on Cl- secretion 213
6.2.6 Statistical analysis 214
6.3 Results 215
6.3.1 XTT assay 215
6.3.2 Effect of lapatinib on permeability 221
6.3.3 Effect of lapatinib on Cl- secretion 230
6.4 Discussion 238
6.5 Conclusion 243
Chapter 7 244
General discussion 244
7.1 Introduction 244
7.2 Mechanisms of lapatinib-induced diarrhoea in breast cancer therapy 244
7.3 Future directions 250
7.4 Conclusion 251
References 252
Appendix 312

List of Figures

Figure 1.1. Cellular activation of ErbB1 receptor that generates two different pathways which are MAPK/ERK and PI3K/Akt pathways. 5

Figure 1.2. Location of ErbB1expression in intestinal epithelial cells (small intestine). 29

Figure 1.3. Location of ErbB1 expression in intestinal epithelial cells (colon). 29

Figure 1.4. Regulation of Cl- secretion in intestinal epithelial 46

Figure 3.1. Phase contrast micrograph of Walker 256 rat breast carcinoma cell line 65

Figure 3.2. Phase contrast micrograph of IEC-6 rat jejunum cell line. 66

Figure 3.3. The effect of lapatinib on proliferation of Walker 256 cells (A) and IEC-6 cells (B) assessed using the XTT assay.....71

Figure 3.4. The effect of lapatinib on Walker 256 (A) and IEC-6 (B) cells at different incubation time as evaluated in trypan blue exclusion analysis. 74

Figure 3.5. The percentage of viable, early apoptotic, late apoptotic and necrotic cells in lapatinib-treated Walker 256 cells compared to control untreated at 6 (A) 24 (B) and 48 (C) hours incubation as quantified via FACS analysis 77

Figure 3.6. The percentage of viable, early apoptotic, late apoptotic and necrotic cells in lapatinib-treated IEC-6 cells compared to control untreated at 6 (A) 24 (B) and 48 (C) hours incubation as quantified via FACS analysis. 78

Figure 3.7. *ErbB2* (A) mRNA expression in control untreated and lapatinib-treated Walker 256 cells 81

Figure 3.8. *ErbB1* (A) and *ErbB2* (B) mRNA expression in control untreated and lapatinib-treated IEC-6 cells 82

Figure 3.9. ErbB1 protein immunofluorescence staining in Walker 256 rat breast tumour cell line at 6 hours incubation. 85

Figure 3.10. ErbB1 protein immunofluorescence staining in Walker 256 rat breast tumour cell line at 24 hours incubation. 86

Figure 3.11. ErbB1 protein immunofluorescence staining in Walker 256 rat breast tumour cell line at 48 hours incubation. 87

Figure 3.12. ErbB2 protein immunofluorescence staining in Walker 256 rat breast tumour cell line at 6 hours incubation. 88

Figure 3.13. ErbB2 protein immunofluorescence staining in Walker 256 rat breast tumour cell line at 24 hours incubation. 89

Figure 3.14. ErbB2 protein immunofluorescence staining in Walker 256 rat breast tumour cell line at 48 hours incubation. 90

Figure 3.15. pErbB1 protein immunofluorescence staining in Walker 256 rat breast tumour cell line at 6 hours incubation. 91

Figure 3.16. pErbB1 protein immunofluorescence staining in Walker 256 rat breast tumour cell line at 24 hours incubation. 92

Figure 3.17. pErbB1 protein immunofluorescence staining in Walker 256 rat breast tumour cell line at 48 hours incubation. 93

Figure 3.18. pErbB2 protein immunofluorescence staining in Walker 256 rat breast tumour cell line at 6 hours incubation. 94

Figure 3.19. pErbB2 protein immunofluorescence staining in Walker 256 rat breast tumour cell line at 24 hours incubation. 95

Figure 3.20. pErbB2 protein immunofluorescence staining in Walker 256 rat breast tumour cell line at 48 hours incubation. 96

Figure 3.21. ErbB1 protein immunofluorescence staining in IEC-6 rat jejunal cell line at 6 hours incubation 97

Figure 3.22. ErbB1 protein immunofluorescence staining in IEC-6 rat jejunal cell line at 24 hours incubation 98

Figure 3.23. ErbB1 protein immunofluorescence staining in IEC-6 rat jejunal cell line at 48 hours incubation 99

Figure 3.24. ErbB2 protein immunofluorescence staining in IEC-6 rat jejunal cell line at 6 hours incubation 100

Figure 3.25. ErbB2 protein immunofluorescence staining in IEC-6 rat jejunal cell line at 24 hours incubation 101

Figure 3.26. ErbB2 protein immunofluorescence staining in IEC-6 rat jejunal cell line at 48 hours incubation 102

Figure 3.27. pErbB1 protein immunofluorescence staining in IEC-6 rat jejunal cell line at 6 hours incubation 103

Figure 3.28. pErbB1 protein immunofluorescence staining in IEC-6 rat jejunal cell line at 24 hours incubation 104

Figure 3.29. pErbB1 protein immunofluorescence staining in IEC-6 rat jejunal cell line at 48 hours incubation 105

Figure 3.30. pErbB2 protein immunofluorescence staining in IEC-6 rat jejunal cell line at 6 hours incubation 106

Figure 3.31. pErbB2 protein immunofluorescence staining in IEC-6 rat jejunal cell line at 24 hours incubation.....107

Figure 3.32. pErbB2 protein immunofluorescence staining in IEC-6 rat jejunal cell line at 48 hours incubation.....108

Figure 4.1. Percentage weight change after Walker 256 tumour inoculation.....122

Figure 4.2. Walker 256 tumour growth with different tumour cell concentrations.....123

Figure 4.3. Walker 256 tumour regression with different tumour cell concentration 123

Figure 4.4. Histology images of Walker 256 tumour tissue from different concentrations of tumour cells injected.....144

Figure 4.5. Histology images of jejunum from rats injected with different concentration of Walker 256 tumour.....145

Figure 4.6. Histology images of colon from rats injected with different concentration of Walker 256 tumour. 146

Figure 4.7. Villus height and crypt depth of jejunum and colon in Walker 256 tumour-bearing rats.....149

Figure 4.8. Villus height and crypt depth of jejunum and colon in rats injected with i) $1x10^5$ cells/0.1 ml (1 flank) ii) $2x10^6$ cells/0.2 ml (1 flank) iii) $2x10^6$ cells/0.2 ml (both flanks).....150

Figure 4.9. Changes in cell apoptosis as identified by caspase-3 immunohistochemistry staining in jejunum and colon of Walker 256 tumour-bearing rats 151

Figure 4.10. Changes in cell apoptosis as identified by caspase-3 immunohistochemistry staining in jejunum and colon of rats injected with i) $1x10^5$ cells/0.1 ml (1 flank) ii) $2x10^6$ cells/0.2 ml (1 flank) iii) $2x10^6$ cells/0.2 ml (both flanks).....152

Figure 4.11. Caspase-3 immunohistochemistry in the jejunum of control non-tumour rat and rats injected with different concentration of Walker 256 tumour cells 153

Figure 4.12. Caspase-3 immunohistochemistry in the colon of control non-tumour-bearing rat and rats injected with different concentration of Walker 256 tumour cells.....154

Figure 4.13. Changes in cell apoptosis as identified by caspase-3 immunohistochemistry staining in tumours of Walker 256 tumour rats. 155

Figure 4.14. Changes in cell apoptosis as identified by caspase-3 immunohistochemistry staining in tumours of rats injected with i) $1x10^5$ cells/0.1 ml (1 flank), ii) $2x10^6$ cells/0.2 ml (1 flank) and iii) $2x10^6$ cells/0.2 ml (both flanks).....156

Figure 4.15. Caspase-3 immunohistochemistry staining in the tumours of rats injected with different concentration of Walker 256 tumour cells.....157

Figure 4.16. Changes in cell proliferation as identified by Ki-67 immunohistochemistry staining in jejunum and colon of Walker 256 tumour rats 158

Figure 4.17. Changes in cell proliferation as identified by Ki-67 immunohistochemistry staining in jejunum and colon of rats injected with i) $1x10^5$ cells/0.1 ml (1 flank) ii) $2x10^6$ cells/0.2 ml (1 flank) iii) $2x10^6$ cells/0.2 ml (both flanks) 159

Figure 4.18. Ki-67 positively stained cells of jejunal crypts in control non-tumour rat andrats injected with different concentration of Walker 256 tumour cells 160

Figure 4.19. Ki-67 positively stained cells of colonic crypts in control non-tumour rat and rats injected with different concentration of Walker 256 tumour cells. 161

Figure 4.20. Changes in cell proliferation as identified by Ki-67 immunohistochemistry staining in tumour tissues of Walker 256 tumour rats 162

Figure 4.21. Changes in cell proliferation as identified by Ki-67 immunohistochemistry staining in tumour tissues of rats injected with i) $1x10^5$ cells/0.1 ml (1 flank) ii) $2x10^6$ cells/0.2 ml (1 flank) iii) $2x10^6$ cells/0.2 ml (both flanks) 163

Figure 4.22. Ki-67 positively stained cells of tumours in rats injected with different concentration of Walker 256 tumour cells.....164

Figure 4.23. *ErbB1* and *ErbB2* mRNA expression in Walker 256 tumour tissues. Rat stomach was used as positive control for calibration. 165

Figure 5.1. Experimental flow chart. 176

Figure 5.2. (A) Body weight and (B) Adjusted body weight to percentage tumour weight for all groups.....182

Figure 5.3. (A) Percentage weight change and (B**)** percentage weight change of adjusted weight compared to the starting weight on day 5 pre-initial treatment for all groups.....183

Figure 5.4. Percentage of tumour burden over body weight for all groups after treatment. .184

Figure 5.5. (A) Tumour weight and (B) percentage tumour weight over body weight of all experimental groups.....185

Figure 5.6. Tumour mitotic index for all groups after treatment. 186

Figure 5.7. Mitotic cells of tumour rats treated with saline/vehicle: Control, lapatinib 240 mg/kg once daily: L240 1x and lapatinib 200 mg/kg twice daily: L200 2x.....187

Figure 5.8. A. Total organ weight B. Organ weight as a percentage of body weight. 188

Figure 5.9. Incidence of diarrhoea 189

Figure 5.10. Histological images of jejunum and colon from tumour rats treated with saline/vehicle (Control), lapatinib 240 mg/kg once daily (L240 1x) and lapatinib 200 mg/kg twice daily (L200 2x).....190

Figure 5.11. Villus height and crypt depth of jejunum and colon in tumour rats treated with saline/vehicle (Control), lapatinib 240 mg/kg once daily (L240 1x) and lapatinib 200 mg/kg twice daily (L200 2x).....191

Figure 5.12. Changes in cell apoptosis as identified by caspase-3 immunohistochemistry staining in jejunum and colon of tumour rats treated with saline/vehicle (Control), lapatinib 240 mg/kg once daily (L240 1x) and lapatinib 200 mg/kg twice daily (L200 2x).....192

Figure 5.13. Caspase-3 immunohistochemistry staining in the jejunum and colon of tumour rats treated with saline/vehicle (Control), lapatinib 240 mg/kg once daily (L240 1x) and lapatinib 200 mg/kg twice daily (L200 2x) 193

Figure 5.14. Changes in cell proliferation as identified by Ki-67 immunohistochemistry staining in jejunum and colon of tumour rats treated with saline/vehicle (Control), lapatinib 240 mg/kg once daily (L240 1x) and lapatinib 200 mg/kg twice daily (L200 2x).....194

Figure 5.15. Ki-67 immunohistochemistry staining in the jejunum and colon of tumour rats treated with saline/vehicle (Control), lapatinib 240 mg/kg once daily (L240 1x) and lapatinib 200 mg/kg twice daily (L200 2x) 195

Figure 5.16. Changes in Erbb1, ErbB2, pErbB1 and pErbB2 staining in the (A) Jejunum: crypts and villi (B) Colon: apical and basal regions of tumour rats treated with saline/vehicle (Control), lapatinib 240 mg/kg once daily (L240 1x) and lapatinib 200 mg/kg twice daily (L200 2x). 197

Figure 5.17. ErbB1, ErbB2, pErbB1 and pErbB2 immunohistochemistry staining in the jejunum of tumour rats treated with saline/vehicle (Control), lapatinib 240 mg/kg once daily (L240 1x) and lapatinib 200 mg/kg twice daily (L200 2x).....198

Figure 5.18. ErbB1, ErbB2, pErbB1 and pErbB2 immunohistochemistry staining in the colon of tumour rats treated with saline/vehicle (Control), lapatinib 240 mg/kg once daily (L240 1x) and lapatinib 200 mg/kg twice daily (L200 2x).....199

Figure 6.1. The effect of lapatinib 1-20 µM (A) and 10-100 µM (B) treatment on T84 cells as assessed by XTT assay 217

Figure 6.2. The effect of paclitaxel 1-10 µM (A) and 10-100 µM (B) treatment on T84 cells as assessed by XTT assay 218

Figure 6.3. The effect of DMSO as a control treatment on T84 cells, as assessed by XTT assay.....219

Figure 6.4. The effect of 50% EtOH as a control treatment on T84 cells as assessed by XTT assay.....220

Figure 6.5. The effect of lapatinib at 10 and 100 µM on T84 colonic epithelial monolayer permeability as evaluated by TEER.....224

Figure 6.6. The effect of paclitaxel at A. lower concentrations (2, 5 and 10 µM), and B. higher concentrations (20 and 50 µM) on T84 colonic epithelial monolayer permeability as evaluated by TEER. 226

Figure 6.7. The effect of lapatinib in combination with paclitaxel at A. lower concentrations (2, 5 and 10 µM), and B. higher concentrations (20 and 50 µM) on T84 colonic epithelial monolayer permeability as evaluated by TEER 227

Figure 6.8. Baseline readings of T84 monolayer after 48 hours pre- treatment with LAP +/- PAC.....233

Figure 6.9. Effect of LAP +/- PAC after 48 hours pre-treatment on T84 cell monolayer on Cl^- secretion induced by carbachol as evaluated by I_{sc} measurement.....234

Figure 6.10. Effect of LAP +/- PAC after 48 hours pre-treatment on T84 cell monolayer on Cl^- secretion induced by forskolin as evaluated by *Isc* measurement.....235

Figure 6.11. Secondary analysis on baseline readings of effect of LAP +/- PAC after 48 hours pre-treatment on T84 cell monolayer.....236

Figure 6.12. Secondary analysis on effect of LAP +/- PAC after 48 hours pre-treatment on T84 cell monolayer as evaluated by I_{sc} measurement.....237

List of Tables

Table 1.1. ErbB1 monoclonal antibodies.....20

Table 1.2. ErbB1 tyrosine kinase inhibitors. 21

Table 1.3. National Cancer Institute Common Toxicity Criteria for Diarrhoea Grading.....34

Table 1.4. Diarrhoea incidence in ErbB1 targeted therapies. 35

Table 1.5. Chloride secretagogues.....43

Table 1.6. Chloride inhibitors.....44

Table 2.1. Primer sequences used in Real-time Polymerase Chain Reaction analysis.....55

Table 3.1. IC_{50} values of lapatinib on Walker 256 and IEC-6 cells as assessed using the XTT assay.....72

Table 3.2. Percentage of cell viability for Walker 256 and IEC-6 after treatment with lapatinib at different incubation time as assessed using trypan blue exclusion assay. 75

Table 3.3. Percentage of viable, early apoptotic, late apoptotic and necrotic cells after treatment with lapatinib at different incubation time as assessed using FACS analysis. 79

Table 4.1. Serum biochemistry and liver enzymes in response to Walker 256 tumour inoculation. 127

Table 4.2. Blood haematology profile in response to Walker 256 tumour inoculation.....129

Table 4.3. Comparison of serum biochemistry and liver enzymes between growing and regressing tumours for $1x10^5$ cells/0.1 ml 1 flank. 131

Table 4.4. Comparison of blood haematology profile between growing and regressing tumours for $1x10^5$ cells/0.1 ml 1 flank. 133

Table 4.5. Comparison of serum biochemistry and liver enzymes between growing and regressing tumours for $2x10^6$ cells/0.2 ml 1 flank. 135

Table 4.6. Comparison of blood haematology profile between growing and regressing tumours for $2x10^6$ cells/0.2 ml 1 flank. 137

Table 4.7. Comparison of serum biochemistry and liver enzymes between growing and regressing tumours for $2x10^6$ cells/0.2 ml both flanks.....139

Table 4.8. Comparison of blood haematology profile between growing and regressing tumours for $2x10^6$ cells/0.2 ml both flanks.....141

Table 5.1. Description of the antibodies used in immunohistochemistry staining. 179

Table 6.1. The effect of lapatinib (10 and 100 μM) on T84 colonic epithelial monolayer permeability as evaluated by TEER.....225

Table 6.2. The effect of lapatinib (10 and 100 µM) in combination with paclitaxel (2, 5 and 10 µM) on T84 colonic epithelial monolayer permeability as evaluated by TEER. 228

Table 6.3. The effect of lapatinib (10 and 100 µM) in combination with paclitaxel (20 and 50 µM) on T84 colonic epithelial monolayer permeability as evaluated by TEER. 229

List of Abbreviations

$2^{-\Delta Ct}$	Delta threshold cycle
ALP	Alkaline phosphatase
ALT	Alanine aminotransferase
ASCO	American Society of Clinical Oncology
AST	Aspartate aminotransferase
ATCC	American Type Culture Collection
ATP	Adenosine triphosphate
b.i.d	Twice daily administration
B2M	Beta-2-microglobulin
BSA	Bovine serum albumin
Ca^{2+}	Calcium ion
$CaCl_2.2H_2O$	Calcium chloride dihydrate
cAMP	Cyclic adenosine 5'-monophosphate
CFTR	Cystic fibrosis transmembrane conductance regulator
Cl^-	Chloride ion
CO2	Carbon dioxide
COX-2	Cyclooxygenase 2
Ct	Threshold cycle
CYP	Cytochrome
DAB	3, 3'-diaminobenzidine
DAPI	4′,6-Diamidino-2-phenylindole dihydrochloride
DEGs	Delayed early genes
DMEM	Dulbecco's Modified Eagle's Medium
DMSO	Dimethyl sulfoxide

DNA	Deoxyribonucleic acid
EDTA	Ethylenediaminetetraacetic acid
EGF	Epidermal growth factor
EGFR	Epidermal growth factor receptor
ELISA	Enzyme-linked immunosorbent assay
EMEA	European Medicines Agency
ErbB1	Epidermal growth factor receptor 1
ErbB2	Epidermal growth factor receptor 2
ERK	Extracellular regulated kinase
EtOH	Ethanol
FACS	Fluorescence activated cell sorting
FBS	Foetal bovine serum
FDA	US Food and Drug Association
FITC	Fluorescein isothiocyanate
G	Conductance
GGT	Gamma-glutamyl transferase
GI	Gastrointestinal
GPCR	G-protein coupled receptor
Grb2	Growth factor receptor bound protein 2
GSK	Glaxo Smith Kline
H&E	Haematoxylin and eosin
H_2O	Water
HB-EGF	Heparin-binding epidermal growth factor
HER	Human epidermal growth factor receptor
IC_{50}	Half maximal inhibitory concentration

IEC-6	Rat jejunal cell line
IEGs	Immediate early genes
IgG	Immunoglobulin
I_{sc}	Short circuit current
K^+	Potassium ion
K_2HPO_4	Potassium hydrogen phosphate
kDa	kilodalton
L200 2x	Lapatinib 200 mg/kg twice daily
L240 1x	Lapatinib 240 mg/kg once daily
LAP	Lapatinib
LD	Lactate dehydrogenase
LPS	Lipopolysaccharide
M.C.H	Mean corpuscular haemoglobin
M.C.H.C	Mean corpuscular haemoglobin concentration
M.C.V	Mean corpuscular volume
mAbs	Monoclonal antibodies
MAPK	Mitogen activated protein kinase
MBC	Metastatic breast cancer
mCRC	Metastatic colorectal cancer
$MgCl_2.6H_2O$	Magnesium chloride hexahydrate
mRNA	Messenger ribonucleic acid
Na^+	Sodium ion
Na^+/K^+-ATPase	Sodium potassium adenosine triphosphatase
NaCl	Sodium chloride
$NaHCO_3$	Sodium hydrogen carbonate

NEC	Necrotising enterocolitis
NGS	Normal goat serum
NSCLC	Non-small cell lung cancer
P.C.V	Packed cell volume
PAC	Paclitaxel
PBS	Phosphate buffered saline
PCR	Polymerase chain reaction
pErbB1	Phosphorylated ErbB1
pErbB2	Phosphorylated ErbB2
Pgp	P-glycoprotein
PI	Propidium iodide
PI3K	Phosphatidylinositol-3-kinase
PS	Phospholipid phosphatidylserine
q.d.	Once daily administration
R.B.C	Red blood cell
R.D.W	Red blood cell distribution width
Raf	Rapidly accelerated fibrosarcoma
Ras	Reticular activating system
RM-SCCHN	Recurrent and/or metastatic squamous cell carcinoma of head and neck
RNA	Ribonucleic acid
S.E.M	Standard error mean
SCCHN	Squamous cell carcinoma of head and neck
Sh2	Src-homology 2
T84	Human colon carcinoma
TEER	Transepithelial electrical resistance

TGF-α	Transforming growth factor alpha
TKI	Tyrosine kinase inhibitor
TNF-α	Tumour necrosis factor alpha
TX-100	Triton X-100
UBC	Ubiquitin C
Walker 256	Rat breast carcinoma cell line
XTT	2,3-bis-(2-methoxy-4-nitro-5-sulfophenyl)-2H-tetrazolium-5-carboxanilide

Abstract

Lapatinib, an ErbB1/ErbB2 tyrosine kinase inhibitor is effective in breast cancer treatment but is associated with diarrhoea. ErbB1 inhibition by lapatinib may interfere with the normal functioning in the intestines. However, the underlying mechanisms remain unclear. This PhD project was conducted to investigate the mechanism of lapatinib-induced diarrhoea.

First study was conducted to determine the cytotoxic properties of lapatinib on rat breast carcinoma (Walker 256) and jejunal (IEC-6) cells and to evaluate the relationship between ErbB1 expression and sensitivity to growth inhibition by lapatinib. The cytotoxic effect of lapatinib on Walker 256 and IEC-6 was evaluated via XTT assay and FACS analysis. Cell lines were incubated with lapatinib for 6, 24 or 48 hours before evaluation. ErbB1 and ErbB2 mRNA and protein expression were determined via RT-PCR and immunofluorescence staining, respectively. Lapatinib inhibited 50% Walker 256 and IEC-6 cell growth at 8.2 ± 0.18 and 3.03 ± 0.26 μM respectively. Higher percentage of necrotic cells (37.91 ± 7.08 %) were observed in lapatinib-treated Walker 256 compared to control untreated cells (11.86 ± 5.62 %) ($p<0.01$), at 48 hours. Lapatinib-treated IEC-6 at 24 hours showed higher percentage of late apoptotic cells (53.56 ± 15.37 %) compared to controls (12.91 ± 4.70 %) ($p<0.01$). Similarly, at 48 hours incubation lapatinib-treated IEC-6 showed a higher percentage of late apoptotic cells (56.82 ± 11.53 %) compared to the control untreated samples that exhibited 22.70 ± 12.81 % late apoptotic cells ($p<0.05$). *ErbB1* mRNA was unable to be detected in Walker 256 due to low expression. Both mRNA expression of *ErbB1* and *ErbB2*, as well as immunofluorescence staining of ErbB1, ErbB2, pErbB1 and pErbB2 showed no differences between control untreated and lapatinib-treated cells. Lapatinib induced necrosis in tumour cells, while inducing late apoptosis in jejunal cells. This may explain lapatinib-induced diarrhoea in patients administered with the drug which could be due to apoptosis of small intestinal epithelial cells leading to barrier disruption and

consequently diarrhoea. However, much remains to be learned on the molecular mechanisms related to lapatinib's cytotoxic effect.

The second study was performed to develop Walker 256 tumour-bearing rat model to study lapatinib-induced diarrhoea. Walker 256 cells were then injected into the right flanks of female albino Wistar rats and grown over 3 weeks. This correlates with the peak of lapatinib-induced diarrhoea in Wistar rats. A concentration of $2x10^6$ cells/0.2 ml resulted in consistent tumour growth. Tumours were measurable by day 4 and reached 10% of body weight 25 days post-inoculation, without metastasis to distant sites. *ErbB1* and *ErbB2* mRNA were expressed in the tumour tissue. Walker 256 tumour did not cause any changes in jejunum and colon, thus there will be no interference of tumour on the intestines in the study of lapatinib-induced diarrhoea. As tumour regression was seen, this matter was taken into consideration in the following study in which the tumour growth was observed intently.

The animal model now provides a framework which enables the study of lapatinib-induced diarrhoea in tumour-bearing animals. Thus, the third study was carried out which aimed to identify histological changes in intestines following lapatinib treatment and to determine the mechanism of diarrhoea related to the treatment. Female albino Wistar rats were injected subcutaneously with Walker 256 breast tumour cells. When the tumour reached 0.01% of body weight, rats were divided into three groups: control, lapatinib 240mg/kg once daily gavaged (L240 1x) and lapatinib 200mg/kg twice daily gavaged (L200 2x). Rats were assessed for indicators of intestinal injury. Upon necropsy, jejunum and colon were collected for histological assessment via H&E staining. Expression of ErbB1, ErbB2 and markers for apoptosis (caspase-3) and proliferation (ki-67) were detected via immunohistochemistry. From the results, diarrhoea was seen in L200 2x group but not in other groups. However, both L240 1x and L200 2x showed significant changes in the intestines compared to controls such as villus blunting in jejunum (L240 1x $p<0.01$, L200 2x $p<0.0001$) and increased apoptosis in colon (L240 1x $p<0.01$, L200 2x $p<0.001$). ErbB2

expression in jejunal crypt was significantly lower than controls in both L240 1x ($p<0.05$) and L200 2x ($p<0.05$). Lapatinib twice daily administration caused diarrhoea. However, it was not related to ErbB1 expression as was expected. The current study was unable to find a dose and a schedule of lapatinib that was able to induce diarrhoea with tolerable levels of systemic toxicity. As such, further research is required to test a number of different schedules to find an appropriate way to model lapatinib-induced diarrhoea in breast cancer-bearing rats. This will enable future work to focus on uncovering mechanisms of lapatinib-induced diarrhoea and to test interventions for diarrhoea management.

The fourth and final study was carried out to investigate the effect of lapatinib and paclitaxel treatment on chloride secretion in the T84 model of colonic epithelium. Lapatinib and paclitaxel were first tested for their cytotoxic effect on proliferating cells that revealed T84 cells were relatively resistant to lapatinib with an IC_{50} of 26.48 ± 1.64 µM in serum-free-medium, 43.24 ± 2.73 µM in 5% serum-medium and 58.59 ± 1.37 µM in 10% serum-medium. In comparison, the effect of paclitaxel was more potent with an IC_{50} reached at 7.52 ± 0.25 µM in serum-free-medium, 12.58 ± 1.13 µM in 5% serum-medium and 18.48 ± 0.77 µM in 10% serum-medium. The lack of response of T84 cells to lapatinib is likely due to low target expression. As it has been shown in the current study that lapatinib and paclitaxel have cytotoxic effects on the T84 human colonic epithelial cell line, TEER experiments were conducted to determine the effect of both drugs on cell permeability. It was observed that lapatinib at both higher and lower concentrations, treated either from apical, basal or both apical and basal sides, as well as at different incubation hours does not affect colonic epithelial cell permeability, suggesting that lapatinib does not damage cell-cell adhesion properties, and likely spares epithelial tight junctions. To examine the effect of lapatinib as well as paclitaxel on intestinal chloride transport, T84 human colonic epithelial cell monolayers were mounted in Ussing chambers and the changes in short circuit current (I_{sc}) were measured. Experiments were conducted at established monolayer resistance and it was

observed that pre-treatment of T84 cells with lapatinib or paclitaxel did not affect baseline $I_{sc.}$ Chloride secretion was measured as I_{sc} across the T84 cell monolayers that were mounted in Ussing chambers, thus the findings reflected that pre-treatment with both drugs does not alter baseline chloride secretion. The present study exhibited higher baseline conductance of cell monolayer pre-treated with a high concentration of paclitaxel which reflected higher permeability, consequently lower barrier function/resistance, compared to control untreated monolayers. The finding is supported by the TEER results that showed that higher concentration of paclitaxel increased cell monolayer permeability. Lapatinib and paclitaxel also do not affect chloride secretion, however, due to lapatinib being an ErbB1 inhibitor which could interfere with chloride secretion, further investigations are required. Effect of lapatinib on chloride secretion might occur via other mechanisms unrelated to calcium or cAMP regulated chloride secretion. The mechanism of lapatinib-induced diarrhoea may be mediated by other unknown mechanisms. The cytotoxic effect of lapatinib as well as paclitaxel on T84 colonic cell line was also shown not to contribute to its effect on T84 monolayer permeability and chloride secretion. Overall, further investigations are needed to clarify the possible mechanisms of lapatinib-induced diarrhoea.

Finally, investigations in this PhD study managed to describe the minor impact of lapatinib on the gastrointestinal mucosa. Thus, much remains to be learned on the mechanisms related to lapatinib or ErbB1 targeted therapy-induced diarrhoea. Understanding the mechanism of damage will lead to an ability to target prevention or treatment as well as managing targeted therapy-induced diarrhoea appropriately.

Acknowledgement

First and foremost, I would like to express my special gratitude to my supervisors Professor Dorothy Keefe, Dr Joanne Bowen and Dr Emma Bateman for their supervision, guidance, ideas and discussion throughout my PhD. Thank you Dorothy, Jo and Emma for being patient and supportive throughout my long PhD journey.

I would like to acknowledge the previous and present members of the Mucositis Research Group who assisted me in my animal studies and other experiments throughout my PhD studies: Erin Plews, Bronwen Mayo, Anthony Wignall, Belinda Wozniak, Imogen White and Kate Secombe. Not to forget Dr Khloud Fakiha, Masooma Sultani, Hannah Wardill, Ysabella van Sebille and Romany Stansborough for their friendship, support and technical assistance in the lab. Thank you all. I truly appreciate it.

I would like to thank Dr Erin Lousberg and Dr Susan Christo for their help with my FACS analysis. Not to forget their friendship and other technical assistance.

Special thanks to Dr Agatha Labrinidis and Lynnette Waterhouse from Adelaide Microscopy Unit for their assistance in confocal microscopy usage.

Thank you to previous and present fellow Malaysian friends in Adelaide for their friendship, support and assistance throughout my PhD studies: Arnida Hani Teh, Dr Noor Alia Lokman, Dr Muhammad Arshad Sidek, Dr Ismaniza Ismail, Sazlyni Lim, Shifa Faizal, Roniza Ismail and Norfaridah Ali Azizan. I will cherish all the moments we shared together in Adelaide.

I sincerely acknowledge the scholarships I received from Ministry of Higher Education and Universiti Teknologi MARA, Malaysia.

Thank you to my friends in Malaysia: Dr Azizah Othman, Dr Nor Ashikeen Mukti, Dr Mudiana Muhammad, Dr Sharaniza Ab Rahim and Associate Professor Dr Narimah Abdul Hamid Hassani for their continuous support in good and hard times and being good listeners throughout my PhD journey.

My heartiest thanks to my loving siblings, my mother and sisters'in-law for their endless love, support and encouragement.

For my parents who are not in this world anymore, Chik and Ayah, who raised me with love and made me who I am today..may Allah bless you always.

Last but not least, to my loving husband, Yasser and my precious children, Ammar and Yasmin. Words can never express how truly grateful I am for your endless love, support, care, patience, encouragement and sacrifice throughout my PhD journey. I am always grateful to have all of you in my life.

Thank you.

Presentations at scientific meeting

1. *Investigating Walker 256 Tumour-Bearing Rat Model to Study Lapatinib-Induced Mucosal Injury,* Australian Society for Medical Research (ASMR) South Australia (SA) Annual Scientific Meeting, 8 June 2013, Adelaide Convention Centre, Adelaide, South Australia.
2. *Development of a Walker 256-TC Tumour-Bearing Rat Model to Study Lapatinib-Induced Mucosal Injury*, Multinational Association of Supportive Care in Cancer/International Society of Oral Oncology (MASCC/ISOO) International Cancer Care Symposium, 27-29 June 2013, Berlin, Germany.
3. *Effects of the Dual ErbB Tyrosine Kinase Inhibitor, Lapatinib, on Walker 256 and IEC-6 cell lines.* Australian Society for Medical Research (ASMR) South Australia (SA) Annual Scientific Meeting, 4 June 2014, Adelaide Convention Centre, Adelaide, South Australia.
4. *Comparative Effects of the Dual ErbB Tyrosine Kinase Inhibitor, Lapatinib, on Tumour and Intestinal Cell Lines*, Florey International Postgraduate Research Conference, 25 September 2014, National Wine Centre of Australia, Adelaide, South Australia.
5. *Investigating Lapatinib-Induced Diarrhoea in a Tumour-Bearing Rat Model*, Malaysian Society of Pharmacology and Physiology 29th Scientific Conference, 24-25 August 2015, Setia City Convention Centre, Shah Alam, Selangor, Malaysia.
6. *Cytotoxic Effects of the Dual ErbB Tyrosine Kinase Inhibitor, Lapatinib, on Tumour and Intestinal Cell Lines,* Malaysian Society of Pharmacology and Physiology 30th Scientific Conference, 15-16 August 2016, Shangri-La Putrajaya, Putrajaya, Selangor, Malaysia.

Thesis explanation

This thesis is composed of eight chapters as follows: literature review, general methods, four distinct research chapters, general discussion, references and appendix. Each research chapter was written with introduction, material and methods, results, discussion and conclusion. All references are included in the final chapter.

Chapter 1

Introduction

1.1 Background of study

Cancer treatment causes significant injury to normal mucosal tissues and is a major cause of morbidity in patients. Recently, a new class of agents known as molecularly targeted agents has been introduced into the clinical setting to treat a range of cancers. These agents which include monoclonal antibodies (Baselga and Arteaga 2005) and small molecule tyrosine and non-tyrosine kinase inhibitors (TKIs) have been approved by the US Food and Drug Administration (FDA) and the European Medicines Agency for cancer treatment (Cohen, Williams et al. 2003, Cohen, Johnson et al. 2005, Giusti, Shastri et al. 2007, Loriot, Perlemuter et al. 2008, Medina and Goodin 2008, Dungo and Keating 2013). The agents often target specific receptors that are upregulated in the cancer cells, although normal cells also express these receptors to varying extents (Loriot, Perlemuter et al. 2008). As such, like other cancer treatments including chemotherapy and radiotherapy, these targeted drugs cause damage to normal tissues which leads to diverse adverse effects such as hepatotoxicity (Loriot, Perlemuter et al. 2008, Asnacios, Naveau et al. 2009), dermal toxicity (Robert, Sibaud et al. 2012), cardiotoxicity (Hedhli and Russell 2011), ocular toxicity (Renouf, Velazquez-Martin et al. 2012) and gastrointestinal (GI) toxicity (Burris, Hurwitz et al. 2005, Moy and Goss 2007, Loriot, Perlemuter et al. 2008, Asnacios, Naveau et al. 2009, Dungo and Keating 2013). GI toxicity is one of the most common toxicities associated with molecularly targeted drugs (Cohen, Williams et al. 2003, Cohen, Johnson et al. 2005, Giusti, Shastri et al. 2007, Burris, Taylor et al. 2009, Dungo and Keating 2013). Apparently, damage to the GI

mucosa, referred as mucosal injury, is caused by inhibiting the specific targeted receptors in normal cells lining the tract, thus leading to GI adverse events, mainly diarrhoea (Moy and Goss 2007, Bowen 2014). Diarrhoea can affect patients' well-being, reduce compliance with medication and thus reduce the efficacy of cancer therapy (Loriot, Perlemuter et al. 2008). More importantly, diarrhoea may lead to dehydration, infection and other serious complications (Richardson and Dobish 2007, Cherny 2008, Loriot, Perlemuter et al. 2008). Most of the diarrhoea incidence in targeted cancer therapy has been reported to be associated with ErbB1 inhibitors (Medina and Goodin 2008, Shi, Zhang et al. 2013, Soria, Felip et al. 2015, Van Sebille, Gibson et al. 2015).

ErbB1, or epidermal growth factor receptor (EGFR) as it is also known, is one member of the epidermal growth factor receptor family. It plays an essential role not just in the development of epithelial cells but also in tumours of epithelial cell origin (Singh and Harris 2005). When activated by ligands, ErbB1 generates diverse cellular responses that include proliferation, growth arrest, differentiation and transformation (Yarden and Sliwkowski 2001). Interruption of ErbB1 signalling with various inhibitors has been shown to inhibit tumour cell proliferation, which clearly suggests that ErbB1 inhibition is an effective approach in cancer treatment (Arteaga 2003).

ErbB1 inhibition in the GI tract, however, may interfere with normal functioning. In the colon, epithelial sodium absorption and chloride secretion are stimulated directly by intracellular messengers such as cyclic adenosine monophosphate (cAMP) and intracellular calcium (Ca^{+}) (Uribe, Gelbmann et al. 1996). ErbB1 is known to be widely expressed in the cells of epithelial origin including in the GI tract (Ullrich, Coussens et al. 1984, Slieker, Martensen et al. 1986) and it is known that ErbB1 is a negative regulator of chloride (Cl^{-}) secretion (Uribe, Gelbmann et al. 1996, Uribe, Keely et al. 1996, Deachapunya and Poonyachoti 2013). Therefore, interference of ErbB1 inhibitors with Cl^{-} secretion

homeostasis may potentiate other mucosal insults to increase diarrhoea. ErbB1 inhibitors could increase Cl^- secretion, thus contributing to secretory diarrhoea which results from excessive Cl^- secretion and deficient sodium (Na^+) absorption (Loriot, Perlemuter et al. 2008).

Despite the evidence that ErbB1 is a negative regulator of Cl^- secretion, the mechanisms of ErbB1 inhibitor-induced diarrhoea have not been entirely elucidated. To date, no study has looked specifically at the mechanisms of ErbB1 inhibitor-induced-diarrhoea in cancer treatment (EMEA 2008, Bowen, Mayo et al. 2012). The importance of this toxicity is only just being realised, thus investigations are required to increase our understanding of injury mechanisms which will be translated to both improved management of this side effect, and potentially improved therapeutic utility of this class of drug.

This chapter discusses ErbB1 characteristics and the mechanisms of action of ErbB1 targeted drugs. The roles of ErbB1 in the GI tract which further lead to how ErbB1-signaling inhibition mediates diarrhoea are also discussed further. From this basis, the possible mechanisms of ErbB1 inhibitor-induced diarrhoea may be better understood.

1.2 ErbB1

1.2.1 ErbB1 properties

ErbB1, or EGFR or HER, is a member of the epidermal growth factor family of receptors, or ErbB family of receptors. It is a 170 kDa transmembrane protein (Carpenter 1987). It is synthesised from a 1210-residue polypeptide precursor in which after cleavage of the N-terminal sequence, a 1186-residue protein, is inserted into the cell membrane (Ullrich, Coussens et al. 1984). Over 20% of the receptor's 170 kDa mass is N-linked glycosylated and this is required for translocation to the cell surface and subsequent acquisition of ErbB1 functions (Slieker, Martensen et al. 1986).

The other receptors of the epidermal growth factor receptor family are ErbB2 (HER2), ErbB3 (HER3) and ErbB4 (HER4) (Arteaga 2003). ErbB1 and the other receptors are composed of an extracellular ligand binding site, a transmembrane domain and an intracellular tyrosine kinase tail (Arteaga 2003). The intracellular tyrosine kinase tail contains the tyrosine autophosphorylation sites, the adenosine triphosphate (ATP) binding site and regions involved in Ca^{2+} regulation, internalisation and substrate binding (Levitzki and Gazit 1995). Under normal physiological conditions, activation of ErbB family receptors is controlled by spatial and temporal expression of their ligands (Holbro and Hynes 2004), which consist of seven known structurally related polypeptides, namely epidermal growth factor (EGF), transforming growth factor-α (TGF-α), amphiregulin, heparin-binding EGF (HB-EGF), betacellulin, epiregulin and epigen (Carpenter, Ingraham et al. 1991, Strachan, Murison et al. 2001). All of these ligands bind and activate ErbB1. ErbB2 is a ligand-less receptor, whereas only epiregulin binds to ErbB3, and ErbB4 is activated via binding with HB-EGF, betacellulin and epiregulin (Avraham and Yarden 2011).

Once bound by a ligand, ErbB1 undergoes homodimerisation or forms heterodimers with ErbB2, ErbB3 and ErbB4 (Carpenter 2000). Ligand-bound ErbB1 undergoes autophosphorylation on specific tyrosine residues in the intracellular tail. Once activated, the tyrosine autophosphorylated domain of ErbB1 can serve as a binding site for Src-homology 2 (Sh2) and phosphotyrosine-binding domain-containing proteins such as growth-factor-receptor-bound protein 2 (Grb2) and Src homology and collagen protein (Shc) (Carpenter and Cohen 1990, Ullrich and Schlessinger 1990). Grb2 or Shc then interacts with reticular activating system (Ras), leading to an interaction with rapidly accelerated fibrosarcoma (Raf), which will in turn activate the mitogen activated protein kinase (MAPK) / extracellular regulated kinase (ERK) pathway (Carpenter and Cohen 1990, Ullrich and Schlessinger 1990, Schlessinger 2000). The activation of ErbB1 can also provide a binding site for p85, which is

the protein subunit of phosphatidylinositol 3-kinase (Xu, Huang et al.) pathway (Rodrigues, Falasca et al. 2000). Once activated, it will in turn phosphorylate Akt also known as protein kinase B (Rodrigues, Falasca et al. 2000, Collin de L'hortet, Gilgenkrantz et al. 2012). Although acting through the same intracellular pathways, there appears to be a different capacity for different ligands (e.g. EGF and TGF-α) to activate either the proliferation factor MAPK or the survival factor Akt (DeHaan, Wolters et al. 2009). The pathway is illustrated in Figure 1.1.

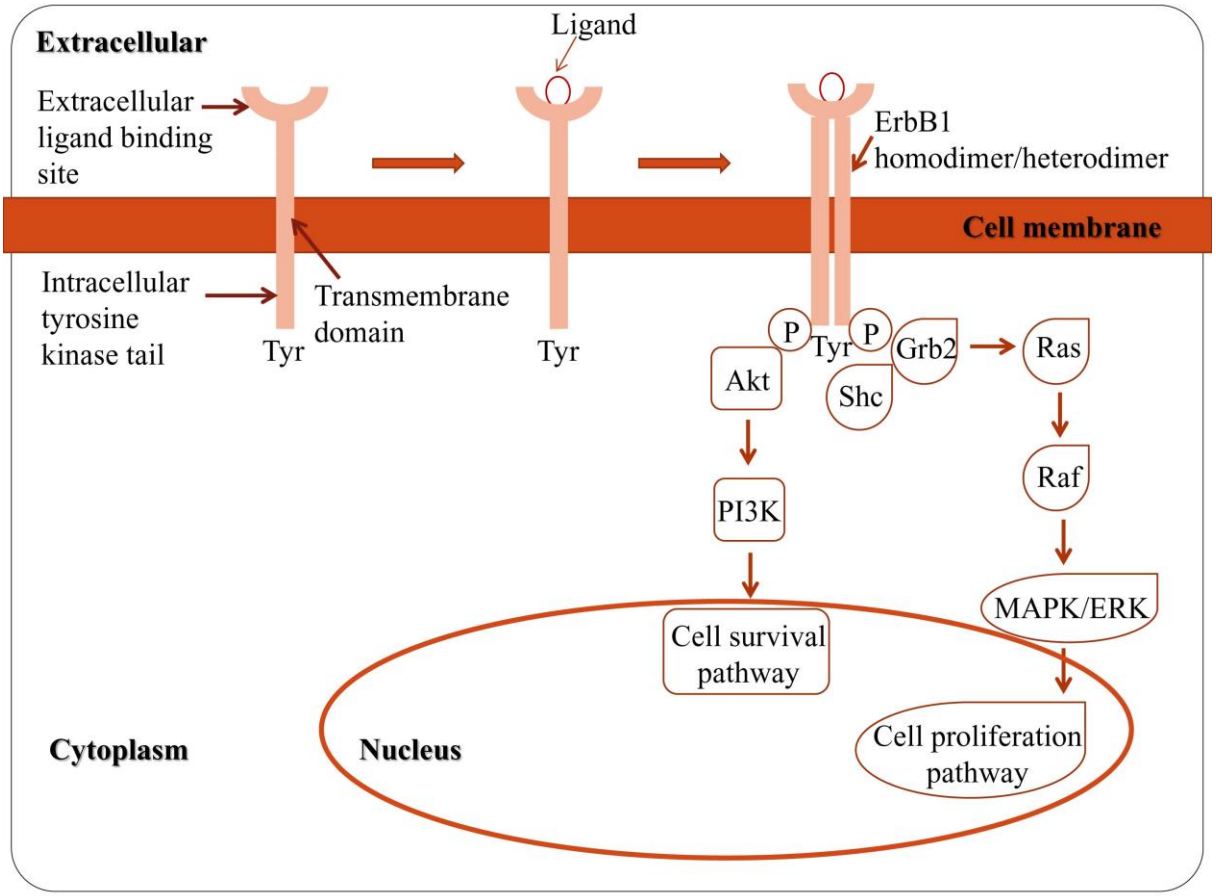

Figure 1.1. Cellular activation of ErbB1 receptor that generates two different pathways which are MAPK/ERK and PI3K/Akt pathways. *Tyr: tyrosine, P: phosphorylated*

1.2.2 Location of expression and normal functions

In normal cells, the expression of ErbB1 ranges from 40, 000 to 100, 000 receptors per cell (Holbro and Hynes 2004). It is expressed on healthy cells that originate from all three germ cell layers, particularly those of epithelial origin (e.g. the skin and GI tract) (Ullrich,

Coussens et al. 1984). Upon ErbB1 activation by its ligands, several important events for ErbB1 are triggered. ErbB1 plays a vital role in wound healing (Schreiber, Winkler et al. 1986, Schultz, White et al. 1987, Nakamura and Nishida 1999) and in the development of skin (Chailler and Menard 1999, Jost, Kari et al. 2000), gastrointestinal (Miettinen, Berger et al. 1995, Dvorak, Halpern et al. 2002) and neonatal development (Chailler and Menard 1999, Dvorak, Halpern et al. 2002). Besides that, ErbB1 is also important in reproduction (Park, Su et al. 2004) and liver regeneration (Berasain, Garcia-Trevijano et al. 2005), as well as in the development of lung (Taniguchi, Yamamoto et al. 2011), eye (Rall, Scott et al. 1985) and bone (Zhu, Jia et al. 2007). In general, the main functions of ErbB1 are in the regulation of epithelial cell proliferation, survival and differentiation during physiological development (Yano, Kondo et al. 2003).

ErbB1 ligands have been reported to have a number of overlapping functions *in vitro* (Strachan, Murison et al. 2001, Lee, Pearsall et al. 2004), thus analysis such as null mutations of the ErbB1 ligands have been crucial to unravel their functions *in vivo* and reveal that each ligand has its own specific function in addition to having redundant activities (Schneider and Wolf 2009, Dahlhoff, Schafer et al. 2012). Generation of transgenic mice overexpressing ErbB1 ligands have also been very informative concerning the role of these molecules in tumorigenesis and other diseases (Schneider and Wolf 2009). The roles of ErbB1 ligands have been covered widely (Jorissen, Walker et al. 2003, Holbro and Hynes 2004, Schneider and Wolf 2009). In this review, the roles of ErbB1 in the GI tract will be discussed in detail.

1.2.3 Post-translational regulation

ErbB1 is regulated extensively by post-translational modifications (Linggi and Carpenter 2006). Ligand-induced tyrosine autophosphorylation mediates the initiation of ErbB1 downstream signalling pathways while N-glycosylation of the extracellular domain is important for the membrane transport and maturation of nascent receptor and ligand binding

activity of the mature surface receptor (Hsu, Chen et al. 2011). Serine/threonine phosphorylation by protein kinase C (PKC), MAPK and calcium/calmodulin-dependent protein kinase II (CaMKII) modulates receptor tyrosine kinase activity and internalisation (Paik, Paik et al. 2007).

Unbound ErbB1 receptor is randomly distributed on the cell surface. After ligand binding, the EGF/ErbB1 complexes cluster in clathrin-coated pits and are internalised. Studies have shown that the half-life of ErbB1 decreased approximately 3-4 fold in the presence of EGF from 6.5 hours to 1.5 hours which indicates that the occupied ErbB1 is rapidly internalised or degraded (Baulida, Kraus et al. 1996) followed by a rapid downregulation of receptors on the cell surface, while the unbound ErbB1 is also internalised but at a slower rate, and is not followed by downregulation of receptors (Wiley, Herbst et al. 1991). Cell surface receptors can be internalised by both clathrin-mediated endocytosis and non-clathrin endocytosis. The mode of internalisation is dependent on ligand concentration (Sigismund, Woelk et al. 2005). In particular, at low doses of EGF, the ErbB1 is internalised through clathrin-mediated endocytosis while at higher doses of EGF, the receptor is internalised through both clathrin-mediated endocytosis and non-clathrin endocytosis (Sigismund, Woelk et al. 2005). Internalisation via clathrin-mediated endocytosis results in recycling of ErbB1 to the cell surface and sustained ErbB1 signalling (Sigismund, Argenzio et al. 2008). By contrast, internalisation via non-clathrin endocytosis is regulated by receptor ubiquitination and commits the ErbB1 to degradation (Sigismund, Argenzio et al. 2008). The regulation of ErbB1 is important as dysregulated ErbB1 signalling is strongly associated with cancer (Appert-Collin, Hubert et al. 2015).

1.2.4 Transcriptional regulation

ErbB1 signalling involves three temporal phases of feedback regulation that is crucial in maintaining the normal phenotype of cells (Avraham, Sas-Chen et al. 2010). The first

mechanism is immediate feedback regulation, which consists of immediate early genes (IEGs), that have primarily positive activities and occurs within 20-45 minutes after stimulation The second mechanism which occurs within 45-120 minutes comprises delayed early genes (DEGs) and consists of both positively- and negatively-acting components (Amit, Citri et al. 2007). The third mechanism involves the late, secondary response genes and occurs after 120 minutes. These confer stable phenotypes in a cell (Avraham and Yarden 2011).

The first regulation which comprises IEGs, depends on post-translational protein modifications, for instance, phosphorylation and dephosphorylation or ubiquitination (Amit, Citri et al. 2007). IEGs are being rapidly induced in response to activation by ErbB family ligands, for example EGF. Activation induced by EGF is mediated by the MAPK pathway, thus aberrant activation of the ligand constitutes a positive feedback mechanism that sustains growth factor signals and often converts a transient stimulus into a sustained signal (Avraham and Yarden 2011).

Consequently, after being rapidly induced by EGF, IEGs are abruptly downregulated through a delayed feedback regulation which involves DEGs. DEGs normally undergo ligand-induced upregulation to gradually shut down ErbB1 signalling, however, DEGs that restrain the transcriptional activation of oncogenic IEGs are commonly downregulated in tumours which explains their tumour-suppressive functions (Amit, Citri et al. 2007). The delayed feedback regulation involves newly induced phosphatases, as well as DNA- and RNA-binding proteins that are encoded primarily by DEGs (Avraham and Yarden 2011). In many cases, the EGF-induced attenuator forms a complex with the protein encoded by the stimulating IEG to repress its function (Amit, Citri et al. 2007). EGF-induced DEGs robustly shut down IEGs by either inhibiting upstream signal transduction pathways or by promoting

transcriptional attenuation. Signal prolongation as well as increased expression of growth factors are associated with aggressive malignant lesions (Avraham and Yarden 2011).

The last phase in ErbB transcriptional regulation which involves secondary response genes determines new phenotypes. Along with genes encoding enzymes involved in metabolism and membrane biogenesis, the late-induced wave of transcription comprises sets of mRNAs that collectively confer new phenotypes (Avraham and Yarden 2011).

1.2.5 Role in cancer

ErbB1 is well-known to be involved in malignant transformation and cancer progression (Baselga and Arteaga 2005). Carcinogenesis caused by ErbB1 dysregulation occurs by different mechanisms, including receptor as well as ligand overexpression, altered dimerization processes, deficiency of specific phosphatases, decreased receptor turnover and mutations (Kamath and Buolamwini 2006). ErbB1 is commonly hyperactivated in different epithelial tumours (Baselga and Arteaga 2005) and overexpression of this receptor has been found in tumours including head and neck, ovarian, colon and lung cancer and leads to poor prognosis among patients (Herbst and Langer 2002, Wood, Truesdale et al. 2004). A smaller percentage of bladder cancers, pancreatic cancers and gliomas are also known to overexpress ErbB1 (Salomon, Brandt et al. 1995). Consequences of such overexpression are constitutively activated downstream signalling pathways, resulting in aggressive and invasive metastatic cancers (Ethier 2002).

It was originally thought that ErbB1 amplification promoted tumour development exclusively by increasing ligand-activated signalling through wild-type ErbB1. However, in addition to that, it is now known that tumours exhibiting ErbB1 amplification have ErbB1 mutations (Frederick, Wang et al. 2000). A number of ErbB1 mutants have been observed in tumours where gene amplification has occurred (Kuan, Wikstrand et al. 2001). ErbB1 class

III variant, or ErbB1vIII, is the most common ErbB1 mutant and was first identified in glioblastoma multiforme (Wikstrand, Reist et al. 1998) and has been reported also in breast, ovarian, prostate and lung carcinoma (Garcia de Palazzo, Adams et al. 1993, Wikstrand, Hale et al. 1995, Moscatello, Holgado-Madruga et al. 1998). The ErbB1vIII mutant receptor has a molecular mass of 145 kDa compared to 170 kDa of wild-type ErbB1. It is truncated due to an in-frame deletion of 801 base pairs, corresponding to exons 2-7 in the mRNA, resulting in the deletion of amino acids 6-273 in the extracellular domain (Wikstrand, Reist et al. 1998). There is no evidence of activation of ErbB1vIII by EGF or TGF-α, in that the truncated receptor is ligand-independent, constitutively active and has a defective downregulation behaviour which can be seen by an increase in tumour cell proliferation and a decrease in apoptosis (Batra, Castelino-Prabhu et al. 1995, Nagane, Coufal et al. 1996, Khattri, Zuo et al. 2015). This indicates that the ligand-independent ErbB1 mutant receptor is more potent in tumour growth than the overexpression of wild-type ErbB1 which must be activated by ligand for maximum activation (Nagane, Coufal et al. 1996, Khattri, Zuo et al. 2015).

Roles of ErbB1 in cancer become a rationale to be exploited in cancer therapeutics. Interruption in the activation of ErbB1 can be accomplished through the use of the ErbB1 mAbs, which block the binding of endogenous ligands, or by the use of ErbB1 TKIs, that inhibit specific downstream components of the ErbB1 pathway (Huang and Harari 1999).

1.3 Mechanism of action of ErbB1 targeted drugs

The intravenously administered monoclonal antibodies (mAbs) target the extracellular surface of ErbB1 and block the ligand binding to the receptor which further inhibits dimerization and subsequent signal transduction (Herbst and Shin 2002). On the other hand, the orally administered TKIs can easily penetrate extracellular membranes and bind intracellularly to the ErbB1 tyrosine kinase domain thus blocking the signal transduction

cascade (Moy and Goss 2007). In this review, ErbB1 targeted drugs are classified into mAbs, single target TKIs, dual target TKIs and multitarget TKIs and the mechanism of action of the drugs are discussed further.

1.3.1 mAbs

Early clinical trials of mAbs utilised only murine mAbs which unfortunately were associated with the development of a human anti-mouse antibody response against the murine proteins (Herbst and Shin 2002). This immune response increases the risk of serious allergic reactions. However, developments in genetic engineering have made it possible to produce antibodies comprised of both murine and human sequences which are known as chimeric antibodies (Herbst and Shin 2002). Chimeric mAbs have been reported to demonstrate specificity and a diminished incidence of human anti-mouse antibody reactions (Shitara, Kuwana et al. 1993). Additionally, humanized and fully human mAbs have also been developed to overcome the immune responses that initially limited the applicability of the early mAbs (Herbst and Shin 2002). Examples of mAbs that inhibit ErbB1 signalling are cetuximab and panitumumab.

In Europe (EU) and the US, cetuximab has been approved for use with concomitant radiotherapy in patients with locally advanced squamous cell carcinoma of the head and neck (SCCHN) and in combination with irinotecan for the treatment of metastatic colorectal cancer (mCRC) in patients with ErbB1-expressing tumours who are refractory to irinotecan-based therapy (Blick and Scott 2007). In the US, cetuximab has also been approved as monotherapy in patients with recurrent or metastatic SCCHN for whom platinum-based therapy has failed and in patients with mCRC who are intolerant of irinotecan-based regimens (Blick and Scott 2007). In 2011, the FDA approved cetuximab in combination with cisplatin or carboplatin and 5-fluorouracil for the first-line treatment of patients with recurrent locoregional or metastatic SCCHN (Cohen, Chen et al. 2013). Cetuximab is a recombinant human/mouse

chimeric mAb for the immunoglobulin G1 (IgG1) subclass and has a five-fold higher affinity for ErbB1 than the natural ligands and inhibits ligand-induced activation of ErbB1 (Yarden and Ullrich 1988). Cetuximab stimulates ErbB1 internalisation, effectively removing the receptor from the cell surface for interaction with the ligands. In addition, due to its IgG1 construct, *in vitro* cetuximab has been shown to mediate antibody-dependent cellular cytotoxicity against certain tumour types (Goldstein, Prewett et al. 1995). Both *in vitro* and *in vivo* studies demonstrate that cetuximab inhibits lung cancer cell lines and tumour xenografts in nude mice (Hanna, Lilenbaum et al. 2006).

Panitumumab (Vectibix^{TM}) is another example of a mAb that was granted approval by the FDA in 2006 for the treatment of patients with ErbB1-expressing metastatic colorectal carcinoma with disease progression on or following fluoropyrimidine-, oxaliplatin- and irinotecan-containing chemotherapy regimens (Giusti, Shastri et al. 2007). However, panitumumab has also undergone early clinical testing in prostate cancer (Wang, Fredlin et al. 2003). Phase II trials of panitumumab monotherapy were in hormone-resistant prostate cancer, colorectal cancer (first line) and NSCLC (Meropol, Berlin et al. 2003). A phase III trial of third-line panitumumab in chemotherapy-refractory metastatic colorectal cancer showed that panitumumab significantly improved progression-free survival with manageable toxicity (Van Cutsem, Peeters et al. 2007). Panitumumab is a fully humanized IgG_2 monoclonal antibody, thus it does not induce antibody-dependent cell-mediated cytotoxicity. It is directed at the ErbB1 and binds with high affinity (Heymach, Nilsson et al. 2006). In preclinical as well as xenograft models, panitumumab has been shown to be effective on ErbB1-overexpressing tumours (Calvo and Rowinsky 2005, Heymach, Nilsson et al. 2006).

Other examples of ErbB1-targeting mAbs that are in clinical development phases are matuzumab (Hartmann, Kollmannsberger et al. 2013) , necitumumab (Dienstmann and Felip 2011) and nimotuzumab (Satoh, Lee et al. 2015). Details are listed in Table 1.1.

1.3.2 Single target TKIs

A second major category of targeted therapies are the small molecule inhibitors which are low molecular weight inhibitors that compete with adenosine triphosphate (ATP) for binding to the intracellular tyrosine kinase domain of ErbB1 and thereby abolish ErbB1 catalytic activity (Arteaga 2003).

An example of a single target TKI which inhibits ErbB1 is gefinib. Gefinib was the first ErbB1 small molecule inhibitor approved by the FDA in 2003 for monotherapy treatment for patients with locally advanced or metastatic NSCLC after failure of both platinum-based and docetaxel chemotherapies (Cohen, Williams et al. 2003). A high response rate was observed in women and in non-smokers with median duration of response of 7.0 months (range 4.6-18.6+ months) whereby the drug was approved under accelerated approval that requires further studies to be conducted to verify that gefinib therapy produced benefit (Cohen, Williams et al. 2003). The *in-vitro* preclinical studies showed effective antiproliferative activity of gefinib on human ovarian (OVCAR-3), breast (MCF-10A ras; ZR-75-1) and colon (GEO) cancer cell lines (Cohen, Williams et al. 2003). In a colon cancer xenograft study, a combined treatment of gefinib and cytotoxic agents produced tumour growth arrest and extended the survival of tumour-bearing animals (Cohen, Williams et al. 2003). Maximum plasma concentrations resulting from clinically relevant gefinib doses are 0.5-1 μM or more, similar to or greater than the 50% inhibitory concentration values of other intracellular transmembrane tyrosine specific protein kinases. Therefore gefinib cytotoxicity could be the result of inhibition of downstream signal proteins or ATP-dependent kinases other than ErbB1 (Cohen, Williams et al. 2003). Current studies have shown that detection of ErbB1 mutation state is beneficial as an important predictive factor for gefinib treatment in NSCLC patients (Aroldi, Bertocchi et al. 2014, Wang, Xiang et al. 2014).

Another example of an ErbB1 single TKI is erlotinib. Studies have shown that erlotinib is effective on human colon and head and neck tumour cells as well as in tumour xenografts (Moyer, Barbacci et al. 1997, Pollack, Savage et al. 1999). Erlotinib also inhibits ErbB1 tyrosine kinase autophosphorylation by inhibiting the intracellular domain (Cohen, Johnson et al. 2005), however, there were insufficient data to support whether erlotinib was more selective for ErbB1 compared to other receptor tyrosine kinases (Pollack, Savage et al. 1999, Johnson, Cohen et al. 2005). Erlotinib received approval by the FDA in 2004 as monotherapy for the treatment of patients with locally advanced or metastatic NSCLC after failure of at least one prior chemotherapy regimen (Cohen, Johnson et al. 2005). The survival rate of erlotinib-treated patients was higher in patients who never smoked and had ErbB1-positive tumours (Cohen, Johnson et al. 2005). However, a study also showed that some NSCLC patients without ErbB1 mutations respond to erlotinib, suggesting that there may be a mechanism other than the ErbB1 pathway that mediated the tumouricidal effects of the drug (Ciuleanu, Stelmakh et al. 2012).

Other examples of ErbB1 single target TKIs that have been approved for NSCLC are icotinib (Conmana®) (Shi, Zhang et al. 2013, Hu, Han et al. 2014), osimertinib (DiGiulio 2015, Tan, Gilligan et al. 2015) and rociletinib (DiGiulio 2015, Yang, Popat et al. 2015), while WZ4002 is in pre-clinical development. Details are listed in Table 1.2.

1.3.3 Dual target TKIs

In the situation where co-expression of ErbB1 and ErbB2 occurs, dual target small molecule inhibitors that simultaneously target both receptors may have therapeutic advantages. This interaction prevents the phosphorylation and subsequent signal transduction of both the MAPK and the PI3K/Akt pathways, leading to an increase in apoptosis and decreased cellular proliferation (Medina and Goodin 2008).

Lapatinib was the first dual target small molecule inhibitor targeting both ErbB1 and ErbB2 and was approved by the FDA in 2007 to be used in combination with capecitabine for the treatment of patients with advanced or metastatic breast cancer that overexpress ErbB2 who have already received previous therapy with anthracyclines, taxanes and trastuzumab (Burris, Taylor et al. 2009). Lapatinib is effective in patients with metastatic breast cancer, particularly those overexpressing ErbB2 (Rusnak, Lackey et al. 2001, Spector, Xia et al. 2005, Konecny, Pegram et al. 2006, Chien, Munster et al. 2014). Lapatinib is a competitive and reversible-dual TKI of both ErbB1 and ErbB2 and inhibits not only baseline activation of both receptors but also interrupts downstream activation of MAPK/ERK1/2 and Akt (Xia, Mullin et al. 2002). Although ErbB1 inhibitors have been largely associated with reversible growth inhibition, Akt inhibition in lapatinib-treated ErbB2 expressing cells was associated with significant apoptosis (Xia, Mullin et al. 2002, Konecny, Pegram et al. 2006). Lapatinib was also found to inhibit signal transduction in EGF-stimulated tumour cell lines that do not overexpress ErbB1 in which EGF was found to be unable to reverse the anti-tumour effects of lapatinib (Xia, Mullin et al. 2002). This is interesting as some tumours may not quantitatively overexpress either ErbB2 or ErbB1 but remain dependent on these receptors for growth and survival signals (Rusnak, Lackey et al. 2001, Rusnak, Alligood et al. 2007). Even low levels of ErbB1 may be activated in the presence of ligands such as EGF followed by formation of ErbB1/ErbB2 heterodimers and ErbB2 transactivation (Xia, Mullin et al. 2002). Thus, lapatinib has a distinct clinical advantage as a potent reversible dual inhibitor of both ErbB2 and ErbB1 in which effects of lapatinib on pathways involved in regulating tumour progression and survival are not reversed in the presence of EGF (Xia, Mullin et al. 2002).

TAK-285 is an investigational, dual TKI inhibitor that was designed and synthesised by Takeda Pharmaceutical Company, Osaka, Japan and has been shown to be both selective and potent in inhibiting ErbB1/ErbB2 kinase activities (Doi, Takiuchi et al. 2012). The anti-

tumour activity of TAK-285 was evaluated in several murine models employing ErbB2 and ErbB1-overexpressing human tumour xenografts, which revealed that orally administered TAK-285 effectively inhibited xenograft tumours and this effect appeared to correlate with its ability to inhibit ErbB1 and ErbB2 (Iwahara A 2008). The similar mechanism of action of anti-tumour activity was also observed in mouse and rat xenograft tumour models (Nakayama, Takagi et al. 2013). TAK-285 also demonstrated no potential elevated cardiac risks, whereas other TKIs can elicit secondary effects including heart toxicity (Shell, Wrappel et al. 2008) . In the phase I study, based on its safety, tolerability profile, pharmacokinetic characteristics and potential antineoplastic activity in patients with advanced solid tumours, further evaluation of TAK-285 was permitted for the treatment of patients with solid tumours (Doi, Takiuchi et al. 2012). Unlike lapatinib, TAK-285 is not a substrate for P-glycoprotein (Pgp) efflux, thus it is useful in the development of an agent to potentially treat brain metastases (Nakayama, Takagi et al. 2013). Lapatinib, which is a Pgp substrate has demonstrated insignificant central nervous system penetration across either an intact (Polli, Olson et al. 2009) or a tumour-compromised blood brain barrier (Taskar, Rudraraju et al. 2012), and has low clinical activity in this setting (Lin, Carey et al. 2008, Lin, Diéras et al. 2009). Key drug efflux transporters operating in preserving the blood brain barrier are the Pgp transporter, which belongs to the ATP-binding cassette transporter family and the breast cancer resistance protein (Sun, Dai et al. 2003, Lin 2004). These transport systems are responsible for the rapid removal of therapeutic agents from the central nervous system following local or systemic administration and thus contribute to relatively ineffective concentrations in the brain of many antineoplastic agents. Thus, due to the characteristic that enables TAK-285 to have access to the central nervous system, this drug may be useful in the treatment of brain metastases (Nakayama, Takagi et al. 2013). However, further investigations are required as TAK-285 was shown to be distributed in human cerebrospinal

fluid but the free concentration of the drug was below that associated with biologically relevant target inhibition (LoRusso, Venkatakrishnan et al. 2014).

Another example of an ErbB1 dual TKI under investigation is selatinib (Zhang, Fan et al. 2013) . Details are listed in Table 1.2.

1.3.4 Multitarget TKIs

Multitarget TKIs for the epidermal growth factor (ErbB) family of receptors are also known as pan-ErbB inhibitors, which inhibit the entire ErbB family of receptors. Afatinib (Gilotrif^{TM}) is one of the potent orally bioavailable, irreversible pan-ErbB inhibitors. It was approved by the US FDA on 12 July 2013 for the first-line treatment of patients with metastatic NSCLC who have tumours with ErbB1 exon 19 deletions or exon 21 (L858R) substitution mutations as detected by a US FDA approved test (Dungo and Keating 2013). Afatinib inhibits ErbB1, ErbB2 and ErbB4 at significantly low concentrations (Li, Ambrogio et al. 2008, Solca, Dahl et al. 2012). It has been proposed that irreversible binding to the target receptor as well as inhibition of multiple ErbB family members, including inhibition of trans-phosphorylation of ErbB3 (Li, Ambrogio et al. 2008), may help to overcome resistance that can develop with reversible small-molecule ErbB1 TKIs (Li, Ambrogio et al. 2008). This has been attributed to clonal selection of tumour cells which exhibit resistance mechanisms such as additional mutations in ErbB1, for example T790M that reduces the efficacy of gefinib and erlotinib (Li, Ambrogio et al. 2008). Several studies have been conducted to evaluate the efficacy of afatinib. Afatinib has demonstrated antiproliferative activities in ErbB2-positive and triple-negative breast cancer cell lines as well as in xenograft models (Schuler, Awada et al. 2012). However, in a phase II trial, afatinib was shown to have a limited activity in ErbB2-negative metastatic breast cancer (Schuler, Awada et al. 2012). Afatinib has also shown its efficacy in the treatment of solid tumours after docetaxel treatment (Awada, Dumez et al. 2013) and also in patients with advanced NSCLC who had

received prior platinum-doublet chemotherapy and/or erlotinib/gefinib therapy (Murakami, Tamura et al. 2012). Afatinib was also recommended to patients with advanced NSCLC that have failed at least 12 weeks of previous ErbB1 TKI treatment (Miller, Hirsh et al. 2012).

Neratinib is an oral, small-molecule inhibitor that irreversibly binds to ErbB receptor tyrosine kinases and is 12- to 16-fold more potent than lapatinib when inhibiting proliferation of ErbB2-positive breast cancer cell lines (Rusnak, Lackey et al. 2001, Rabindran, Discafani et al. 2004, Hegde, Rusnak et al. 2007). Neratinib in combination with trastuzumab and paclitaxel has been shown to be effective in ErbB2-positive metastatic breast cancer in which inhibiting multiple ErbB family receptors may be more advantageous than single-agent inhibition (Jankowitz, Abraham et al. 2013). The efficacy of neratinib as compared to lapatinib can be explained by the incomplete inhibition of ErbB1 by lapatinib which resulted in selection of ligand-driven feedback that sustained ErbB1 activation in the face of constant exposure to the drug (Xia, Petricoin et al. 2013). Although lapatinib is considered as an equipotent inhibitor of ErbB2 and ErbB1 (Rusnak, Lackey et al. 2001, Wood, Truesdale et al. 2004), its clinical efficacy has been limited to ErbB2-positive breast cancers (Johnston, Trudeau et al. 2008) Despite its significant effect in the ErbB2-positive breast cancers, the clinical efficacy of lapatinib has been limited by the development of therapeutic resistance (Geyer, Forster et al. 2006, Johnston, Trudeau et al. 2008). It was also reported that ErbB2 mutation does not play a role in resistance and phosphorylation of ErbB2 remains inhibited in models of acquired lapatinib resistance (Xia, Bacus et al. 2006, Martin, Miller et al. 2008, Huang, Park et al. 2011). Inadequate target inhibition driven by a ligand-mediated autocrine feedback loop may represent a broader mechanism of therapeutic resistance to ErbB TKIs and a different strategy for selecting more effective TKIs (such as pan-ErbB inhibitors) could have a significant impact not only on the treatment of ErbB2- and ErbB1-dependent tumours

but also on the treatment of other kinase-dependent tumours or diseases (Xia, Petricoin et al. 2013).

Dacomitinib is other example of an ErbB1 multitarget TKI which is effective on the treatment of recurrent/metastatic-squamous cell cancer of the head and neck (RM-SCCHN) (Abdul Razak, Soulieres et al. 2012). Sapitinib (Tjulandin, Moiseyenko et al. 2014), pelitinib (Erlichman, Hidalgo et al. 2006) and BMS-599626 (Rixe, Franco et al. 2009) are also in development phases for the treatment of advanced solid tumours while canertinib (Soria, Cortes et al. 2012) is under investigation for metastatic breast cancer (MBC). Details are listed in Table 1.2.

Table 1.1. ErbB1 monoclonal antibodies.

Drug	*Targeted receptor*	*Type of tumour*	*Therapy setting*	*Development phase*	*References*
mAbs					
Cetuximab *(Erbitux®)*	ErbB1	SCCHN, mCRC	Combination/Monotherapy & Second-line	Approved	Blick and Scott 2007
		SCCHN	Combination & First-line	Approved	Cohen, Chen et al. 2013
Panitumumab *(Vectibix™)*	ErbB1	mCRC	Combination/Second-line	Approved	Giusti, Shastri et al. 2007
Matuzumab	ErbB1	Advanced NSCLC	Combination	Phase I	Hartmann, Kollmannsberger et al. 2013
Necitumumab	ErbB1	Stage IV squamous & nonsquamous NSCLC	Combination & First-line	Phase III	Dienstmann and Felip 2011
Nimotuzumab	ErbB1	Advanced gastric cancer	Combination & Second-line	Phase II	Satoh, Lee et al. 2015

Abbreviations- SCCHN: squamous cell carcinoma head and neck, mCRC: metastatic colorectal cancer, NSCLC: non-small cell lung cancer

Table 1.2. ErbB1 tyrosine kinase inhibitors.

Drug	*Targeted receptor*	*Type of tumour*	*Therapy setting*	*Development phase*	*References*
Single targeted TKIs					
Gefinib *(Iressa®)*	ErbB1	Advanced/metastatic NSCLC	Monotherapy & Second-line	Approved	Cohen, Williams et al. 2003
Erlotinib *(Tarceva®)*	ErbB1	NSCLC	Monotherapy & Second-line	Approved	Cohen, Johnson et al. 2005
Icotinib *(Conmana®)*	ErbB1	Advanced NSCLC	Monotherapy & Second or Third-line	Approved	Shi, Zhang et al. 2013, Hu, Han et al. 2014
Osimertinib *(Tagrisso™)*	ErbB1	Advanced NSCLC	Monotherapy & Second-line	Approved	DiGiulio 2015, Tan, Gilligan et al. 2015
Rociletinib	ErbB1	Advanced NSCLC	Monotherapy & Second-line	Approved	DiGiulio 2015,Yang, Popat et al. 2015
WZ4002	ErbB1	Mutant NSCLC	N/A	Pre-clinical	Cortot, Repellin et al. 2013

Dual targeted TKIs					
Lapatinib *(Tykerb/Tyverb®)*	ErbB1, ErbB2	ErbB2 +ve mBC	Combination/Second-line	Approved	Burris, Taylor et al. 2009
TAK-285	ErbB1, ErbB2	Solid tumours	Monotherapy & First-line	Phase I	LoRusso, Venkatakrishnan et al. 2014
Selatinib	ErbB1, ErbB2	ErbB2+ve ovarian tumour	N/A	Pre-clinical	Zhang, Fan et al. 2013
Multitargeted TKIs					
Afatinib *(Gilotrif^{TM})*	ErbB1, ErbB2, ErbB4	Advanced NSCLC	Monotherapy/First-line	Approved	Dungo and Keating 2013
Neratinib	ErbB1, ErbB2, ErbB4	ErbB2 +ve mBC	Combination	Phase I	Jankowitz, Abraham et al. 2013
Dacomitinib	ErbB1, ErbB2, ErbB4	RM-SCCHN	Monotherapy/First-line	Phase II	Abdul Razak, Soulieres et al. 2012

Sapitinib *(AZD8931)*	ErbB1, ErbB2, ErbB3	Advanced solid tumours	Monotherapy	Phase I	Tjulandin, Moiseyenko et al. 2014
Pelitinib	ErbB1, ErbB2, ErbB4	Advanced solid tumours	Monotherapy	Phase I	Erlichman, Hidalgo et al. 2006
Canertinib *(CI-1033)*	ErbB1, ErbB2, ErbB4	mBC	Monotherapy	Phase II	Rixe, Franco et al. 2009
BMS-599626 (AC480)	ErbB1, ErbB2, ErbB4	Advanced solid tumours	Monotherapy	Phase I	Soria, Cortes et al. 2012

Abbreviations- SCCHN: squamous cell carcinoma head and neck, mCRC: metastatic colorectal cancer, mBC: metastatic breast cancer, RM: recurrent and/or metastatic, NSCLC: non-small cell lung cancer

1.4 ErbB1 role in gastrointestinal tract

ErbB1 targeted drugs have been associated with gastrointestinal toxicities. In order to understand why these drugs cause symptoms which are most probably related to altered functions of the gastrointestinal tract, the roles of ErbB1 in the normal gastrointestinal mucosa need to be fully understood.

The expression of ErbB1 in the human gastrointestinal tract is observed during foetal development, in which ErbB1 has been found in the oesophagus, stomach, and small and large intestines, suggesting ErbB1 has vital roles in the development of the digestive tract (Ghizdavat, Raduly et al. 2015). This is not surprising, as Dvorak and Halpem have reported that foetal intestine is exposed to EGF which is present in amniotic fluid, thus supporting vital roles of ErbB1during foetal development (Dvorak, Halpern et al. 2002). In the early postnatal period, breast milk is the major source of EGF for the developing intestinal mucosa (Dvorak, Halpern et al. 2002). Heparin-binding-EGF, which is also one of the ligands that bind to ErbB1, is also detected in both amniotic fluid and breast milk, but in lower concentrations than EGF. The biological actions of EGF and HB-EGF are mediated via interaction with all of the four members of ErbB family receptors (ErbB1, ErbB2, ErbB3 and ErbB4) (Dvorak, Halpern et al. 2002).

In adults, ErbB1 as well as its ligands, are widely expressed in the gastrointestinal tract. EGF, (one of ErbB1's ligands) is present in a relatively high concentration in the salivary glands and it has also been reported that EGF secreted from the salivary glands is necessary for liver regeneration (Jones, Tran-Patterson et al. 1995). In the stomach, EGF has been reported to stimulate the production of gastric mucus (Kelly and Hunter 1990). Studies by Ichikawa et al on rat gastric mucosa reported higher ErbB1 mRNA expression in the surface mucosal layer but lower in the submucosa and muscle layers of the stomach, thus suggesting

EGF-induced stimulation of mucin biosynthesis is limited to the surface mucus cells of the rat gastric mucosa (Ichikawa, Endoh et al. 2000).

The intestinal epithelium is one of the most rapidly proliferating tissues in the body. Intestinal epithelial cells proliferate at a high rate to preserve the balance with continuous cell loss through mechanical abrasion and terminal differentiation (Podolsky 1993). Research has shown that ErbB1 has various physiological functions, particularly within the gastrointestinal tract (Sequist, Besse et al.). ErbB1 is expressed widely in the basolateral membranes of intestinal epithelial cells (Uribe and Barrett 1997) (refer to Figure 1.2 and 1.3). In addition, the duodenal enterocytes were shown to express ErbB1 in the apical membrane and in the supranuclear area along the length of villi. ErbB1 was also detected in the crypts of Lieberkühn and Brunner's glands (Montaner and Perez-Tomas 1999). Gastric parietal cells are also known to secrete at least three ErbB1 ligands: TGF-α, amphiregulin and HB-EGF which are the critical regulators of differentiation and epithelial cell function within the gastrointestinal mucosa (Levitzki and Gazit 1995, Richardson and Dobish 2007, Reardon, Cloughesy et al. 2012, Soria, Cortes et al. 2012).

The wide expression of ErbB1 and its ligands in the gastrointestinal tract contributes to its important functions. The protective effects of ErbB1 are observed as early as during intestinal development with HB-EGF playing an important role against injury in the developing intestine (Dvorak, Khailova et al. 2008). This is also observed in the small intestine of adult animals (Dvorak, Halpern et al. 2002). It has been reported that ErbB1 is involved in the regulation of electrolyte and glucose transport in the small intestine (Opleta-Madsen, Hardin et al. 1991, Donowitz, Montgomery et al. 1994), as well as in the regulation of gastric acid secretion in the GI mucosa (Rhodes, Tam et al. 1986). ErbB1 also plays a significant role in GI mucosa healing by increasing the blood flow at the region of injury (Konturek, Brzozowski et al. 1997). It also protects the mucosa via stimulation of mucus

secretion from goblet cells (Ishikawa, Cepinskas et al. 1994). In the colon, ErbB1 is also involved in the regulation of chloride secretion and sodium absorption by colonocytes (McCole and Barrett 2009).

The functions of ErbB1 are able to be understood further from *in vivo* or *in vitro* models that feature the symptoms caused by ErbB1 activation or inhibition where the ErbB1 ligand or receptor has been modified. In an experimental model of necrotizing enterocolitis (NEC), EGF has been shown to decrease the incidence and severity of NEC which is a common and devastating GI disease predominantly affecting premature infants (Dvorak, Halpern et al. 2002). ErbB1 inactivation leads to impaired epithelial development of the gastrointestinal tract which was shown by intestinal epithelial defects of ErbB1 knockout mice (Miettinen, Berger et al. 1995), thus suggesting that ErbB1 signalling plays important roles in embryonic gut development.

In an experimental NEC model, ErbB1 activation was shown to induce cyclooxygenease-2 (COX-2) expression via transactivation by bacterial lipopolysaccharide (LPS). LPS is known to mediate inflammation through toll-like receptor 4 activation and is a key molecule in the pathogenesis of NEC. However, LPS also induces COX-2 which promotes intestinal barrier restitution through stimulation of intestinal cell survival, proliferation and migration. ErbB1 activation prevents experimental NEC and may play a critical role in LPS-stimulated COX-2 production, thus showing that ErbB1 is required for LPS induction of COX-2 expression. LPS induction of COX-2 also requires Src-family kinase signalling while LPS transactivation of ErbB1 requires matrix metalloprotease activity. It was also reported that inhibition of ErbB1 blocks LPS stimulation of MAPK/ERK, suggesting an important role of the MAPK/ERK pathway in ErbB1-mediated COX-2 expression (McElroy, Hobbs et al. 2012).

An *in vitro* study also showed that TGF-α, another ErbB1 ligand, also plays an important role in gastric epithelial wound healing. It was reported that COX-2 is involved in this process in which TGF-α induced expression of COX-2, is followed by gastric epithelial replication and morphogenesis (Sawaoka, Tsuji et al. 1999). ErbB1 activation by EGF was also reported to stimulate COX-2 expression via transactivation by tumour necrosis factor (TNF). Induction of COX-2 protein expression protects confluent monolayers of colon epithelial cells from TNF cytotoxicity. It was also shown that TNF-induced COX-2 expression in colon and gastric epithelial cells is via a tumour necrosis factor receptor 1 (TNFR1), ErbB1, Src and p38 MAPK-dependent mechanism (Hobbs, Goettel et al.).

In the enterocytes of adults, after direct activation by EGF, ErbB1 induces repair mechanisms following mucosal injury, promotes cell survival and reduces intestinal inflammation (Dvorak, Halpern et al. 2002). Increase of gastric barrier damage in the epithelial membrane increased the level of the expression of ErbB1 (Lin, Zhao et al. 2012) and the protective effect of ErbB1 on colonic mucosa was also reported, in which ErbB1, upon the binding of EGF and TGF-α, controlled colonic mucosal repair processes following injury by stimulating epithelial migration (Wilson 1999). Migration of the intestinal epithelial cell is important during intestinal development, epithelial cell turnover and also during disease states involving ulceration of the gastrointestinal lining. Mucosal integrity is thus re-established by rapid migration of epithelial cells across the wound margins (Dignass and Podolsky 1993).

Amphiregulin and epiregulin are also ligands of ErbB family receptors and were shown to stimulate the proliferation of human colonic subepithelial myofibroblasts, which is significant, as subepithelial myofibroblasts are reported to play an important role in promoting repair processes following mucosal injury (Inatomi, Andoh et al. 2006). Although all ErbB1 ligands elicit a similar spectrum of biological activities, such as stimulation of cell

migration and proliferation, through interaction with ErbB1 (Kavanaugh and Williams 1994, Jost, Kari et al. 2000, Yano, Kondo et al. 2003), recent investigations have indicated that individual ligands may produce different physiologic responses (Cohen and Elliott 1963, Chailler and Menard 1999). For example, TGF-α knockout in mice did not influence the induction of intestinal metaplasia, which is considered as a precursor of gastric cancer, however, amphiregulin knockout in mice caused an acceleration and augmentation of the induction of intestinal metaplasia (Gibson 2011).

Intestinal injury is a frequent complication of cancer therapies such as radiotherapy and chemotherapy, which disrupts mucosa surface integrity and most frequently manifests in diarrhoea (Beck, Wong et al. 2004). A study has been conducted showing that treatment with EGF protected against 5-fluorouracil-induced mucositis in hamsters (Sonis, Costa et al. 1992). However, despite the beneficial effects of ErbB1 and its ligands, particularly EGF, a study by Huang et al does not support a critical role for EGF or its receptor in the prevention or repair of chemotherapy-induced intestinal injury (Huang, Kemp et al. 2002).

Thus, further investigations are required to elucidate the roles of ErbB1 in cancer therapy-induced intestinal injury, as previous studies have shown its important roles in maintaining normal gastrointestinal function.

Figure 1.2. Location of ErbB1expression in intestinal epithelial cells (small intestine).

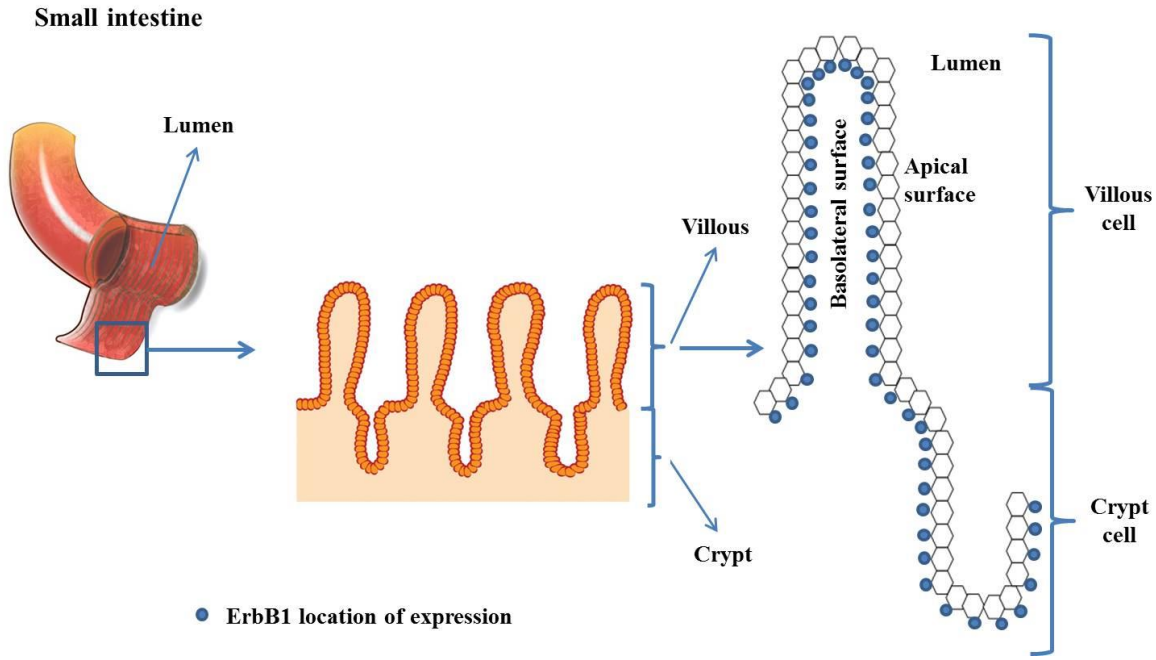

Figure 1.3. Location of ErbB1 expression in intestinal epithelial cells (colon).

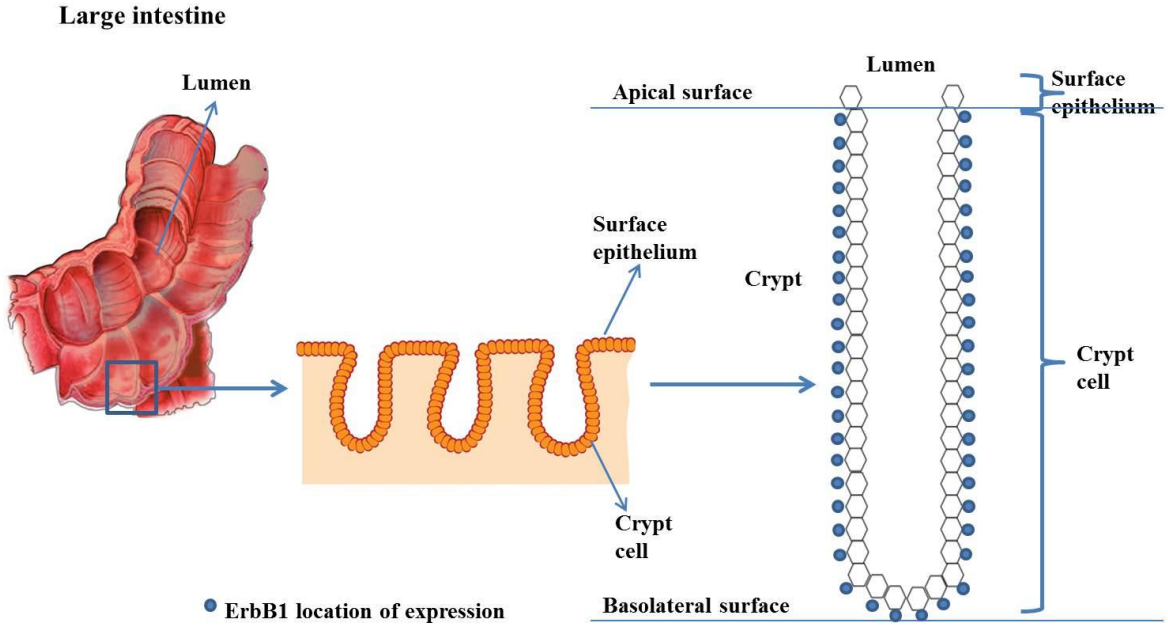

1.5 Diarrhoea associated with ErbB1 targeted therapies

Similarly to patients administered with conventional chemotherapy drugs, cancer patients treated with ErbB1 targeted drugs also experience diarrhoea (Cohen, Johnson et al. 2005, Hanna, Lilenbaum et al. 2006, Crown, Burris et al. 2008, Loriot, Perlemuter et al. 2008, Medina and Goodin 2008, Asnacios, Naveau et al. 2009, Abdul Razak, Soulieres et al. 2012).

Post-chemotherapy diarrhoea is the end result of damage to the crypts of the small bowel and colon, resulting in an excess of fluid remaining in the bowel lumen (Gibson and Keefe 2006). However, it is unclear whether targeted therapies cause the same sort of damage as chemotherapy. The importance of ErbB1 in the gastrointestinal tract has been described in the previous sections. However, the inhibition of intestinal ErbB1 which may lead to the gastrointestinal adverse events, as well as the exact pathophysiology of ErbB1 targeted therapy-induced diarrhoea, remains unclear. The following section will discuss the possible mechanisms of diarrhoea in ErbB1 targeted therapies.

1.5.1 Mechanisms of diarrhoea in ErbB1 targeted therapies

The proposed mechanisms of action of both ErbB1 targeted mAbs and TKIs are apoptosis induction, anti-angiogenesis or tyrosine kinase inhibition in target-expressing cells, which all could damage mucosa and lead to diarrhoea (Keefe and Gibson 2007). However, diarrhoea is more common in patients receiving oral ErbB1 TKIs, compared to those receiving ErbB1 mAbs which are administered intravenously (Asnacios, Naveau et al. 2009). This might be explained by the more specific selective inhibition of ErbB1 mAbs on the targeted receptors compared to ErbB1 TKIs that show varying degrees of cross-reactivity for a spectrum of receptor tyrosine kinases that could lead to higher toxicity (Huang, Armstrong et al. 2004, Widakowich, de Castro et al. 2007). Among all types of ErbB1 TKIs, incidence of diarrhoea is higher in the multitarget TKIs compared to the single and dual target TKIs (Table 1.3). TKIs that can inhibit multiple targets simultaneously also lead to a higher risk for other toxicities (Xia, Gerard et al. 2005). In addition, TKIs are expected to present more gastrointestinal toxicities as a result of their oral administration and hence direct damage to the intestinal mucosa (Widakowich, de Castro et al. 2007). Although adverse effects of targeted therapies are reported to be better tolerated than conventional chemotherapy, the risk of side effects are usually greater when targeted therapies are used in combination with

conventional chemotherapy or when mAbs are combined with TKIs (Keefe and Gibson 2007).

Knowledge of pharmacokinetic profile of ErbB1 TKIs may also help in understanding the mechanism of diarrhoea induced by the drugs. The maximum plasma level (C_{max}) of ErbB1 TKI, for example lapatinib, occurs 3 to 6 hours after oral administration with the effective plasma half-life is approximately 24 hours. Lapatinib is eliminated through hepatic metabolism by cytochrome P450 (CYP) 3A4 and is excreted in faeces. The drug should be used with caution with medications that are CYP3A4 substrates that could affect its elimination (Wilkinson 2005). Antacid should generally be avoided for 1 hour before and after lapatinib administration as the antacid could modify gastric pH which may affect absorption of lapatinib (Moy and Goss 2007). Systemic exposure (AUC) to lapatinib was increased when the drug was taken with food especially with a high-fat meal (Burris, Taylor et al. 2009, Koch, Reddy et al. 2009). As clinical studies of lapatinib were performed with administration on an empty stomach, thus, it is recommended that the drug to be taken in the same manner (Medina and Goodin 2008, Burris, Taylor et al. 2009). Approximately 40% of patients treated with lapatinib experienced a first diarrhoea event within 6 days of treatment initiation (Crown, Burris et al. 2008). Incidence of diarrhoea with lapatinib treatment was reported to be linearly related to dose and there was no apparent relationship between diarrhoea and serum concentration of the drug, suggesting that this toxicity evolves from a local effect of the drug on the gut epithelium (Burris, Hurwitz et al. 2005). Diarrhoea is a dose limiting toxicity not just for lapatinib but also for most ErbB1 TKIs (Keefe and Gibson 2007). Similar and more severe toxicities were also reported in other ErbB1 TKIs such as gefinib and erlotinib (Hidalgo, Siu et al. 2001, Baselga, Rischin et al. 2002).

Genetic variations have also been reported to give impact on susceptibility to side effects such as diarrhoea. Diarrhoea related to drug toxicity was correlated in some studies

with a clinical benefit and/or was a predictive factor of tumour response to ErbB1 TKIs (Thomas, Fossella et al. 2006, Shah, Shah et al. 2013). A polymorphism of the drug transporter *ABCG2* (also known as breast cancer resistance gene *BCRP*) and also *CYP3A4* and *CYP3A5* genes may modify the pharmacokinetics and therefore the toxicities of the drug. This is observed in both gefinib and erlotinib. It was reported that the 141K-*ABCG2* polymorphism is associated with a lower expression and activity of *ABCG2*, which consequently leads to a higher accumulation of both gefinib and erlotinib (Li, Cusatis et al. 2007). The similar 141K-*ABCG2* polymorphism was also correlated with the incidence of diarrhoea in patients treated with gefinib (Cusatis, Gregorc et al. 2006). Diarrhoea was also observed in gefinib-treated patients carrying *ABCG2* -15622T/T genotype or at least one TT copy in the 1143C/T and -15622C/T haplotype (Lemos, Giovannetti et al. 2011). Additionally, two ErbB1 promoter polymorphisms, -216 G/T and -191 C/A, were shown to be associated with grade ≥ 2 erlotinib-related diarrhoea (Rudin, Liu et al. 2008). Lapatinib is also a substrate and inhibitor of efflux transporters ABCB1 (also known as P-glycoprotein Pgp) and ABCG2 (Dai, Tiwari et al. 2008). Similar to gefinib and erlotinib, one of the most frequent adverse events of lapatinib in patients is also diarrhoea. Therefore, these functional single nucleotide polymorphisms of *ABCG2* in patients may also affect the pharmacokinetics and pharmacodynamics of lapatinib, resulting in an attenuation of its adverse events (Dai, Tiwari et al. 2008). Thus, it is important to note that certain polymorphisms may be related to susceptibility to ErbB1 TKI-induced-diarrhoea.

1.5.2 Incidence of diarrhoea in ErbB1 targeted therapies

Diarrhoea incidence in ErbB1 targeted therapies was graded on a scale from 1 to 5 using the National Cancer Institute Common Toxicity Criteria for Diarrhoea (Table 1.3) (Burris, Taylor et al. 2009, Health and Services 2009). Grade 1 or 2 diarrhoea is classified as

mild or moderate, grade 3 is severe, while grade 4 is life threatening or causing disabling adverse events and grade 5 is death (Moy and Goss 2007).

Diarrhoea occurs in about 21-26% of patients undergoing treatment with ErbB1 mAbs but is rarely severe, with only 1-3% experiencing grade 3-4 (Hanna, Lilenbaum et al. 2006, Giusti, Shastri et al. 2007, Cohen, Chen et al. 2013, Hartmann, Kollmannsberger et al. 2013, Satoh, Lee et al. 2015) (Table 1.4). The incidence and severity of diarrhoea is higher with ErbB1 TKIs than the mAbs with an incidence of 8.5-90.5% with <1-42.9% grade 3-4 (Table 1.4). Among the ErbB1 TKIs, multitarget TKIs possess higher incidences of diarrhoea (Erlichman, Hidalgo et al. 2006, Rixe, Franco et al. 2009, Abdul Razak, Soulieres et al. 2012, Soria, Cortes et al. 2012, Dungo and Keating 2013, Jankowitz, Abraham et al. 2013, Tjulandin, Moiseyenko et al. 2014), followed by dual target TKIs (Burris, Taylor et al. 2009, LoRusso, Venkatakrishnan et al. 2014) and single target TKIs (Cohen, Williams et al. 2003, Cohen, Johnson et al. 2005, Hu, Han et al. 2014, Sequist, Soria et al. 2015, Tan, Gilligan et al. 2015) (Table 1.4).

Diarrhoea related to erlotinib required 1% of patients to undergo dose treatment reduction in a randomized trial in metastatic NSCLC patients (Cohen, Johnson et al. 2005). A similar situation could also be seen in other ErbB1 TKIs such as gefinib, lapatinib, afatinib and dacomitinib which clearly suggests that diarrhoea is a dose limiting toxicity associated with ErbB1 TKIs (Fukuoka, Yano et al. 2003, Crown, Burris et al. 2008, Abdul Razak, Soulieres et al. 2012, Awada, Dumez et al. 2012). Since diarrhoea appears to correlate with dose and not serum concentration, this suggests a direct effect of the drugs on the gut (Burris, Hurwitz et al. 2005). This hypothesis is also supported by the fact that TKIs are more frequently associated with diarrhoea than mAbs which are administered intravenously rather than orally (Asnacios, Naveau et al. 2009). However, diarrhoea associated with ErbB1 targeted therapies were reported to be well-tolerated, self-limiting and manageable (Burris,

Hurwitz et al. 2005, Abdul Razak, Soulieres et al. 2012, Hu, Han et al. 2014). A summary of diarrhoea incidence associated with ErbB1 targeted therapies is shown in Table 1.4.

Table 1.3. National Cancer Institute Common Toxicity Criteria for Diarrhoea Grading (Health and Services 2009).

Grade of toxicity	Diarrhoea[a]
1	Increase of <4 stools/day over baseline; Mild increase in ostomy output compared with baseline
2	Increase of 4–6 stools/day over baseline; Intravenous fluids >24 h; Moderate increase in ostomy output compared with baseline; Not interfering with daily living
3	Increase of >7 stools/day over baseline; Incontinence; Intravenous fluids; Severe increase in ostomy output compared with baseline; Interfering with daily living activities
4	Life-threatening consequences (e.g., haemodynamic collapse)
5	Death

[a] Includes diarrhoea of small bowel or colonic origin and/or ostomy diarrhoea

Table 1.4. Diarrhoea incidence in ErbB1 targeted therapies.

Drug	*Targeted receptor*	*Administration*	*Therapy setting*	*Diarrhoea incidence (%)*		*References*
				Grade 3/4	*All grades*	
mAbs						
Cetuximab *(Erbitux®)*	ErbB1	Intravenous	Monotherapy&Second-line Combination&First-line	1.5 Not reported	22.7 26	Hanna et al. 2006 Cohen, Chen et al. 2013
Panitumumab *(Vectibix™)*	ErbB1	Intravenous	Combination/Second-line	2	21	Giusti, Shastri et al. 2007
Matuzumab	ErbB1	Intravenous	Combination	2	23	Hartmann, Kollmannsberger et al. 2013
Nimotuzumab	ErbB1	Intravenous	Combination&Second-line	3	25	Satoh, Lee et al. 2015
Single targeted TKIs						
Gefinib *(Iressa®)*	ErbB1	Oral	Monotherapy&Second-line	3	49	Cohen, Williams et al. 2003
Erlotinib *(Tarceva®)*	ErbB1	Oral	Monotherapy&Second-line	7	54	Cohen, Johnson et al. 2005
Icotinib *(Conmana®)*	ErbB1	Oral	Monotherapy&Second or Third-line	<1	8.5	Hu, Han et al. 2014

Osimertinib *(Tagrisso™)*	ErbB1	Oral	Monotherapy&Second-line	1	33	Tan, Gilligan et al. 2015
Rociletinib	ErbB1	Oral	Monotherapy&Second-line	0	20	Sequist, Soria et al. 2015
Dual targeted TKIs						
Lapatinib *(Tykerb/Tyverb®)*	ErbB1, ErbB2	Oral	Combination/Second-line	7	51	Burris, Taylor et al. 2009
TAK-285	ErbB1, ErbB2	Oral	Monotherapy&First-line	6	46	LoRusso, Venkatakrishnan et al. 2014
Multitargeted TKIs						
Afatinib *(Gilotrif™)*	ErbB1, ErbB2, ErbB4	Oral	Monotherapy/First-line	5	50	Dungo and Keating 2013
Neratinib	ErbB1, ErbB2, ErbB4	Oral	Combination	38	90.5	Jankowitz, Abraham et al. 2013
Dacomitinib	ErbB1, ErbB2, ErbB4	Oral	Monotherapy/First-line	15.9	84.1	Abdul Razak, Soulieres et al. 2012
Sapitinib *(AZD8931)*	ErbB1, ErbB2, ErbB3	Oral	Monotherapy	25	75	Tjulandin, Moiseyenko et al. 2014

Pelitinib	ErbB1, ErbB2, ErbB4	Oral	Monotherapy	27	70	Erlichman, Hidalgo et al. 2006
Canertinib *(CI-1033)*	ErbB1, ErbB2, ErbB4	Oral	Monotherapy	42.9	85.7	Rixe, Franco et al. 2009
BMS-599626 *(AC480)*	ErbB1, ErbB2, ErbB4	Oral	Monotherapy	0	41	Soria, Cortes et al. 2012

1.5.3 Management of diarrhoea in ErbB1 targeted therapies

Diarrhoea induced by ErbB1 targeted therapies is thought to be a result of excess chloride secretion, causing a secretory form of diarrhoea (Keefe and Gibson 2007, Crown, Burris et al. 2008), however, this has no supporting evidence and TKI-induced diarrhoea may be quite different to chemotherapy-induced diarrhoea (Bowen 2014). Chemotherapy-induced diarrhoea suggest direct mucosal damage (Pritchard, Potten et al. 1998, Gibson, Bowen et al. 2003, Gibson, Bowen et al. 2005), however, in ErbB1 TKI-induced diarrhoea, no significant pathology in the rats' intestines was observed despite rats displaying a dose-dependent diarrhoea profile consistent with that observed clinically (Bowen, Mayo et al. 2012). Histopathological findings on the effect of ErbB1 inhibitors on gastrointestinal are discussed further in the next section.

Diarrhoea may affect patients' well-being, reduce compliance with oral medications and thus reduce the efficacy of cancer therapy. The management of diarrhoea events may also increase the cost of cancer treatment (Wadler, Benson et al. 1998, Viele 2003, Crown, Burris et al. 2008). More importantly, severe diarrhoea can result in fluid and electrolyte losses, which may lead to dehydration, electrolyte imbalance and renal insufficiency (Melosky 2012).

A crucial challenge associated with management of toxicity is differentiating between side effects that may correlate with treatment response versus those that do not correlate with treatment response (Liu and Kurzrock 2014). In order to maximise the beneficial effects, the former would require management of the toxicity rather than dose reduction, while the latter might optimally be managed by dose reduction, though supportive/supplemental care to ameliorate toxicities should always be considered (Liu and Kurzrock 2014).

Currently, management of ErbB1 TKI-induced diarrhoea is very similar to management of chemotherapy-induced diarrhoea. The key to managing ErbB1 TKI-induced diarrhoea is to educate patients about this adverse event before treatment starts. Patients should be monitored weekly for the first 4 weeks of treatment, which is the period during which diarrhoea will most likely occur (Hirsh, Blais et al. 2014). Non-pharmacologic management strategies include dietary changes, supplemental hydration and electrolyte replenishment. Pharmacologic management of ErbB1 TKI-induced diarrhoea is largely limited to loperamide, with the dose based on the grade of diarrhoea experienced by the patient (Hirsh, Blais et al. 2014).

Loperamide, a synthetic oral opioid drug, works by a number of different mechanisms of action that decrease peristalsis and fluid secretion, resulting in longer gastrointestinal transit time and increased absorption of fluids and electrolytes from the gastrointestinal tract (Baker 2006). Alternatives to loperamide are also available for managing diarrhoea, however their use and effectiveness can differ by geographic location and the diarrhoea severity. Some of these include diphenoxylate–atropine and codeine, either of which can be used with loperamide (Hirsh, Blais et al. 2014). Dose reductions are not recommended for grade 1 diarrhoea. At grade 2, if the patient does not respond to loperamide after 48 hours, it is recommended the ErbB1 TKI is temporarily discontinued until the diarrhoea returns to grade 1, at which time the ErbB1 TKI is resumed, often at a lower dose (Hirsh, Blais et al. 2014). It is recommended that the ErbB1 TKI should be permanently discontinued if diarrhoea does not reach grade 1 within 14 days despite best supportive care and withholding of the ErbB1 TKI (Hirsh, Blais et al. 2014). Patients presenting with grade 3 - 4 diarrhoea should be admitted to hospital for the administration of intravenous fluids and electrolyte replacement. Early management of ErbB1 TKI-induced diarrhoea can lower the incidence of high-grade

events that could lead to hospitalisation and drug discontinuation and most importantly can improve quality of life of the patients (Hirsh, Blais et al. 2014).

It is also known that targeted therapies are rarely administered as a monotherapy and normally combined with chemotherapy or radiation therapy. Thus, management of diarrhoea induced by targeted therapy in combination with other cancer therapies becomes more complex. Most of the guidelines on management of cancer therapy-induced diarrhoea are meant for the management of chemotherapy-induced diarrhoea. Loperamide and octreotide are recommended in the treatment guidelines for the management of chemotherapy-induced diarrhoea. Management of lapatinib-paclitaxel combination-induced diarrhoea following the treatment guidelines by the American Society of Clinical Oncology (ASCO) (Benson, Ajani et al. 2004) has been found to decrease the frequency and severity of gastrointestinal complications (Crown, Burris et al. 2008). Thus far, there have been no developed guidelines on the specific management of diarrhoea induced by targeted therapy in combination with other cancer therapies. This is due to limited investigations on the mechanism of action of molecular targeted drugs.

1.6 Role of ErbB1 in diarrhoea mechanisms

One of the vital functions of ErbB1 is in the regulation of Cl^- secretion and Na^+ absorption by colonocytes (McCole, Rogler et al. 2005, McCole and Barrett 2009). The regulation is critical in maintaining normal gut homeostasis. The secretion of water (H_2O) across the intestinal epithelial cells is a passive process driven by the active secretion of Cl^- ions (Barrett and Keely 2000) while Na^+ may be absorbed both passively and actively (Sherwood 2007). When the electrochemical gradient favours movement of Na^+ from the lumen to the blood, passive diffusion of Na^+ can occur between the intestinal epithelial cells

(intercellular) through the 'leaky' tight junctions into the interstitial fluid while movement of Na^+ through the cells (transcellular) is energy-dependent (Sherwood 2007).

The sodium/potassium adenosine triphosphatase (Na^+/K^+-ATPase), also known as the sodium-potassium pump (Na^+/K^+ pump), is critical for active transepithelial transport. The Na^+/K^+-ATPase catalyses the efflux of three Na^+ ions from the cell and the uptake of two K^+ ions at the expense of hydrolysing one ATP molecule per cycle (Montrose MH 2003). Because more cations are pumped out than are replaced, the Na^+ pump is electrogenic and generates a negative intracellular electrical potential (Montrose MH 2003).

Na^+/K^+-ATPase is localized basolaterally and is expressed in all intestinal epithelial cells. It acts to maintain a low intracellular Na^+ concentration and a high intracellular K^+ concentration. The Na^+ electrochemical gradient is then used as a driving force for Na^+ influx through Na^+ channels or through secondary active cotransporters (Montrose MH 2003).

Chloride then passively follows down the electrical gradient created by Na^+ absorption (Sherwood 2007). Most H_2O absorption in the digestive tract depends on the active carrier that pumps Na^+ into the lateral spaces, resulting in a concentrated area of high osmotic pressure in that localised region between the cells. This localised high osmotic pressure provides the driving force for passive water absorption. Meanwhile, more Na^+ is pumped into the lateral space to encourage more H_2O absorption (Sherwood 2007).

Excessive secretion of Cl^- into the intestinal lumen could result in the osmotic movement of water into the lumen, resulting in diarrhoea (Montrose MH 2003, Gibson and Keefe 2006). This theory could be applied to altered ErbB1 signalling, as one of the vital functions of ErbB1 is in the regulation of Cl^- secretion; thus inference with ErbB1 signalling might affect the downstream pathways and channels, leading to excess chloride secretion which may lead to diarrhoea.

Chloride secretion from the apical membrane of intestinal epithelial cells is normally stimulated by hormones, neurotransmitters and immune cell mediators which act on specific basolateral membrane receptors on the surface of epithelial cells to increase intracellular levels of second messengers (Keely and Barrett 2000, Keely and Barrett 2003). The second messengers that are involved in initiating Cl^- secretion are cyclic adenosine 5'-monophosphate (cAMP) and calcium (Ca^{2+}) (Keely and Barrett 2003). Elevation of intracellular levels of second messengers promotes Cl^- and consequently fluid secretion (Keely, Calandrella et al. 2000). While fluid secretion is important in normal intestinal physiology, pathological conditions such as inflammatory bowel disease are characterised by increased neuroimmune mediator release which may give rise to excessive Cl^- and fluid secretion, resulting in the onset of secretory diarrhoea (Montrose MH 2003).

As described above, cAMP and Ca^{2+} initiate the Cl^- secretory mechanism in intestinal epithelial cells. Secretion can be stimulated via increases of either cAMP or cytosolic Ca^{2+}. Chloride is taken up into the cell across the basolateral membrane via a cotransporter directed by Na^+ concentration gradient established by the basolateral Na^+/K^+ ATPase (secondary active Cl^- transport). Then Cl^- is transported across the apical membrane either via the cAMP-dependent cystic fibrosis transmembrane conductance regulator (CFTR) Cl^- channel or Ca^{2+} activated Cl^- channel. Substances that are capable of stimulating Cl^- secretory response are also known as Cl^- secretagogues. The regulation of Cl^- secretory response is also controlled by Cl^- secretory inhibitors. A list of Cl^- secretagogues and inhibitors are summarized in Tables 1.5 and 1.6. ErbB1 as well as its ligands (EGF, TGF-α, heregulin) are examples of Cl^- inhibitors. The mechanism of inhibition is thought to be via the Ca^{2+} -dependent Cl^- secretion (Uribe, Gelbmann et al. 1996, Barrett and Keely 2000). It has been shown that carbachol, which is an acetylcholine analogue, acts as both Cl^- secretagogue and inhibitor (Table 1.5 and 1.6). This will be explained further in the next paragraph.

Table 1.5. Chloride secretagogues (Barrett and Keely 2000, Wapnir and Teichberg 2002, Christofi, Wunderlich et al. 2004, Marchelletta, Gareau et al. 2013).

Chloride secretagogues	*Mechanism of action*
Neurotransmitters	
Vasoactive intestinal polypeptides	cAMP-dependent Cl^- secretion
Acetylcholine e.g. Carbachol	Ca^{2+}-dependent Cl^- secretion
Substance P	cAMP-dependent Cl^- secretion
Immune mediators	
Histamine	cAMP-dependent Cl^- secretion
Reactive oxygen species (ROS)	cAMP-dependent Cl^- secretion
Platelet activating factor	cAMP-dependent Cl^- secretion
Lipoxygenase metabolites of arachidonic acid	cAMP-dependent Cl^- secretion
Cytokines e.g. Interleukin-11	cAMP-dependent Cl^- secretion
Endocrine mediators	
Digestive hormones e.g. Uroguanylin	cGMP-dependent Cl^- secretion
Paracrine mediators	
Prostanoids	Ca^{2+}-dependent Cl^- secretion
5-hydroxytryptamine (5-HT)	Ca^{2+}-dependent Cl^- secretion
Exogenous agents	
Bacteria & bacterial toxins *e.g. V. cholerae, E. coli*	cAMP-dependent Cl^- secretion
C. difficile	Ca^{2+}-dependent Cl^- secretion
S. typhimurium	Modulates colonic ion transport
Bile acids	Ca^{2+} dependent Cl^- secretion
Nucleotide	
Adenosine triphosphate (ATP)	Ca^{2+} dependent Cl^- secretion

cAMP: cyclic adenosine monophosphate, cGMP: cyclic guanosine monophosphate,
V. cholerae : *Vibrio cholerae, E. coli* : *Escherichia coli* ,
C. difficile : *Clostridium difficile* , *S. typhimurium* : *Salmonella typhimurium* ,
Cl^-: chloride, Ca^{2+}: calcium

Table 1.6. Chloride inhibitors (Breen, Mannon et al. 1998, Barrett and Keely 2000).

Chloride inhibitors	*Mechanism of inhibition*
Acetylcholine e.g. Carbachol	Ca^{2+}-dependent Cl^- secretion
Neuropeptides Somatostatin	cAMP-dependent Cl^- secretion
Peptides e.g. 1. Neuropeptide Y 2. Peptide YY	cAMP- and Ca^{2+}-dependent Cl^- secretion Vasopressin-dependent Cl^- secretion
Growth factors ErbB ligands e.g. EGF, TGF-α, heregulin	Ca^{2+}-dependent Cl^- secretion
Insulin	Ca^{2+}-dependent Cl^- secretion
Insulin-like growth factors	Ca^{2+}-dependent Cl^- secretion

Cl^-: chloride, Ca^{2+}: calcium, cAMP: cyclic adenosine monophosphate,
EGF: epidermal growth factor, TGF-α: transforming growth factor-α

Chloride secretory responses may be limited in order to prevent excessive fluid loss from the body which results from secretory diarrhoea (Keely, Calandrella et al. 2000). ErbB1 has been shown in previous studies to be involved in the regulation of epithelial Cl^- secretion (Uribe, Gelbmann et al. 1996, McCole, Keely et al. 2002, McCole, Rogler et al. 2005, McCole and Barrett 2009). Not only via activation of ErbB1 by its ligand that exerts a direct inhibitory effect on Ca^{2+}-dependent Cl^- secretion, but by ErbB1 itself also participating in mediating the secretory processes activated by a variety of Cl^- secretagogues that act via G-protein coupled receptors (GPCR) (Bertelsen, Barrett et al. 2004).

ErbB1 is involved in carbachol activated Ca^{2+}-dependent Cl^- secretion. Carbachol, a Ca^{2+}-dependent Cl^- secretagogue, binds to a muscarinic GPCR to stimulate Ca^{2+} dependent signals that initially activate Cl^- secretion. This leads to an increase in intracellular K^+ concentration and a decrease in intracellular Na^+ which establishes a concentration gradient

for passive movement of Na^+ from the lumen into the intestinal cell. Sodium is then extruded to the interstitial fluid by the basolateral Na^+/K^+ pump (Barrett and Keely 2000). Sodium continues to diffuse down a concentration gradient from its high concentration in the interstitial fluid into the capillary. Chloride, which always passively follows Na^+ down the electrical gradient established by Na^+ movement, further leads to salt retention that osmotically promotes H_2O retention encouraging more H_2O absorption (Chow, Uribe et al. 2000).

However, there are subsequent signals which show that carbachol transactivates ErbB1, through the soluble tyrosine kinases Pyk2 and Src, and also the release of TGF-α (ErbB1 ligand) from the epithelial cells. The effect of these subsequent signalling events, which involve the formation of ErbB1 homodimers, limits Cl^- secretion (McCole, Keely et al. 2002), showing that Cl^- secretory response to carbachol which is mediated by an increase in intracellular Ca^{2+} is transient in nature (McCole, Keely et al. 2002). This finding which shows that carbachol acts as both Cl^- secretagogue and inhibitor also shows the ability of ErbB1 to recruit the MAPK/ERK to inhibit an apical Ca^{2+} activated Cl^- channel (Uribe, Gelbmann et al. 1996, Barrett and Keely 2000).

On the other hand, besides TGF-α, EGF, (another ligand of ErbB1), can also act to inhibit Cl^- secretion (Uribe, Gelbmann et al. 1996). However, the signalling pathways and targets that underlie the effect of EGF on Cl^- secretion are apparently distinct from TGF-α. Binding of EGF to ErbB1 involves the formation of heterodimers of ErbB1/ErbB2 which appears to signal via a PI3K/AKT pathway, to recruit downstream effectors including protein kinase C-ε (PKC-ε) that inhibit Cl^- secretion by reducing the activity of a basolateral Ca^{2+}-activated K^+ channel (Keely and Barrett 1999). This process is summarised in Figure 1.4.

Figure 1.4. Regulation of Cl- secretion in intestinal epithelial (McCole and Barrett 2009).

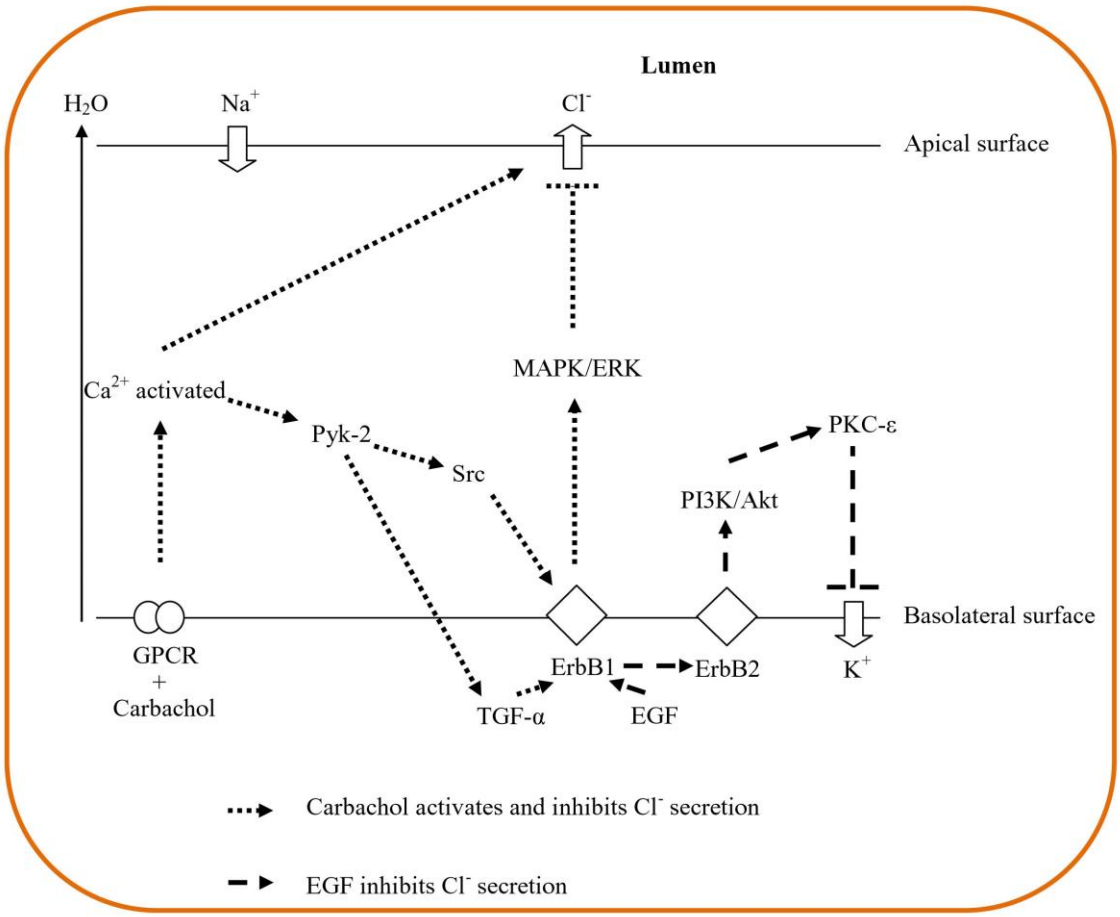

Very few studies have been carried out to investigate mechanisms of ErbB1 inhibitor–induced diarrhoea. When ErbB1 is inhibited, the normal function of ErbB1 is disrupted and this may lead to excessive secretion of chloride into the intestinal lumen which consequently causes diarrhoea. This might be the answer to why ErbB1 inhibitors cause gastrointestinal toxicities. However, histopathological findings on the effect of ErbB1 inhibitors on gastrointestinal epithelial cells are also limited, and are conducted solely in animal models. In a study on ErbB1 single TKI-induced diarrhoea, mice administered with gefinib showed gastrointestinal damage with significant reduced in small intestinal and colon weight as well as significant epithelial atrophy of the duodenum due to inhibited intestinal homeostasis and healing (Hare, Hartmann et al. 2007). Another study on ErbB1 single TKI-induced diarrhoea, involved mice administered with erlotinib via intraperitoneal injection and showed reduced

small intestinal and colon weight as well as reduced villus height of jejunum and ileum, which was worsened when given in combination with cisplatin (Rasmussen, Viby et al. 2010). In a study on ErbB1 multitarget TKI-induced diarrhoea, mice administered with canertinib had decreased jejunal villus height and small intestinal wet weight (Yusta, Holland et al. 2009). In an earlier study, canertinib was found to induce duodenal injury in Apc^{Min} mice genetic model of intestinal tumourigenesis but no significant inhibition of intestinal adenoma was observed (Ritland, Gendler et al. 2000). In an ErbB1 dual target TKI-induced diarrhoea model, lapatinib-administered rats showed no macroscopic or microscopic tissue injury seen within the jejunum or colon (Bowen 2014, Bowen, Mayo et al. 2014). This study also does not support lapatinib altering chloride secretion, as blood biochemical analysis found that lapatinib had no significant effect on serum chloride (Bowen, Mayo et al. 2014). As such, the role of chloride secretion, or other ion transport mechanisms in lapatinib-induced diarrhoea (or diarrhoea induced by other ErbB1 TKIs), is still unclear. Thus, further studies are required to explore its mechanism of action in detail.

1.7 Other factors of ErbB1 inhibitor-induced diarrhoea

There are also other factors that may oppose the theory of ErbB1 inhibitor-induced diarrhoea. Studies using ErbB1 knockout mice and other ErbB1 TKIs have described mucosal atrophy supporting a role for direct mucosal damage (Roberts, Arteaga et al. 2004, Hare, Hartmann et al. 2007). Another potential avenue is accumulation of unabsorbed drug in the lumen due to its low bioavailability, thus may lead to mucus secretion and therefore result in the osmotic movement of water into the lumen, resulting in diarrhoea (Stringer, Gibson et al. 2009).

1.8 Conclusion

Novel agents such as ErbB1 inhibitors are revolutionising the treatment of cancer. However, gastrointestinal adverse effects such as diarrhoea are associated with this type of drug. These effects must be considered with caution as they can lead to poor compliance, reduced dose and even discontinuation of treatment leading to compromised cancer control. Investigations are warranted to determine the precise pathophysiologic mechanisms of this side effect to improve efficacy and tolerance of treatment. Knowledge of the mechanisms may also lead to a better drug dosage in the individual patient and contribute to reducing the cost of cancer treatment therapy. Therefore, it is important that a better understanding of the effects of ErbB1inhibitors on gastrointestinal toxicity in cancer therapy is achieved.

1.9 Research question, hypothesis and aims of study

Targeted cancer therapy remains a mainstream treatment for patients with advanced malignant tumours, but the success of this cancer therapy is often limited by the occurrence of side effects particularly diarrhoea. Lapatinib, a molecular targeted agent, is a dual inhibitor of ErbB1 and ErbB2 that has a proven activity in ErbB2-positive metastatic breast cancer. It has an *in vitro* and *in vivo* activity as a single agent or as part of combination regiment. Despite its efficacies in the treatment of breast cancer, diarrhoea remains a major problem with the clinical use of lapatinib. The mechanism of how lapatinib induces diarrhoea is still unknown. More importantly, a model that could reflect a patient setting is required. Development of an animal tumour model will enable the investigations on the underlying mechanisms as patients receiving lapatinib will have tumours. Furthermore, preliminary study has been conducted in non-tumour animal model, thus further clarification is required to improve understanding.

Thus, this study aims to answer the following research question:

> What is the underlying mechanism of diarrhoea pertaining to the use of lapatinib as an anticancer therapy?

This research question is supported by the following hypothesis:

Lapatinib-induced diarrhoea is due to an inhibition of ErbB1 activity in enterocytes leading to increased chloride secretion.

In order to answer the question and support the hypothesis above, this research has the following specific aims and objectives:

1. To determine the inhibitory concentration 50% (IC_{50}) of lapatinib on rat tumour and intestinal cell lines.

2. To identify the candidate markers which are involved in inhibitory effects of lapatinib on rat tumour and intestinal cell lines.

3. To develop a tumour-bearing rat model to study lapatinib-induced diarrhoea.

4. To develop lapatinib-induced diarrhoea in the tumour rat model to best reflect a patient setting.

5. To examine the underlying mechanism of diarrhoea in relation to the use of lapatinib *in vivo*.

6. To assess the permeability changes in colonic epithelial monolayer pertaining to the use of lapatinib as an anticancer therapy.

Chapter 2

General methods

2.1 Cell lines, chemicals and reagents

The Walker 256 (rat breast carcinoma) cell line was obtained from the Cell Resource Centre for Medical Research at Tohoku University, Japan. The IEC-6 (rat small intestinal) cell line was obtained from the American Type Culture Collection (ATCC), USA. Walker 256 cells are derived from female Wistar rat breast carcinoma while IEC-6 cells are derived from adult rat jejunum. The T84 (human colon carcinoma) cell line was obtained from the European Collection of Cell Cultures (ECACC), UK, and is derived from a lung metastasis of colon carcinoma in a 72 year old male. Assays using these cell lines were carried out between passages 2 and 10. All of the cell lines had tested negative for mycoplasma contamination by Dr Nicholas Eyre from Hepatitis C Virus Research Laboratory, School of Molecular and Biomedical Science, University of Adelaide, Australia.

The growth media: RPMI-1640 and Dulbecco's Modified Eagle's Medium (DMEM), 1x phosphate buffered saline (PBS), L-glutamine, penicillin-gentamicin with fungizone and trypsin were supplied by Gibco®, Australia. DMEM/Nutrient F-12 Ham, dimethyl sulfoxide (DMSO), ethylenediaminetetraacetic acid (EDTA) solution and 0.4% trypan blue were purchased from Sigma Aldrich, Australia. Foetal bovine serum (FBS) was purchased from Bovogen Pty Ltd, VIC, Australia.

The 2,3-bis-(2-methoxy-4-nitro-5-sulfophenyl)-2H-tetrazolium-5-carboxanilide (XTT) kit, which consists of the XTT labelling reagent and the electron-coupling reagent, was obtained from Roche Diagnostics GmbH, Germany.

In cell culture studies, lapatinib powder was supplied by GlaxoSmithKline (GSK, Australia). Lapatinib powder was dissolved in 100% DMSO to 10 mM (Rusnak, Alligood et al. 2007). The drug solution was then diluted with serum-free medium for cell culture assays (Zhou, Li et al. 2006).

In animal studies, lapatinib 250 mg/tablet (Tykerb®, Glaxo Smith-Kline) was supplied by the Royal Adelaide Hospital pharmacy. Prior to usage, lapatinib tablets were crushed and dissolved in normal saline to a final concentration of 100 mg/ml.

2.2 Cell culture

Walker 256 cells were grown in RPMI-1640 supplemented with 10% foetal bovine serum and 1% penicillin-gentamicin with fungizone. IEC-6 and T84 cells were grown in DMEM and DMEM/ Nutrient F-12 Ham, respectively, supplemented with 10% FBS, 1% penicillin-gentamicin with fungizone and 2mM L-glutamine. All of the cells were cultured using 75 cm^2 flasks in a 37^oC incubator with 5% CO_2.

In order to subculture, the cells were divided and the culture medium replaced with fresh medium as follows; first, the old medium was removed, and then the cells were rinsed briefly with PBS. Walker 256 cells were subcultured with 2 ml of 0.02% EDTA in PBS while IEC-6 and T84 were subcultured with 2-3 ml of 0.01% trypsin in PBS. Flasks were incubated at 37^oC and 5% CO_2 for 3-5 minutes. After the cells had detached from the lower surface of the flask, 20 ml of medium was added to the flask (to stop the enzymatic digestion) and the culture was divided in two parts. One part was then transferred to a new flask.

2.3 XTT cell proliferation assay

Cells were harvested and the number of viable cells were counted with a haemacytometer to prepare a cell suspension. One hundred microliters of suspension

containing $5x10^3$ cells for Walker 256 and IEC-6 and $1x10^4$ cells for T84, respectively, were seeded in each well of a 96-well microtiter flat-bottom plate (Becton Dickinson, USA). The plate was then incubated for 24 hours at 37ºC with 5% CO_2.

Lapatinib stock 10 mM (refer to Section 2.1) was diluted with serum-free medium to a concentration series (1-10 µM). After 24 hours incubation, the old medium was replaced and the cells were treated with lapatinib at the dose of 1-10 µM and incubated at 37ºC with CO_2 for 48 hour. An equivalent serial dilution of DMSO was used as control treatment (Mosesson and Yarden 2004). After the incubation period, the old media was replaced with 100 µl fresh media and 50 µl of XTT solution (composed of 5 ml XTT labelling reagent and 100 µl of electron coupling), was added to each well. The microtiter plate was then incubated again for 6 hours at 37ºC with 5% CO_2. Then, the cell viability was measured using an ELISA reader (Bio-Rad 550, USA) at 490 nm. This assay is based on the cleavage of the tetrazolium salt XTT in the presence of an electron-coupling reagent, producing a soluble formazan salt. This conversion only occurs in viable cells. Inhibition of cell proliferation was calculated as follow:

$$\text{Cell viability (\%)} = \frac{\text{Absorbance490 value of sample}}{\text{Absorbance490 value of control}} \times 100$$

A graph of percentage of cell viability versus concentration of lapatinib was then plotted and the IC_{50} (a dose that inhibited 50% cell growth) was determined from the graph.

2.4 RNA isolation

2.4.1 Cell lines

Cell lines were subcultured into a sterile tissue culture dish plate (Becton Dickinson, USA) in a final volume of 10 ml culture medium per well that contained $5x10^4$ cells/ml and was incubated for 24 hours at 37ºC with 5% CO_2. The cells were then treated with lapatinib

at a dose that inhibited 50% cell growth (IC_{50}). Cultures were maintained at 37ºC with CO_2 for 6, 24 and 48 hours. After the incubation period, the cells were dislodged using the subculture procedure above and spun at 250xg for 5 minutes. The supernatant was discarded and 500 µl of TRIzol® reagent (Invitrogen Life Technologies, Australia) was added to the cell pellet. The cell pellet was resuspended using a pipette and vortexed and incubated for 5 minutes at room temperature. Samples were left at room temperature for 5 minutes before adding 100 µl chloroform (Sigma, Australia). Then, samples were resuspended using a pipette and vortexed for 15 seconds before sitting at room temperature for 3 minutes. Samples were centrifuged at 13, 350xg for 15 minutes at 4ºC to separate aqueous and solvent phases subsequently. The upper, aqueous phase was collected and placed into a new tube. Three hundred microliters of 70% ethanol was added to change binding conditions of the RNA so as to be purified through a silica gel membrane (Macherey-Nagel GmbH & Co., Germany) which results in enriched mRNA. The following procedure was then carried out as per manufacturer's protocol (Macherey-Nagel GmbH & Co., Germany).

The highly pure RNA was eluted with 40 µl RNAse-free sterile water (Qiagen, Australia) and the concentration was quantified by measuring the absorbance at 260 nm (A_{260}) and 280 nm (A_{280}) on a nanodrop spectrophotometer (Nano Drop Technologies Inc, Wilmington, DE, USA). Concentration of RNA was determined by the following formula (assuming that an optical density reading of 1.0 represents 40 µg/ml of RNA):

A_{260} x 40 x 20 = RNA ng/µL;

The quality of RNA was also checked by A_{260}/A_{280} ratio of samples.

2.4.2 Animal tissues

The rat stomach and tumours from the animal study (described in detail in Chapter 4) were freshly stored in RNAlater (Ambion®, Life technologies, Australia) and were cut into 1-2

mm^2 pieces and homogenized (TissueLyser LT, Qiagen, Australia) in 500 µl of TRIzol® reagent (Invitrogen Life Technologies, Australia) at 50 Hz for 2 minutes. The supernatant was then transferred into a 1.5 ml tube before adding 100 µl chloroform, followed by the same protocols as described above for the cell line.

2.5 Reverse transcription

Total RNA was quantified for yield and integrity using the nanodrop spectrophotometer. Up to 1 µg of total RNA was reverse-transcribed to generate cDNA using the iScript cDNA Synthesis Kit (Bio-Rad, Hercules, CA, USA). For each reaction (up to 1 µg of RNA), iScript reaction mix, iScript reverse transcriptase was added and reaction volume was made up to 20 µl using nuclease-free water (Biorad, USA) according to the manufacturer's instructions. Samples were incubated for 5 minutes at 25ºC, 30 minutes at 42ºC and 5 minutes at 85ºC. Total cDNA concentration was measured using the nanodrop program and samples were diluted to100 ng/µl with nuclease-free water.

2.6 Primer design

Oligonucleotide primers for *ErbB1* were obtained from previous study (Nasrollahzadeh, Siassi et al. 2008) and have been tested for stability, primer dimers and cross priming using the Net Primer program (PREMIER Biosoft International). Oligonucleotide primers for *ErbB2* were designed using the published sequences (as listed in Entrez Nucleotide) for rat. The sequences were inserted into the PRIMER 3 primer design program version 0.4.0 (Untergasser, Cutcutache et al. 2012) to identify possible primer pairs. This program listed the best 8 pairs and stated the product length, difference in melting temperature, and priming position in the sequence for each. Theoretical primer pairs were checked for stability, primer dimers and cross priming using the Net Primer program. Two housekeeping genes were used

which are *Ubiquitin C* (*UBC*) and *β2 microglobulin* (*B2M*). The oligonucleotide primers for the housekeeping genes were obtained from previous study (Al-Dasooqi, Bowen et al. 2011). All of the primers were synthesized by GeneWorks (Adelaide, SA) and resuspended with sterile H_2O to a working concentration of 50 nmol/ml. A list of primer pairs is shown in Table 2.1.

Table 2.1. Primer sequences used in Real-time Polymerase Chain Reaction analysis.

Gene	Nucleotide sequence (5'-3')	Nucleotide position	Amplicon length (bp)	Tm (°C)	NCBI accession no.
ErbB1	F:CCCACAGCAAGGCTTCTTCA	3181-3301	119	61; 61	NM_031507.1
	R:CACGGCAGCTCCCATTTCTA				
ErbB2	F:AACCTTTCCTTGCTGCTTGA	4021-4201	212	57; 57	NM_017003.2
	R:GTTCCCTCCAGACCTCTTCC				
UBC	F:TCGTACCTTTCTCACCACAGTATCTAG	2406-2487	82	58; 56	NM_017314.1
	R:GAAAACTAAGACACCTCCCCATCA				
B2M	F:CGAGACCGATGTATATGCTTGC	286-399	114	55; 55	NM_012512.1
	R:GTCCAGATGATTCAGAGCTCCA				

2.7 Real-time Polymerase Chain Reaction (PCR)

Real-time PCR amplification of cDNA was performed using the QuantiTect SYBR Green Mastermix (Qiagen, Australia) and the gene was amplified using the Rotor-Gene Q Series Rotary Cycler (Qiagen, Australia). Amplification mixes contained 1 µl of cDNA sample, 5 µl of fluorescent dye QuantiTect SYBR green (Qiagen, Australia), 3 µl of nuclease-free water (Bio-Rad, USA) and 0.5 µl of each forward and reverse primers which had been

pre-diluted as mentioned in the previous section, to makeup a final volume of 10 µl. Thermal cycling conditions for all primers included denaturation step at 95ºC for 15 minutes, and then 45 cycles of denaturation at 95ºC for 10 seconds, annealing at 54ºC for 15 seconds and extension at 72ºC for 20 seconds. Amplification was followed by melt curve analysis to confirm product specificity.

2.8 Calculation of relative expression of genes

All samples were run in triplicate. Two different methods were used to calculate the relative expression of genes. For the cell culture study (Chapter 3), Delta CT ($2^{-\Delta Ct}$) method was used to acquire the fold change in *ErbB1* and *ErbB2* mRNA expressions. The experimental threshold (Ct) values were calculated manually by converting the Ct values into relative quantities relative to 2 housekeeping genes which are *UBC* and *B2M*.

For the animal tumour tissues (Chapter 4), Ct values were calculated by the Rotor-Gene Q Series program. The delta-delta Ct ($2^{-\Delta\Delta Ct}$) was used to calculate relative quantities relative to rat stomach as a control calibrator over the time course and data was normalized by the 2 housekeeping genes (*UBC* and *B2M*).

2.9 Preparation of tumour inoculum

Walker 256 cells were cultured as described in the previous section. Culture flasks of 75 cm^2 were checked every day and once the confluence reached >90%, the cells were passaged with the addition of 2.0 ml of 0.02% EDTA in PBS to the culture and left for 2-3 minutes. The reaction was stopped by adding serum-containing growth medium. The cells were spun down at 250xg for 5 minutes to form a pellet and then resuspended in a serum-free medium. The number of cells were calculated by using a haemocytometer and then diluted to the required concentration.

2.10 Histological examination

This method was carried out to determine the histopathological changes in the animal tissues. Briefly, sections of the animal tissues such as tumour, jejunum and colon were collected, weighed and fixed in 10% neutral buffered formalin. Fixed tissues were processed in a tissue processor and embedded in paraffin wax. Four µm thick tissue sections were cut using a Rotary Microtome Micron 8N325 and mounted onto silane-coated slides, dewaxed in xylene (HDS Scientific, South Australia) (SA) (3x5 minutes) and rehydrated through a graded series of ethanol (100% 3x1 minutes, 10x quick dips in 90%, 70%, 50%). Slides were then rinsed in water prior to staining with Lillie-Mayer's haematoxylin (Fronine Laboratory Supplies, Australia) for 10 minutes. Slides were then briefly dipped in 1% acid alcohol (10 ml hydrochloric acid, 1 L 70% ethanol) and rinsed in running tap water. Next, the slides were blued in Scott's tap water (10 g magnesium sulphate, 1 g sodium hydrogen carbonate, 500 ml distilled water) for 2 minutes and counterstained in eosin (HDS Scientific, SA) for 3 minutes. After that, slides were rinsed again under running tap water prior to dehydration in ethanol (90%, 100%) for 30 seconds to 1 minute, clearing in xylene (3x5 minutes) and mounting with DPX (Sigma, Australia). Slides were examined using a light microscope (Olympus BX51, USA) prior to digital analysis using NDPview version 1.2.25 (NanoZoomer Digital Pathology, Hamamatsu, Japan) and confirmed by expertise in the Mucositis Research Group and by a professional veterinary pathologist, Professor John Finnie, at the Institute of Medical and Veterinary Sciences (IMVS, Adelaide, Australia).

2.11 Measurement of villus height and crypt depth in jejunum and colon

From the histological images, villus height and crypt depth in jejunum and colon were measured by using NDPview software version 1.2.25 (NanoZoomer Digital Pathology, Hamamatsu, Japan) to determine any histopathological changes in jejunum and colon. Fifteen

jejunal villi with their crypts and fifteen colonic crypts were selected in even randomisation on each sectional area for each sample. Measurements were carried out at 5-10x magnification. All measurements were done blinded to treatment.

2.12 Immunohistochemistry staining for caspase-3 and Ki-67

This method is commonly used to demonstrate the presence and location of specific proteins in tissue sections using antibodies that recognize target proteins and has been established by the Mucositis Research Group (Bowen, Gibson et al. 2005, Bowen, Mayo et al. 2014). Paraffin wax embedded tissue samples were cut into 4 µm sections and carefully placed on coated glass slides (FLEX IHC Microscope Slides, Dako, Australia) and left to dry on a hot plate set to 60^{o}C. Slides were dewaxed in xylene (3x5 minutes) and rehydrated through decreasing concentrations of ethanol (100% 3x1 minute, 1x1 minute in 90%, 70%, 50%). Slides were then briefly rinsed in running tap water followed by 1x PBS. This was then followed by antigen retrieval. Slides were placed in 10 nM sodium citrate buffer (pH 6.0) and heated on 'high' in a pressure cooker (Breville) for 3 minutes. Then, the sections were allowed to cool at room temperature for 20 minutes prior to rinsing in PBS. Endogenous peroxidase was blocked with 3% H_2O_2 in methanol for 10 minutes followed with rinsing in PBS. Non-specific binding was blocked by incubating slides in 20% normal goat serum (NGS) (Sigma, USA) in PBS for 20 minutes at room temperature. Endogenous avidin and biotin was blocked using the Avidin-Biotin Blocking Kit (Vector Laboratories, Burlingame, CA), 15 minutes each. Following washing in PBS, sections were then incubated overnight for 16 hours with a rabbit primary antibody (Ki-67 or caspase-3) (Abcam, UK) diluted in 5% NGS (1:100) at 4^{o}C in a humidified chamber.

Slides were washed in PBS (3x) following incubation with primary antibody and were incubated with biotinylated anti-rabbit IgG secondary antibody (Vector Laboratories,

Burlingame, CA) diluted in 5% NGS (1:200) and for 30 minutes at room temperature. Then, horse radish peroxidase (HRP) enzyme (available as a Vectastain ABC kit (Vector Laboratories, Burlingame, CA)) was applied to the sections and incubated for 30 minutes at room temperature. Slides were rinsed in PBS prior to the application of 3,3'-diaminobenzidine (DAB) solution (Sigma, USA) for antibody visualisation. Sections were carefully watched at this step as a brown precipitate appears on positive control tissues. Slides were then rinsed in running tap water. Nuclei were counterstained with Lillie Mayer's Haematoxylin for 2 minutes and rinsed through running tap water prior to a quick dip in 1% acid alcohol. Then, slides were rinsed and blued in Scott's tap water for 2 minutes and immediately rinsed again under running tap water prior to dehydration with ethanol (50%, 70%, 90%, 100% 3x) and cleared with xylene (3x5 minutes). Sections were coverslipped using DPX mounting medium. Slides were examined using a light microscope prior to digital analysis using the NanoZoomer and confirmed by experts in the Mucositis Research Group.

Using the NDPview version 1.2.25, caspase-3 staining for jejunum and colon were assessed by counting positive cells in 15 fields (20x magnification) and calculating the mean number of positive cells/crypt for each sample. For tumours, caspase-3 positively stained cells were counted in a 0.1 mm^2 area in 10 fields (20x magnification) and the mean number of positive cells/0.1 mm^2 area were calculated. Ki-67 staining was assessed by counting stained cells/20 half crypts (40x magnification) and calculating the mean number of positive cells/half crypt. Results were presented as percentage of stained cells/half crypt. For tumours, Ki-67 positively stained cells were counted in 10 fields (40x magnification) and the mean number of positive cells/field were calculated. Results were presented as the percentage of positive cells/field. All assessments were done blinded to treatment.

2.13 Statistical analysis

Data in this thesis were analysed as mean ± standard error mean (SEM). All analyses were performed using Graph Pad Prism version 6. Statistical significance was accepted as $p<0.05$. Statistical analyses were described in detail in each of the following experimental chapters.

Chapter 3

Cytotoxic effect of lapatinib on rat breast tumour (Walker 256) and rat jejunum (IEC-6) cell lines and assessment of ErbB1 and ErbB2 expression

3.1 Introduction

ErbB1 and ErbB2 play significant roles in ligand-activated signalling pathways that regulate cell proliferation and cell death (Rusnak, Alligood et al. 2007). Numerous tumour cell lines overexpress these receptors and/or display constitutive activation of the pathways (Mosesson and Yarden 2004). Overexpression of ErbB1 has been implicated in the development and progression of head and neck, lung, pancreas, bladder and breast cancer (Salomon, Brandt et al. 1995). High ErbB2 expression correlates with poor prognosis in cancers of the colon, ovary, breast and bladder (Slamon, Godolphin et al. 1989, Salomon, Brandt et al. 1995, Kapitanovic, Radosevic et al. 1997). ErbB2 is the most common heterodimerisation partner of ErbB1 (Graus-Porta, Beerli et al. 1997) in which ErbB2 potentiates ErbB1 signalling via an *in trans* mechanism by enhancing the binding affinity of the ErbB1 ligand, EGF (Karunagaran, Tzahar et al. 1996), reducing its degradation (Worthylake, Opresko et al. 1999), and predisposing the receptor to recycling (Lenferink, Pinkas-Kramarski et al. 1998). It has also been shown that EGF-induced stimulation of ErbB1 leads to activation of ErbB2 by transduction through heterodimerisation (King, Borrello et al. 1988, Wada, Qian et al. 1990). Previous studies have shown that ErbB1-specific inhibitors can reduce ErbB2-signalling and growth of breast cancer cells that express high levels of ErbB2 (Lenferink, Simpson et al. 2000, Moasser, Basso et al. 2001, Moulder, Yakes et al. 2001). It has also been reported that ErbB2 plays an important role in the oncogenic activity of ErbB1. Preclinical experiments have shown that ErbB2 and ErbB1 act synergistically to transform NIH 3T3 rodent fibroblasts (Kokai, Myers et al. 1989). As such,

combined inhibition of both ErbB1 and ErbB2 may be more efficacious than targeting either one of them. Thus, these proteins show potential as targets for anticancer drugs (Mosesson and Yarden 2004).

Lapatinib is an orally administered small molecule dual tyrosine kinase inhibitor (Wadler, Atkins et al.) of ErbB1 and ErbB2 and has been approved for the treatment of metastatic breast cancer patients (Rusnak, Lackey et al. 2001, Geyer, Forster et al. 2006). Structural and biochemical studies have indicated that lapatinib *in vitro* is a potent inhibitor of the tyrosine kinase activity of ErbB1 and ErbB2, by which lapatinib binds to an inactive-like conformation of ErbB1 and has a slow dissociation rate (half-life ≥300 minutes) from its target receptor *in vitro* and *in vivo* (Wood, Truesdale et al. 2004) which may result in prolonged inhibition of tyrosine kinase activity of tumour cells. Lapatinib reversibly inhibits ErbB1 and ErbB2 tyrosine kinases leading to inhibition of Ras/Raf MAPK and PI3K/Akt pathways, leading to an increase in apoptosis and a decrease in cellular proliferation (Spector, Xia et al. 2005, Lackey 2006).

Lapatinib cytotoxic activity has been tested on several cancer cell lines such as gastric, head and neck, lung, epidermal, breast and others and it has been proven that lapatinib inhibits the cancer cell growth at low concentrations within the range of 0.01 to 9.8 μM (Konecny, Pegram et al. 2006, Rusnak, Alligood et al. 2007). The studies also show that the cytotoxic activity of lapatinib on the cancer cell lines was due to overexpression of ErbB1 and/or ErbB2 or varying levels of both ErbB1 and ErbB2 expression (Konecny, Pegram et al. 2006, Rusnak, Alligood et al. 2007). Among all the cancer cell lines tested, lapatinib has been shown to have the highest cytotoxic effect on the breast cancer cell lines (UACC182: 0.01 μM, SUM190: 0.018 μM, BT474: 0.022 μM, SK-BR-3: 0.037 μM, SUM225: 0.083 μM and MDA-MB-453: 3.9 μM) and this correlated to higher ErbB2 expression (108 to1161 ng/mg) (Konecny, Pegram et al. 2006, Rusnak, Alligood et al. 2007). However, there were also

breast cancer cell lines which showed high lapatinib cytotoxic effect (MDA-MB-175: 0.012 µM, EFM-19: 4.6 µM, MCF-7: 7.7 µM and MDA-MB-435: 8.5 µM) but expressed a moderate or low level of both ErbB1 and ErbB2 (2.2 to 20 ng/mg) (Konecny, Pegram et al. 2006, Rusnak, Alligood et al. 2007). There were also breast cancer cell lines with high lapatinib cytotoxic effect (MDA-MB-468: 4.7 µM and BT20: 9.8 µM) that correlated with higher ErbB1 expression (295 to 908 ng/mg). Thus, much remains to be learned about molecular mechanisms that determine lapatinib sensitivity in cancer cell lines.

This study is conducted to determine *in vitro* toxicity of lapatinib on tumour and intestinal cell lines which may explain the significant association between lapatinib and gastrointestinal toxicities, particularly diarrhoea (Melosky 2012). Lapatinib is effective on human tumour cell lines, however, no study has been conducted to evaluate the effect of lapatinib on normal intestinal cell lines. As far as the author is concerned, lapatinib also has not yet been tested on any rat cell line including rat breast tumour and intestinal cell lines. Two cell lines, Walker 256 and IEC-6, were used in this study (refer to Chapter 2 Section 2.1). Walker 256 is a rat breast carcinoma syngeneic to Wistar rats and commonly used to induce secondary brain tumours (Lewis, Harford-Wright et al. 2013) and bone metastases (Biesalski, Yilmaz et al. 2012). It has also been used to develop cachectic tumour-bearing rat model to study metabolic changes characteristic of cancer cachexia (de Lima, Lima et al. 2005, Rebeca, Bracht et al. 2008). Thus, using Walker 256 cell line might be able to best develop a tumour-bearing Wistar rat model to best reflect a clinical cancer patient setting in the following study (Chapter 4). The other rationale is that lapatinib is known to be effective in inhibiting breast cancer metastasis; hence Walker 256 breast tumour cell line was used in this study. While inhibiting cancer metastasis, at the same time, lapatinib also has a significant effect on the gastrointestinal tract; thus IEC-6 was also used in this study. IEC-6 is a non-transformed intestinal cell line derived from rat jejunal crypt cells (Mannon and Mele

2000). It is a homogeneous population of epithelial-like cells commonly used as a model to elucidate the mechanism of intestinal epithelial cell differentiation, growth and wound healing (Wood, Zhao et al. 2003). Use of these cell lines allows for further investigation of the underlying mechanisms on lapatinib efficacy on breast cancer cells, as well as its toxicity on the normal intestinal cells.

In this study, the cytotoxic effect of lapatinib on Walker 256 and IEC-6 was evaluated and the mechanism of cell death induced by lapatinib was determined using fluorescence activated cell sorting (FACS) analysis. The relative expression of ErbB1 and ErbB2 was also assessed using real-time polymerase chain reaction (Real-time PCR), western blot and immunofluorescence staining. The outcomes were used to evaluate the relationship between ErbB1 and/or ErbB2 expression and sensitivity to growth inhibition by lapatinib. This *in vitro* model provides a framework for future animal tumour model development to further understand the mechanisms of diarrhoea induced by this targeted agent.

3.2 Materials and Methods

3.2.1 Chemicals and reagents

The 2,3-bis-(2-methoxy-4-nitro-5-sulfophenyl)-2H-tetrazolium-5-carboxanilide (XTT) kit was obtained from Roche Diagnostics GmbH, Germany as described in Chapter 2 (Section 2.1). The fluorescein isothiocyanate (FITC) Annexin V Apoptosis Detection Kit I, which consists of 10x Annexin V binding buffer, FITC Annexin V and propidium iodide (PI) staining solutions was purchased from BD Pharmingen, USA.

Rabbit polyclonal anti-ErbB1 (0.2 mg/ml), anti-ErbB2 (0.2 mg/ml) and anti-ErbB2 (phospho Y1248) (pErbB2) (1 mg/ml) primary antibodies were supplied by Abcam, UK. Rabbit polyclonal anti-ErbB1 (Tyr 1173) (pErbB1) (0.1 mg/ml) was obtained from Santa

Cruz Biotechnology, USA. Fluorophore-labelled donkey anti-rabbit IgG (H+L) secondary antibodies Alexa Fluor® 568 and 488 (2 mg/ml) were purchased from Invitrogen, USA. Normal rabbit IgG control (polyclonal rabbit IgG) was obtained from R&D Systems, Australia while 4′,6-Diamidino-2-phenylindole dihydrochloride (DAPI) (1 mg) was supplied by Sigma, Australia.

Lapatinib (GlaxoSmithKline (GSK), Australia) was dissolved in 100% DMSO to 10 mM (Rusnak, Alligood et al. 2007). Drug solutions for treatment were diluted with serum-free medium from the stock solution (Zhou, Li et al. 2006).

3.2.2 Cell harvesting

Cell culturing of Walker 256 and IEC-6 (Figure 3.1 and 3.2) was carried out as described in Chapter 2 Section 2.2. Cells were harvested once they reached 80-90% confluence for further experiments. Experiments were carried out using serum-free media.

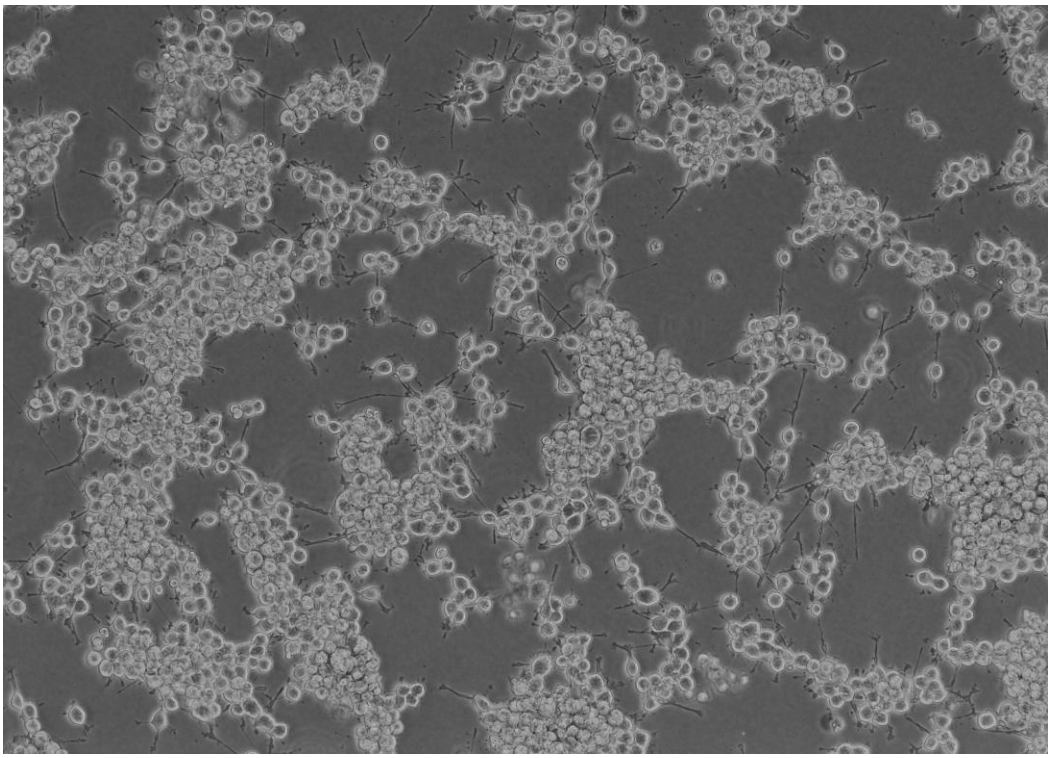

Figure 3.1. Phase contrast micrograph of Walker 256 rat breast carcinoma cell line. Image is of x10 original magnification.

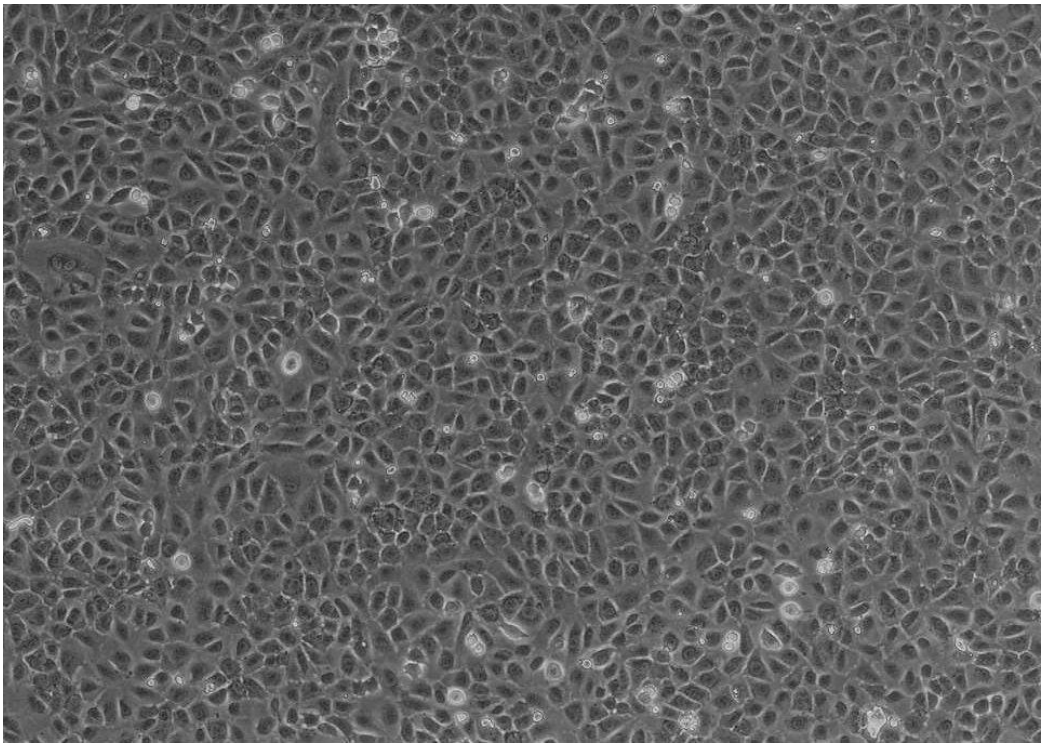

Figure 3.2. Phase contrast micrograph of IEC-6 rat jejunum cell line. Image is of x10 original magnification.

3.2.3 Cytotoxicity assays

The cytotoxic effects of lapatinib on Walker 256 rat breast tumour and IEC-6 rat jejunum cell lines were assessed via the XTT assay and trypan blue exclusion method as described below in Section 3.2.3.1 and 3.2.3.2.

3.2.3.1 XTT cell proliferation assay

This assay was carried out as detailed in Chapter 2 (section 2.3). The experiment was repeated until the final IC_{50} value of lapatinib was confirmed. The final concentration of lapatinib that had been determined to inhibit 50% cell growth was used in the following experiments and cells were incubated for 6, 24 and 48 hours to evaluate the cell growth at different time points.

3.2.3.2 Trypan blue exclusion method

Each cell line was grown in a 6-well plate (Becton Dickinson, USA) in a final volume of 3 ml culture medium per well that contained $5x10^4$ cells/ml and was incubated for 24 hours

at 37ºC with 5% CO_2. Cells were then treated with lapatinib and incubated for 6, 24 and 48 hours. An equivalent dilution of DMSO was used as a control treatment. After the incubation period, the cell suspension was mixed with 0.4% trypan blue and was examined under an inverted microscope. Viable cells had a clear cytoplasm, while nonviable cells had a blue cytoplasm. This test is based on the principle that live cells possess intact cell membranes that exclude certain dyes such as trypan blue whereas the dead cells will take up the dye. The cytotoxic effect of lapatinib on the cell line was calculated as follow:

$$\text{Cell viability (\%)} = \frac{\text{Viable cells in sample}}{\text{Viable cells in control}} \times 100$$

3.2.4 Fluorescence activated cell sorting (FACS) analysis

This experiment was carried out to evaluate cell apoptosis. Each cell line was grown in a sterile tissue culture dish plate (Becton Dickinson, USA) in a final volume of 10 ml culture medium per dish that contained $5x10^4$ cells/ml and was incubated for 24 hours at 37ºC with 5% CO_2. Cells were treated with lapatinib and incubated for 6, 24 and 48 hours. After the incubation period with lapatinib, the old medium potentially containing dead cells was collected in a 50 ml falcon tube. The remaining cells were then dislodged (refer to Chapter 2 Section 2.2) and the cell solution was then added to the 50 ml falcon tube. The tubes were spun at 1400 rpm for 5 minutes. Supernatant was removed and the cells were washed with cold PBS and spun again for 2 minutes. The supernatant was then removed and the cell pellet was resuspended in 100 µl of 1x Annexin V binding buffer and transferred to a 5 ml FACS tube. Five microlitres of FITC Annexin-V and propidium iodide (PI) were added to the tubes. Cells were gently vortexed and incubated for 15 minutes at room temperature in the dark. Four hundred microliters of 1x Annexin V binding buffer was then added to each tube. Three tubes of untreated cells were prepared as follows - unstained cells, cells stained with FITC Annexin V (no PI) and cells stained with PI (no FITC Annexin V), in order to set up

compensation and quadrants for flow cytometry analysis (Appendix 1). Samples were kept on ice and analysed by a flow cytometry machine (FACSCalibur, BD Biosciences, San Jose, CA, USA) within 1 hour.

In apoptotic cells, the membrane phospholipid phosphatidylserine (PS) is translocated from the inner to the outer leaflet of the plasma membrane, thereby exposing PS to the external cellular environment. This analysis is based on the principle that Annexin V which is a calcium (Ca^{2+}) dependent phospholipid-binding protein has a high affinity for PS and binds to cells with exposed PS. Staining with FITC Annexin V is typically used in conjunction with a vital dye such as PI to allow identification of early apoptotic cells (PI negative, FITC Annexin V positive). Viable cells with intact membranes exclude PI, whereas the membranes of dead and damaged cells are permeable to PI.

At least 10, 000 cells were examined in the gated region used for calculation. Dual parameter cytometric data were analysed using CellQuest software from BD Biosciences. Viable cells were indicated as FITC Annexin V and PI negative, whereas FITC Annexin V negative and PI positive staining indicated necrosis, FITC Annexin V positive and PI negative staining indicated early apoptosis, and cells that were FITC Annexin V and PI positive were considered to be in late apoptosis (Sukhotnik, Shteinberg et al. 2008).

3.2.5 Real-time PCR

Each cell line was subjected to real-time PCR analysis to determine the mRNA expression of *ErbB1* and *ErbB2*. Analysis was carried out based on the methods described in Chapter 2 (refer to Section 2.3-2.7).

3.2.6 Immunofluorescence staining of total ErbB1 and ErbB2 & phosphorylated ErbB1 and ErbB2 (pErbB1 and pErbB2)

This method is used to demonstrate the presence and location of specific proteins in cells using antibodies that recognise target proteins by utilising fluorescent-labelled antibodies to detect specific target antigens. Cells ($5x10^4$ cells/ml) were seeded in 8-well chamber slide (Millicell® EZ Slide, Millipore, USA) which were coated with poly-L-lysine (Sigma Aldrich, Australia) (1:10) prior to cell seeding. Cells were then incubated for 48 hours to allow cell adherence. Then, cells were treated with lapatinib and incubated for 6, 24 and 48 hrs. After the incubation period, medium was carefully aspirated. Cells were then washed with PBS for 1 minute. Next, PBS was aspirated prior to cell fixation in 4% paraformaldehyde (Sigma Aldrich, Australia) for 20 minutes at room temperature. The fixative solution was aspirated prior to 2x5 minutes washing in PBS and following that, cells were permeabilised with 0.5% Triton-X solution (Sigma Aldrich, Australia) for 10 minutes at room temperature. Next, cells were rinsed with PBS for 3x5 minutes and were blocked with 1% bovine serum albumin (BSA) (Sigma, Australia) in PBS for 1 hour at room temperature. After the incubation hour, the blocking solution was aspirated and cells were incubated with primary antibodies diluted in 1% BSA (ErbB1: 5 µg/ml, ErbB2: 8 µg/ml, pErbB1: 2.5 µg/ml and pErbB2: 40 µg/ml) for 18 hours at 4ºC. Then, the primary antibodies were aspirated and cells were washed with PBS for 2x3 minutes. Following that, cells were incubated with fluorophore-labelled secondary antibodies diluted in 1% BSA (10 µg/ml) for 1 hour at room temperature, protected from light. Following washing with PBS for 2x3 minutes, cells were incubated with DAPI diluted in PBS (1 µg/ml) for 15 minutes at room temperature, protected from light. The cells were washed again in PBS (2x3 minutes), then the chamber was removed from the 8-well slide and the slide was coverslipped with an aqueous mounting media, Fluoroshield (Sigma Aldrich, Australia) The coverslip was then sealed with nail polish and left to dry at room temperature for 20 minutes prior to storage at 4ºC. Slides were viewed using a confocal

microscope (Leica TCS SP5) within 48 hours. Cells treated with rabbit IgG (40 µg/ml) or BSA (1%) only were used as controls for comparison.

3.2.7 Statistical analysis

Data were presented as mean ± S.E.M. Statistical analysis of *ErbB2* mRNA expression results in Walker 256 cells were carried out using Kruskal Wallis test to identify differences between control untreated samples and treated samples at different incubation time. One-way ANOVA with Tukey's multiple comparisons test was used to analyse *ErbB1* and *ErbB2* mRNA expression in IEC-6 cells. Trypan blue exclusion results as well as FACS results were analysed using two-way ANOVA with Tukey's multiple comparisons test to compare means of each group at different incubation time. Statistical significance was accepted as $p<0.05$.

3.3 Results

3.3.1 Cytotoxic effect of lapatinib on Walker 256 and IEC-6

The cytotoxic effects of lapatinib on Walker 256 and IEC-6 as assessed via the XTT assay and trypan blue exclusion method are explained below in Section 3.3.1.1 and 3.3.1.2. Results were compared between control untreated and lapatinib-treated cells.

3.3.1.1 XTT assay

Walker 256 and IEC-6 were treated with lapatinib at a series of concentrations (1-10 µM) to determine the lapatinib dosage that could inhibit 50% cell growth (Figure 3.3 A and B). Lapatinib was found to inhibit 50% of Walker 256 rat breast tumour cell growth at 8.20 ± 0.18 µM, and at 3.03 ± 0.26 µM in the IEC-6 rat jejunum cell line (Table 3.1). Experiments were also carried out with DMSO (lapatinib vehicle), which was assayed in a series of concentrations equivalent to the concentration of lapatinib treatment. DMSO did not cause

50% cell inhibition (Figure 3.3 A and B) at any of the concentrations, which signifies that the vehicle did not influence lapatinib cytotoxic effect on both cell lines.

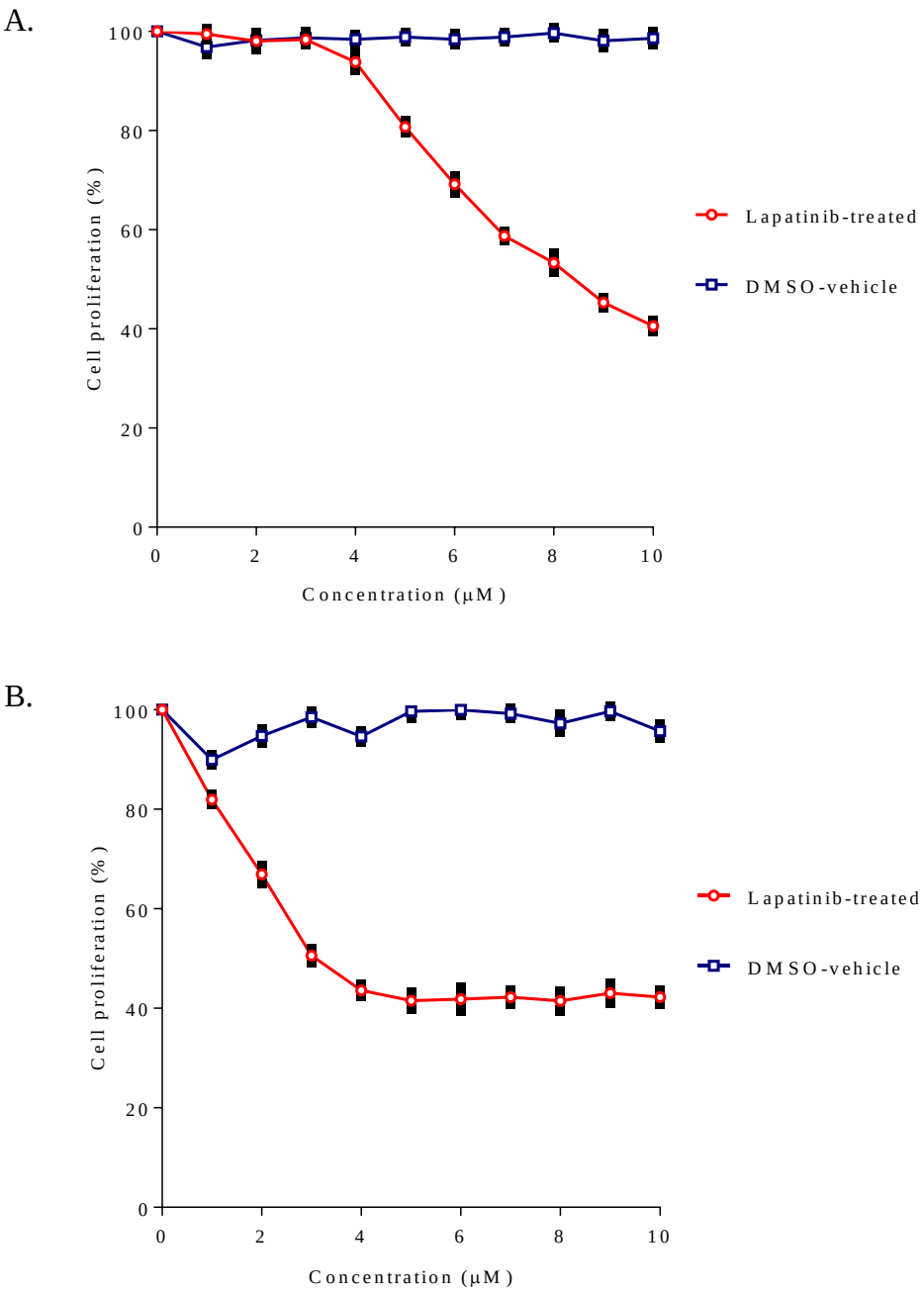

Figure 3.3. The effect of lapatinib on proliferation of Walker 256 cells **(A)** and IEC-6 cells **(B)** assessed using the XTT assay. Experiment was repeated 4 times with 3 replicates in each experiment. Graph shown for each cell line is representative of experiments conducted. Results shown on the graph are presented as mean ± standard deviation (n=3).

Table 3.1. IC_{50} values of lapatinib on Walker 256 and IEC-6 cells as assessed using the XTT assay.

Cell line	Experiment 1	Experiment 2	Experiment 3	Experiment 4	Mean ± S.E.M
Walker 256	7.9 µM	8.0 µM	8.2 µM	8.7 µM	8.20 ± 0.18 µM
IEC-6	2.3 µM	3.0 µM	3.5 µM	3.3 µM	3.03 ± 0.26 µM

*Data presented as mean ± S.E.M (n=4).

3.3.1.2 Trypan blue exclusion assay

The cytotoxic effects of lapatinib on Walker 256 and IEC-6 were further evaluated using a trypan blue exclusion assay. The effects of lapatinib on the cell lines were tested in a time-dependent manner (Figure 3.4 A and 3.4 B).

As shown in Table 3.2, at 6 and 24 hours incubation, viability of lapatinib-treated Walker 256 cells (6 hours: 94.96 ± 1.08 %, 24 hours: 85.51 ± 2.51 %) did not show any difference to control untreated (6 hours: 92.48 ± 1.44 %, 24 hours: 90.58 ± 0.85 %) or DMSO-treated (6 hours: 90.56 ± 4.09 %, 24 hours: 84.18 ± 0.97 %) cells ($p>0.05$). However, at 48 hours incubation, lapatinib-treated cells (55.83 ± 4.85 %) showed a significant difference in cell viability compared to the control untreated (88.12 ± 1.09 %) and DMSO-treated (85.30 ± 1.11%) cells ($p<0.0001$). There were no significant differences between control untreated and DMSO-treated cells at 6, 24 and 48 hours ($p>0.05$) (Table 3.2).

As for IEC-6, lapatinib-treated cells (90.49 ± 4.31 %) did not show any difference in inhibition of cell viability at 6 hours incubation compared to control untreated (92.19 ± 3.18 %) and DMSO-treated (89.33 ± 0.57 %) cells ($p>0.05$). However, at 24 hours incubation, lapatinib-treated cells (55.69 ± 3.06 %) decreased in cell viability as compared to control untreated (84.08 ± 3.39 %) and DMSO-treated (83.50 ± 1.49 %) cells ($p<0.0001$). At 48 hours incubation, lapatinib-treated cells (46.85 ± 2.89 %) also showed a significant difference in cell viability compared to control-untreated (80.61 ± 3.36 %) ($p<0.0001$) and DMSO-treated cells (77.72 ± 2.45 %) ($p<0.0001$). As shown in Table 3.2, DMSO-treated cells did not show a significant difference with control-untreated cells at all incubation hours but indicated a difference with lapatinib-treated cells.

As DMSO did not show any significant effect on viability in both cell lines, further experiments were carried out on control untreated and lapatinib-treated cells only.

A.

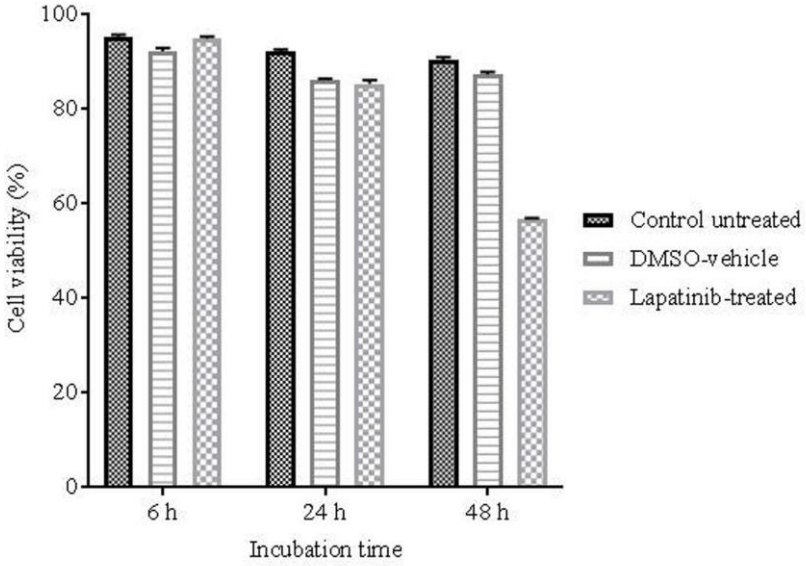

B.

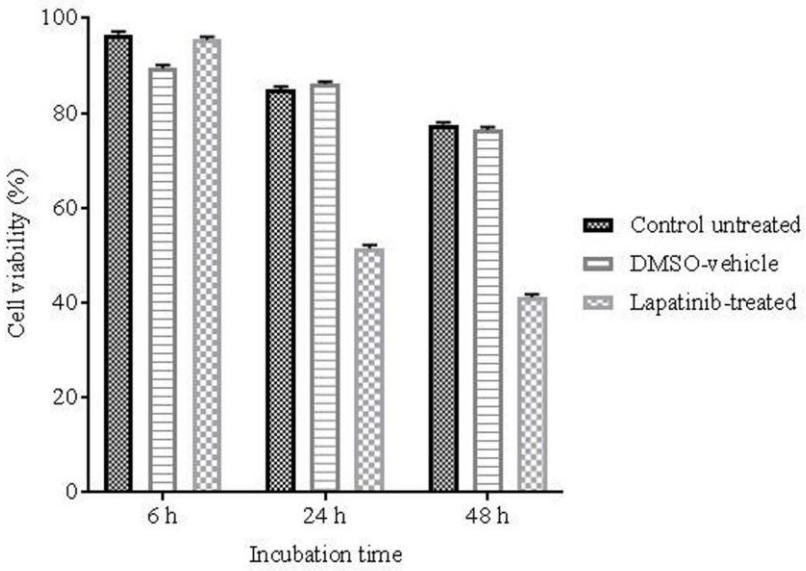

Figure 3.4. The effect of lapatinib on Walker 256 **(A)** and IEC-6 **(B)** cells at different incubation time as evaluated in trypan blue exclusion analysis. Experiment was repeated 3 times with 2 replicates in each experiment. Results were compared with control untreated and DMSO-vehicle treated cells. Graph shown for each cell line is representative of experiments conducted. Results shown on the graph are presented as mean ± S.E.M (n=2). Significant level was not taken into account as further statistical analysis was shown in the summarised data presented in Table 3.2.

Table 3.2. Percentage of cell viability for Walker 256 and IEC-6 after treatment with lapatinib at different incubation time as assessed using trypan blue exclusion assay.

Cell line	Incubation time	Control untreated	DMSO-vehicle	Lapatinib-treated
Walker 256	6 h	92.48 ± 1.44 %	90.56 ± 4.09 %	94.96 ± 1.08 %
	24 h	90.58 ± 0.85 %	84.18 ± 0.97 %	85.51 ± 2.51 %
	48 h	88.12 ± 1.09 %	85.30 ± 1.11 %	55.83 ± 4.85 % $_{AB}$
IEC-6	6 h	92.19 ± 3.18 %	89.33 ± 0.57 %	90.49 ± 4.31 %
	24 h	84.08 ± 3.39 %	83.50 ± 1.49 %	55.69 ± 3.06 % $_{AB}$
	48 h	80.61 ± 3.36 %	77.72 ± 2.45 %	46.85 ± 2.89 % $_{AB}$

*Data presented as mean ± S.E.M (n=3). Results were compared with control untreated and DMSO-vehicle treated cells. Data showing the subscript letters were significantly different at the level of $p<0.05$. $_{A}$ for $p<0.0001$ compared to control untreated cells, $_{B}$ for $p<0.0001$ compared to DMSO-vehicle treated cells.

3.3.2 Mechanism of cell death induced by lapatinib

As indicated in the results above, lapatinib was shown to induce cell death in both Walker 256 and IEC-6 cells. Thus, flow cytometry was carried out to evaluate the mechanism of cell death induced by lapatinib. Percentage of viable, early apoptotic, late apoptotic and necrotic cells in Walker 256 and IEC-6, after treatment with lapatinib at different incubation time were presented in Figure 3.5 and 3.6. At 6 hours, lapatinib-treated samples showed a significantly lower number of viable cells (58.99 ± 3.21 %) ($p<0.0001$) and higher numbers of early apoptotic cells (24.71 ± 1.39 %) ($p<0.0001$), compared to control untreated (viable cells: 79.97 ± 0.99 %, early apoptotic cells: 7.30 ± 2.51 %) (Table 3.3), as determined by flow cytometry. However, lapatinib-treated samples did not show any difference in the percentage of viable, early apoptotic, late apoptotic and necrotic cells at 24 hours incubation (Table 3.3) compared to control untreated samples ($p>0.05$), while at 48 hours incubation, lapatinib-treated samples were shown to have a lower percentage of viable cells (50.70 ± 7.27 %) ($p<0.05$) and higher percentage of necrotic cells (37.91 ± 7.08 %) ($p<0.01$), compared to control untreated samples (viable cells: 71.93 ± 6.71 %, necrotic cells: 11.86 ± 5.62 %) (Table 3.3).

As for IEC-6, the results did not show any significant differences in cell viability at 6 hours incubation ($p>0.05$) (Table 3.3). However, lapatinib-treated samples at 24 hours incubation showed a lower percentage of viable cells (27.72 ± 9.59 %) ($p<0.05$) and a higher percentage of late apoptotic cells (53.56 ± 15.37 %) ($p<0.01$) compared to control untreated samples (viable cells: 65.00 ± 9.70 %, late apoptotic cells: 12.91 ± 4.70 %) (Table 3.3). Similarly, at 48 hours incubation lapatinib-treated samples showed a lower percentage of viable cells (25.68 ± 10.78 %) ($p<0.05$) and a higher percentage of late apoptotic cells (56.82 ± 11.53 %) ($p<0.05$) compared to the control untreated samples that exhibited 65.83 ± 13.11 % alive cells and 22.70 ± 12.81 % late apoptotic cells (Table 3.3).

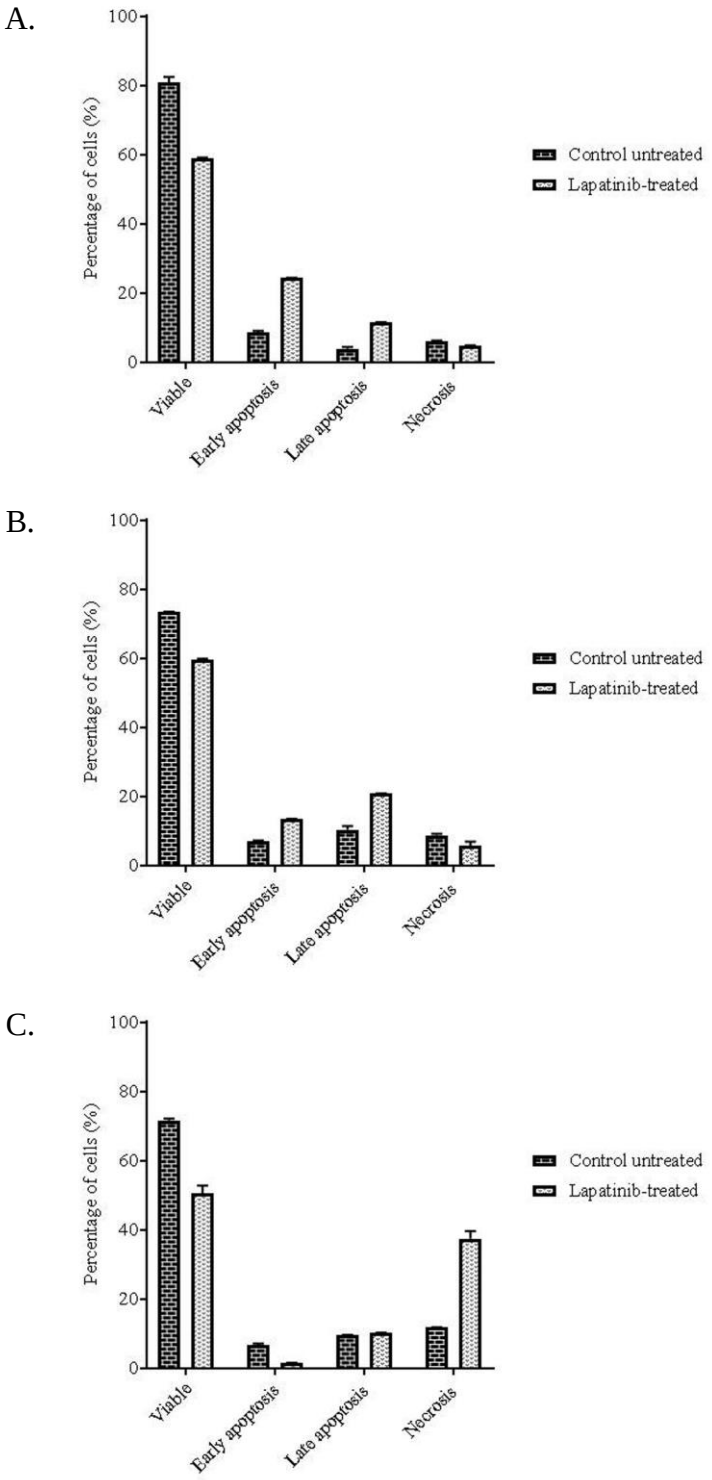

Figure 3.5. The percentage of viable, early apoptotic, late apoptotic and necrotic cells in lapatinib-treated Walker 256 cells compared to control untreated at 6 **(A)** 24 **(B)** and 48 **(C)** hours incubation as quantified via FACS analysis. Each experiment was repeated 3 times with 2 replicates in each experiment. Graph shown for each cell line is representative of experiments conducted. Results shown on the graph are presented as mean ± S.E.M (n=2). Significant level was not taken into account as statistical analysis was shown in the summarised data presented in Table 3.3.

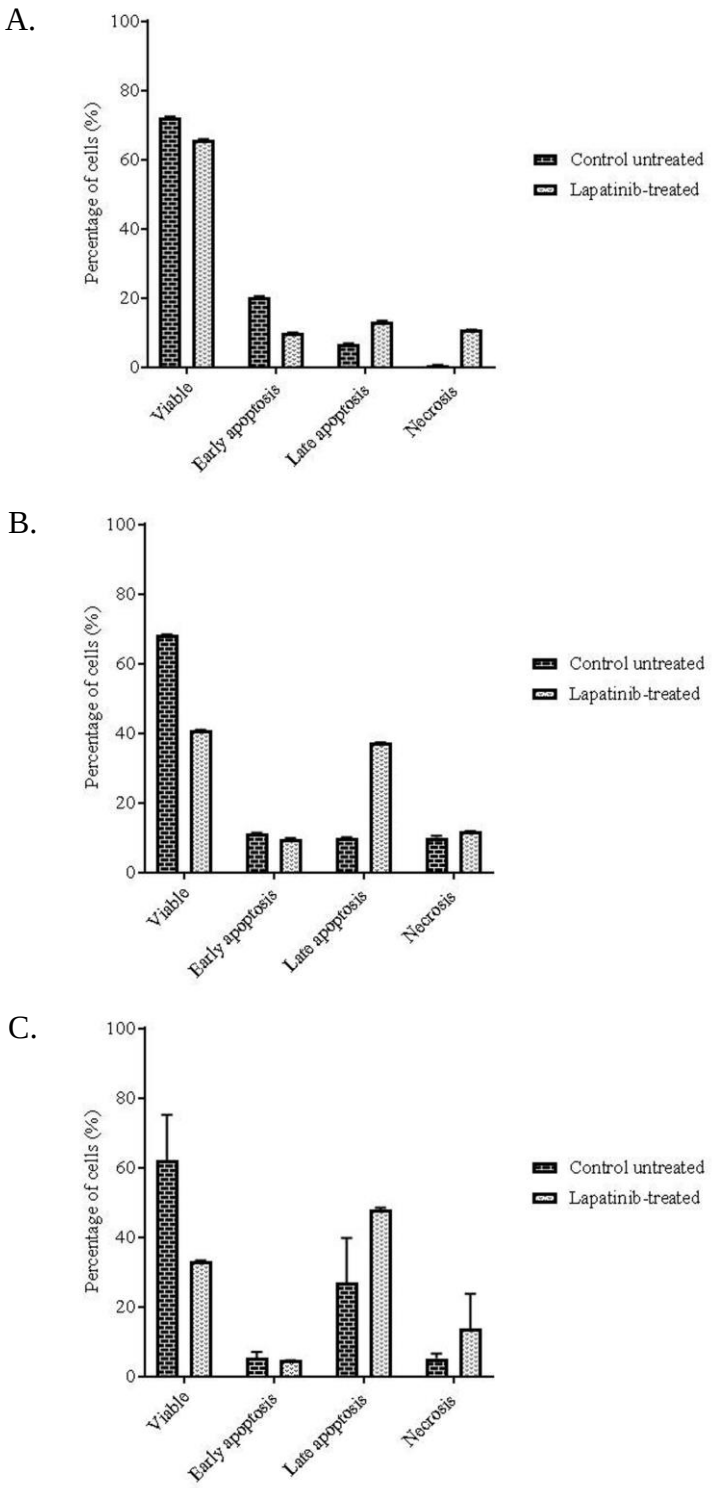

Figure 3.6. The percentage of viable, early apoptotic, late apoptotic and necrotic cells in lapatinib-treated IEC-6 cells compared to control untreated at 6 **(A)** 24 **(B)** and 48 **(C)** hours incubation as quantified via FACS analysis. Each experiment was repeated 3 times with 2 replicates in each experiment. Graph shown for each cell line is representative of experiments conducted. Results shown on the graph are presented as mean ± S.E.M (n=2). Significant level was not taken into account as statistical analysis was shown in the summarised data presented in Table 3.3.

Table 3.3. Percentage of viable, early apoptotic, late apoptotic and necrotic cells after treatment with lapatinib at different incubation time as assessed using FACS analysis.

Cell line	Incubation time	Sample	Viable cells	Early apoptotic cells	Late apoptotic cells	Necrotic cells
Walker 256	6 h	*Control untreated*	79.97 ± 0.99 %	7.30 ± 2.51 %	4.40 ± 1.37 %	8.34 ± 4.05 %
		Lapatinib-treated	58.99 ± 3.21 % $_{A}$	24.71 ± 1.39 % $_{A}$	11.91 ± 1.96 %	4.39 ± 0.65 %
	24 h	*Control untreated*	71.24 ± 1.86 %	7.43 ± 1.49 %	11.33 ± 1.50 %	10.03 ± 2.71 %
		Lapatinib-treated	58.07 ± 11.81 %	12.82 ± 0.73 %	22.26 ± 8.26 %	6.87 ± 3.30 %
	48 h	*Control untreated*	71.93 ± 6.71 %	6.66 ± 1.65 %	9.56 ± 2.63 %	11.86 ± 5.62 %
		Lapatinib-treated	50.70 ± 7.27 % $_{a}$	1.68 ± 0.67 %	9.67 ± 2.77 %	37.91 ± 7.08 % $_{b}$
IEC-6	6 h	*Control untreated*	72.90 ± 7.67 %	16.11 ± 4.22 %	9.87 ± 4.36 %	1.14 ± 0.33 %
		Lapatinib-treated	63.93 ± 8.70 %	10.45 ± 3.39 %	15.23 ± 5.65 %	10.38 ± 5.41 %
	24 h	*Control untreated*	65.00 ± 9.70 %	12.52 ± 2.71 %	12.91 ± 4.70 %	9.57 ± 5.97 %
		Lapatinib-treated	27.72 ± 9.59 % $_{a}$	10.77 ± 3.75 %	53.56 ± 15.37 % $_{b}$	9.27 ± 3.75 %
	48 h	*Control untreated*	65.83 ± 13.11 %	5.37 ± 1.84 %	22.70 ± 12.81 %	6.12 ± 1.40 %
		Lapatinib-treated	25.68 ± 10.78 % $_{a}$	6.82 ± 1.08 %	56.82 ± 11.53 % $_{a}$	10.69 ± 1.41 %

*Data presented as mean ± S.E.M (n=3). Results were compared with control untreated cells at the same incubation time in the same category. Data showing the subscript letters were significantly different at the level of $p<0.05$. $_a$ for $p<0.05$ compared to control untreated cells, $_b$ for $p<0.01$ compared to control untreated cells, $_A$ for $p<0.0001$ compared to control untreated cells.

3.3.3 ErbB1 and ErbB2 mRNA expression

ErbB1 was unable to be detected in Walker 256 cells due to low expression (no data shown). *ErbB2* mRNA expression in lapatinib-treated Walker 256 cells was not significantly different compared to control untreated cells at 6, 24 and 48 hours incubation ($p>0.05$) (Figure 3.7 A). As for IEC-6, *ErbB1* mRNA expressions increased as incubation time increased in both control untreated and lapatinib-treated cells. However, the results were not significantly different between lapatinib-treated cells and control untreated cells (Figure 3.8 A) ($p>0.05$). Figure 3.8 B illustrates *ErbB2* mRNA expression in IEC-6 cells in which control untreated cells showed increasing *ErbB2* mRNA expressions with the increase of incubation hour, while lapatinib-treated cells indicated decreasing *ErbB2* mRNA expression over 6, 24 and 48 hours incubation. However, the results were also not significantly different ($p>0.05$).

A.

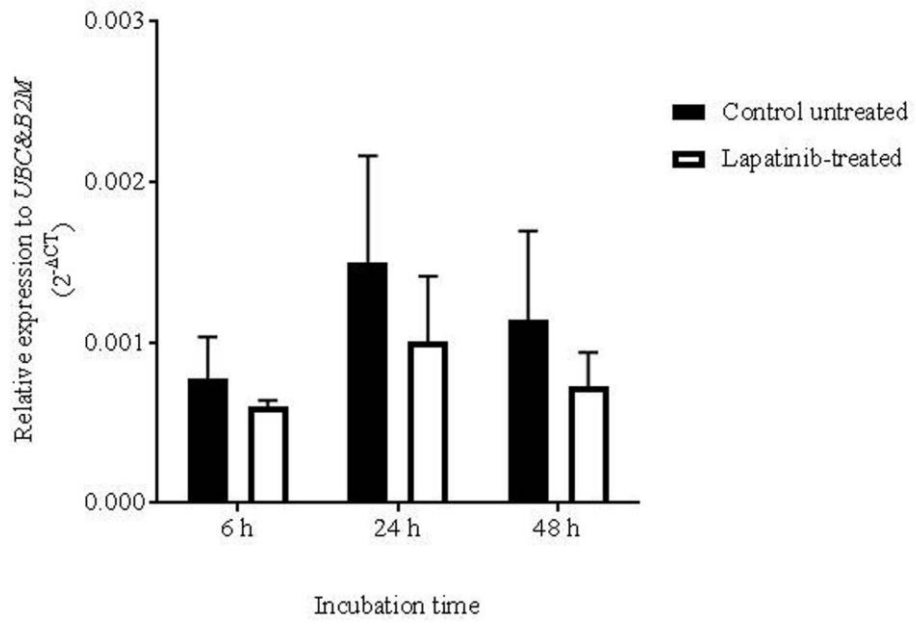

Figure 3.7. *ErbB2* **(A)** mRNA expression in control untreated and lapatinib-treated Walker 256 cells. Data presented as mean ± S.E.M (n=4).

A.

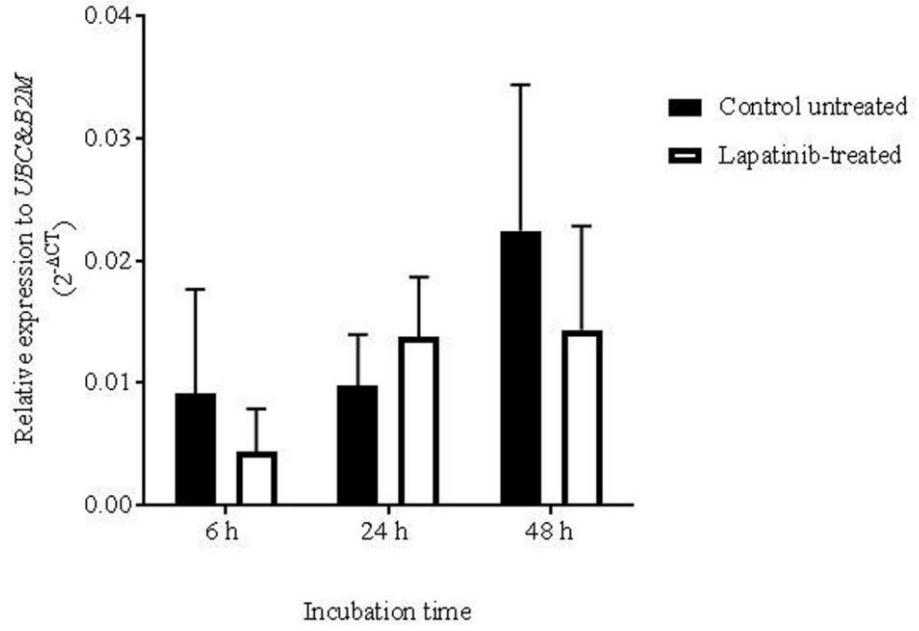

B.

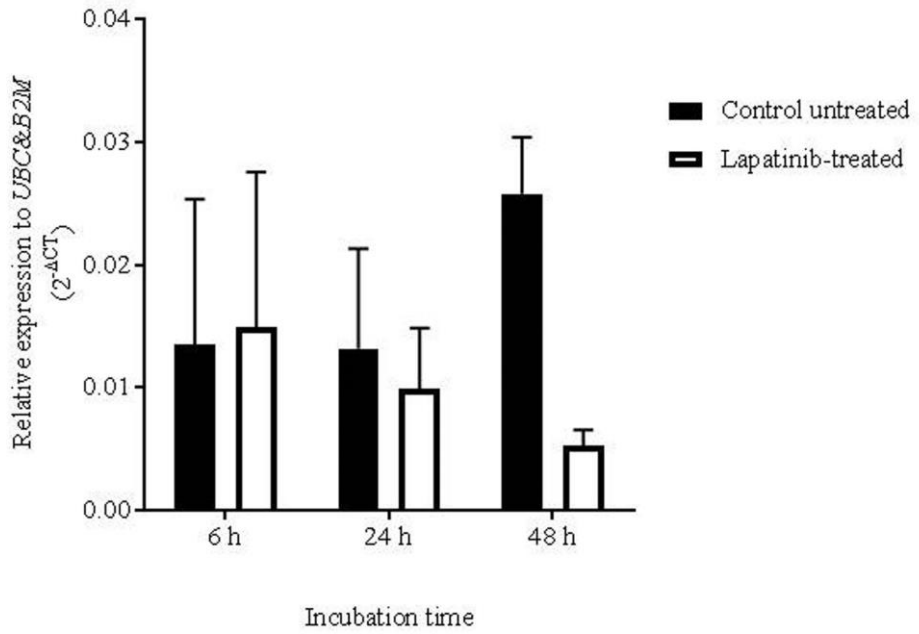

Figure 3.8. *ErbB1* **(A)** and *ErbB2* **(B)** mRNA expression in control untreated and lapatinib-treated IEC-6 cells. Data presented as mean ± S.E.M (n=4).

3.3.4 Detection of total and phosphorylated ErbB1 and ErbB2 proteins

All four proteins (ErbB1, ErbB2, pErbB1 and pErbB2) were expressed in both Walker 256 and IEC-6 cells at all time points but with different staining intensities. Staining can be seen dispersed throughout the cells, with higher intensity at the cytoplasmic membrane of the cells. The nuclei were round and stained blue by DAPI. The staining intensities of control untreated and lapatinib-treated cells from both cell lines were also compared with negative controls (1% BSA and Rabbit IgG) which were stained with secondary antibody only (red or green). Cells which were treated with Rabbit IgG only exhibited intense staining compared to the cells which were treated with 1% BSA only.

The intensity of secondary antibody expression in the Walker 256 cells treated with Rabbit IgG only was comparatively the same as the Walker 256 cells treated with all four primary antibodies (ErbB1, ErbB2, pErbB1 and pErbB2) especially at 6 and 24 hours incubation which might indicate a false positive signal. However, it is important to note that in this experiment the concentration of Rabbit IgG (40 µg/ml) used was equivalent to the highest concentration of primary antibody used which was pErbB2, in which the concentration of Rabbit IgG was higher than the concentrations of other primary antibodies (ErbB1, ErbB2 and pErbB1). Thus, based on the staining intensities shown in the images (Figure 3.9, 3.12 and 3.15), ErBB1, ErbB2 and pErbB1 proteins were expressed in Walker 256 cells but in lower amounts. The concentration of Rabbit IgG used in this experiment was equivalent to the concentration of pErbB2 primary antibody, however, the staining intensity of pErbB2 in Walker 256 cells was slightly higher compared to the cells that were treated with Rabbit IgG only, indicating that pErbB2 protein was also expressed in Walker 256 but in lower amount (Figure 3.18).

The results of lapatinib-treated cells were also compared with control untreated cells. In Walker 256 cells, there were no differences in the ErbB1, ErbB2, pErbB1 and pErbB2

staining intensity between untreated and lapatinib-treated cells at 6 (Figures 3.9, 3.12, 3.15, 3.18), 24 hours (Figures 3.10, 3.13, 3.16, 3.19) or at 48 hours incubation (Figures 3.11, 3.14, 3.17, 3.20). However, at 48 hours incubation, lower cell counts were seen in lapatinib-treated cells compared to control untreated cells (Figures 3.11, 3.14, 3.17, 3.20).

The intensity of secondary antibody expression in the IEC-6 cells treated with Rabbit IgG only was lower compared to the IEC-6 cells treated with all four primary antibodies (ErbB1, ErbB2, pErbB1 and pErbB2), indicating low immunoreactivity of negative control in IEC-6 cells. However, staining intensities of ErbB1, ErbB2, pErbB1 and pErbB2 in IEC-6 cells were no different between untreated and lapatinib-treated cells at 6 hours incubation (Figures 3.21, 3.24, 3.27, 3.30). The cell quantities were also similar between untreated and lapatinib-treated cells. At 24 hours incubation (Figures 3.22, 3.25, 3.28, 3.31) incubation, lower cell counts were seen in lapatinib-treated cells compared to untreated cells. However, all four proteins showed no difference in staining intensity between untreated and lapatinib-treated cells. At 48 hours incubation (Figures 3.23, 3.26, 3.29, 3.32), lower cell counts were seen in both untreated and lapatinib-treated cells. Cell shrinkage was seen in the untreated cells, while lapatinib-treated cells showed slightly increased cell size compared to the untreated cells. However, untreated and lapatinib-treated cells showed no difference in staining intensities of all antibodies. Lower cell counts and shrinking cells in control untreated at 48 hours may be due to prolonged serum-deprivation as the cells were treated with serum-free media.

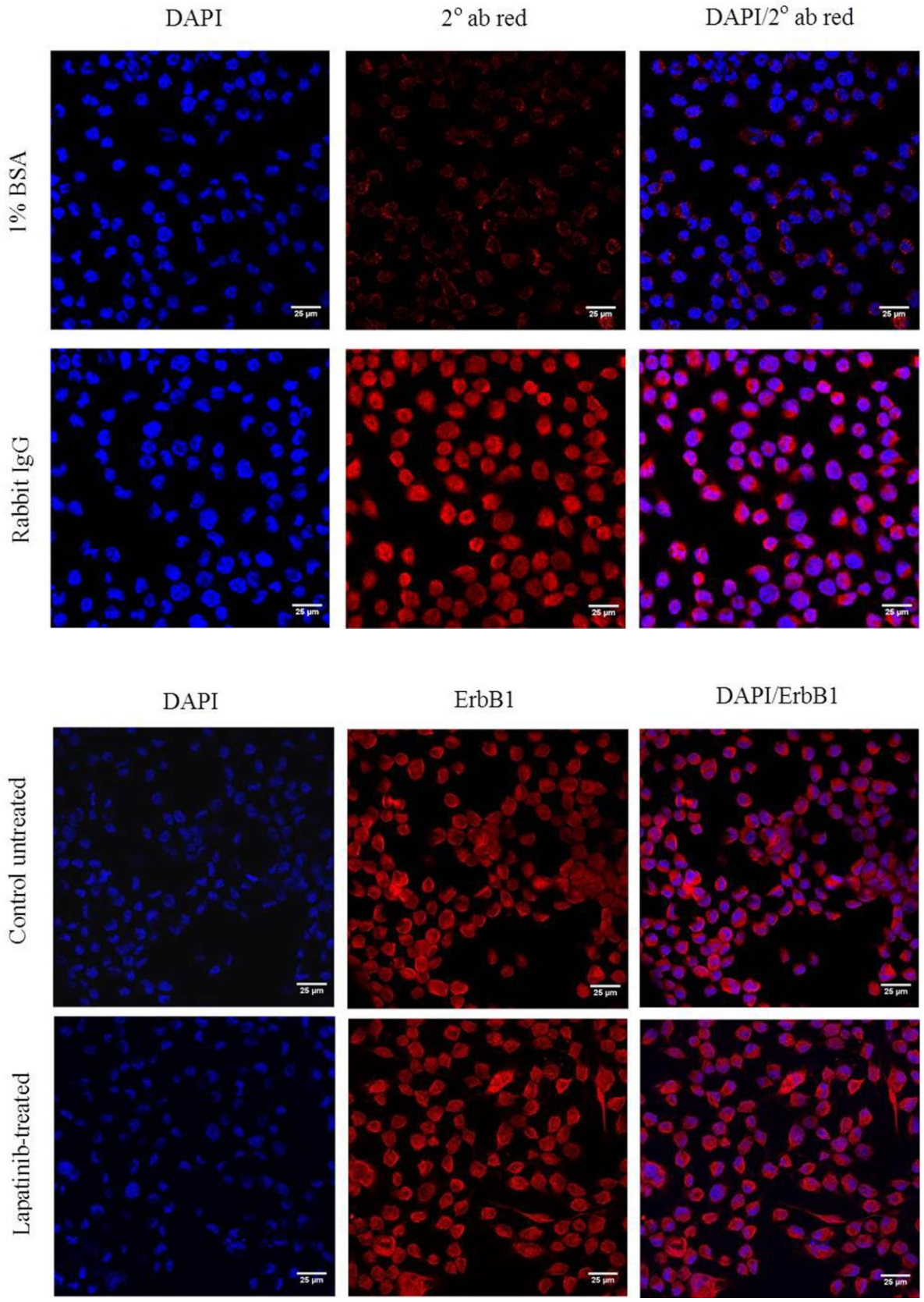

Figure 3.9. ErbB1 protein immunofluorescence staining in Walker 256 rat breast tumour cell line at 6 hours incubation. Images shown are control untreated and lapatinib-treated cells stained with DAPI, ErbB1 and overlay images of DAPI/ErbB1. Images are of x60 original magnification (Scale bar: 25 µm). Results were compared with negative controls (1% BSA and Rabbit IgG) stained with secondary antibody only.

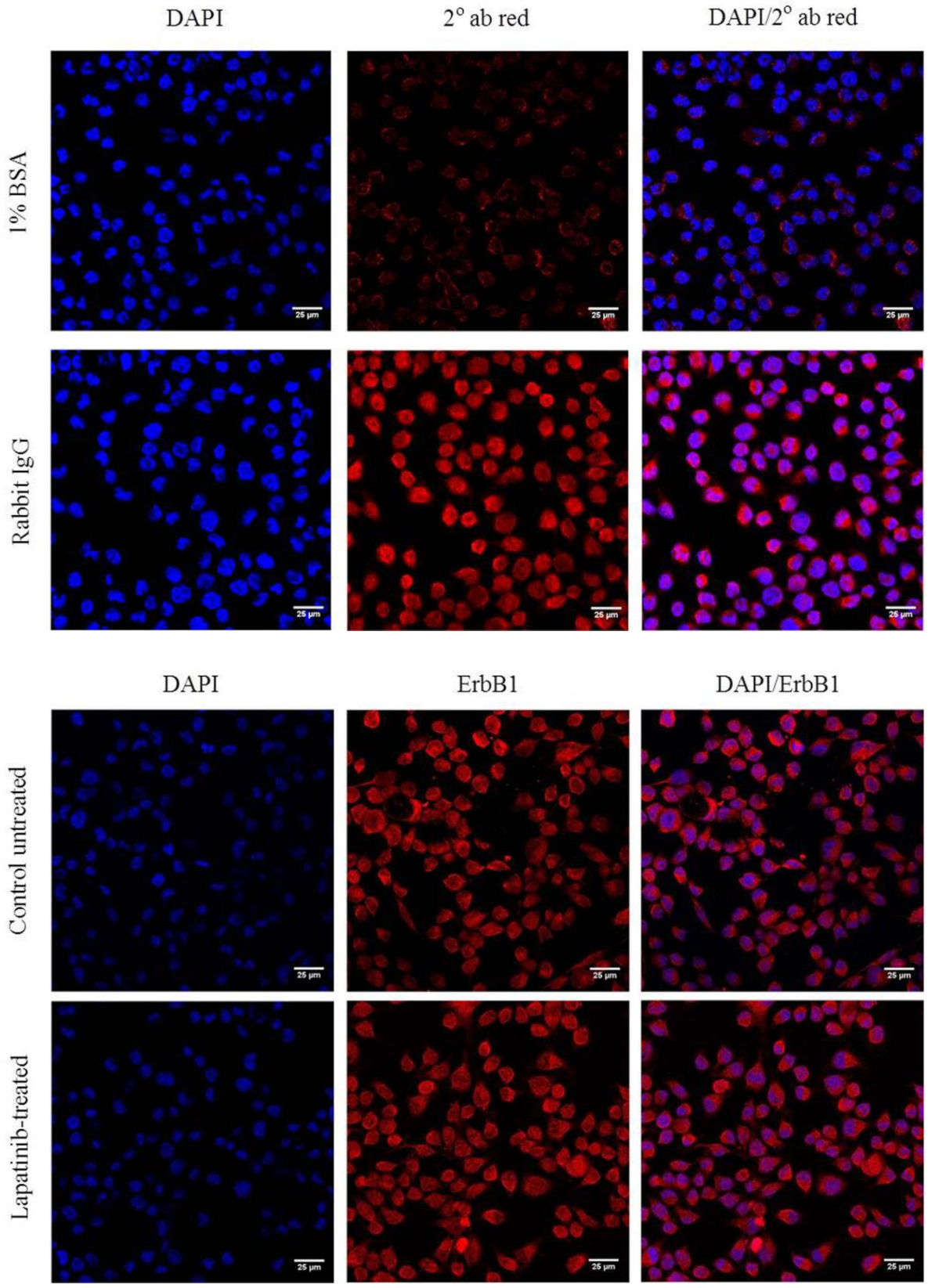

Figure 3.10. ErbB1 protein immunofluorescence staining in Walker 256 rat breast tumour cell line at 24 hours incubation. Images shown are control untreated and lapatinib-treated cells stained with DAPI, ErbB1 and overlay images of DAPI/ErbB1. Images are of x60 original magnification (Scale bar: 25 µm). Results were compared with negative controls (1% BSA and Rabbit IgG) stained with secondary antibody only.

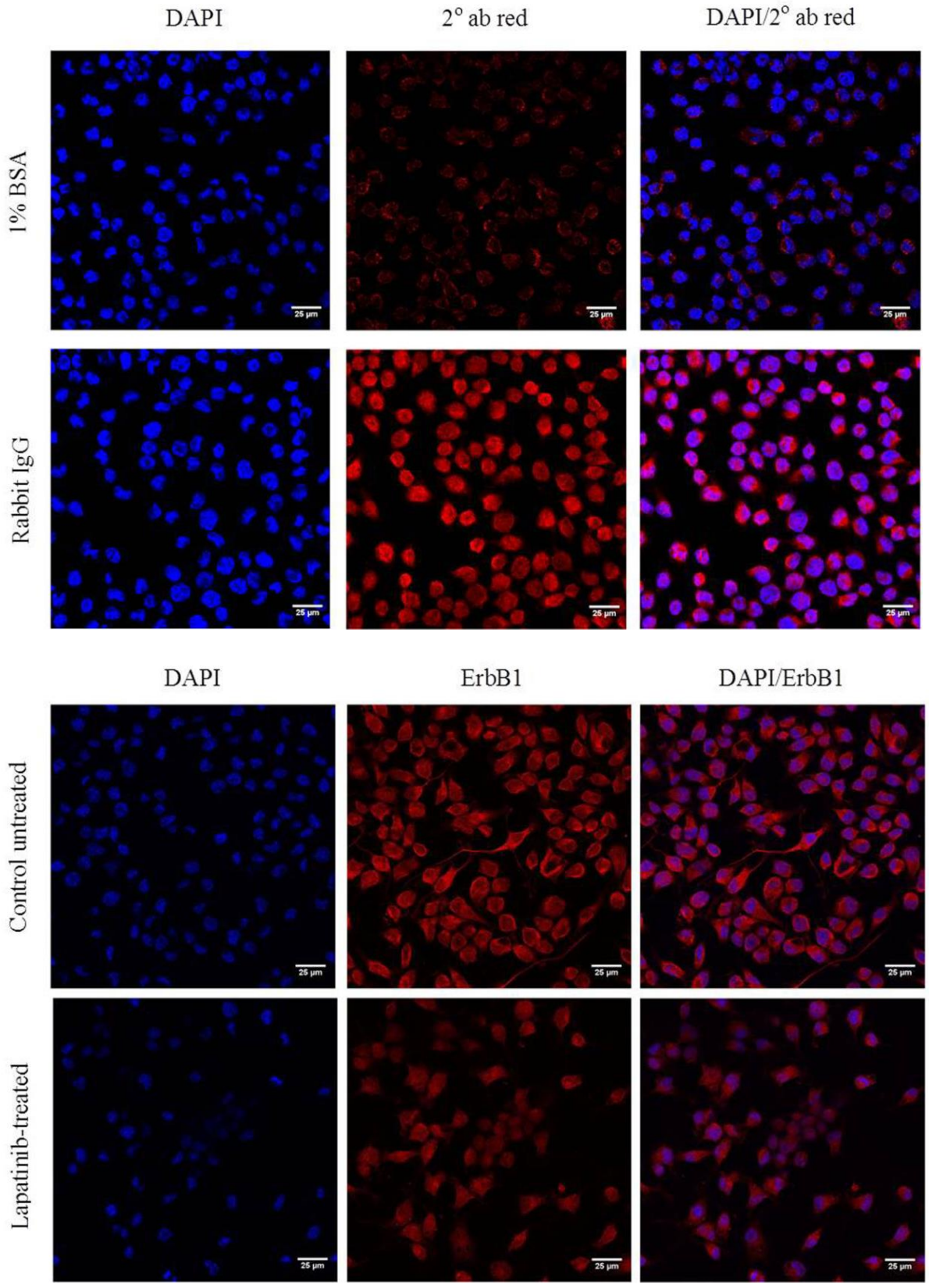

Figure 3.11. ErbB1 protein immunofluorescence staining in Walker 256 rat breast tumour cell line at 48 hours incubation. Images shown are control untreated and lapatinib-treated cells stained with DAPI, ErbB1 and overlay images of DAPI/ErbB1. Images are of x60 original magnification (Scale bar: 25 µm). Results were compared with negative controls (1% BSA and Rabbit IgG) stained with secondary antibody only.

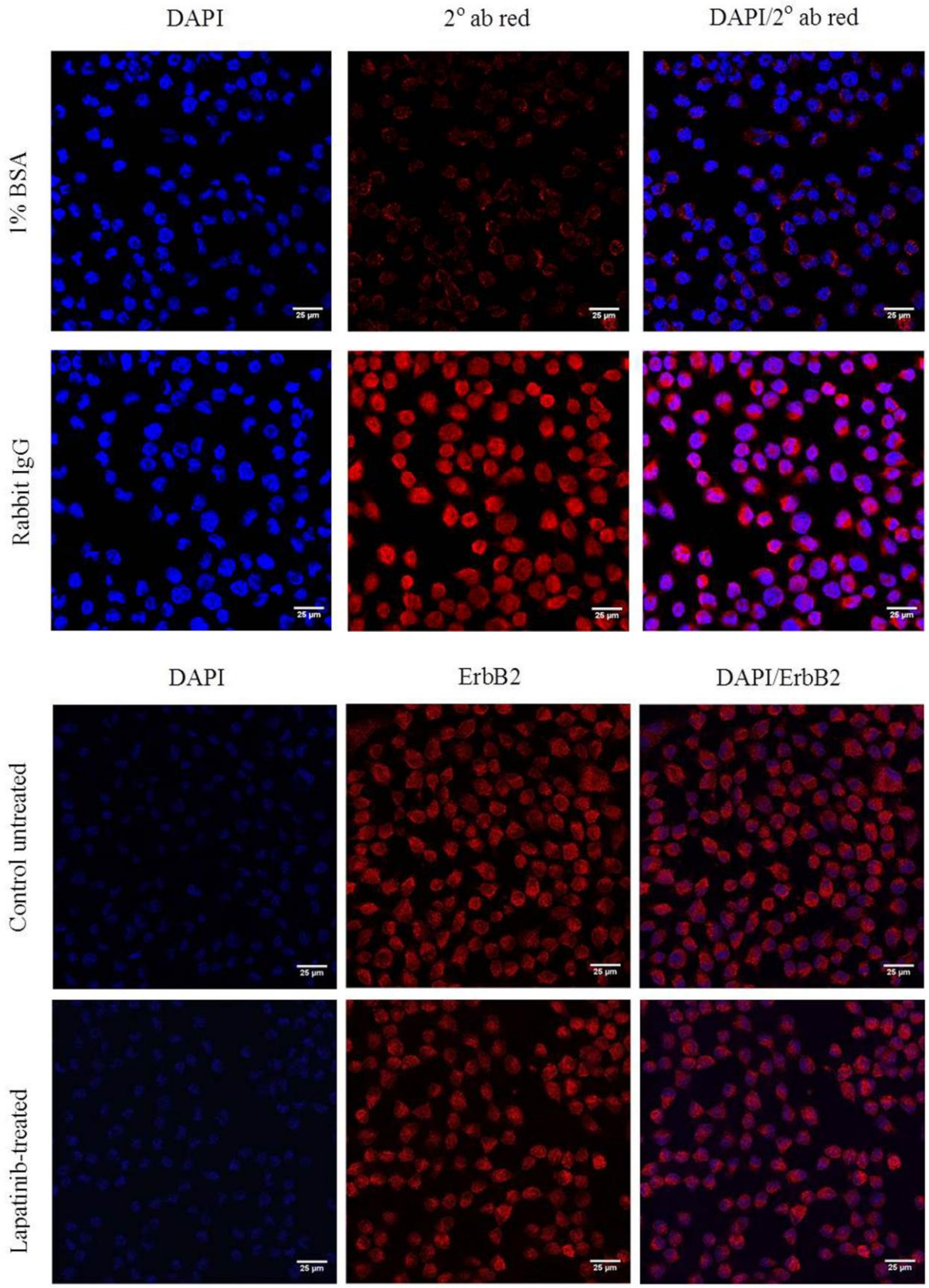

Figure 3.12. ErbB2 protein immunofluorescence staining in Walker 256 rat breast tumour cell line at 6 hours incubation. Images shown are control untreated and lapatinib-treated cells stained with DAPI, ErbB2 and overlay images of DAPI/ErbB2. Images are of x60 original magnification (Scale bar: 25 µm). Results were compared with negative controls (1% BSA and Rabbit IgG) stained with secondary antibody only.

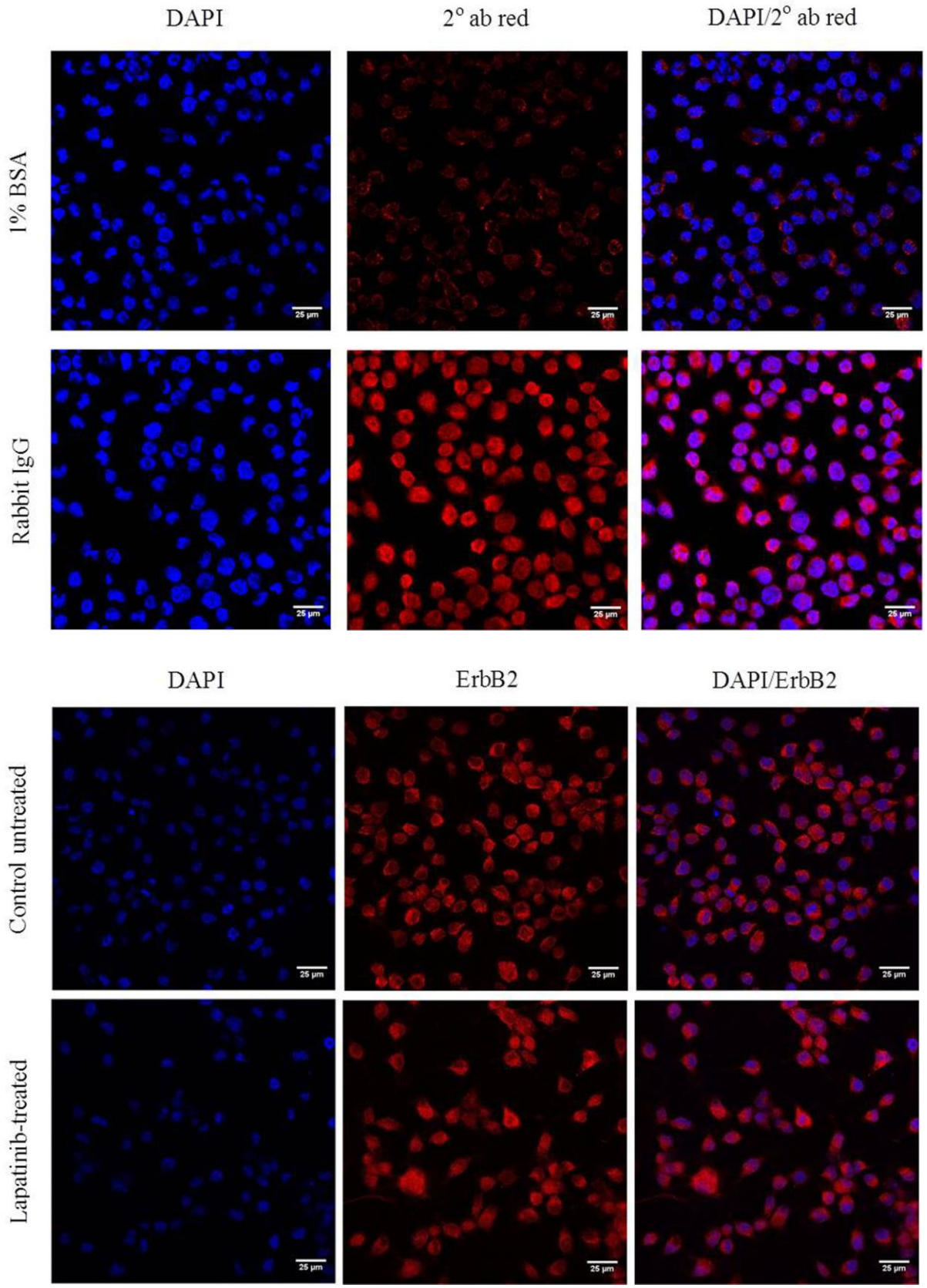

Figure 3.13. ErbB2 protein immunofluorescence staining in Walker 256 rat breast tumour cell line at 24 hours incubation. Images shown are control untreated and lapatinib-treated cells stained with DAPI, ErbB2 and overlay images of DAPI/ErbB2. Images are of x60 original magnification (Scale bar: 25 µm). Results were compared with negative controls (1% BSA and Rabbit IgG) stained with secondary antibody only.

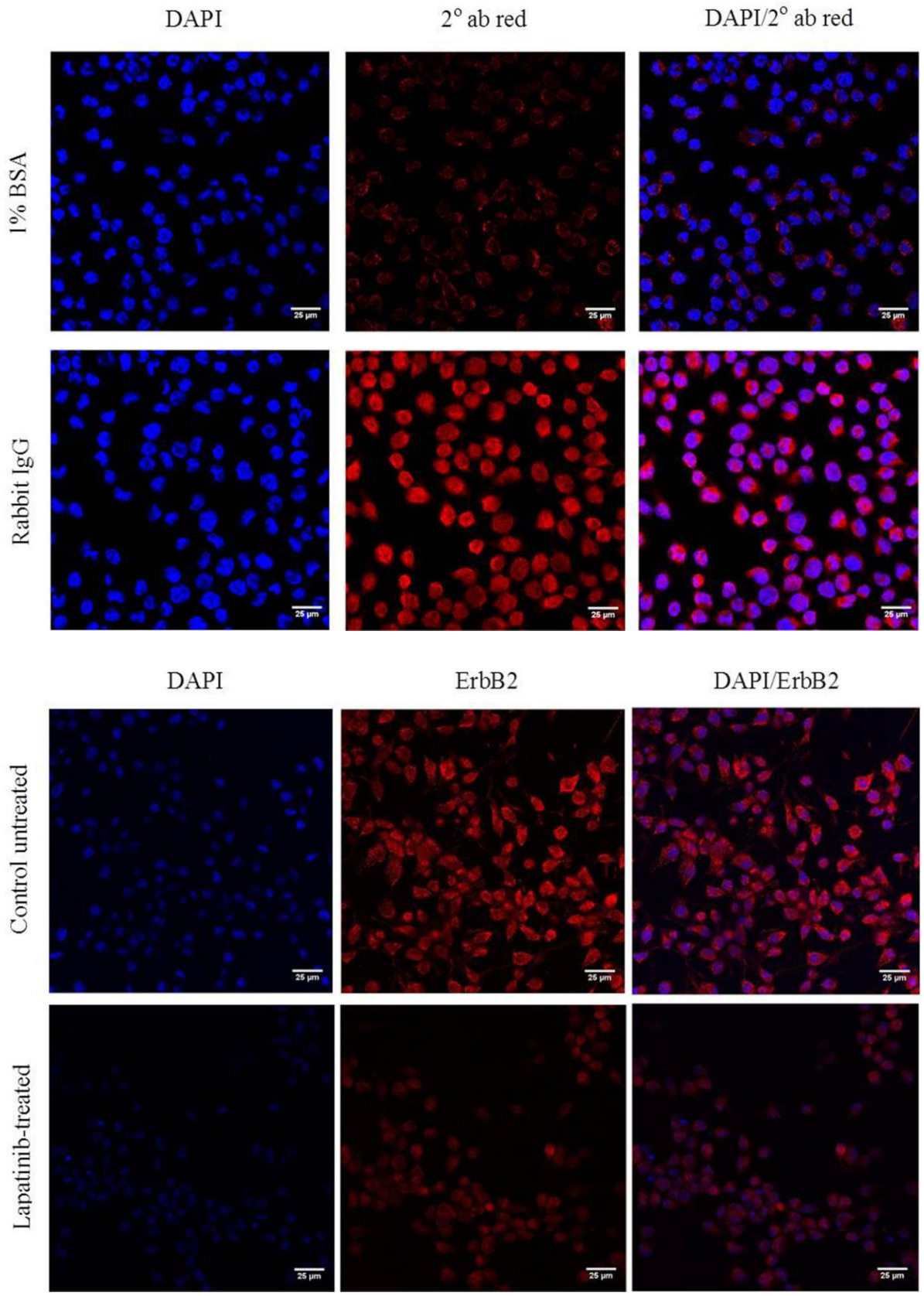

Figure 3.14. ErbB2 protein immunofluorescence staining in Walker 256 rat breast tumour cell line at 48 hours incubation. Images shown are control untreated and lapatinib-treated cells stained with DAPI, ErbB2 and overlay images of DAPI/ErbB2. Images are of x60 original magnification (Scale bar: 25 µm). Results were compared with negative controls (1% BSA and Rabbit IgG) stained with secondary antibody only.

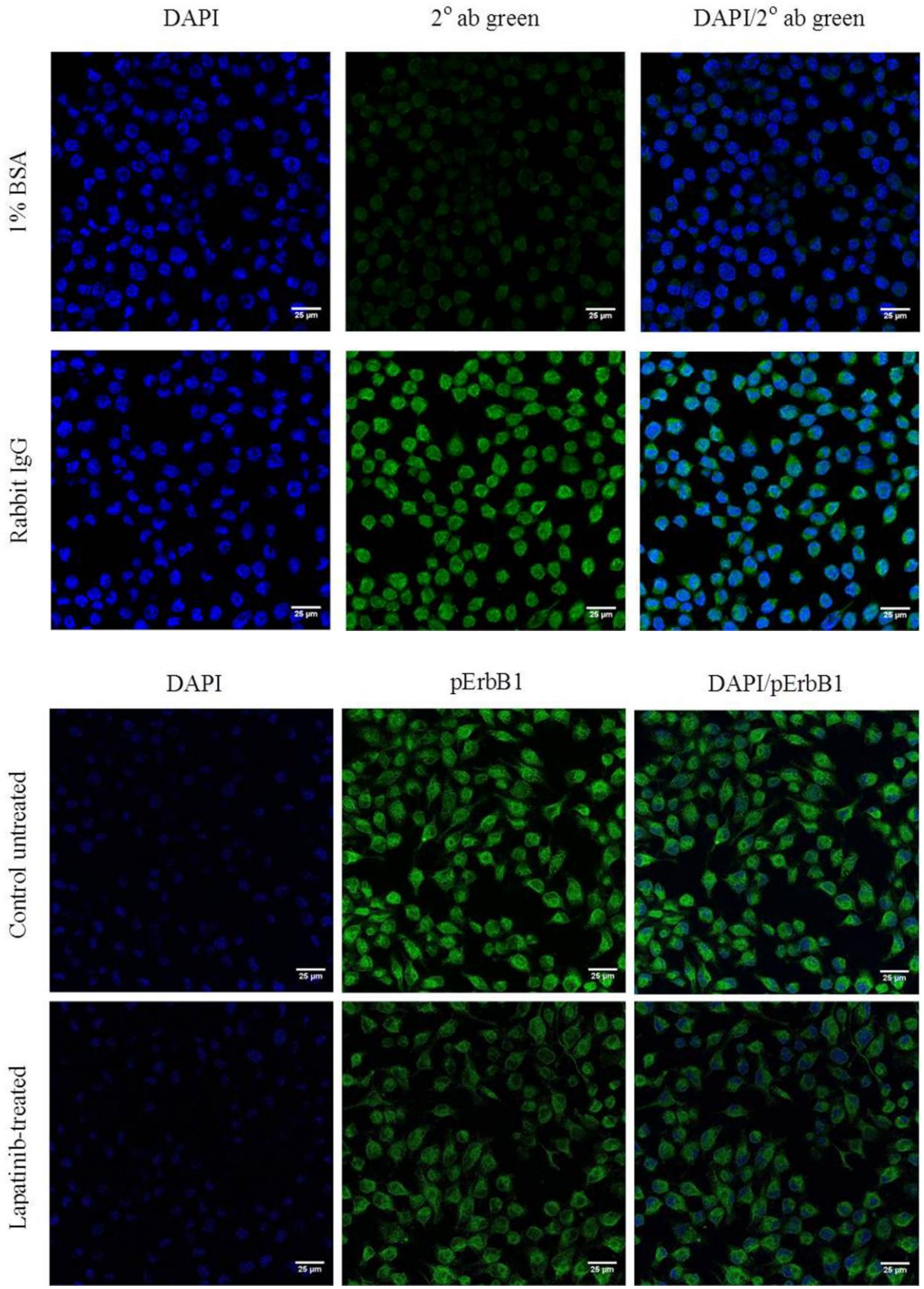

Figure 3.15. pErbB1 protein immunofluorescence staining in Walker 256 rat breast tumour cell line at 6 hours incubation. Images shown are control untreated and lapatinib-treated cells stained with DAPI, pErbB1 and overlay images of DAPI/pErbB1. Images are of x60 original magnification (Scale bar: 25 µm). Results were compared with negative controls (1% BSA and Rabbit IgG) stained with secondary antibody only.

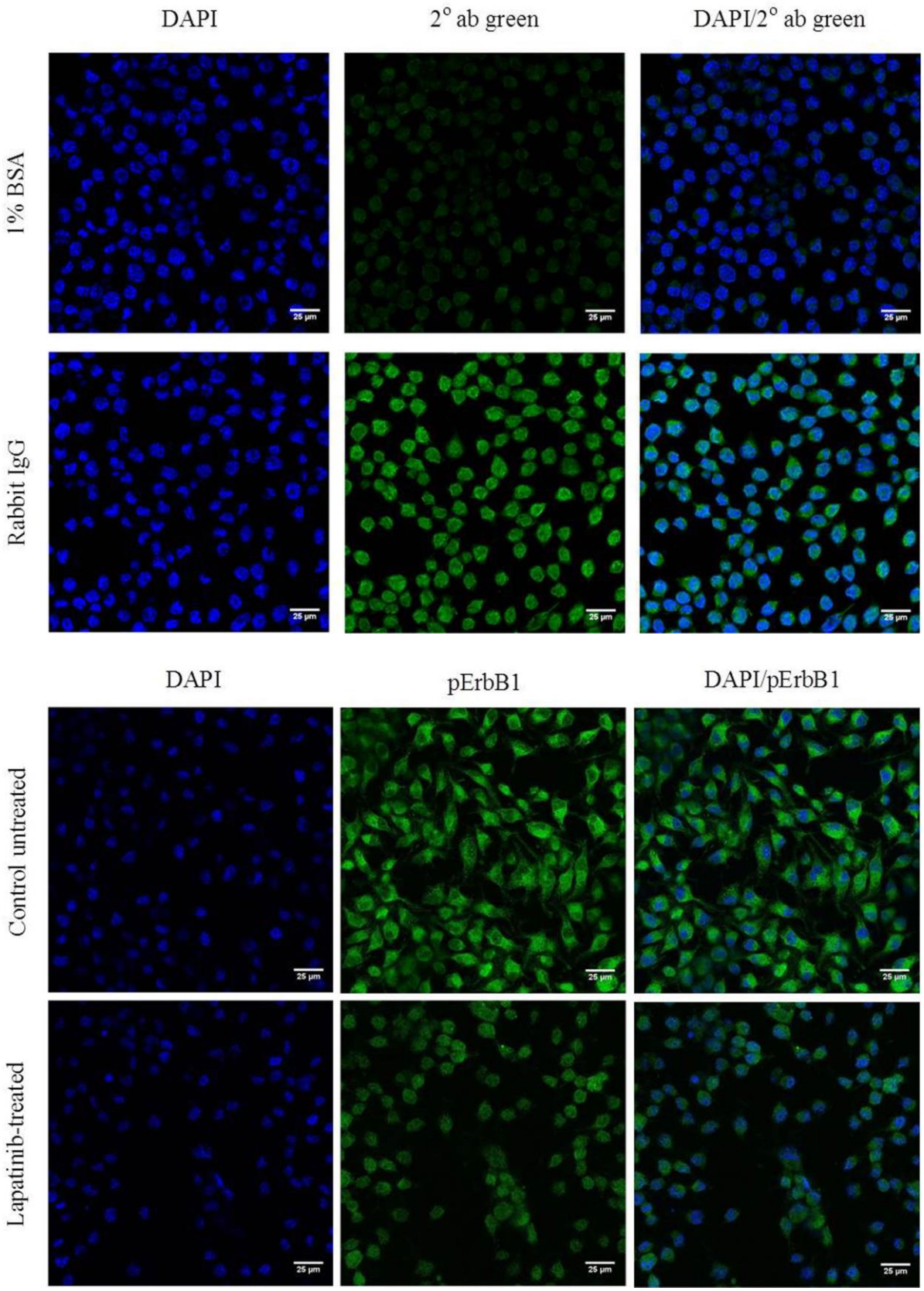

Figure 3.16. pErbB1 protein immunofluorescence staining in Walker 256 rat breast tumour cell line at 24 hours incubation. Images shown are control untreated and lapatinib-treated cells stained with DAPI, pErbB1 and overlay images of DAPI/pErbB1. Images are of x60 original magnification (Scale bar: 25 µm). Results were compared with negative controls (1% BSA and Rabbit IgG) stained with secondary antibody only.

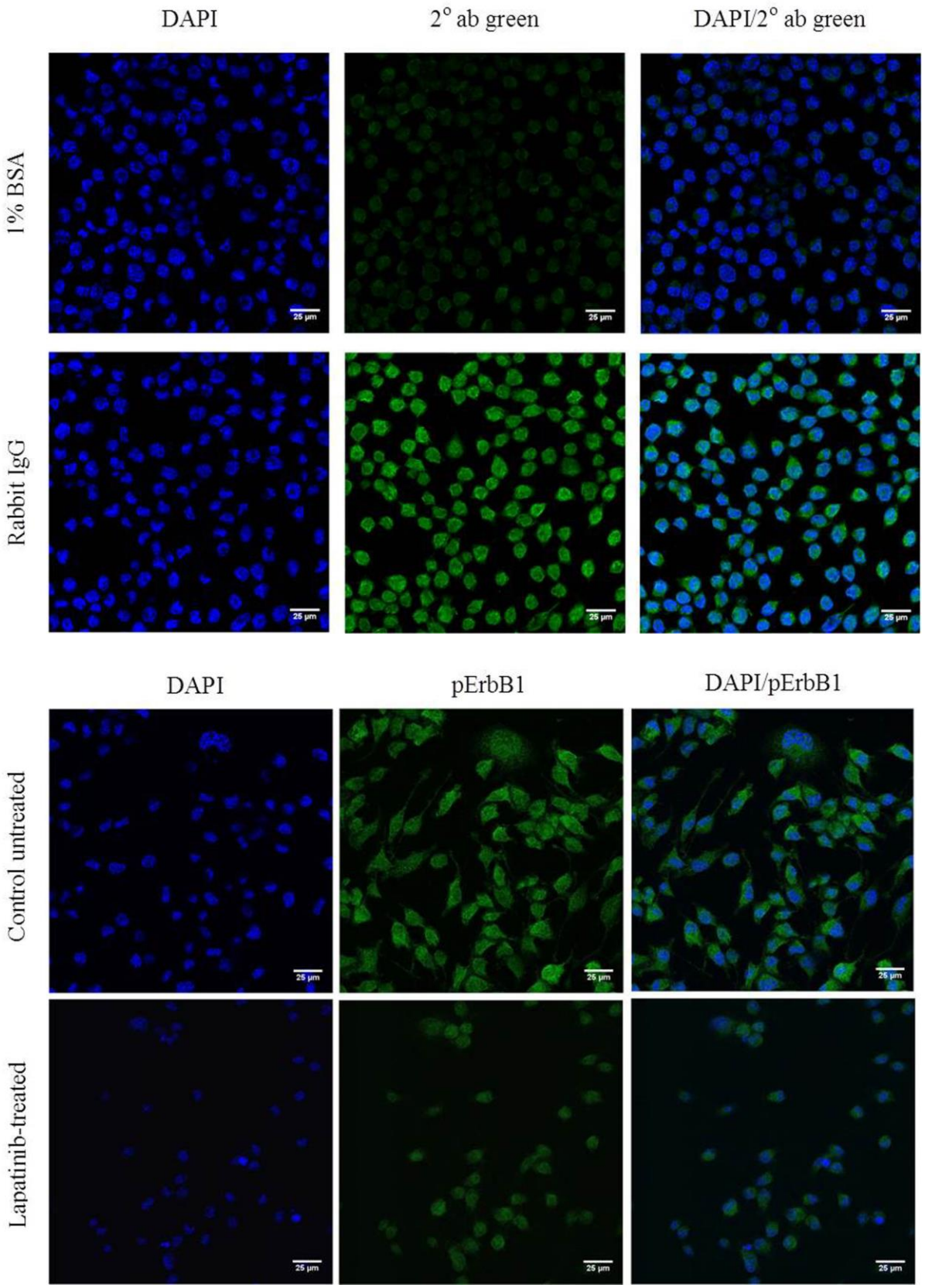

Figure 3.17. pErbB1 protein immunofluorescence staining in Walker 256 rat breast tumour cell line at 48 hours incubation. Images shown are control untreated and lapatinib-treated cells stained with DAPI, pErbB1 and overlay images of DAPI/pErbB1. Images are of x60 original magnification (Scale bar: 25 µm). Results were compared with negative controls (1% BSA and Rabbit IgG) stained with secondary antibody only.

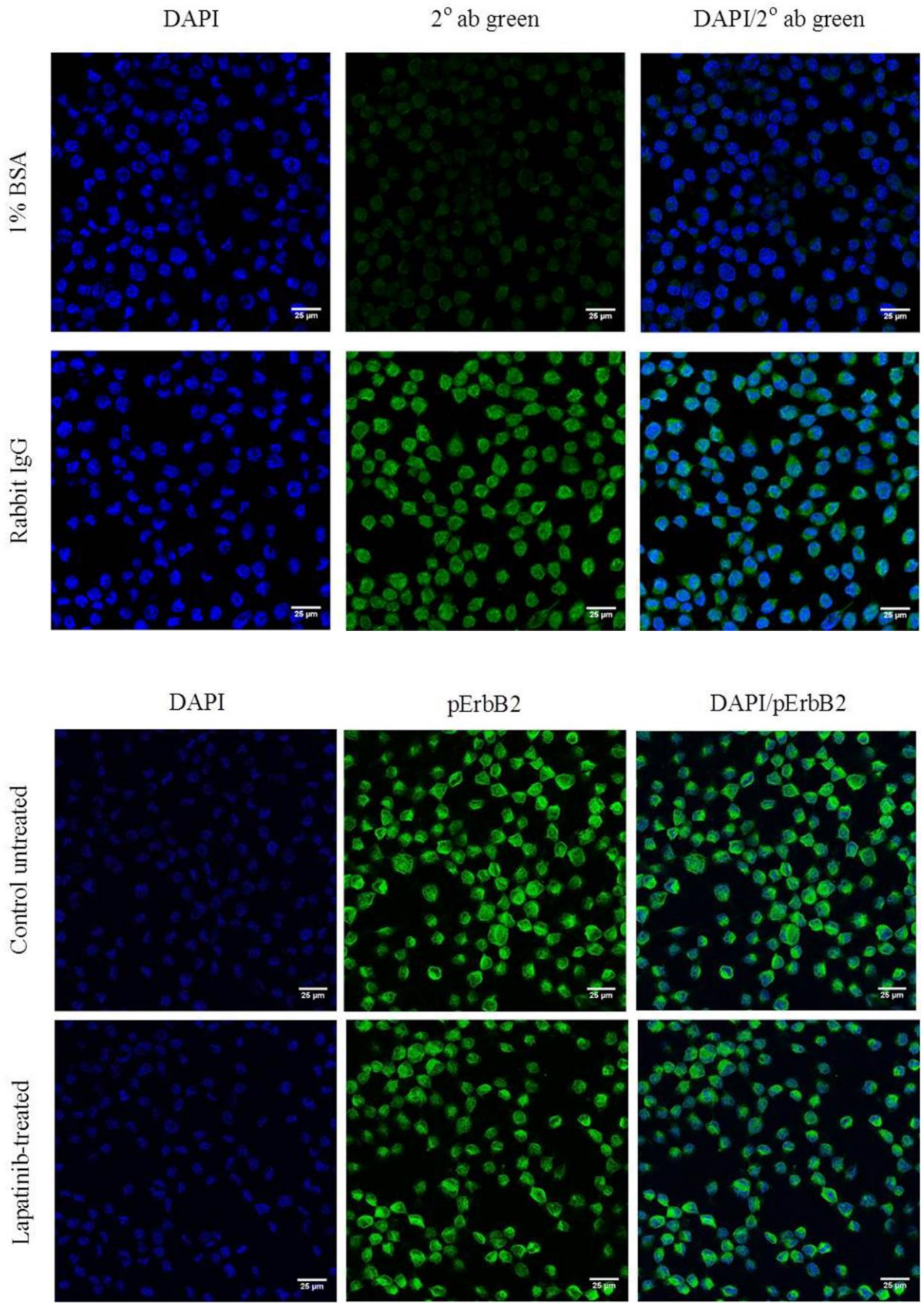

Figure 3.18. pErbB2 protein immunofluorescence staining in Walker 256 rat breast tumour cell line at 6 hours incubation. Images shown are control untreated and lapatinib-treated cells stained with DAPI, pErbB2 and overlay images of DAPI/pErbB2. Results were compared with negative controls (1% BSA and Rabbit IgG) stained with secondary antibody only.

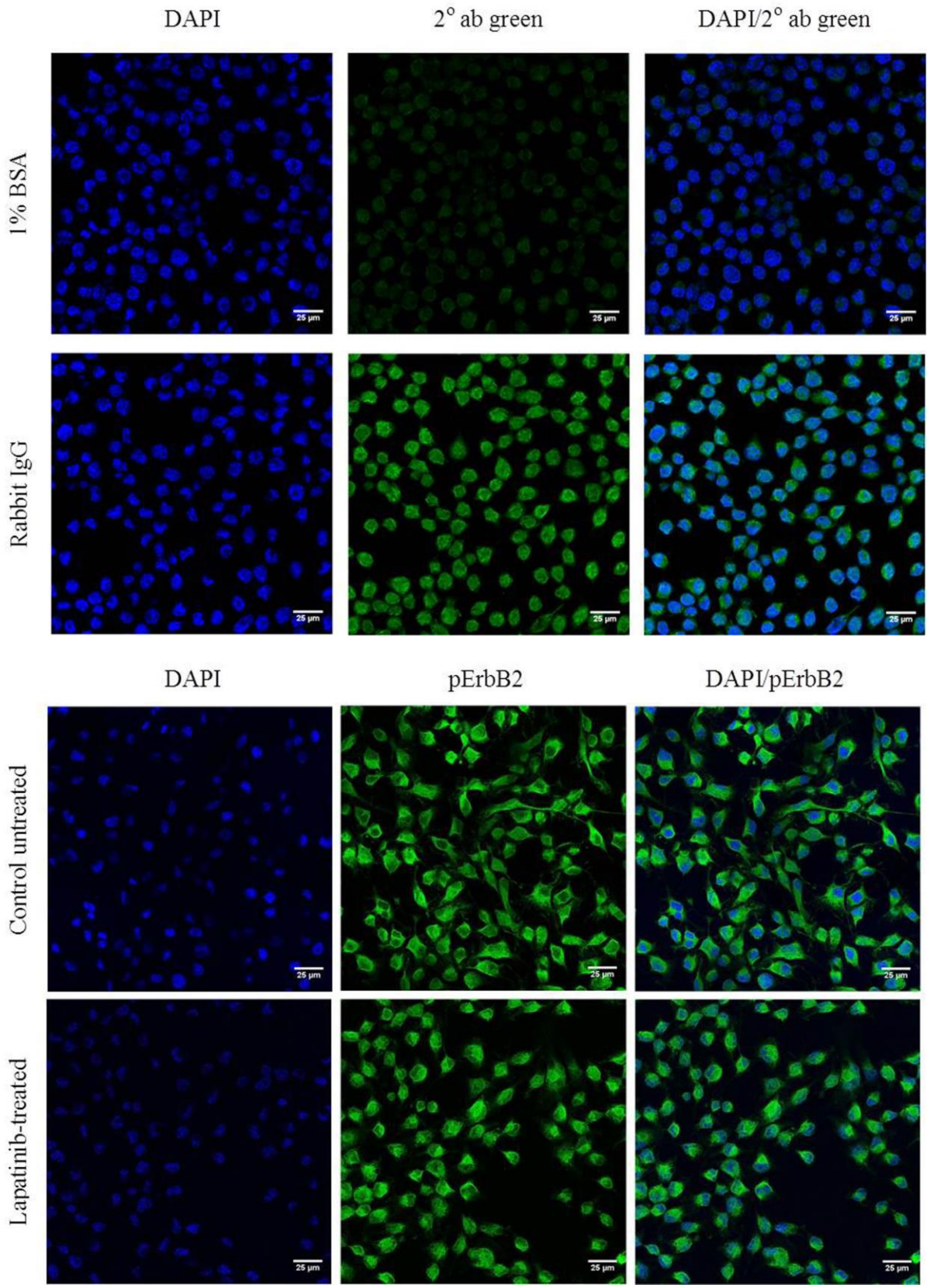

Figure 3.19. pErbB2 protein immunofluorescence staining in Walker 256 rat breast tumour cell line at 24 hours incubation. Images shown are control untreated and lapatinib-treated cells stained with DAPI, pErbB2 and overlay images of DAPI/pErbB2. Images are of x60 original magnification (Scale bar: 25 µm). Results were compared with negative controls (1% BSA and Rabbit IgG) stained with secondary antibody only.

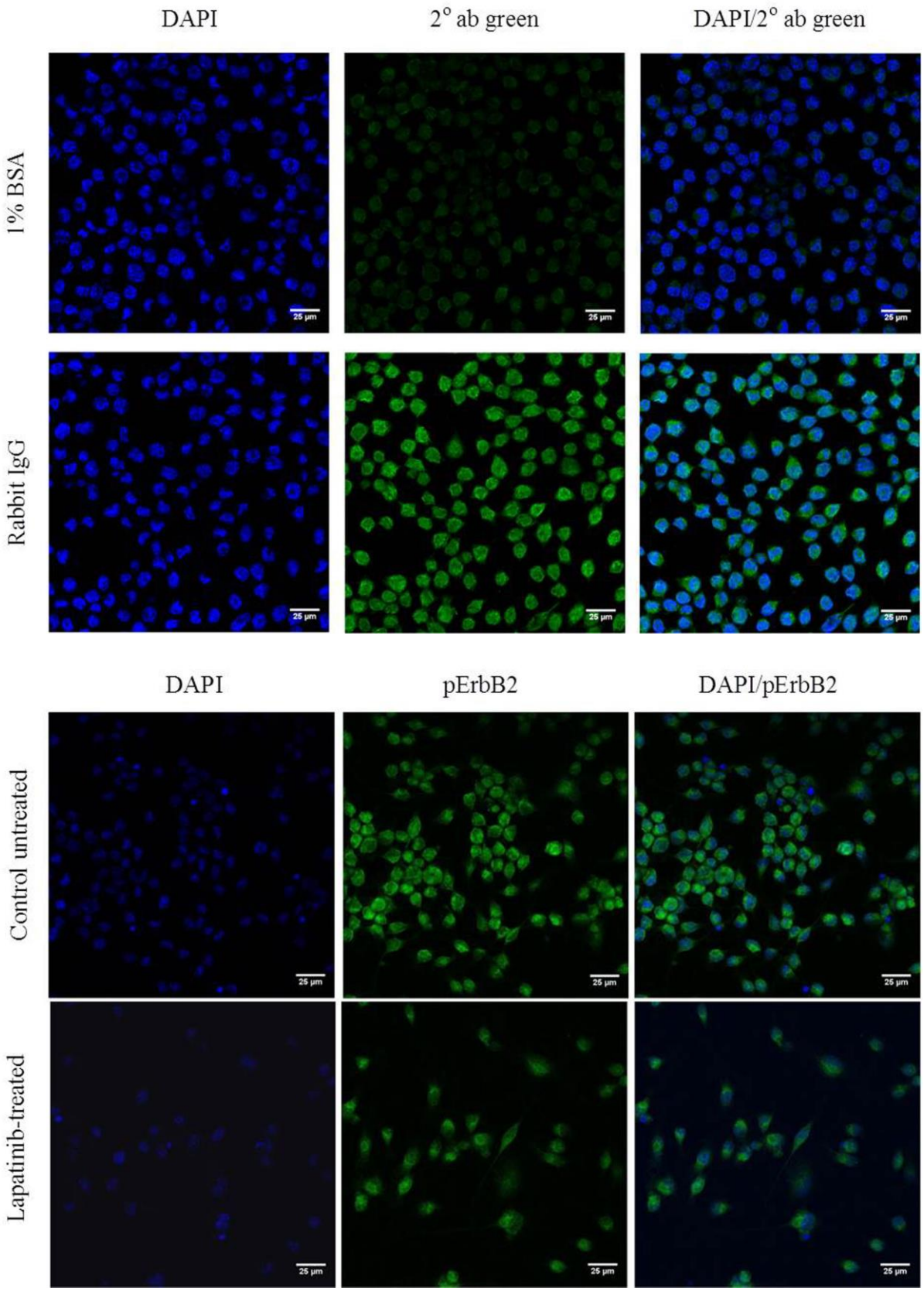

Figure 3.20. pErbB2 protein immunofluorescence staining in Walker 256 rat breast tumour cell line at 48 hours incubation. Images shown are control untreated and lapatinib-treated cells stained with DAPI, pErbB2 and overlay images of DAPI/pErbB2. Images are of x60 original magnification (Scale bar: 25 µm). Results were compared with negative controls (1% BSA and Rabbit IgG) stained with secondary antibody only.

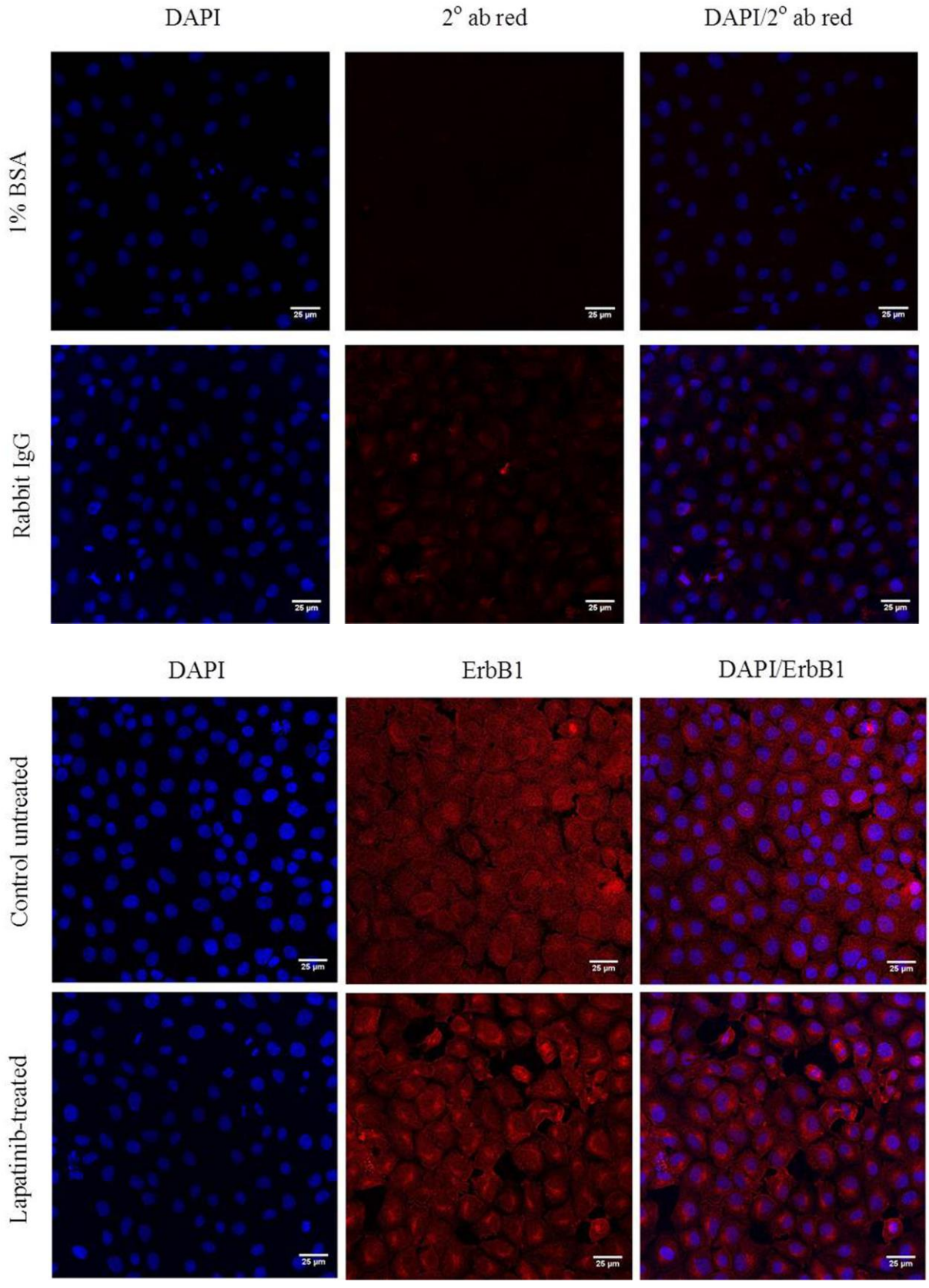

Figure 3.21. ErbB1 protein immunofluorescence staining in IEC-6 rat jejunal cell line at 6 hours incubation. Images shown are control untreated and lapatinib-treated cells stained with DAPI, ErbB1 and overlay images of DAPI/ErbB1. Images are of x60 original magnification (Scale bar: 25 µm). Results were compared with negative controls (1% BSA and Rabbit IgG) stained with secondary antibody only.

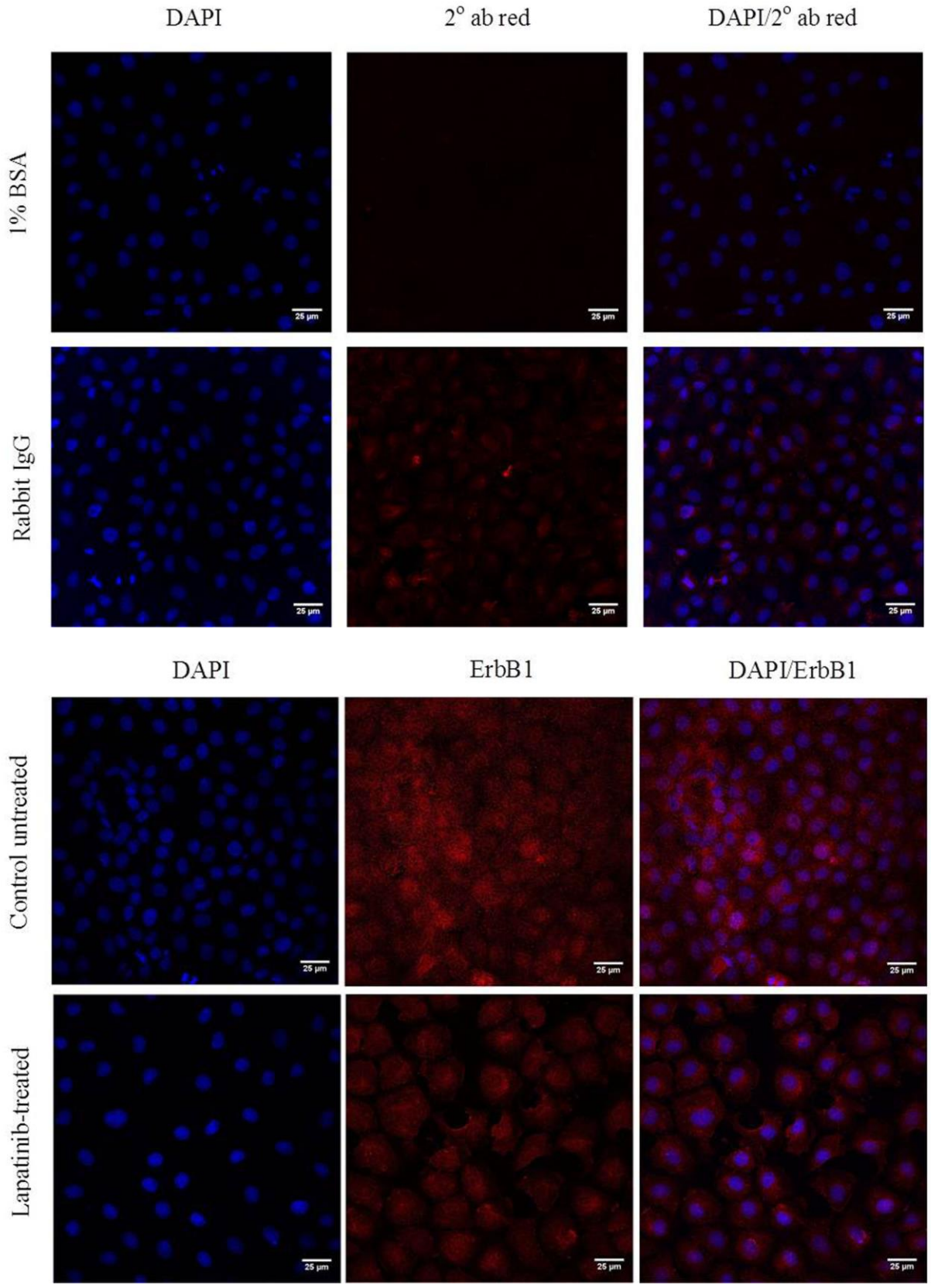

Figure 3.22. ErbB1 protein immunofluorescence staining in IEC-6 rat jejunal cell line at 24 hours incubation. Images shown are control untreated and lapatinib-treated cells stained with DAPI, ErbB1 and overlay images of DAPI/ErbB1. Images are of x60 original magnification (Scale bar: 25 µm). Results were compared with negative controls (1% BSA and Rabbit IgG) stained with secondary antibody only.

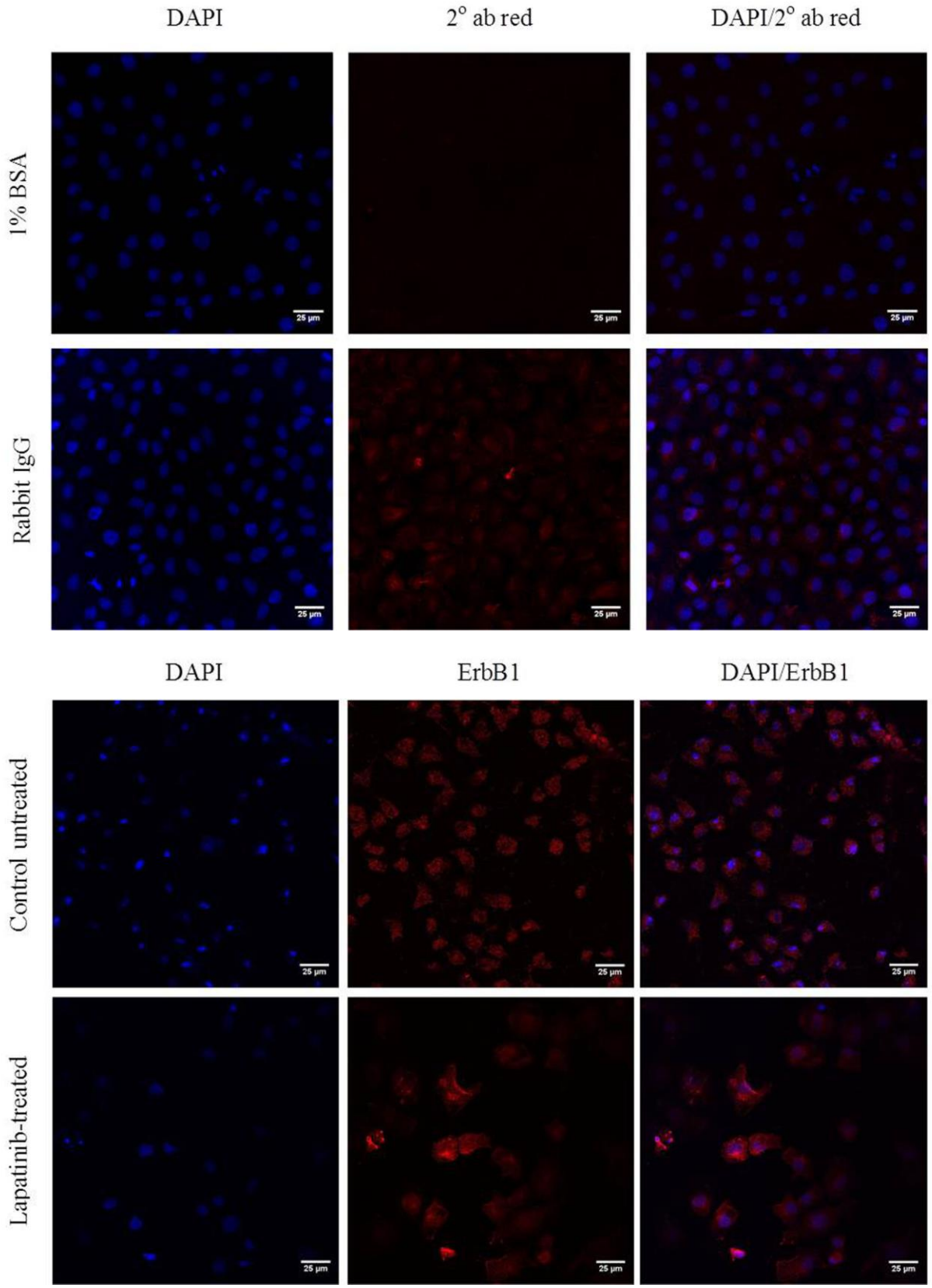

Figure 3.23. ErbB1 protein immunofluorescence staining in IEC-6 rat jejunal cell line at 48 hours incubation. Images shown are control untreated and lapatinib-treated cells stained with DAPI, ErbB1 and overlay images of DAPI/ErbB1. Images are of x60 original magnification (Scale bar: 25 µm). Results were compared with negative controls (1% BSA and Rabbit IgG) stained with secondary antibody only.

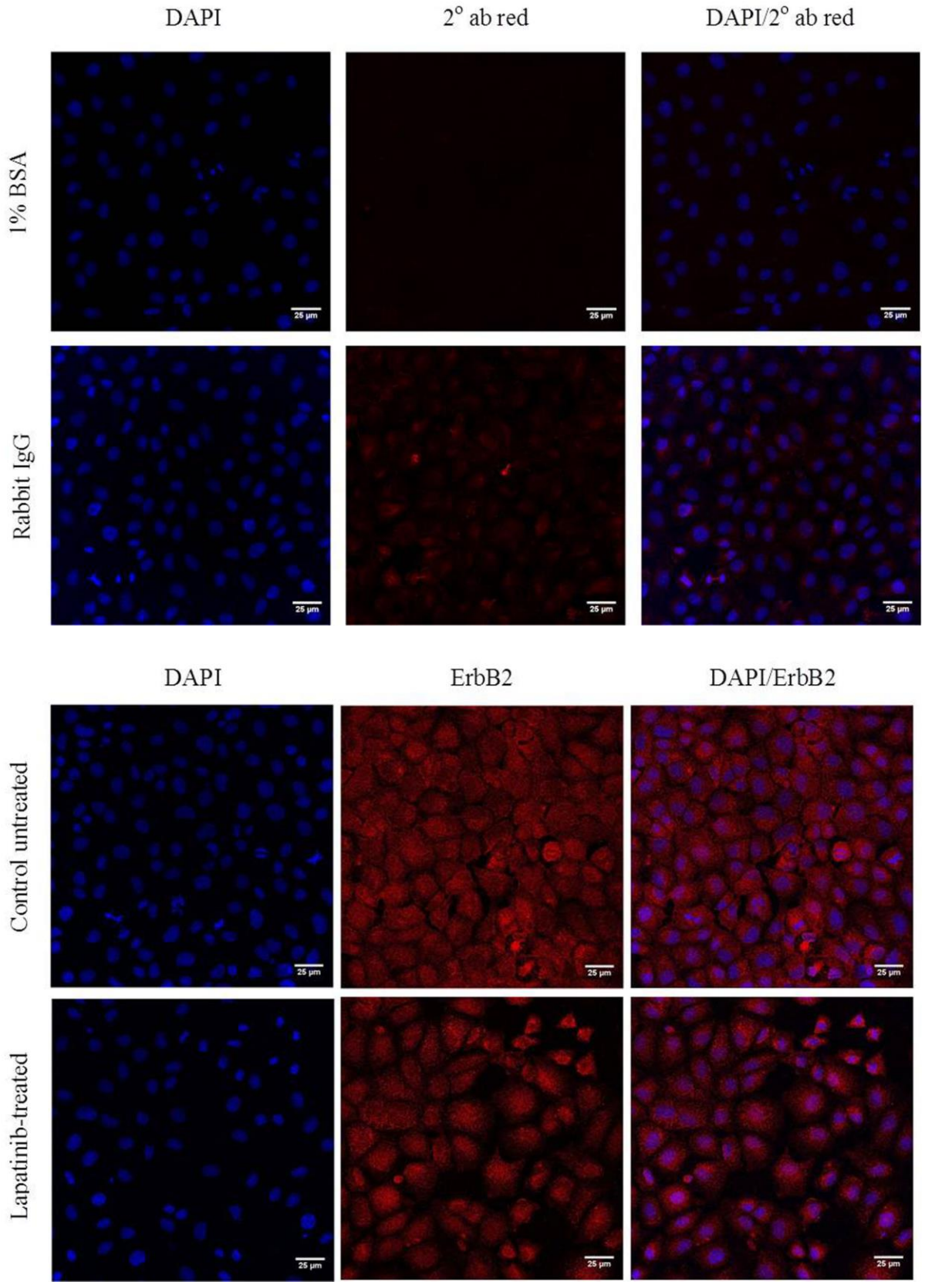

Figure 3.24. ErbB2 protein immunofluorescence staining in IEC-6 rat jejunal cell line at 6 hours incubation. Images shown are control untreated and lapatinib-treated cells stained with DAPI, ErbB2 and overlay images of DAPI/ErbB2. Images are of x60 original magnification (Scale bar: 25 µm). Results were compared with negative controls (1% BSA and Rabbit IgG) stained with secondary antibody only.

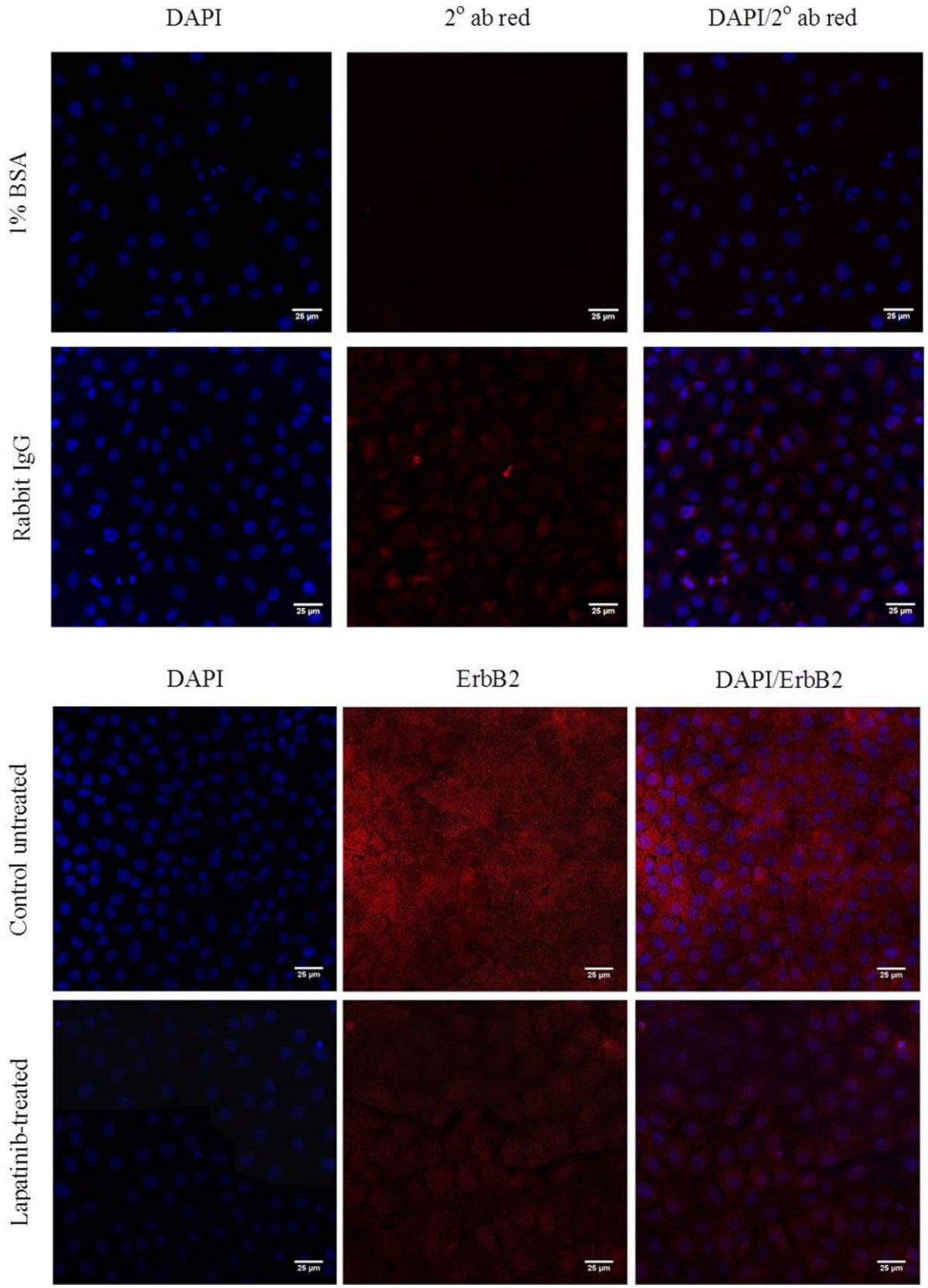

Figure 3.25. ErbB2 protein immunofluorescence staining in IEC-6 rat jejunal cell line at 24 hours incubation. Images shown are control untreated and lapatinib-treated cells stained with DAPI, ErbB2 and overlay images of DAPI/ErbB2. Images are of x60 original magnification (Scale bar: 25 µm). Results were compared with negative controls (1% BSA and Rabbit IgG) stained with secondary antibody only.

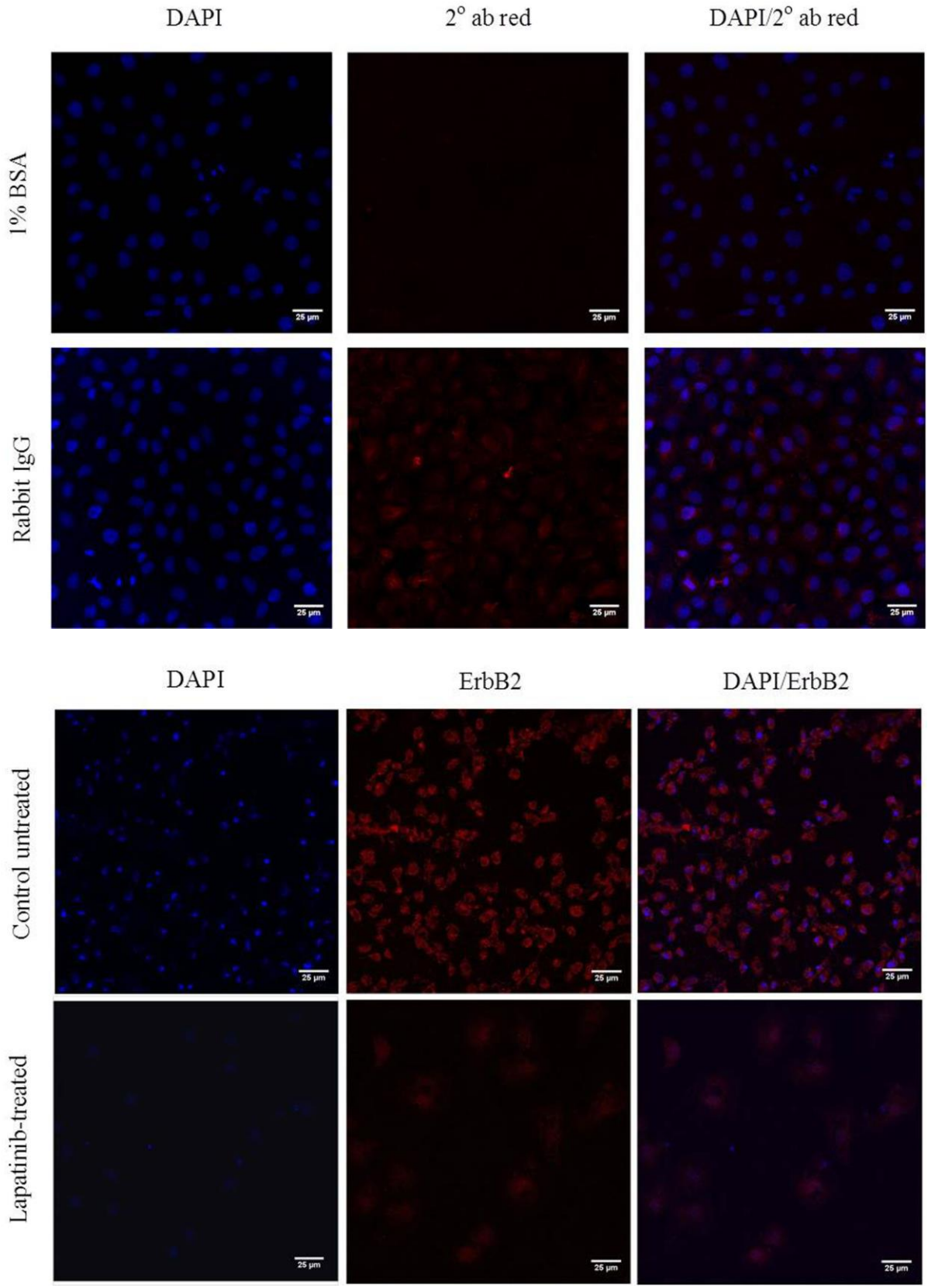

Figure 3.26. ErbB2 protein immunofluorescence staining in IEC-6 rat jejunal cell line at 48 hours incubation. Images shown are control untreated and lapatinib-treated cells stained with DAPI, ErbB2 and overlay images of DAPI/ErbB2. Images are of x60 original magnification (Scale bar: 25 µm). Results were compared with negative controls (1% BSA and Rabbit IgG) stained with secondary antibody only.

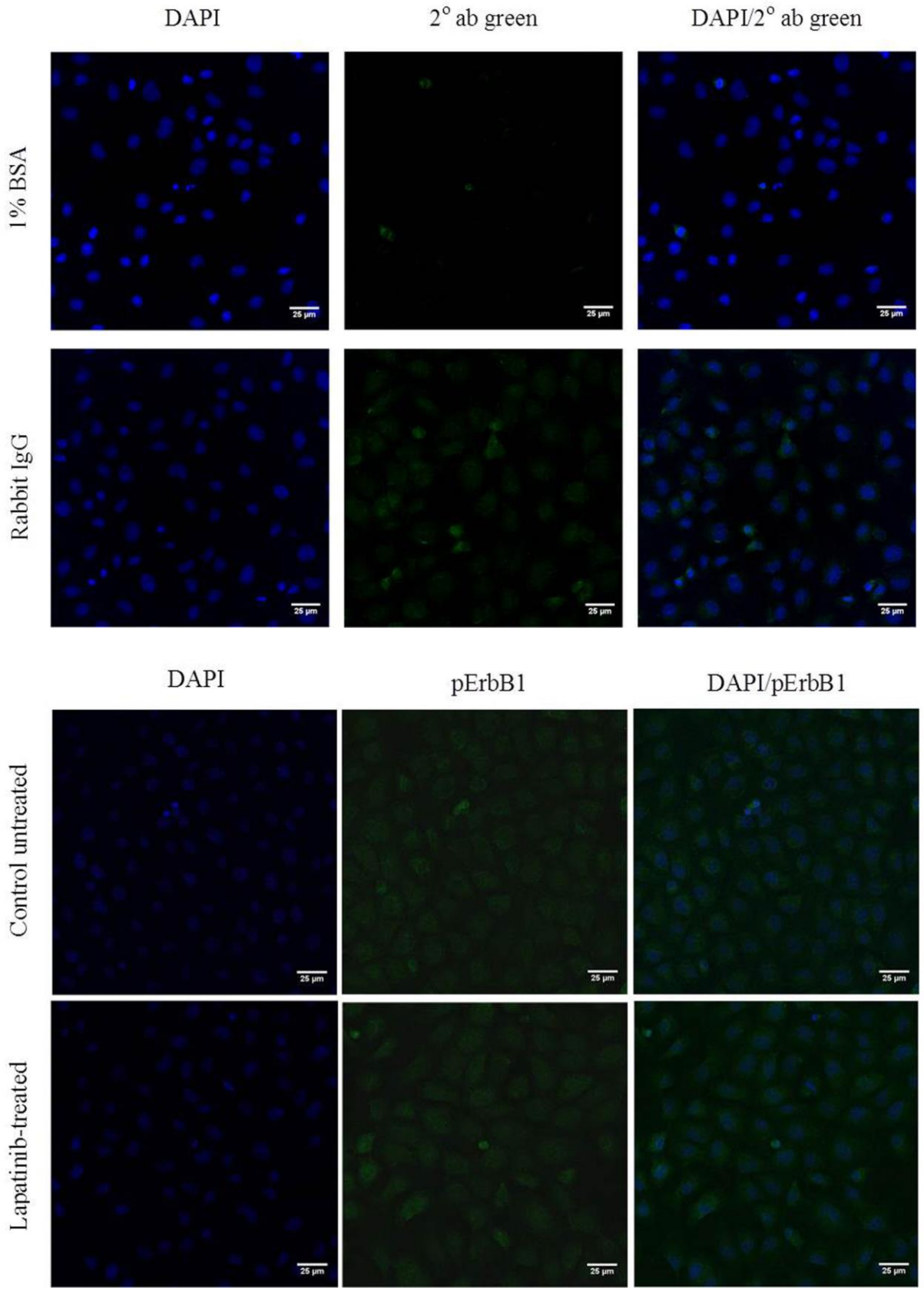

Figure 3.27. pErbB1 protein immunofluorescence staining in IEC-6 rat jejunal cell line at 6 hours incubation. Images shown are control untreated and lapatinib-treated cells stained with DAPI, pErbB1 and overlay images of DAPI/pErbB1. Images are of x60 original magnification (Scale bar: 25 µm). Results were compared with negative controls (1% BSA and Rabbit IgG) stained with secondary antibody only.

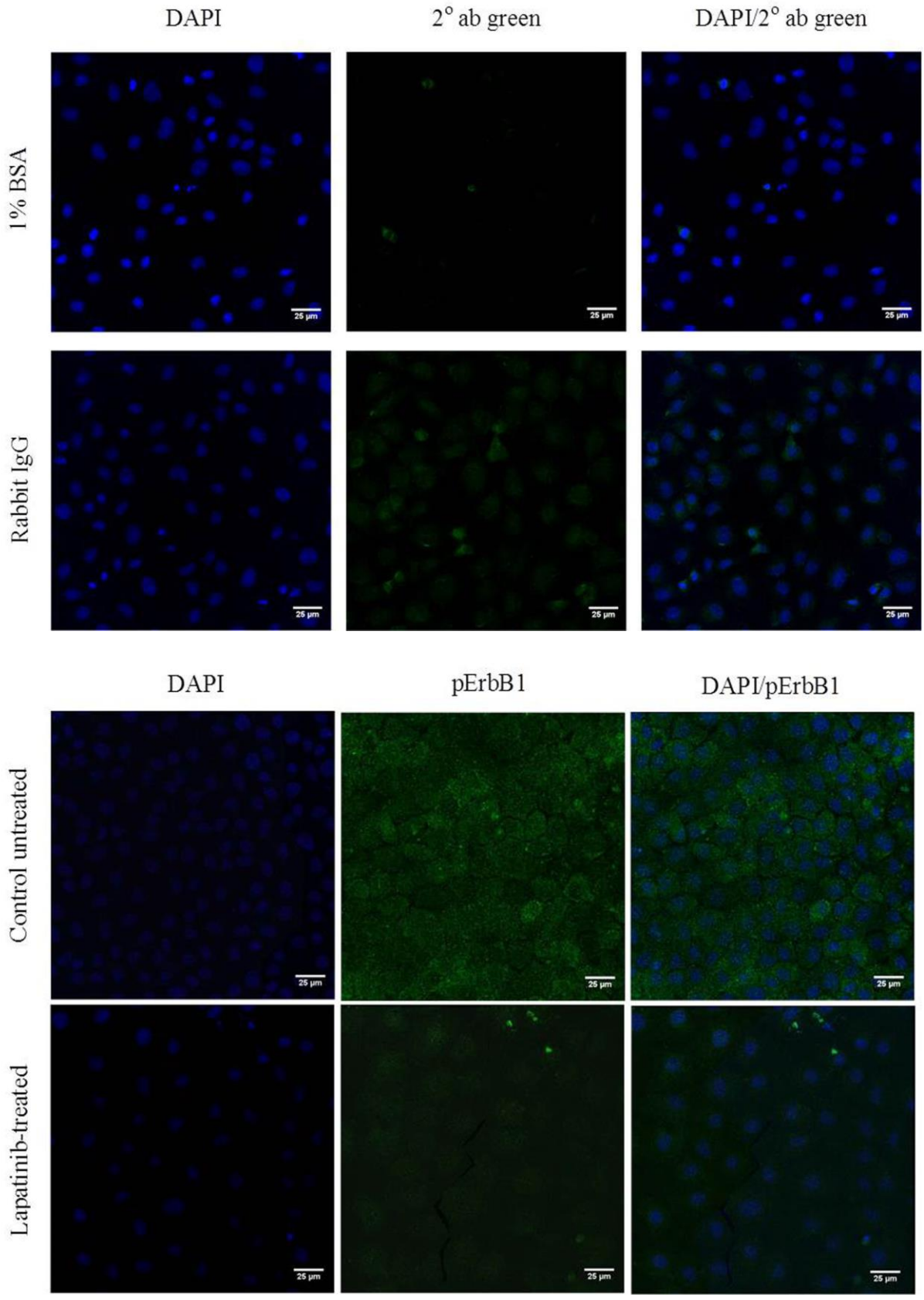

Figure 3.28. pErbB1 protein immunofluorescence staining in IEC-6 rat jejunal cell line at 24 hours incubation. Images shown are control untreated and lapatinib-treated cells stained with DAPI, pErbB1 and overlay images of DAPI/pErbB1. Images are of x60 original magnification (Scale bar: 25 µm). Results were compared with negative controls (1% BSA and Rabbit IgG) stained with secondary antibody only.

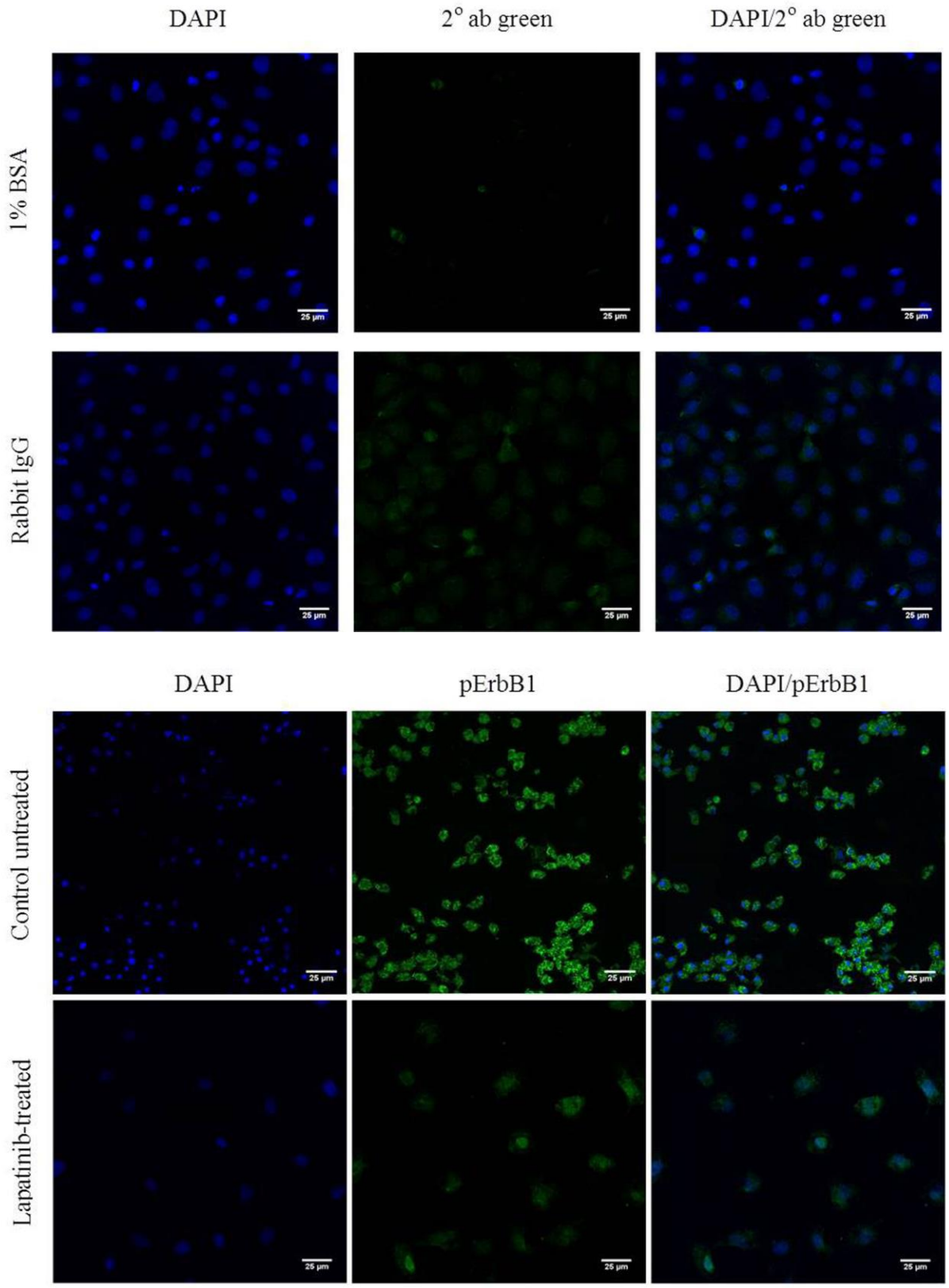

Figure 3.29. pErbB1 protein immunofluorescence staining in IEC-6 rat jejunal cell line at 48 hours incubation. Images shown are control untreated and lapatinib-treated cells stained with DAPI, pErbB1 and overlay images of DAPI/pErbB1. Images are of x60 original magnification (Scale bar: 25 µm). Results were compared with negative controls (1% BSA and Rabbit IgG) stained with secondary antibody only.

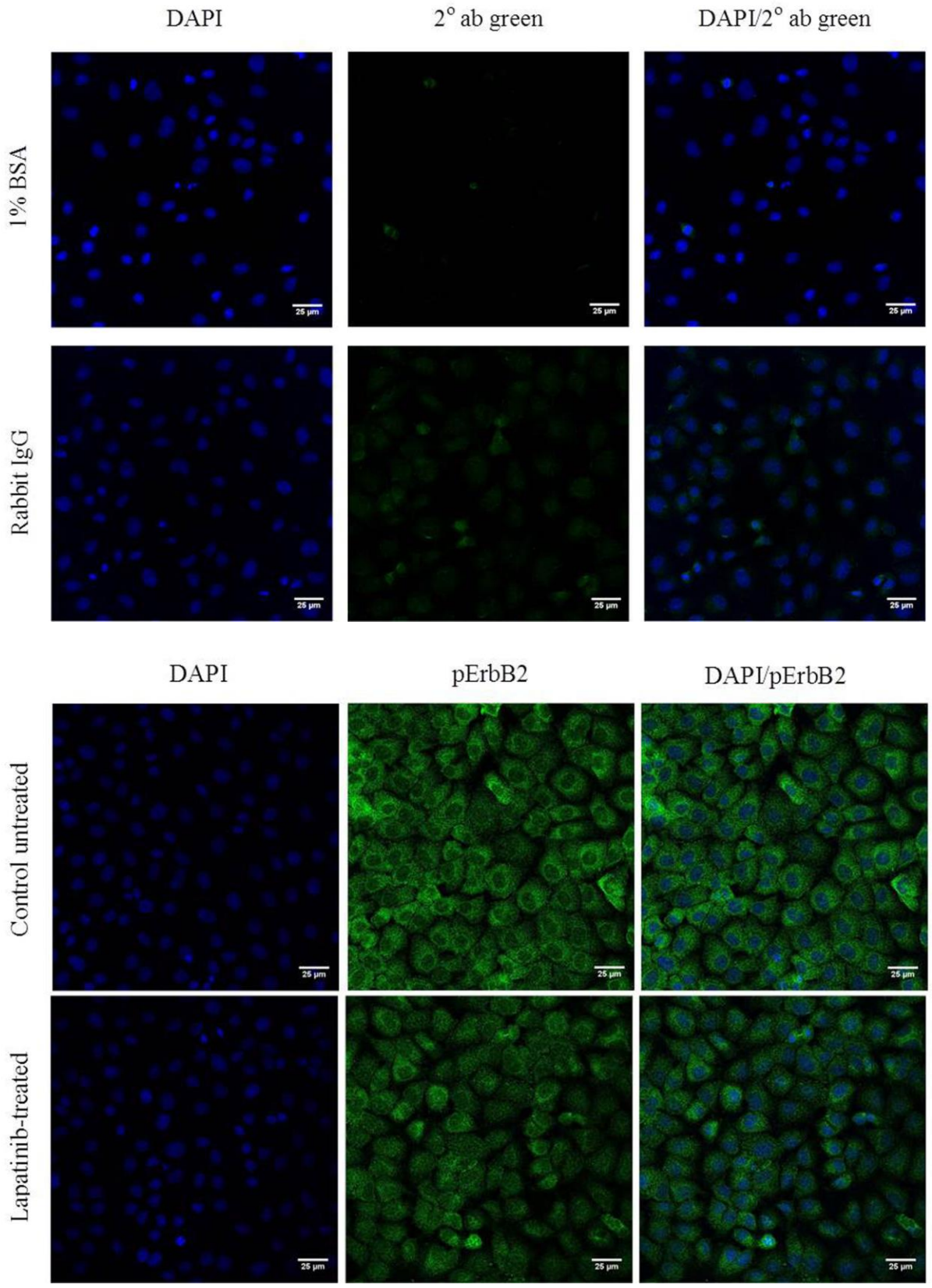

Figure 3.30. pErbB2 protein immunofluorescence staining in IEC-6 rat jejunal cell line at 6 hours incubation. Images shown are control untreated and lapatinib-treated cells stained with DAPI, pErbB2 and overlay images of DAPI/pErbB2. Images are of x60 original magnification (Scale bar: 25 µm). Results were compared with negative controls (1% BSA and Rabbit IgG) stained with secondary antibody only.

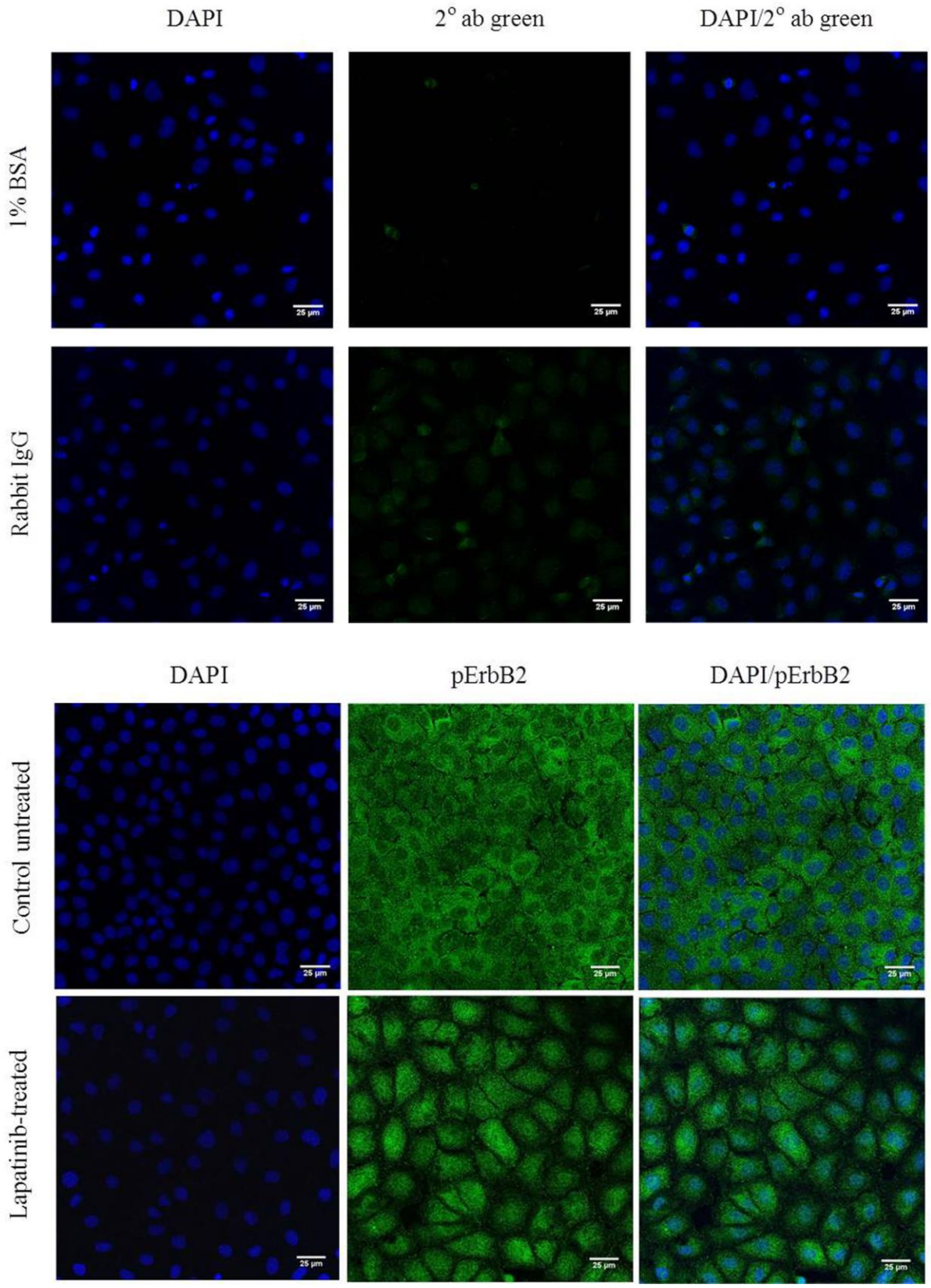

Figure 3.31. pErbB2 protein immunofluorescence staining in IEC-6 rat jejunal cell line at 24 hours incubation. Images shown are control untreated and lapatinib-treated cells stained with DAPI, pErbB2 and overlay images of DAPI/pErbB2. Images are of x60 original magnification (Scale bar: 25 µm). Results were compared with negative controls (1% BSA and Rabbit IgG) stained with secondary antibody only.

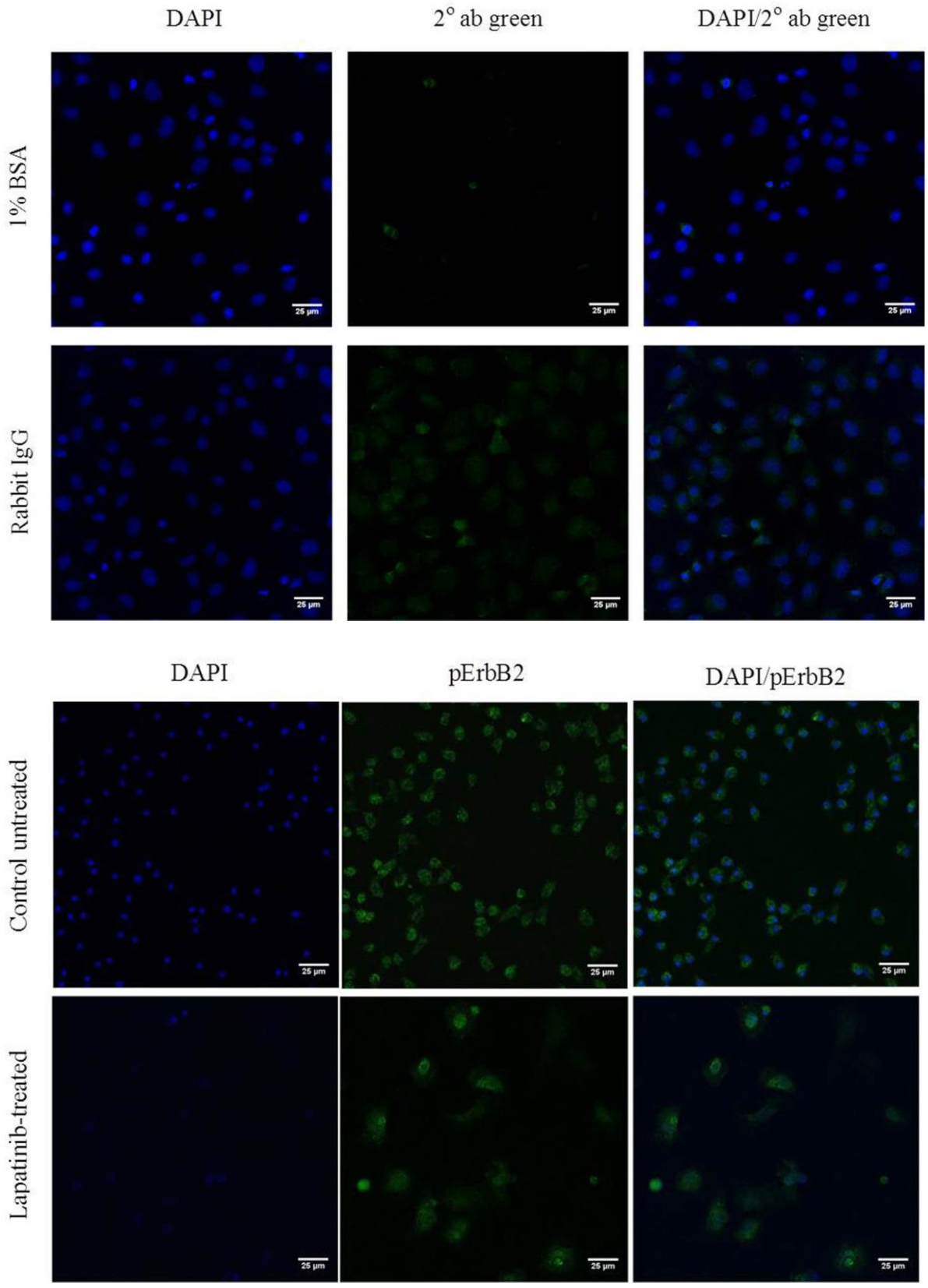

Figure 3.32. pErbB2 protein immunofluorescence staining in IEC-6 rat jejunal cell line at 48 hours incubation. Images shown are control untreated and lapatinib-treated cells stained with DAPI, pErbB2 and overlay images of DAPI/pErbB2. Images are of x60 original magnification (Scale bar: 25 µm). Results were compared with negative controls (1% BSA and Rabbit IgG) stained with secondary antibody only.

3.4 Discussion

Lapatinib is a dual inhibitor of ErbB1/ErbB2 which is used to treat ErbB2-positive breast cancer. The formation of ErbB1/ErbB2 or ErbB2/ErbB3 heterodimers can enhance the ligand binding, receptor tyrosine phosphorylation and cell proliferation compared to ErbB1 homodimers, thus, lapatinib has superior potency compared to single inhibitors of ErbB1 in inhibiting signal transduction of tumour proliferation and survival pathways (Johnston and Leary 2006).

Evaluation of the antiproliferative effect of lapatinib on rat breast tumour and jejunal cell lines indicated that lapatinib showed cytotoxic effects on both cell lines. The cytotoxic effect of lapatinib on Walker 256 rat breast tumour and IEC-6 rat jejunal cell lines was confirmed via XTT assay and trypan blue exclusion method. However, it was shown that lapatinib is more potent in inhibiting jejunal cell growth compared to breast tumour cell growth. The IC_{50} value of lapatinib on Walker 256 rat breast tumour cell line (8.2 µM) was comparable to the IC_{50} value of lapatinib on human breast tumour cell lines; CAMA-1 (8.3 µM) and MDA-MB-435 (8.5 µM) (Konecny, Pegram et al. 2006). While IEC-6 rat jejunal cell line (3.03 µM) showed slightly higher IC_{50} compared to HME human normal mammary (1.34 µM), but lower than HFF human fibroblast (6.45 µM) (Rusnak, Alligood et al. 2007). The cytotoxic effect of lapatinib on IEC-6 rat jejunal was not able to be compared with either human or rat normal intestinal cells as lapatinib has never been tested on these cell lines. Lapatinib also has never been tested on rat tumour cell lines. It is noted that all of the human cell lines mentioned above possessed moderate or low levels of both ErbB1 and ErbB2 (Konecny, Pegram et al. 2006, Rusnak, Alligood et al. 2007), although lapatinib showed higher cytotoxic effects on the cell lines.

In the current study, the cytotoxic effect of lapatinib also showed an increase with the increasing incubation period, which was observed in trypan blue exclusion results. This is

may be explained in part by the fact that cells were maintained in serum-free media following addition of lapatinib or vehicle; this may have sensitised the cells after 24 hours and caused a greater response to lapatinib. However, results showed no major decrease in viability of control untreated cells based on XTT and trypan blue exclusion experiments. Thus suggesting that lapatinib may have sensitised both normal intestinal and breast tumour cells to cytotoxicity rather than the serum-deprived medium. Previous study has reported that treatment with chemotherapeutic agent also sensitises normal human epithelial cells to cell death which may pose a risk of developing chemotherapy-induced toxicity (Finnberg, Gokare et al. 2016).

In FACS analysis, the mechanisms of cell death induced by lapatinib on Walker 256 and IEC-6 cells were evaluated. Cells that were treated with lapatinib at different incubation periods were then sorted and were classified as viable, early apoptosis, late apoptosis and necrosis. Viable cells have an intact membrane, while early apoptotic cells are dying cells in which the plasma membrane remains intact but exposes phosphatidylserine (PS) on the cell surface to mediate its recognition by phagocytes. Early apoptotic cells can become late apoptotic cells, also known as secondary necrotic cells, when the plasma membrane becomes permeabilised (Gregory and Devitt 2004, Elmore 2007). Alternatively, direct exposure of healthy viable cells to trauma, such as extreme temperature or, mechanical and chemical insults, can lead to the generation of membrane-permeabilised necrotic cells which are also known as primary necrotic cells (Gregory and Devitt 2004, Elmore 2007). Lapatinib was shown to induce early apoptosis in Walker 256 tumour cells at early incubation with lapatinib, however at 48 hours incubation, lapatinib induced necrosis in Walker 256 tumour cells. In IEC-6 cells, lapatinib induced late apoptosis at 24 hours as well as at 48 hours incubation. This findings show that lapatinib causes tumour cell necrosis which explains the drug's role in tumour inhibition, however, lapatinib-induced late apoptosis in intestinal cells might well be

involved in gastrointestinal toxicity which leads to diarrhoea in patients administered with the drug. Nevertheless, further investigation such as cell cycle analysis will further clarify the mechanism of cell death induced by lapatinib on both tumour and normal intestinal cells.

A significant decrease of viable cells in lapatinib-treated Walker 256 cells were observed at 6 hours incubation using FACS analysis. This is in contrast with the results obtained in trypan blue exclusion assay that showed a significant decrease in viable cells only at 48 hours. However, different method has different principles and techniques that may contribute to the discrepancy in the viable cells (Altman, Randers et al. 1993).

Previous studies have reported that at a very high level of ErbB2 expression, lapatinib sensitivity is increased, while at a lower level of ErbB2, lapatinib sensitivity is decreased. The lowest sensitivity of lapatinib is mostly seen in cell lines with a low level of ErbB2 and nearly undetectable levels of ErbB1 (Rusnak, Alligood et al. 2007). These findings support the results obtained from this study which showed lower *ErbB2* mRNA expression and undetectable *ErbB1* mRNA expression in Walker 256 rat breast tumour cells, thus explaining lower sensitivity of lapatinib on this cell line. Although Walker 256 breast tumour cells are less sensitive towards lapatinib due to lower *ErbB2* mRNA expression and undetectable *ErbB1* mRNA expression, the drug exhibited cytotoxic effect on the cell line, suggesting involvement of other unknown mechanisms which could be an off-target cytotoxic effect (Rudmann 2012). The possible reason could also be lapatinib inhibition on ErbB2/ErbB3 heterodimers. However, the expression of *ErbB3* mRNA was not assessed in this study as lapatinib is known to be targeting ErbB1 and ErbB2. Furthermore, lower *ErbB2* mRNA expression was observed in Walker 256 with no significant difference between untreated and lapatinib-treated cells, showing no significant inhibition on *ErbB2* mRNA expression. Expression of *ErbB3* mRNA as well as other *ErbB* receptor mRNAs also has never been tested in Walker 256. Thus, further investigation is required as other mechanism might

contribute to lapatinib cytotoxic properties on Walker 256 rat breast tumour cells. The relatively high *ErbB1* and *ErbB2* mRNA expression in IEC-6 jejunal cells compared to Walker 256 tumour cells may partially explain differential sensitivity to lapatinib.

Lapatinib inhibited Walker 256 rat breast tumour cell proliferation but with lower cytotoxic effect that could be due to lower *ErbB2* mRNA with *ErbB1* mRNA was not able to be detected in the cells. The drug induced necrosis in Walker 256 rat breast tumour cells, explaining the drug's role in tumour inhibition. In contrast, lapatinib exhibited higher cytotoxic effect on the IEC-6 rat jejunal cells that could be due to higher levels of *ErbB1* and *ErbB2* mRNAs in IEC-6 cells. The drug induced IEC-6 rat jejunal cell death via late apoptosis which might well cause gastrointestinal toxicity. Previous works have proven lapatinib ability to reduce tyrosine phosphorylation of ErbB1 and ErbB2, and inactivation of Erk1/2 and AKT, the downstream effectors of cell proliferation and cell survival, respectively (Xia, Mullin et al. 2002, Wood, Truesdale et al. 2004, Konecny, Pegram et al. 2006, Zhou, Li et al. 2006). However, in this study the downstream mechanism of cell death induced by lapatinib on both Walker 256 rat breast tumour and IEC-6 rat jejunal cells are not known. Further investigations will be able to explain the downstream mechanisms.

The expression and localisation of all four proteins (ErbB1, ErbB2, pErbB1 and pErbB2) in Walker 256 and IEC-6 cells were seen in the immunofluorescence staining. In Walker 256, the negative control which was incubated with Rabbit IgG only showed high immunoreactivity which was shown by comparable staining with the cells that was incubated with primary antibodies. However, it has to be noted that the concentration of Rabbit IgG used in this study was higher than the concentration of all primary antibodies except pErbB2. Thus, based on the images obtained in results, ErbB1, ErbB2 and pErbB1 might be expressed in Walker 256 cells but in lower amounts. Similar to pErbB2, though the negative control showed high immunoreactivity, however based on the images obtained, pErbB2 might also be

expressed in Walker 256 but in a very low amount. In IEC-6, the negative control which was incubated with Rabbit IgG only showed low immunoreactivity. Thus, all four proteins were expressed in both control untreated and lapatinib-treated Walker 256 and IEC-6 cells. Control untreated and lapatinib-treated cells did not show much difference in staining intensity at different incubation hours, except at 48 hours incubation in which both control untreated and lapatinib-treated showed lower staining intensity as well as lower cell counts. This could be due to prolonged incubation with lapatinib and/or serum-deprived medium for lapatinib-treated and control untreated samples, respectively. Previous studies have shown decrease of growth factor expression in terms of relative protein expression following incubation with tyrosine kinase inhibitors (Konecny, Pegram et al. 2006, Takahashi, Lee et al. 2016), yet, as far as is known, no study has been carried out to show decrease of growth factor expression in term of staining intensity following incubation with tyrosine kinase inhibitors or serum starvation.

Both mRNA expression of *ErbB1* and *ErbB2*, as well as immunofluorescence staining of ErbB1, ErbB2, pErbB1 and pErbB2 showed no differences between control untreated and lapatinib-treated cells. This is a limitation in immunofluorescence staining in this study as the quantitative comparison in staining intensity was not able to be carried out due to different cell counts between control untreated and lapatinib-treated samples, wherein most of the lapatinib-treated samples showed lower cell counts which would give a lower percentage of staining intensity when compared to control untreated. Comparison of upregulation or downregulation between all four proteins tested in the cell lines was also not able to be done due to varied cell counts. This limitation could be overcome by conducting an experiment such as Western blot analysis, which would enable determination of relative protein expression, as well as evaluation of lapatinib effects on all four proteins and not just overall expression, as in the current experiment.

Testing of another intestinal and breast tumour cell line may also support further understanding of lapatinib cytotoxic effects and its underlying mechanisms. However, it is impossible due to the time-frame of this study. Nevertheless, it is important to note that this study provides the first information on effect of lapatinib on rat breast tumour cells which may contribute to the understanding of its usage in developing animal tumour model to study tyrosine kinase inhibitor-induced diarrhoea.

Although *ErbB1* mRNA expression was undetectable in Walker 256 cells, both ErbB1 and pErbB1 protein expression were observed via immunofluorescence staining. However, as mentioned earlier in the results, the intensity of expression of secondary antibody in the Walker 256 cells treated with Rabbit IgG only was comparatively the same as the Walker 256 cells treated with all four primary antibodies, especially at 6 and 24 hours incubation. This may indicate that all four proteins might be expressed in lower amounts in Walker 256 cells, which could be supported by the lower mRNA expression. As far as is known, no studies have been conducted to determine mRNA expression of *ErbB1* or other ErbB family members in Walker 256 cells. Thus, further investigations are required to determine *ErbB* gene expression in Walker 256 cells. Importantly, an understanding of differential expression of lapatinib targets in cancer and normal gastrointestinal tissue may allow identification of diarrhoea intervention targets that could preferentially protect gastrointestinal epithelium.

3.5 Conclusion

In summary, lapatinib exhibited cytotoxic properties on ErbB1/ErbB2 expressing cell lines, with jejunal cells being more sensitive to lapatinib compared to tumour cells. Lapatinib induced necrosis in tumour cells, while inducing late apoptosis in jejunal cells. This may explain lapatinib-induced diarrhoea in patients administered with the drug which could be due to apoptosis of small intestinal epithelial cells leading to barrier disruption and consequently

diarrhoea. However, much remains to be learned on the molecular mechanisms related to lapatinib's cytotoxic effect.

3.6 Acknowledgements

Adelaide Microscopy Unit, University of Adelaide, South Australia.

Chapter 4

Development of a Walker 256 tumour-bearing rat model to study the effects of lapatinib on the intestine

4.1 Introduction

Diarrhoea is a major acute complication in the clinical setting that occurs in a large percentage of patients undergoing cytotoxic therapy, particularly targeted therapy (Widakowich, de Castro et al. 2007). One of the major problems with targeted therapy-induced mucosal injury is that the underlying mechanisms behind its development are not entirely understood. Animal models provide a critical source of knowledge when sampling from patients is unavailable or interventions are yet to be fully tested (Bowen, Gibson et al. 2011). This study focuses on developing a tumour-bearing animal model which will provide an opportunity to test a range of targeted drug treatment regimens in a more clinically relevant situation compared to previous work in non-tumour bearing animals. It is vital to develop a tumour-bearing animal model as patients receiving targeted drugs will have tumours. A study using mice with early-stage subcutaneous syngeneic grafts of various tumours have shown serious types of DNA damage which were double-strand breaks and oxidatively induced non-double-strand breaks clustered DNA lesions, which were elevated in tissues distant from the tumour site with most affected areas were crypts in the gastrointestinal tract organs and skin (Redon, Dickey et al. 2010). Thus, a tumour-bearing rat model is essential to assess lapatinib toxicity on the intestine.

In this study, a tumour-bearing Albino Wistar rat model was developed, based on previous preclinical work conducted in this strain of rat (Bowen 2014, Bowen, Mayo et al. 2014). It has also been shown that the Wistar rat has an appropriate metabolic profile to study the pathophysiological effects of tyrosine kinase inhibitors (TKIs) (EMEA 2008, Bowen,

Mayo et al. 2014). Besides that, the Walker 256 tumour cell line which was used to develop this model originated from a spontaneous tumour in a Wistar rat, making it ideal to study (details of Walker 256 cell line has been described in Chapter 3).

The median duration of lapatinib treatment in patients was 19.9 weeks with approximately 40% of patients treated with lapatinib monotherapy or combination therapy experienced a first diarrhoea event within 6 days of treatment initiation, with a median duration of 7 to 9 days (Crown, Burris et al. 2008, Di Leo, Gomez et al. 2008). From previous animal study, it was shown that lapatinib-induced diarrhoea developed 14 days post-initial treatment (Bowen, Mayo et al. 2012). As such, an appropriate rat tumour model is essential to study TKI-induced gut damage in which as the TKIs are given over long time course, thus the tumour needs to be slow growing. In this study Walker 256 which is a rat breast tumour cell was used to develop an appropriate rat tumour model to study TKI-induced gut damage, in particular lapatinib-induced gut damage. This is due to lapatinib is used to treat breast cancer, whereby Walker 256 is a breast cancer cell which would be appropriate to reflect breast cancer patient setting receiving lapatinib treatment.

The Walker 256 tumour-bearing rat model has been successfully used previously to investigate cancer-induced anorexia or cachexia (Bennani-Baiti and Walsh 2011), as well as to study the effect of anticancer drugs (He, Chen et al. 2003). In the current study, the optimum concentration of Walker 256 tumour cells to develop the rat tumour model was determined and the effect of the tumour on the intestines was also evaluated. The development of an appropriate tumour-bearing rat model to study lapatinib-induced diarrhoea will contribute to a better understanding of the mechanisms of diarrhoea in cancer patients treated with lapatinib and other TKIs.

4.2 Materials and Methods

4.2.1 Animals

Thirty six female albino Wistar rats weighing 200-350 g were used in this study. Experiments were carried out in three separate parts. All experimental procedures were approved by the Animal Ethics Committees of SA Pathology and the University of Adelaide. Rats were housed in groups upon arrival at the SA Pathology Animal Care Facility, and were allowed to acclimatise for one week. After tumour inoculation, animals were monitored twice daily and if an animal showed signs of excess distress due to tumour burden (criteria as defined by the Animal Ethics Committee) they were removed from the study. These criteria include >15% weight loss from original body weight, >10% tumour burden (by body weight), a dull ruffled coat with accompanying dull and sunken eyes, coolness to the touch with no spontaneous activity, or a hunched appearance.

4.2.2 Walker 256 tumour rat model

Walker 256 tumour cells were cultured and the tumour inoculum was prepared as described in Chapter 2 Sections 2.2 and 2.8. Rats were divided into 4 groups as follows: 1) control non-tumour, 2) $1x10^5$ Walker 256 cells in 0.1 ml PBS (injected into 1 flank) as according to a previously published protocol (Takasuna, Hagiwara et al. 2006), 3) $2x10^6$ Walker 256 cells in 0.2 ml PBS (injected into 1 flank) and 4) $2x10^6$ Walker256 cells in 0.2 ml PBS (injected into both flanks). The injection site was checked every day for tumour presence and any skin irritation and once the tumour was palpable, the tumour size was measured with digital callipers. Throughout the experiment, all rats had free access to chow and water. The rats were weighed every day and checked for clinical symptoms, including diarrhoea, weight loss, changes in temperament, changes in coat appearance, reluctance to move, and reduced food and water intake at least twice a day. The size of the tumour was

measured by digital callipers every day to assess growth and to enable an estimation of the tumour as a % of bodyweight. The following formulas were used to measure the tumour burden and tumour as % of bodyweight, and have been shown to accurately predict the weight of the tumour:

Tumour burden = (tumour width x tumour height) x tumour length) x $\pi/6$);

$$\text{Tumour as \% of bodyweight} = \frac{\text{Tumour burden}}{\text{Bodyweight}} \times 100$$

Once the tumour reached around 1% of bodyweight, the rats were separated into individual cages to avoid cagemates attacking the tumours and causing injury. Tumours were grown until tumour burden reached 10% of body weight.

At the end of the experiment, all animals were killed by deep anaesthesia before cardiac puncture and cervical dislocation. Blood, tumours and intestines were collected for analysis.

As experiments were carried out in separate parts, it was shown in the first part that rats injected with $1x10^5$ Walker 256 cells in 0.1 ml PBS into 1 flank exhibited either very slow growing tumours or regressing tumours which were not ideal for this study. Thus sample size for rats injected with $2x10^6$ Walker 256 cells in 0.2 ml into 1 flank and $2x10^6$ Walker 256 cells in 0.2 ml into both flanks were increased to 12 in which the tumour growth for both groups were much ideal for this study. Sample size for control non-tumour group remained as 6 while $1x10^5$ Walker 256 cells in 0.1 ml PBS (injected into 1 flank) group was also 6 rats.

4.2.3 Blood analysis

Blood samples were collected by cardiac puncture. Serum was separated by centrifugation at 18, 000 xg for 5 minutes before being analysed by the Department of Clinical Pathology, SA Pathology, Adelaide, South Australia. A multiple blood analysis (serum biochemistry) was carried out which includes measurements for sodium, potassium, chloride, bicarbonate, anion gap, glucose, urea, creatinine, cholesterol, urate, phosphate, total calcium, albumin, globin, protein, total bilirubin, lactate dehydrogenase (LD) and liver enzymes such as gamma-glutamyl transferase (GGT), alkaline phosphatase (ALP), alanine aminotransferase (ALT) and aspartate aminotransferase (AST). Complete blood analysis (blood haematology) was also carried out which includes measurements of haemoglobin, red blood cells, packed cell volume (P.C.V.), mean corpuscular volume (M.C.V.), mean corpuscular haemoglobin (M.C.H.), mean corpuscular haemoglobin concentration (M.C.H.C.) red blood cell distribution width (R.D.W.), platelet count, white cell count, and white cell components such as neutrophils, lymphocytes, monocytes, eosinophils and basophils.

4.2.4 Histological examination

This method was carried out to characterise the histopathological characteristics of the Walker 256 tumour, and to evaluate possible tumour-induced histopathological changes in jejunum and colon. The detailed procedures are described in Chapter 2 Section 2.10.

4.2.5 Measurement of villus height and crypt depth in colon and jejunum

This method was carried out to determine any histopathological changes in jejunum and colon. The methods are described in Chapter 2 (Section 2.11).

4.2.6 Immunohistochemistry of caspase-3 and Ki-67

Markers of apoptosis (caspase-3) and proliferation (Ki-67) in jejunum, colon and tumour were detected via immunohistochemistry. The detailed procedures are described in Chapter 2 (Section 2.12).

4.2.7 Real-time PCR

This method was carried out to determine the mRNA expression of *ErbB1* and *ErbB2* in the Walker 256 tumour. As lapatinib is known to inhibit *ErbB1* and *ErbB2*, it is important to evaluate the mRNA expression of both genes in the Walker 256 tumour. Details of the method were explained in Chapter 2 (Section 2.3.2-2.7).

4.2.8 Statistical analysis

All data are presented as mean ± S.E.M. Results for blood analysis, villus and crypt length measurement, caspase-3 and Ki-67 protein detection in jejunum, colon and tumour as well as real-time PCR were statistically analysed using two-way ANOVA with Tukey's multiple comparisons test to compare means of each group, except for results of caspase-3 and Ki-67 detection in growing and regressing Walker 256 tumours which were analysed via unpaired *t*-test. Statistical significance was accepted as $p<0.05$.

4.3 Results

4.3.1 Body weight

Rats injected with $1x10^5$ cells/0.1 ml (1 flank) gained 0.92 %±4.00 weight average over the experimental period. This was not statistically significant from other groups. Rats injected with $2x10^6$ cells/0.2 ml (1 flank) group lost 3.71 ± 5.00 % weight on average, while rats injected with $2x10^6$ cells/0.2 ml (both flanks) lost 1.48 ± 4.61 % weight on average over the experimental period. These were statistically significant from the control non-tumour

group that gained 1.11 ± 1.94 % weight on average; $p<0.01$ and $p<0.05$, respectively (Figure 4.1).

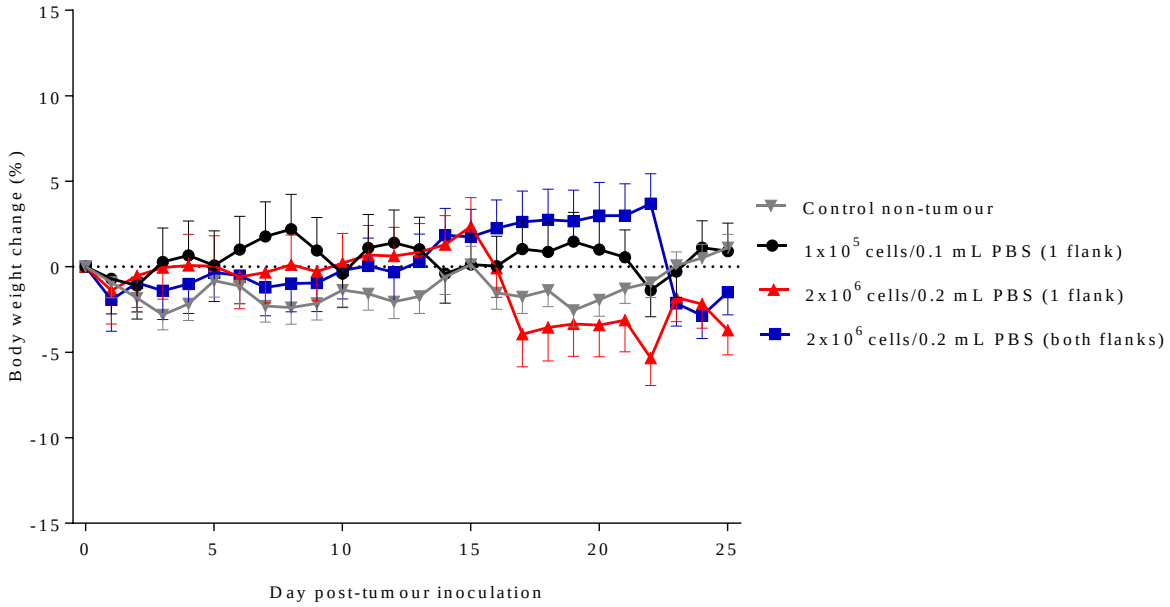

Figure 4.1. Percentage weight change after Walker 256 tumour inoculation. Data presented as mean ± S.E.M (n=6 for control non-tumour, n=6 for $1x10^5$ cells/0.1 ml PBS (1 flank), n=12 for $2x10^6$ cells/0.2 ml PBS (1 flank) and n=12 for $2x10^6$ cells/0.2 ml PBS (both flanks)).

4.3.2 Tumour growth

Rats injected with $1x10^5$ cells/0.1 ml (1 flank) showed a maximum tumour burden of less than 1% of the body weight and showed regression at day 23 post-tumour inoculation (Figure 4.2). Rats injected with $2x10^6$ cells/0.2 ml (1 flank) showed tumour growth, with the tumour burden reaching 10% body weight on day 25 post inoculation (Figure 4.2). However, the tumour burden for the rats which were injected with the same tumour concentration but in both flanks reached 10% of the body weight on day 15 post-tumour inoculation (Figure 4.2).

During the studies, half of the rats in each group - 3 of 6 rats in $1x10^5$ cells/0.1 ml (1 flank), 6 of 12 rats in $2x10^6$ cells/0.2 ml (1 flank) and 6 of 12 rats in $2x10^6$ cells/0.2 ml (both flanks) - showed tumour regression. The tumour regression results are presented in Figure 4.3. In the groups injected with $2x10^6$ cells/0.2 ml into 1 flank and both flanks, the tumours started to regress on day 15 post-tumour inoculation (Figure 4.3). In the group that was

injected with $1x10^5$ cells/0.1 ml into 1 flank, some of the rats showed tumour growth at less than 0.1% of body weight and some of the rats did not show any tumour growth (Figure 4.3).

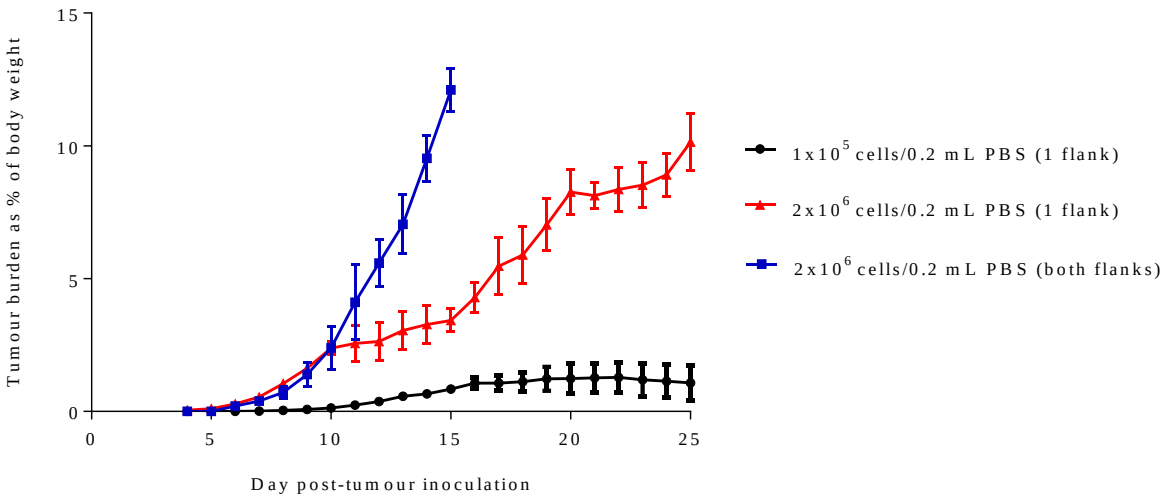

Figure 4.2. Walker 256 tumour growth with different tumour cell concentrations. Data presented as mean ± S.E.M (n=3 for $1x10^5$ cells/0.1 ml PBS (1 flank), n=6 for $2x10^6$ cells/0.2 ml PBS (1 flank) and n=6 for $2x10^6$ cells/0.2 ml PBS (both flanks)).

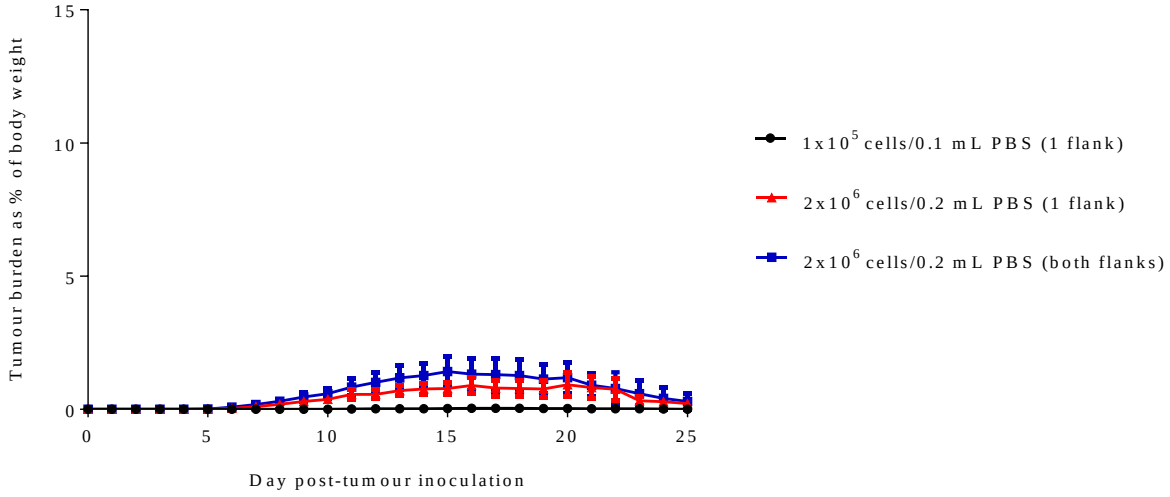

Figure 4.3. Walker 256 tumour regression with different tumour cell concentration. Data presented as mean ± S.E.M (n=3 for $1x10^5$ cells/0.1 ml PBS (1 flank), n=6 for $2x10^6$ cells/0.2 ml PBS (1 flank) and n=6 for $2x10^6$ cells/0.2 ml PBS (both flanks)).

4.3.3 Blood analysis

Rats injected with $1x10^5$ cells/0.1 ml (1 flank) had a significantly increased chloride level (103.00 ± 1.00 mmol/L) ($p<0.01$) and decreased anion gap (13.50 ± 0.5 mmol/L) ($p<0.01$), creatinine level (22.50 ± 1.19 mmol/L) ($p<0.0001$) and lactate dehydrogenase (LD) level (434.00 ± 78 mmol/L) ($p<0.001$) compared to control non-tumour-bearing rats; (99.17 ± 1.49 mmol/L, 19.00 ± 2.08 mmol/L, 32.33 ± 4.31 mmol/L and 1213.33 ± 510.95 mmol/L) respectively (Table 4.1).

Sodium (140.14 ± 0.91 mmol/L) ($p<0.01$) and bicarbonate (28.14 ± 0.77 mmol/L) ($p<0.05$) levels were increased in rats inoculated with $2x10^6$ cells/0.2 ml (1 flank) compared to control non-tumour-bearing rats (137.00 ± 1.37 mmol/L, 25.33 ± 1.26 mmol/L), while the anion gap (14.83 ± 1.19 mmol/L) ($p<0.01$), creatinine (16.43 ± 1.02 µmol/L) ($p<0.0001$) and LD (572.50 ± 75.42 U/L) ($p<0.0001$) levels were decreased compared to controls (Table 4.1).

Rats inoculated with $2x10^6$ cells/0.2 ml (both flanks) showed a decrease in glucose (6.91 ± 0.34 mmol/L) ($p<0.01$) and creatinine (20.63 ± 2.19 µmol/L) ($p<0.0001$) levels compared to control non-tumour-bearing rats (8.43 ± 0.69 mmol/L, 32.33 ± 4.31 µmol/L) and did not show any significant increases in other components tested as compared to controls ($p>0.05$) (Table 4.1).

Significant differences were also observed between tumour-bearing rat groups, including rats inoculated with $2x10^6$ cells/0.2 ml (1 flank) had a higher bicarbonate level (28.14 ± 0.77 mmol/L) compared to rats inoculated with $2x10^6$ cells/0.2 ml (both flanks) (25.75 ± 0.75 mmol/L) ($p<0.05$). Rats inoculated with $2x10^6$ cells/0.2 ml (1 flank) and rats inoculated with $2x10^6$ cells/0.2 ml (both flanks) had a decreased glucose level (7.87 ± 0.24 mmol/L and 6.91 ± 0.34 mmol/L, respectively) compared to rats inoculated with $1x10^5$ cells/0.1 ml (1 flank) (9.57 ± 0.26 mmol/L) ($p<0.05$ and $p<0.0001$, respectively). Rats injected with $1x10^5$ cells/0.1 ml (1 flank) and $2x10^6$ cells/0.2 ml (both flanks) showed higher

creatinine levels (22.50 ± 1.19 µmol/L and 20.63 ± 2.19 µmol/L, respectively) compared to rats inoculated with $2x10^6$ cells/0.2 ml (1 flank) (16.43 ± 1.02 µmol/L; $p<0.01$ and $p<0.05$, respectively). LD was found to be lower in rats inoculated with $1x10^5$ cells/0.1 ml (1 flank) (434.00 ± 78 U/L) compared to rats injected with $2x10^6$ cells/0.2 ml (both flanks) (752.00 ± 101.74 U/L) ($p<0.05$) (Table 4.1).

Only haemoglobin and platelet levels showed changes in response to tumours. In regard to haemoglobin levels, rats injected with $2x10^6$ cells/0.2 ml (1 flank) showed a higher level (138.29 ± 3.72 g/L) compared to control non-tumour-bearing rats (116.33 ± 3.67 g/L) ($p<0.0001$). Rats injected with the same concentration but in both flanks also showed a higher haemoglobin level (133.67 ± 3.65 g/L) compared to controls (116.33 ± 3.67 g/L) ($p<0.01$). Rats injected with $1x10^5$ cells/0.1 ml (1 flank) presented with a lower haemoglobin level (123.00 ± 15.13 g/L) compared to rats injected with $2x10^6$ cells/0.2 ml (1 flank) (138.29 ± 3.72 g/L) ($p<0.01$) (Table 4.2).

All tumour-bearing groups showed a significant increase in platelet levels ($1x10^5$ cells/0.1 ml (1 flank), 477.00 ± 167.09 10^9 cells/L ($p<0.001$); $2x10^6$ cells/0.2 ml (1 flank), 779.57 ± 95.02 10^9 cells/L ($p<0.0001$); $2x10^6$ cells/0.2 ml (both flanks), 778.67 ± 58.50 10^9 cells/L ($p<0.0001$)) compared to controls (191.00 ± 75.34 10^9 cells/L). The platelet concentrations in rats inoculated with $2x10^6$ cells/0.2 ml into 1 flank and both flanks were also significantly higher than the $1x10^5$ cells/0.1 ml group ($p<0.0001$) (Table 4.2).

Serum biochemistry and blood haematology profiles were also compared between control non tumour-bearing rats and rats showing growing and regressing tumours in each tumour group (Tables 4.3-3.5). The LD level was significantly lower in rats showing growing tumours (568.00 ± 56.00 U/L) ($p<0.0001$) and regressing tumours (434.00 ± 78.00 U/L) ($p<0.001$) in the $1x10^5$ cells/0.1 ml group compared to control non-tumour rats (1213.33 ± 510.95 U/L). Platelet levels were significantly higher in rats showing growing tumours

(415.00 ± 261.00 10^9 cells/L) compared to non tumour-bearing rats (191.00 ± 75.34 10^9 cells/L) ($p<0.05$) (Table 4.3).

Similarly to above, LD was also significantly lower in rats with growing tumours (534.00 ± 95.45 U/L) ($p<0.0001$) and regressing tumours (565.50 ± 63.50 U/L) ($p<0.001$) in the $2x10^6$ cells/0.2 ml (1 flank) group compared to the control non-tumour rats (1213.33 ± 510.95 U/L). However, growing (897.80 ± 24.05 10^9 cells/L) ($p<0.0001$) and regressing (424.00 ± 188.00 10^9 cells/L) ($p<0.01$) tumour rats had higher platelet levels compared to control non-tumour rats (191.00 ± 75.34 10^9 cells/L). Rats with growing tumours also exhibited significantly higher platelet levels compared to the rats with regressing tumour rats ($p<0.0001$) (Table 4.4).

Lactate dehydrogenase was also significantly lower in the $2x10^6$ cells/0.2 ml (both flanks) groups with both growing tumours (712.33 ± 121.13 U/L) ($p<0.0001$) and regressing tumours (811.50 ± 231.50 U/L) ($p<0.001$) compared to control non-tumour rats (1213.33 ± 510.95 U/L). Platelets were also significantly increased in rats with growing tumours (808.80 ± 87.55 10^9 cells/L) ($p<0.0001$) and rats with regressing tumours (720.00 ± 13.00 10^9 cells/L) ($p<0.0001$) compared to control non-tumour-bearing rats (191.00 ± 75.34 10^9 cells/L) (Table 4.5).

Some rats, (2 of 6 rats in $1x10^5$ cells/0.1 ml (1 flank), 3 of 12 rats in $2x10^6$ cells/0.2 ml (1 flank) and 2 of 12 rats in $2x10^6$ cells/0.2 ml (both flanks)) did not have results for serum biochemistry and blood haematology profile due to technical problems in conducting cardiac puncture, thus reducing the sample size of each rat group.

Table 4.1. Serum biochemistry and liver enzymes in response to Walker 256 tumour inoculation.

	Rat groups			
	Control non-tumour	**1x10^5 cells/0/1 ml (1 flank)**	**2x10^6 cells/0.2 ml (1 flank)**	**2x10^6 cells/0.2 ml (both flanks)**
Sodium	137.00 ± 1.37	139.33 ± 1.45	140.14 ± 0.91**	138.63 ± 0.84
Potassium	4.63 ± 0.47	3.65 ± 0.15	4.12 ± 0.08	4.42 ± 0.04
Chloride	99.17 ± 1.49	103.00 ± 1.00**	101.43 ± 0.81	100.88 ± 0.93
Bicarbonate	25.33 ± 1.26	27.67 ± 0.33	28.14 ± 0.77*ǂ	25.75 ± 0.75
Anion gap	19.00 ± 2.08	13.50 ± 0.5**	14.83 ± 1.19**	16.00 ± 1.14
Glucose	8.43 ± 0.69	9.57 ± 0.26	7.87 ± 0.24#	6.91 ± 0.34**¥
Urea	6.00 ± 0.38	6.20 ± 0.21	5.81 ± 0.25	5.91 ± 0.28
Creatinine	32.33 ± 4.31	22.50 ± 1.53ϕǂ	16.43 ± 1.02ϕ	20.63 ± 2.19€
Urate	0.08 ± 0.02	0.08 ± 0.02	0.04 ± 0.01	0.07 ± 0.01
Cholesterol	1.87 ± 0.10	2.00 ± 0.06	2.10 ± 0.11	1.88 ± 0.10
Phosphate	1.66 ± 0.11	1.65 ± 0.03	1.83 ± 0.08	1.71 ± 0.11
Total Calcium	2.53 ± 0.03	2.62 ± 0.02	2.56 ± 0.03	2.52 ± 0.02
Albumin	15.17 ± 0.65	16.00 ± 1.15	13.43 ± 0.72	12.63 ± 1.05
Globulin	46.00 ± 0.97	48.67 ± 2.19	46.29 ± 0.71	45.75 ± 1.46

Protein	61.17 ± 1.47	64.67 ± 2.33	59.71 ± 1.41	58.38 ± 2.18
Total Bilirubin	1.00 ± 0.00	1.00 ± 0.00	1.00 ± 0.00	1.00 ± 0.00
GGT	3.00 ± 0.00	3.00 ± 0.00	3.00 ± 0.00	3.00 ± 0.00
ALP	77.00 ± 9.04	63.00 ± 3.21	89.29 ± 10.96	68.38 ± 6.94
ALT	68.17 ± 10.52	51.67 ± 12.25	48.86 ± 4.62	52.63 ± 6.29
AST	124.67 ± 25.73	97.50 ± 19.50	151.00 ± 28.70	170.60 ± 49.22
LD	1213.33 ± 510.95	$434.00 \pm 78_{***\ddagger}$	$572.50 \pm 75.42_{\phi}$	$752.00 \pm 101.74_{\phi}$

Data presented as mean ± S.E.M (n=6 for control non-tumour, n=4 for $1x10^5$ cells/0/1 ml (1 flank), n=9 for $2x10^6$ cells/0.2 ml (1 flank) and n=10 for $2x10^6$ cells/0.2 ml (both flanks)). Units: Sodium, potassium, chloride, bicarbonate, anion gap, glucose, urea, urate, phosphate, total calcium, mmol/L. Creatinine and total bilirubin, µmol/L. Albumin, globulin, protein, g/L. GGT, ALP, ALT, AST, LD, U/L.

GGT Gamma-glutamyl transpeptidase, *ALP* Alkaline phosphatase, *ALT* Alanine aminotransferase, *AST* Aspartate aminotransferase, *LD* lactate dehydrogenase

*Data showing the subscript symbol were significantly different at the level of p<0.05. ** for p<0.05 compared to controls, ** for p<0.01 compared to controls, *** for p<0.001 compared to controls, ϕ for p<0.0001 compared to controls, # for p<0.05 compared to $1x10^5$/0.1 ml (1 flank) group, ¥ for p<0.0001 compared to $1x10^5$/0/1 ml (1 flank) group, € for p<0.05 compared to $2x10^6$/0.2 ml (1 flank) group, ┼ for p<0.01 compared to $2x10^6$/0.2 ml (1 flank) group, ╪ for p<0.05 compared to $2x10^6$/0.2 ml (both flanks) group.*

Table 4.2. Blood haematology profile in response to Walker 256 tumour inoculation.

	Rat groups			
	Control non-tumour	**$1x10^5$/0/1 ml (1 flank)**	**$2x10^6$/0.2 ml (1 flank)**	**$2x10^6$/0.2 ml (both flanks)**
Haemoglobin	116.33 ± 3.67	123.00 ± 15.13┼	138.29 ± 3.72ϕ	133.67 ± 3.65**
R.B.C.	6.59 ± 0.33	6.92 ± 0.89	7.77 ± 0.15	7.45 ± 0.20
P.C.V.	0.36 ± 0.02	0.38 ± 0.04	0.42 ± 0.01	0.40 ± 0.01
M.C.V.	54.20 ± 0.40	54.93 ± 2.09	53.54 ± 0.90	53.68 ± 0.76
M.C.H.	17.73 ± 0.81	17.80 ± 0.46	17.80 ± 0.28	17.93 ± 0.15
M.C.H.C.	327.00 ± 12.66	325.00 ± 10.26	332.29 ± 3.14	334.50 ± 3.17
R.D.W.	12.80 ± 0.31	13.23 ± 0.27	13.29 ± 0.25	13.33 ± 0.23
White cell count	1.84 ± 0.04	2.54 ± 0.20	7.91 ± 0.92	9.06 ± 1.31
Neutrophils	0.14 ± 0.05	0.51 ± 0.04	2.43 ± 0.46	4.31 ± 1.42
Lymphocytes	1.66 ± 0.08	1.92 ± 0.27	5.10 ± 0.63	4.24 ± 0.43
Monocytes	0.03 ± 0.01	0.06 ± 0.04	0.23 ± 0.09	0.34 ± 0.08
Eosinophils	0.01 ± 0.01	0.04 ± 0.01	0.14 ± 0.03	0.19 ± 0.09
Basophils	Not detected	Not detected	Not detected	Not detected
Platelets	191.00 ± 75.34	477.00 ± 167.09***	779.57 ± 95.02ϕ¥	778.67 ± 58.50ϕ¥

Data presented as mean ± S.E.M (n=6 for control non-tumour group, n=4 for $1x10^5$ cells/0/1 ml (1 flank), n=9 for $2x10^6$ cells/0.2 ml (1 flank) and n=10 for $2x10^6$ cells/0.2 ml (both flanks)). Units: Haemoglobin, M.C.H.C. g/L, R.B.C. 10^{12}/L, P.C.V. L/L, M.C.V. fl, M.C.H. pg, R.D.W. %, platelets, white cell count, neutrophils, lymphocytes, monocytes, eosinophils, basophils 10^9/L.

R.B.C. Red blood cell, P.C.V. packed cell volume, M.C.V. mean corpuscular volume, M.C.H mean corpuscular haemoglobin, M.C.H.C mean corpuscular haemoglobin concentration, R.D.W. red blood cell distribution width

*Data showing the subscript symbol were significantly different at the level of $p<0.05$. ** *for $p<0.01$ compared to controls,* *** *for $p<0.001$ compared to controls, ϕ for $p<0.0001$ compared to controls, ¥ for $p<0.0001$ compared to $1x10^5$/0.1 ml (1 flank) group, ┼ for $p<0.01$ compared to $2x10^6$/0.2 ml (1 flank) group.*

Table 4.3. Comparison of serum biochemistry and liver enzymes between growing and regressing tumours for $1x10^5$ cells/0.1 ml 1 flank.

	Control non-tumour rats	**Growing tumour rats**	**Regressing tumour rats**
Sodium	137.00 ± 1.37	140.00 ± 1.00	139.50 ± 2.50
Potassium	4.63 ± 0.47	3.85 ± 0.05	3.70 ± 0.20
Chloride	99.17 ± 1.49	101.00 ± 1.00	103.50 ± 1.50
Bicarbonate	25.33 ± 1.26	28.50 ± 0.50	27.50 ± 0.50
Anion gap	19.00 ± 2.08	14.00 ± 1.00	13.50 ± 0.50
Glucose	8.43 ± 0.69	8.10 ± 1.50	9.55 ± 0.45
Urea	6.00 ± 0.38	5.50 ± 0.80	6.15 ± 0.35
Creatinine	32.33 ± 4.31	23.00 ± 2.00	26.00 ± 6.00
Urate	0.08 ± 0.02	0.05 ± 0.02	0.09 ± 0.04
Cholesterol	1.87 ± 0.10	2.15 ± 0.05	1.95 ± 0.05
Phosphate	1.66 ± 0.11	1.59 ± 0.00	1.68 ± 0.00
Total Calcium	2.53 ± 0.03	2.64 ± 0.01	2.61 ± 0.03
Albumin	15.17 ± 0.65	16.50 ± 0.50	16.00 ± 2.00
Globulin	46.00 ± 0.97	50.00 ± 3.00	46.50 ± 0.50
Protein	61.17 ± 1.47	66.50 ± 2.50	62.50 ± 1.50

Total Bilirubin	1.00 ± 0.00	1.00 ± 0.00	1.00 ± 0.00
GGT	3.00 ± 0.00	3.00 ± 0.00	3.00 ± 0.00
ALP	77.00 ± 9.04	63.50 ± 1.50	63.50 ± 5.50
ALT	68.17 ± 10.52	56.00 ± 13.00	43.00 ± 15.00
AST	124.67 ± 25.73	106.50 ± 10.50	97.50 ± 19.50
LD	1213.33 ± 510.95	$568.00 \pm 56.00_{\phi}$	$434.00 \pm 78.00_{***}$

Data presented as mean ± S.E.M (n=6 for control non-tumour rats, n=2 for growing tumour rats, n=2 for regressing tumour rats). Units: Sodium, potassium, chloride, bicarbonate, anion gap, glucose, urea, urate, phosphate, total calcium, mmol/L. Creatinine and total bilirubin, µmol/L. Albumin, globulin, protein, g/L. GGT, ALP, ALT, AST, LD, U/L.

GGT Gamma-glutamyl transpeptidase, *ALP* Alkaline phosphatase, *ALT* Alanine aminotransferase, *AST* Aspartate aminotransferase, *LD* lactate dehydrogenase

*Data showing the subscript symbol were significantly different at the level of $p<0.05$. *** *for $p<0.001$ compared to controls, ϕ for $p<0.0001$ compared to controls.*

Table 4.4. Comparison of blood haematology profile between growing and regressing tumours for $1x10^5$ cells/0.1 ml 1 flank.

	Control non-tumour rats	**Growing tumour rats**	**Regressing tumour rats**
Haemoglobin	116.33 ± 3.67	119.50 ± 10.50	119.50 ± 25.50
R.B.C.	6.59 ± 0.33	6.64 ± 0.33	6.90 ± 1.54
P.C.V.	0.36 ± 0.02	0.37 ± 0.02	0.37 ± 0.06
M.C.V.	54.20 ± 0.40	55.10 ± 1.40	54.15 ± 3.35
M.C.H.	17.73 ± 0.81	18.00 ± 0.70	17.35 ± 0.15
M.C.H.C.	327.00 ± 12.66	326.50 ± 4.50	322.00 ± 17.00
R.D.W.	12.80 ± 0.31	12.45 ± 0.25	13.50 ± 0.10
White cell count	1.84 ± 0.04	1.97 ± 0.18	2.74 ± 0.05
Neutrophils	0.14 ± 0.05	0.40 ± 0.20	0.48 ± 0.00
Lymphocytes	1.66 ± 0.08	1.44 ± 0.06	2.20 ± 0.05
Monocytes	0.03 ± 0.01	0.08 ± 0.05	0.02 ± 0.01
Eosinophils	0.01 ± 0.01	0.04 ± 0.00	0.05 ± 0.02
Basophils	0.00 ± 0.00	0.00 ± 0.00	0.00 ± 0.00
Platelets	191.00 ± 75.34	415.00 ± 261.00*	377.50 ± 232.50

Data presented as mean ± S.E.M (n=6 for control non-tumour rats, n=2 for growing tumour rats, n=2 for regressing tumour rats). Units: Haemoglobin, M.C.H.C. g/L, R.B.C. 10^{12}/L, P.C.V. L/L, M.C.V. fl, M.C.H. pg, R.D.W. %, platelets, white cell count, neutrophils, lymphocytes, monocytes, eosinophils, basophils 10^{9}/L.

R.B.C. Red blood cell, P.C.V. packed cell volume, M.C.V. mean corpuscular volume, M.C.H mean corpuscular haemoglobin, M.C.H.C mean corpuscular haemoglobin concentration, R.D.W. red blood cell distribution width

*Data showing the subscript symbol were significantly different at the level of $p<0.05$. * *for $p<0.05$ compared to controls.*

Table 4.5. Comparison of serum biochemistry and liver enzymes between growing and regressing tumours for $2x10^6$ cells/0.2 ml 1 flank.

	Control non-tumour rats	**Growing tumour rats**	**Regressing tumour rats**
Sodium	137.00 ± 1.37	140.00 ± 0.71	142.00 ± 2.00
Potassium	4.63 ± 0.47	4.03 ± 0.02	4.40 ± 0.10
Chloride	99.17 ± 1.49	101.40 ± 1.08	102.50 ± 0.50
Bicarbonate	25.33 ± 1.26	28.60 ± 0.98	28.00 ± 0.00
Anion gap	19.00 ± 2.08	14.00 ± 1.58	16.00 ± 2.00
Glucose	8.43 ± 0.69	7.90 ± 0.35	7.30 ± 0.40
Urea	6.00 ± 0.38	5.74 ± 0.24	6.35 ± 0.45
Creatinine	32.33 ± 4.31	16.40 ± 1.25	16.50 ± 2.50
Urate	0.08 ± 0.02	0.04 ± 0.01	0.05 ± 0.03
Cholesterol	1.87 ± 0.10	2.14 ± 0.12	1.80 ± 0.10
Phosphate	1.66 ± 0.11	1.80 ± 0.11	1.62 ± 0.43
Total Calcium	2.53 ± 0.03	2.53 ± 0.03	2.58 ± 0.11
Albumin	15.17 ± 0.65	12.80 ± 0.80	16.50 ± 0.50
Globulin	46.00 ± 0.97	45.60 ± 0.81	48.00 ± 0.00
Protein	61.17 ± 1.47	58.40 ± 1.60	64.50 ± 0.50

Total Bilirubin	1.00 ± 0.00	1.00 ± 0.00	1.00 ± 0.00
GGT	3.00 ± 0.00	3.00 ± 0.00	3.00 ± 0.00
ALP	77.00 ± 9.04	93.00 ± 14.01	78.50 ± 22.50
ALT	68.17 ± 10.52	47.40 ± 6.39	44.00 ± 13.00
AST	124.67 ± 25.73	175.25 ± 38.20	92.00 ± 2.00
LD	1213.33 ± 510.95	534.00 ± 95.45$_{\phi}$	565.50 ± 63.50$_{***}$

Data presented as mean ± S.E.M (n=6 for control non-tumour rats, n=5 for growing tumour rats, n=4 for regressing tumour rats). Units: Sodium, potassium, chloride, bicarbonate, anion gap, glucose, urea, urate, phosphate, total calcium, mmol/L. Creatinine and total bilirubin, µmol/L. Albumin, globulin, protein, g/L. GGT, ALP, ALT, AST, LD, U/L.

GGT Gamma-glutamyl transpeptidase, *ALP* Alkaline phosphatase, *ALT* Alanine aminotransferase, *AST* Aspartate aminotransferase, *LD* lactate dehydrogenase.

*Data showing the subscript symbol were significantly different at the level of $p<0.05$. *** *for $p<0.001$ compared to controls, ϕ for $p<0.0001$ compared to controls.*

Table 4.6. Comparison of blood haematology profile between growing and regressing tumours for $2x10^6$ cells/0.2 ml 1 flank.

	Control non-tumour rats	**Growing tumour rats**	**Regressing tumour rats**
Haemoglobin	116.33 ± 3.67	139.80 ± 5.14	137.50 ± 5.50
R.B.C.	6.59 ± 0.33	7.77 ± 0.22	7.87 ± 0.11
P.C.V.	0.36 ± 0.02	0.42 ± 0.01	0.41 ± 0.02
M.C.V.	54.20 ± 0.40	54.50 ± 0.94	51.45 ± 0.65
M.C.H.	17.73 ± 0.81	18.00 ± 0.34	17.45 ± 0.45
M.C.H.C.	327.00 ± 12.66	329.80 ± 3.75	339.50 ± 4.50
R.D.W.	12.80 ± 0.31	13.10 ± 0.32	13.75 ± 0.15
White cell count	1.84 ± 0.04	9.05 ± 0.77	4.90 ± 0.42
Neutrophils	0.14 ± 0.05	2.96 ± 0.41	1.12 ± 0.45
Lymphocytes	1.66 ± 0.08	5.67 ± 0.75	3.53 ± 0.14
Monocytes	0.03 ± 0.01	0.25 ± 0.13	0.19 ± 0.10
Eosinophils	0.01 ± 0.01	0.16 ± 0.03	0.06 ± 0.02
Basophils	0.00 ± 0.00	0.00 ± 0.00	0.00 ± 0.00
Platelets	191.00 ± 75.34	897.80 ± 24.05ϕ	424.00 ± 188.00**Þ

Data presented as mean ± S.E.M (n=6 for control non-tumour rats, n=5 for growing tumour rats, n=4 for regressing tumour rats). Units: Haemoglobin, M.C.H.C. g/L, R.B.C. 10^{12}/L, P.C.V. L/L, M.C.V. fl, M.C.H. pg, R.D.W. %, platelets, white cell count, neutrophils, lymphocytes, monocytes, eosinophils, basophils 10^{9}/L.

R.B.C. Red blood cell, P.C.V. packed cell volume, M.C.V. mean corpuscular volume, M.C.H mean corpuscular haemoglobin, M.C.H.C mean corpuscular haemoglobin concentration, R.D.W. red blood cell distribution width

*Data showing the subscript symbol were significantly different at the level of $p<0.05$. ** *for $p<0.01$ compared to controls, ϕ for $p<0.0001$ compared to controls, Þ for $p<0.0001$ compared to regressing tumour rats group.*

Table 4.7. Comparison of serum biochemistry and liver enzymes between growing and regressing tumours for $2x10^6$ cells/0.2 ml both flanks.

	Control non-tumour rats	**Growing tumour rats**	**Regressing tumour rats**
Sodium	137.00 ± 1.37	139.00 ± 1.10	137.50 ± 0.50
Potassium	4.63 ± 0.47	4.43 ± 0.07	4.40 ± 0.00
Chloride	99.17 ± 1.49	101.17 ± 1.22	100.00 ± 1.00
Bicarbonate	25.33 ± 1.26	25.83 ± 0.95	25.50 ± 1.50
Anion gap	19.00 ± 2.08	16.00 ± 2.00	16.00 ± 1.00
Glucose	8.43 ± 0.69	7.27 ± 0.32	5.85 ± 0.35
Urea	6.00 ± 0.38	6.18 ± 0.29	5.10 ± 0.30
Creatinine	32.33 ± 4.31	21.33 ± 2.78	18.50 ± 3.50
Urate	0.08 ± 0.02	0.07 ± 0.01	0.07 ± 0.02
Cholesterol	1.87 ± 0.10	1.92 ± 0.09	1.75 ± 0.35
Phosphate	1.66 ± 0.11	1.75 ± 0.15	1.61 ± 0.01
Total Calcium	2.53 ± 0.03	2.51 ± 0.02	2.56 ± 0.08
Albumin	15.17 ± 0.65	11.67 ± 1.15	15.50 ± 0.50
Globulin	46.00 ± 0.97	45.17 ± 0.95	47.50 ± 6.50
Protein	61.17 ± 1.47	56.83 ±1.92	63.00 ± 7.00

Total Bilirubin	1.00 ± 0.00	1.00 ± 0.00	1.00 ± 0.00
GGT	3.00 ± 0.00	3.00 ± 0.00	3.00 ± 0.00
ALP	77.00 ± 9.04	69.50 ± 7.89	65.00 ± 20.00
ALT	68.17 ± 10.52	55.17 ± 8.29	45.00 ± 1.00
AST	124.67 ± 25.73	218.67 ± 72.00	98.50 ± 2.50
LD	1213.33 ± 510.95	$712.33 \pm 121.13_{\phi}$	$811.50 \pm 231.50_{***}$

Data presented as mean ± S.E.M (n=6 for control non-tumour rats, n=5 for growing tumour rats, n=5 for regressing tumour rats). Units: Sodium, potassium, chloride, bicarbonate, anion gap, glucose, urea, urate, phosphate, total calcium, mmol/L. Creatinine and total bilirubin, µmol/L. Albumin, globulin, protein, g/L. GGT, ALP, ALT, AST, LD, U/L.

GGT Gamma-glutamyl transpeptidase, *ALP* Alkaline phosphatase, *ALT* Alanine aminotransferase, *AST* Aspartate aminotransferase, *LD* lactate dehydrogenase.

*Data showing the subscript symbol were significantly different at the level of $p<0.05$. *** *for $p<0.001$ compared to controls, ϕ for $p<0.0001$ compared to controls.*

Table 4.8. Comparison of blood haematology profile between growing and regressing tumours for $2x10^6$ cells/0.2 ml both flanks.

	Control non-tumour rats	**Growing tumour rats**	**Regressing tumour rats**
Haemoglobin	116.33 ± 3.67	133.25 ± 4.87	134.50 ± 7.50
R.B.C.	6.59 ± 0.33	7.36 ± 0.29	7.64 ± 0.25
P.C.V.	0.36 ± 0.02	0.40 ± 0.01	0.40 ± 0.02
M.C.V.	54.20 ± 0.40	54.40 ± 0.91	52.25 ± 0.85
M.C.H.	17.73 ± 0.81	18.10 ± 0.07	17.60 ± 0.40
M.C.H.C.	327.00 ± 12.66	333.25 ± 4.78	337.00 ± 2.00
R.D.W.	12.80 ± 0.31	13.20 ± 0.30	13.60 ± 0.40
White cell count	1.84 ± 0.04	10.10 ± 1.79	6.99 ± 0.39
Neutrophils	0.14 ± 0.05	5.90 ± 1.59	1.12 ± 0.26
Lymphocytes	1.66 ± 0.08	3.59 ± 0.17	5.54 ± 0.06
Monocytes	0.03 ± 0.01	0.39 ± 0.11	0.23 ± 0.03
Eosinophils	0.01 ± 0.01	0.24 ± 0.13	0.11 ± 0.04
Basophils	0.00 ± 0.00	0.00 ± 0.00	0.00 ± 0.00
Platelets	191.00 ± 75.34	$808.00 \pm 87.55_{\phi}$	$720.00 \pm 13.00_{\phi}$

Data presented as mean ± S.E.M (n=6 for control non-tumour rats, n=5 for growing tumour rats, n=5 for regressing tumour rats). Units: Haemoglobin, M.C.H.C. g/L, R.B.C. 10^{12}/L, P.C.V. L/L, M.C.V. fl, M.C.H. pg, R.D.W. %, platelets, white cell count, neutrophils, lymphocytes, monocytes, eosinophils, basophils 10^{9}/L.

R.B.C. Red blood cell, P.C.V. packed cell volume, M.C.V. mean corpuscular volume, M.C.H mean corpuscular haemoglobin, M.C.H.C mean corpuscular haemoglobin concentration, R.D.W. red blood cell distribution width

*Data showing the subscript symbol were significantly different at the level of $p<0.05$. ϕ *for $p<0.0001$ compared to controls.*

4.3.4 Histological analysis

Histological analysis on formalin-fixed, paraffin-embedded tumour, jejunum and colon was carried out on sections stained with haematoxylin and eosin.

4.3.4.1 Tumour histology

The Walker 256 tumour histopathology has been characterised by a professional veterinary pathologist, Professor John Finnie, at SA Pathology (Adelaide, Australia). The tumour is characterised as a solid, partially encapsulated tumour with no evidence of glandular differentiation. The neoplasm is a poorly differentiated carcinoma with multifocal areas of tumour necrosis of varying size, especially in the central core region, and sometimes containing haemorrhage. The tumour nuclei are of greatly varying size and shape, from round to ovoid to more elongated, are sometimes indented or lobulated and are occasionally binucleated. They often contain one or more prominent nucleoli. Ratio of nucleus to cytoplasm is also high, with indistinct cell boundaries, sometimes separated by connective tissue septa. A high mitotic rate was also seen, with many abnormal mitotic figures. Scattered apoptotic bodies which represent dying individual tumour cells were characterised by shrunken, usually deeply eosinophilic, cytoplasm, and fragmented nuclear remnants with the bodies separated from contiguous viable tumour cells by a non-staining clear space. The histological analysis was done on both growing tumours and regressing tumours in each group. No histological differences were found between the growing and regressing tumours. Results are shown in Figure 4.5.

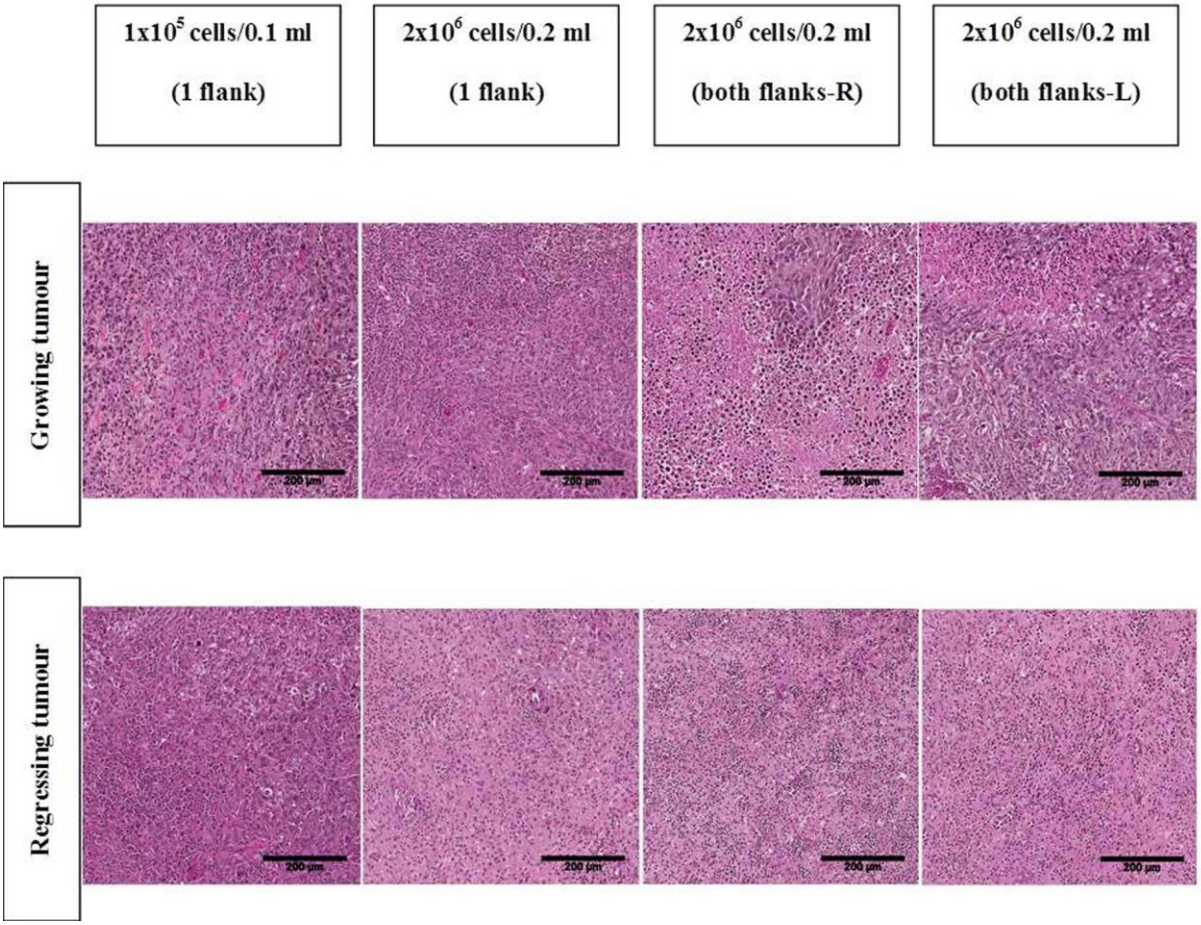

Figure 4.4. Histology images of Walker 256 tumour tissue from different concentrations of tumour cells injected. Photomicrographs are of x100 original magnification (Scale bar: 200 µm). R: right flank tumour, L: left flank tumour. Images are representatives of each group.

4.3.4.2 Jejunum

No histological damage was seen in the jejunum of all tumour-bearing rats compared to the control non-tumour rats and no difference was associated with different concentrations of tumour inoculum. There was also no histological difference between the jejunum from growing and regressing tumour-bearing rats.

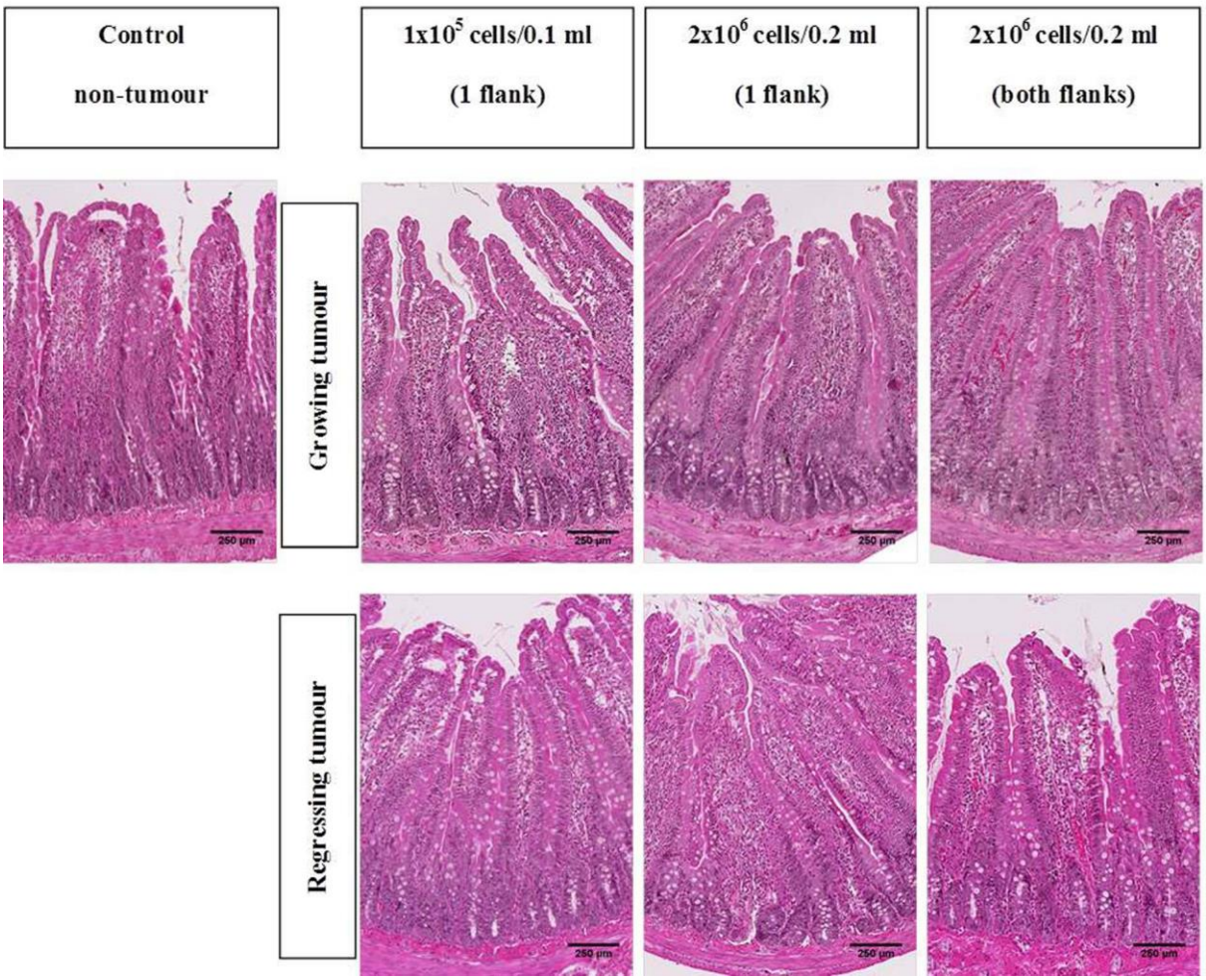

Figure 4.5. Histology images of jejunum from rats injected with different concentration of Walker 256 tumour. Photomicrographs are of x50 original magnification (Scale bar: 250 µm). Images are representatives of each group.

4.3.4.3 Colon

Similarly to jejunum, no histological damage was seen in the colon of all tumour-bearing rats compared to the control non-tumour rats. There was no difference in the colon histology among the rats injected with different concentration of tumour inoculum. There was also no difference between the colon from growing and regressing tumour rats.

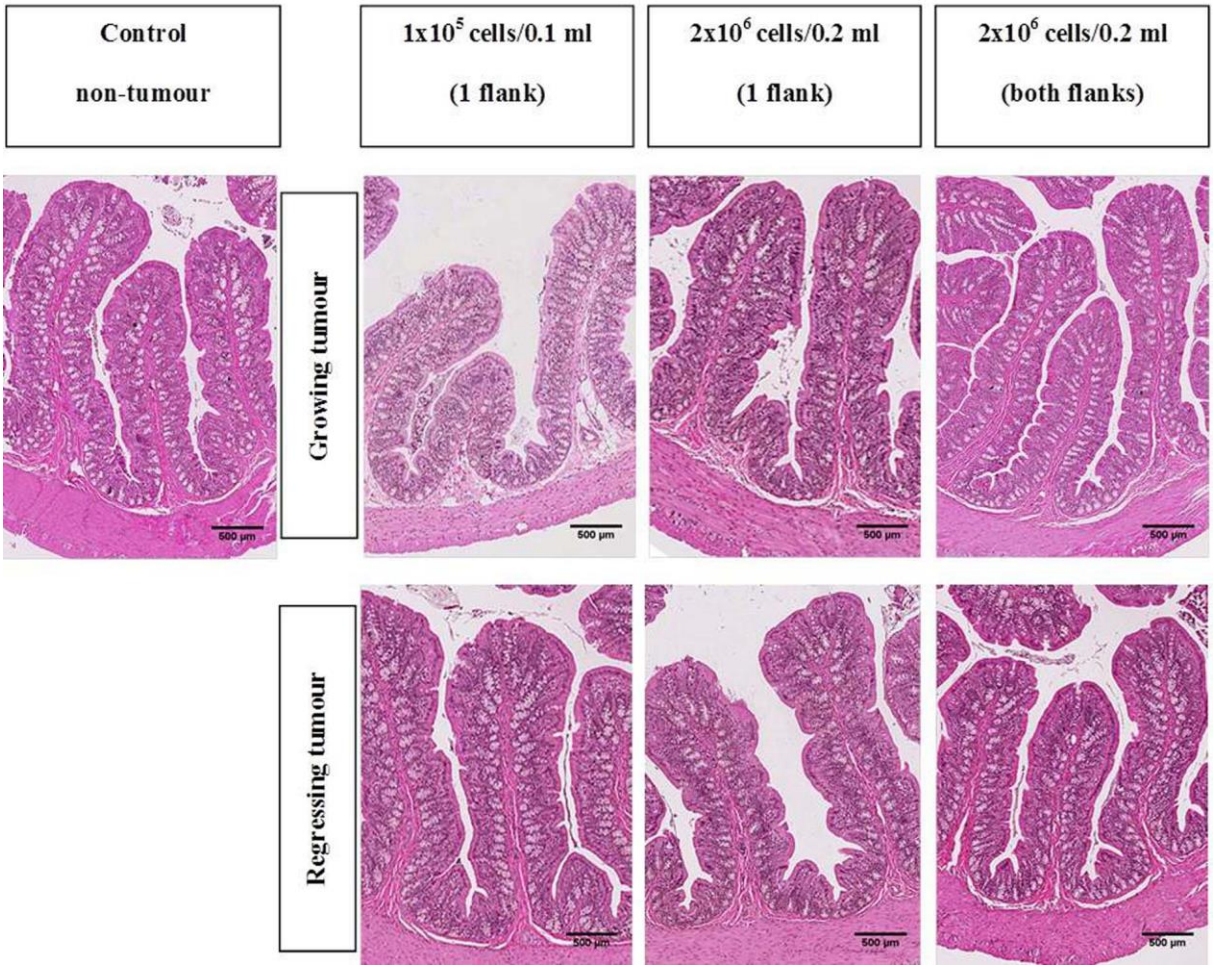

Figure 4.6. Histology images of colon from rats injected with different concentration of Walker 256 tumour. Photomicrographs are of x25 original magnification (Scale bar: 500 µm). Images are representatives of each group.

4.3.5 Measurement of villus height and crypt depth in jejunum and colon

Villus height and crypt depth were measured to further evaluate any histological damage in the jejunum and colon in response to tumours. Results were first compared between control non-tumour rats and each of the tumour-bearing groups (Figure 4.7). Then, the results were compared between rats with growing tumours and with regressing tumours in each group and control non-tumour-bearing rats (Figures 4.8-4.10).

There was a significant difference in the jejunal villus length between control non-tumour rats (546.75 ± 10.21 µm) and rats injected with $1x10^5$ cells/0.1 ml (484.40 ± 13.25 µm) ($p<0.05$) (Figure 4.7). It was also found that the jejunal villus length of rats inoculated with $1x10^5$ cells/0.1 ml was significantly lower than that in the $2x10^6$ cells/0.2 ml (both flanks) group (554.66 ± 26.82 µm) ($p<0.05$). No significant difference was found between controls and rats inoculated with $2x10^6$ cells/0.2 ml in both 1 flank and 2 flanks ($p>0.05$). There was also no significant difference in jejunal crypt and colonic crypt length in any group (Figure 4.7).

Statistical difference in jejunal villi length between $2x10^6$ cells/0.2 ml (both flanks) group and $1x10^5$ cells/0.1 ml (1 flank) could be due to different in sample size. However, significant difference in jejunal villi length between control non tumour and $1x10^5$ cells/0.1 ml (1 flank) is not due to different in sample size as both groups have equal number of rats (Figure 4.7).

Jejunal villus length showed a significant difference between control non-tumour rats, and rats with growing or regressing tumours (Figure 4.8 i-iii). The jejunal villus length of rats injected with $1x10^5$ cells/0.1 ml with growing (493.59 ± 0.52 µm) ($p<0.05$) and regressing (475.20 ± 29.73 µm) ($p<0.01$) tumours were significantly lower than control non-tumour rats (546.75 ± 10.21 µm) (Figure 4.8i).

In tumour-bearing rats injected with $2x10^6$ cells/0.2 ml in 1 flank (Figure 4.8ii), rats with regressing tumours (484.99 ± 17.24 µm) showed a significantly lower jejunal villus length compared to control non-tumour rats ($p<0.01$). A significant difference in the jejunal villus length was also seen between rats with growing (539.85 ± 14.20 µm) and regressing (484.99 ± 17.24 µm) tumours ($p<0.05$).

Jejunal villus length in rats with regressing tumours injected with $2x10^6$ cell/0.2 ml in both flanks (503.01 ± 14.48 µm) was significantly lower than the rats with growing tumours (571.88 ± 32.61 µm) ($p<0.01$).

Again, statistical difference in jejunal villi length between control non tumour rats and $1x10^5$ cells/0.1 ml (1 flank) rats could be due to different in sample size (Figure 4.8i). However, statistical differences in jejunal villi length between groups in rats injected with $2x10^6$ cells/0.2 ml in 1 flank (Figure 4.8ii) and both flanks (Figure 4.8iii) were not due to different in sample size as all groups have equal number of rats.

No significant difference was observed in jejunal and colonic crypt length of control non-tumour-bearing rats, or in rats with growing or regressing tumours in each group ($p>0.05$) (Figures 4.8i, ii and iii).

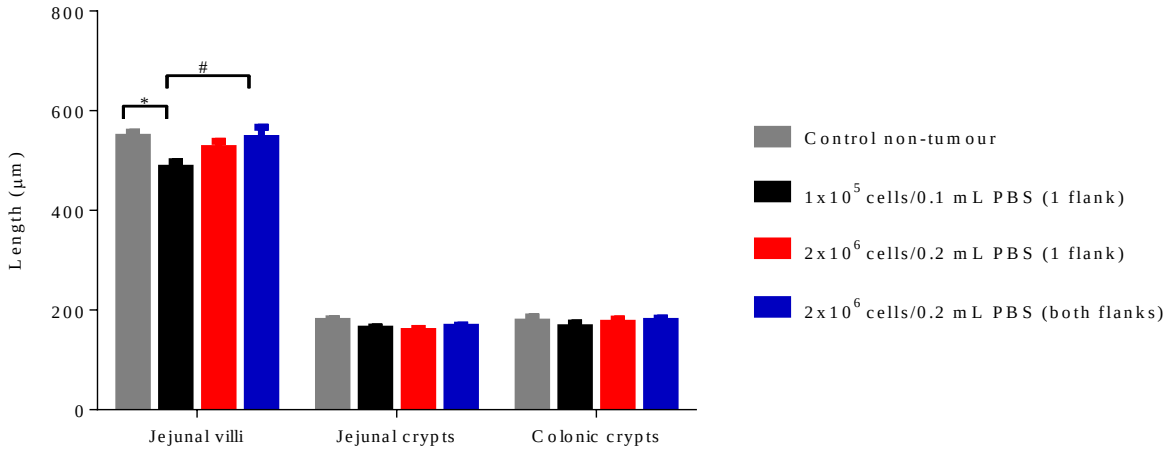

Figure 4.7. Villus height and crypt depth of jejunum and colon in Walker 256 tumour-bearing rats. Data presented as mean ± S.E.M (n=6 for control non-tumour, n=6 for $1x10^5$ cells/0.1 ml PBS (1 flank), n=12 for $2x10^6$ cells/0.2 ml PBS (1 flank) and n=12 for $2x10^6$ cells/0.2 ml PBS (both flanks)). ** for $p<0.05$ compared to controls, # for $p<0.05$ compared to $1x10^5$/0.1 ml (1 flank) group.*

i.

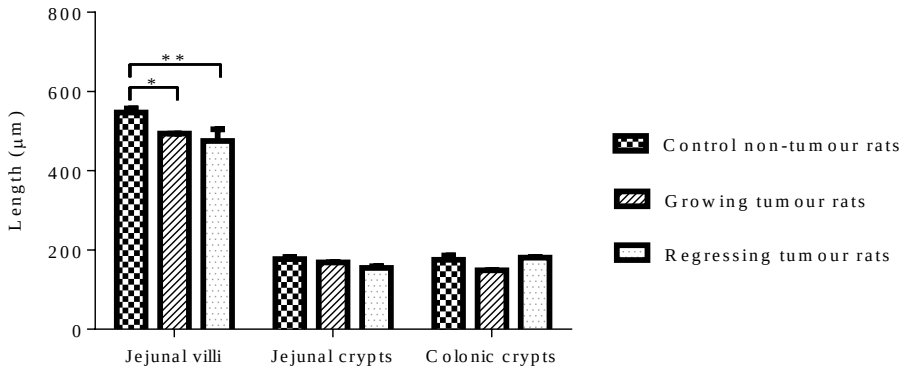

ii.

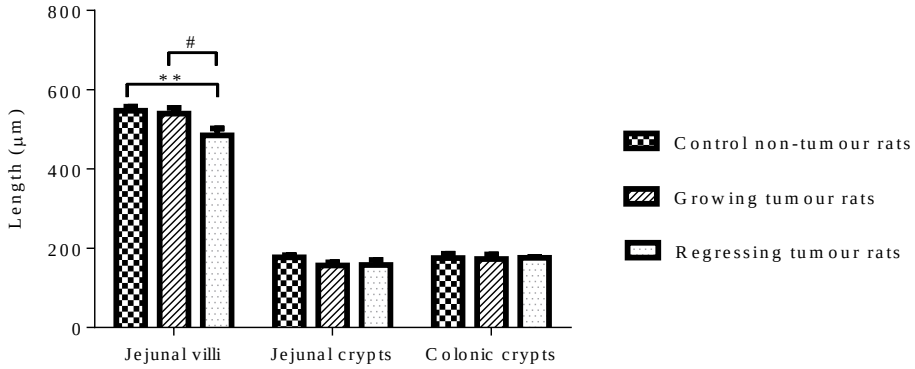

iii.

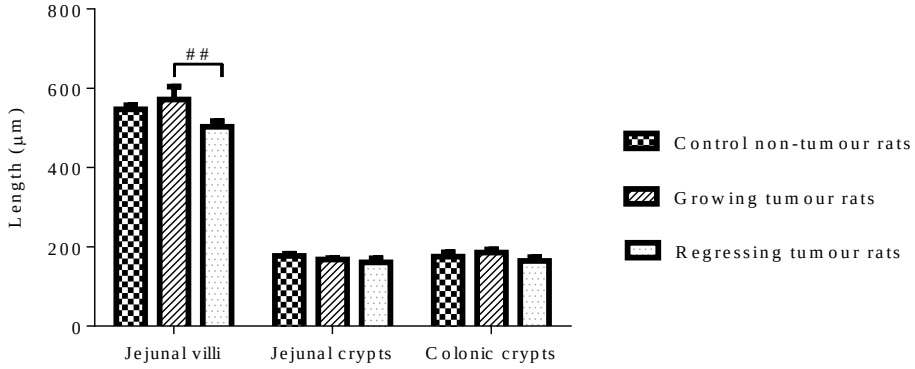

Figure 4.8. Villus height and crypt depth of jejunum and colon in rats injected with **i)** $1x10^5$ cells/0.1 ml (1 flank) **ii)** $2x10^6$ cells/0.2 ml (1 flank) **iii)** $2x10^6$ cells/0.2 ml (both flanks). Data presented as mean ± S.E.M (n=6 for control non-tumour group, n=3 for each growing and regressing tumours of $1x10^5$ cells/0.1 ml PBS (1 flank) group, n=6 for each growing and regressing tumours of $2x10^6$ cells/0.2 ml PBS (1 flank) group, n=6 for each growing and regressing tumours of $2x10^6$ cells/0.2 ml PBS (both flanks)). * *for $p<0.05$ compared to controls, ** for $p<0.01$ compared to controls, # for $p<0.05$ compared to growing tumour rats and ## for $p<0.01$ compared to growing tumour rats.*

4.3.6 Detection of apoptosis (caspase-3) and proliferation (Ki-67)

To assess epithelial apoptosis in the jejunum, colon and tumour, caspase-3 positively-stained crypt cells were counted. There are no significant differences in levels of apoptotic cells between jejunum of control non-tumour rats and all tumour-bearing rats from each group ($p>0.05$) (Figure 4.9). No significant difference was also seen within the colon ($p>0.05$). Figures 4.10i, ii and iii show the changes in cell apoptosis in jejunum and colon of growing and regressing tumours from all tumour-bearing groups. No significant differences were seen in either jejunum or colon in any experimental groups ($p>0.05$). The photomicrographs of jejunum and colon are shown in Figure 4.11 and 4.12.

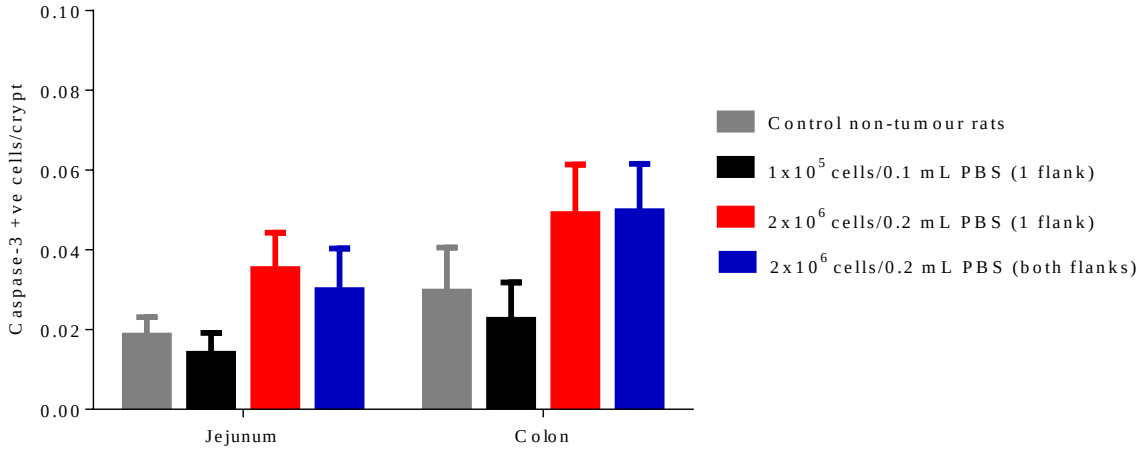

Figure 4.9. Changes in cell apoptosis as identified by caspase-3 immunohistochemistry staining in jejunum and colon of Walker 256 tumour-bearing rats. Data presented as mean ± S.E.M (n=6 for control non-tumour, n=6 for $1x10^5$ cells/0.1 ml PBS (1 flank), n=12 for $2x10^6$ cells/0.2 ml PBS (1 flank) and n=12 for $2x10^6$ cells/0.2 ml PBS (both flanks)).

i.

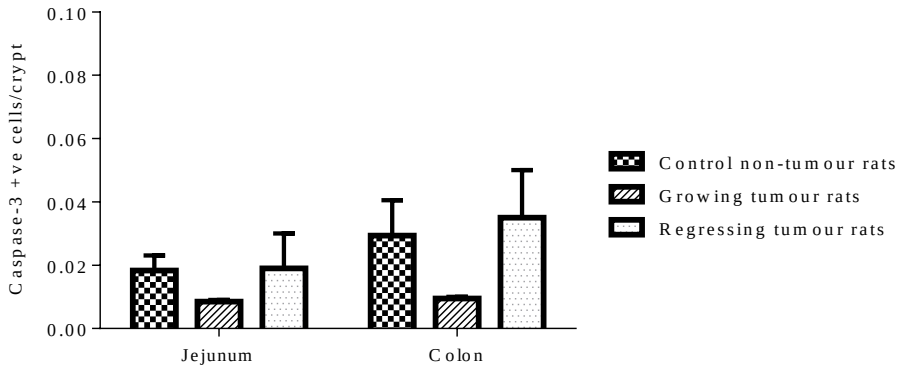

ii.

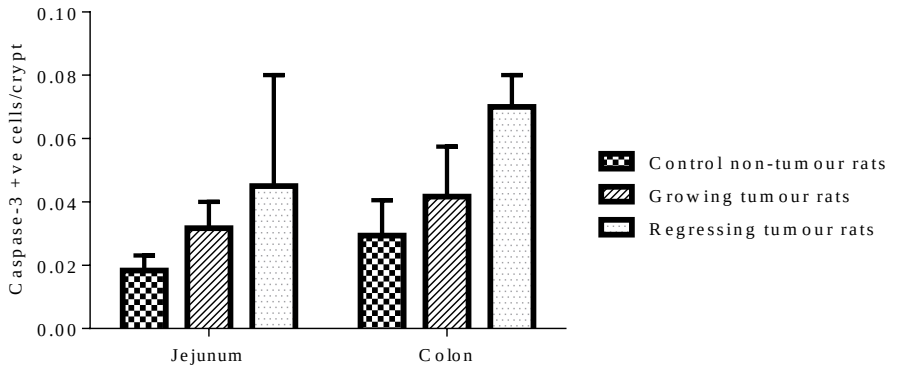

iii.

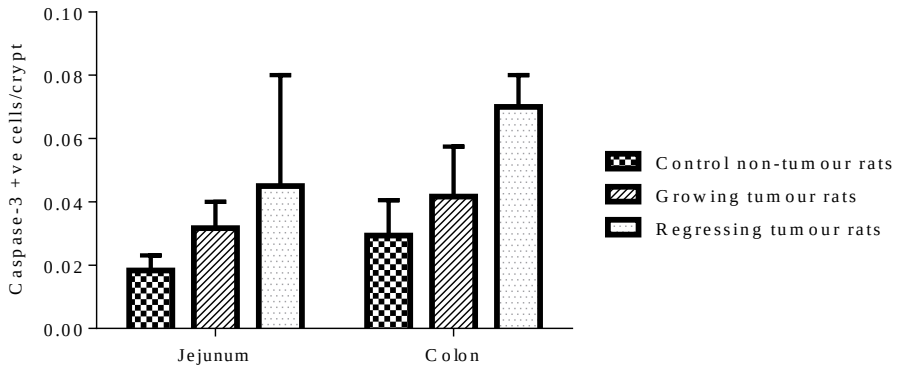

Figure 4.10. Changes in cell apoptosis as identified by caspase-3 immunohistochemistry staining in jejunum and colon of rats injected with **i)** $1x10^5$ cells/0.1 ml (1 flank) **ii)** $2x10^6$ cells/0.2 ml (1 flank) **iii)** $2x10^6$ cells/0.2 ml (both flanks). Data presented as mean ± S.E.M (n=6 for control non-tumour group, n=3 for each growing and regressing tumours of $1x10^5$ cells/0.1 ml PBS (1 flank) group, n=6 for each growing and regressing tumours of $2x10^6$ cells/0.2 ml PBS (1 flank) group, n=6 for each growing and regressing tumours of $2x10^6$ cells/0.2 ml PBS (both flanks)).

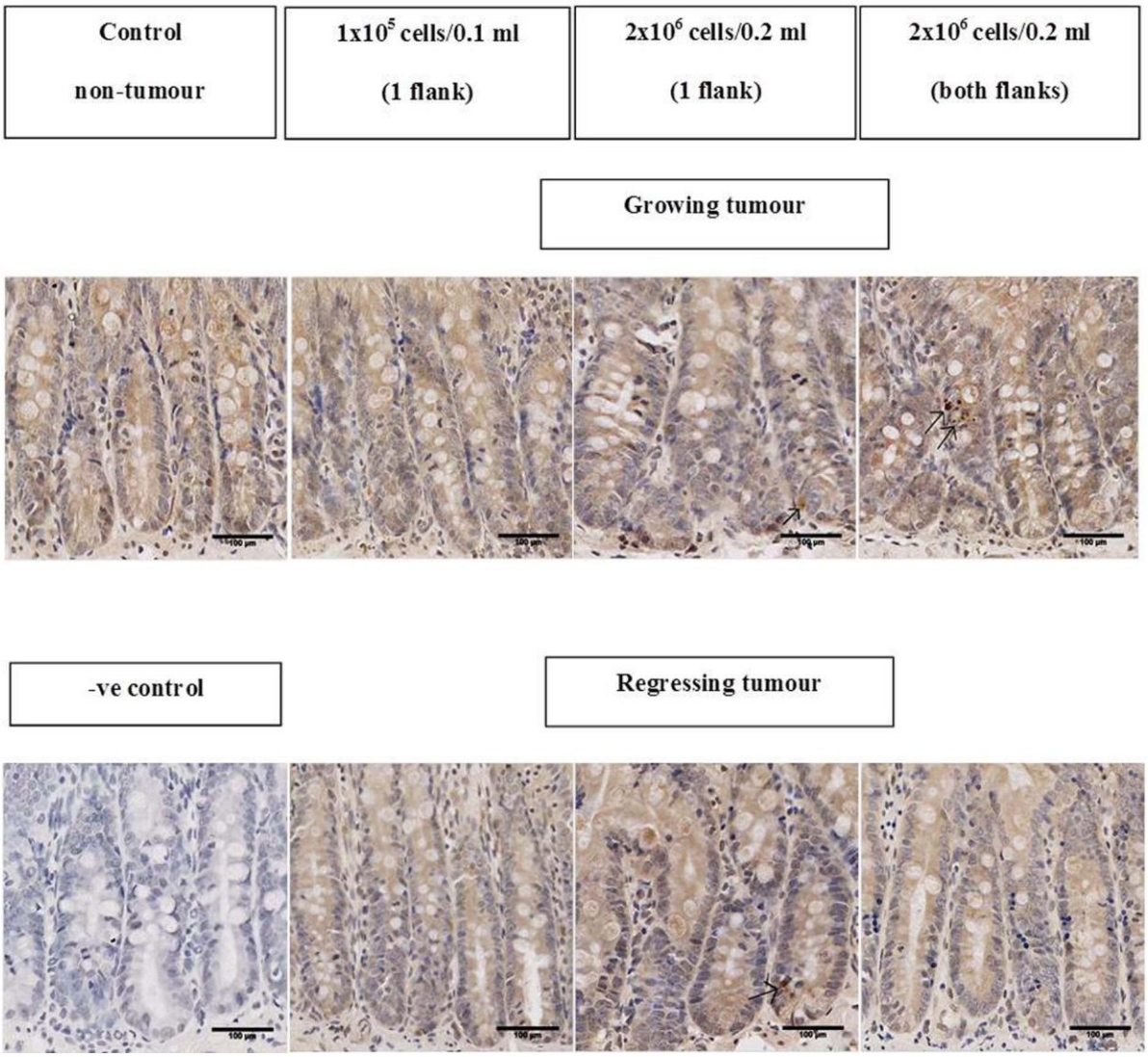

Figure 4.11. Caspase-3 immunohistochemistry in the jejunum of control non-tumour rat and rats injected with different concentration of Walker 256 tumour cells. Photomicrographs are of x200 original magnification (Scale bar: 100 µm). Negative control (-ve control) presents slides stained with secondary antibody only. Arrows indicate apoptotic cells positively stained for caspase-3. Images are representatives of each group.

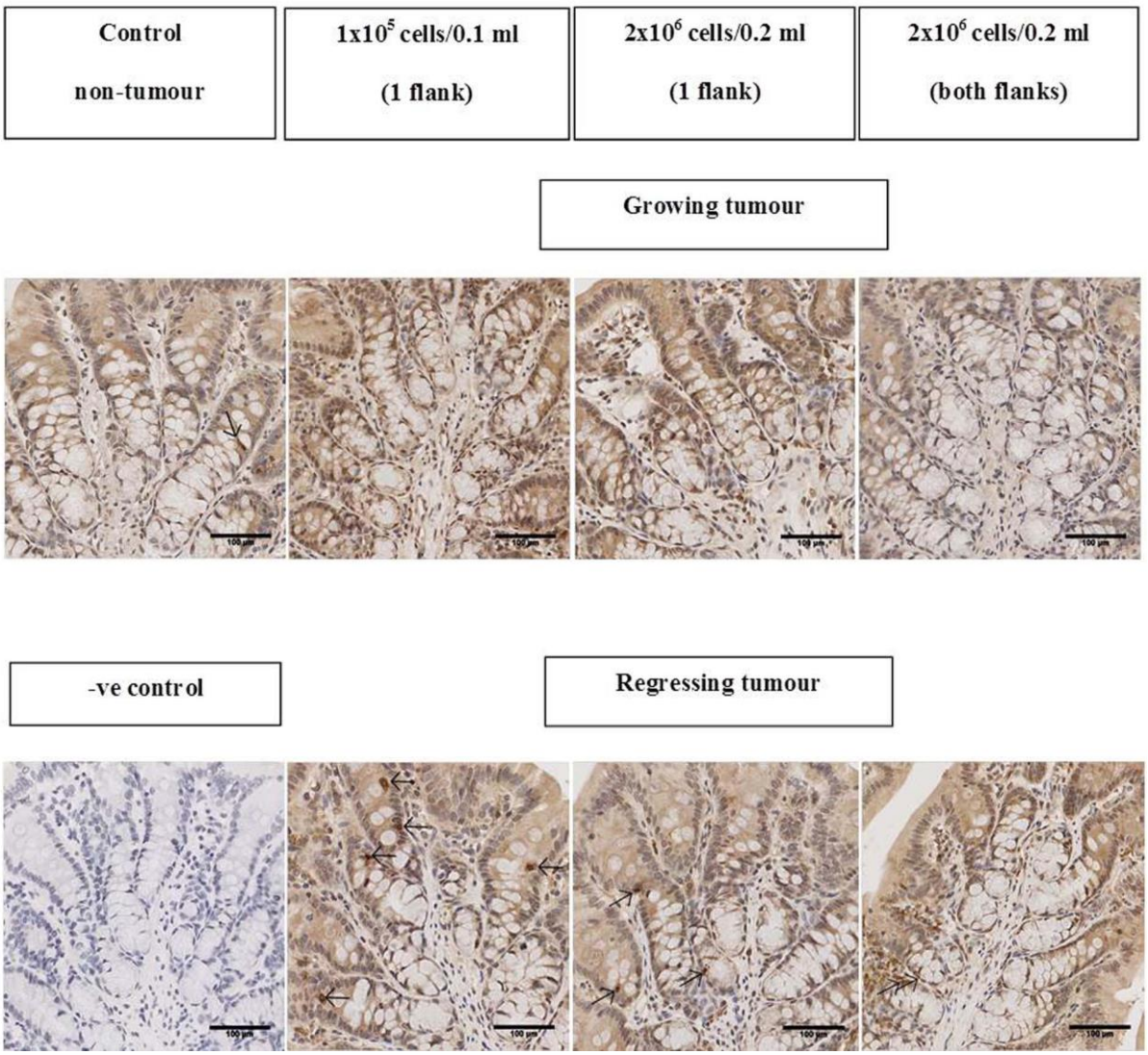

Figure 4.12. Caspase-3 immunohistochemistry in the colon of control non-tumour-bearing rat and rats injected with different concentration of Walker 256 tumour cells. Photomicrographs are of x200 original magnification (Scale bar: 100 µm). Negative control (-ve control) presents slides stained with secondary antibody only. Arrows indicate apoptotic cells positively stained for caspase-3. Images are representatives of each group.

In the Walker 256 tumour tissues, it was found that there was no significant difference in cell apoptosis between any groups of tumour-bearing rats ($p>0.05$) (Figure 4.13). No significant differences in apoptotic cell counts were seen in either regressing or growing tumours of rats injected with $1x10^5$ cells/0.1 ml (1 flank) and $2x10^6$ cells/0.2 ml (1 flank) (Figures 4.14i and ii). However, the caspase-3 positive cells were significantly increased in the regressing tumours of rats injected with $2x10^6$ cells/0.2 ml on both flanks compared in the growing tumours ($p<0.05$) (Figure 4.14iii). Figure 4.15 illustrates the results of caspase-3 immunohistochemistry staining in each tumour-bearing group including the growing and regressing tumours.

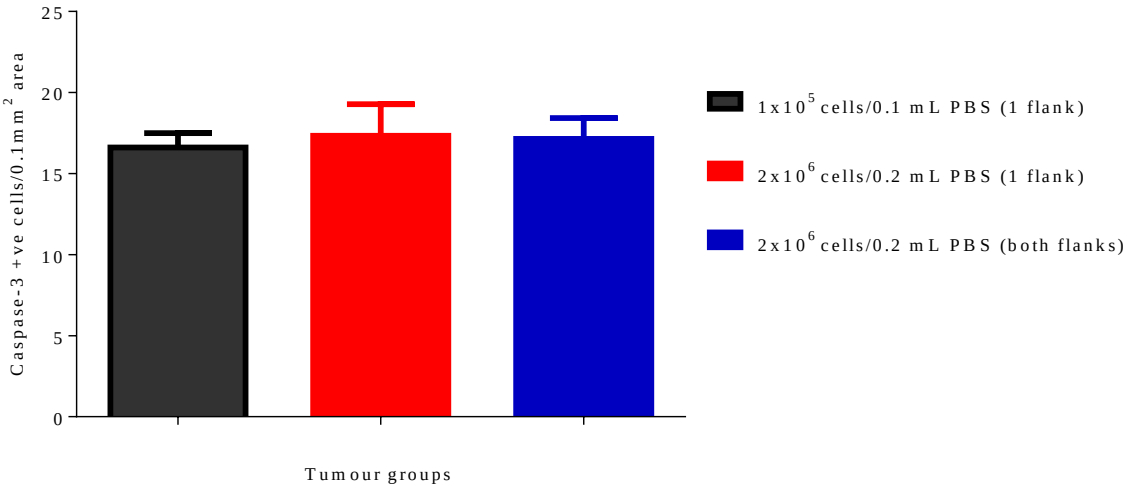

Figure 4.13. Changes in cell apoptosis as identified by caspase-3 immunohistochemistry staining in tumours of Walker 256 tumour rats. Data presented as mean ± S.E.M (n=6 for $1x10^5$ cells/0.1 ml PBS (1 flank), n=12 for $2x10^6$ cells/0.2 ml PBS (1 flank) and n=12 for $2x10^6$ cells/0.2 ml PBS (both flanks)).

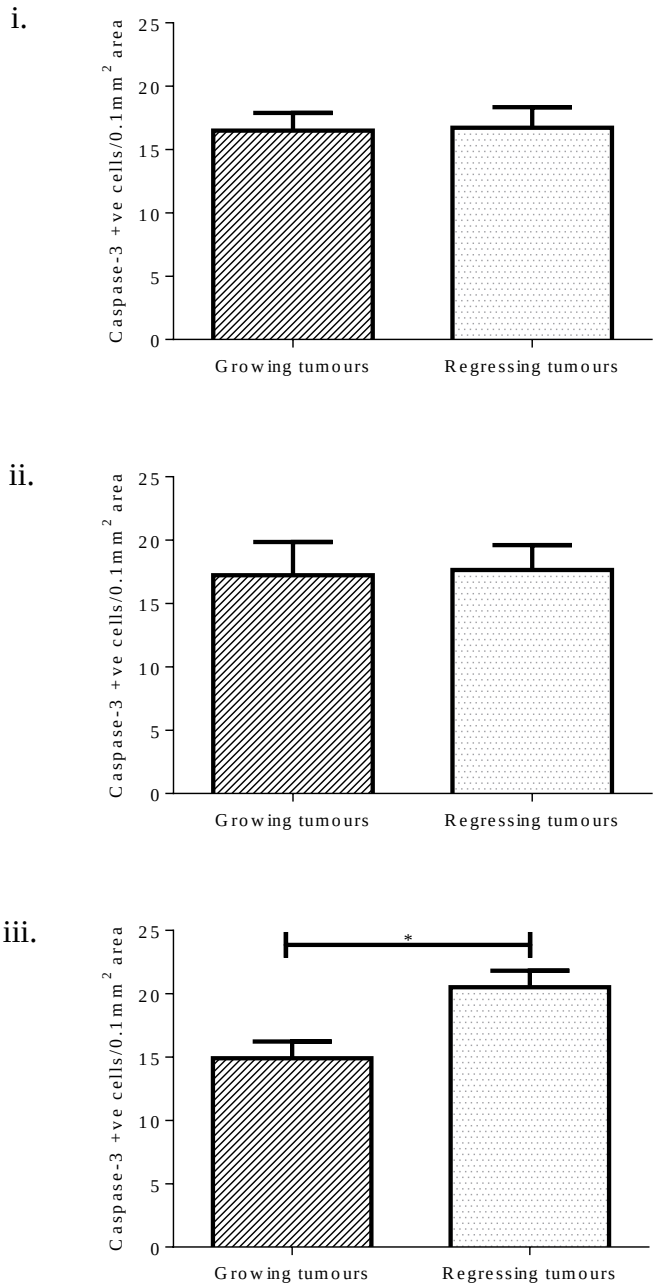

Figure 4.14. Changes in cell apoptosis as identified by caspase-3 immunohistochemistry staining in tumours of rats injected with **i)** $1x10^5$ cells/0.1 ml (1 flank), **ii)** $2x10^6$ cells/0.2 ml (1 flank) and **iii)** $2x10^6$ cells/0.2 ml (both flanks). Data presented as mean ± S.E.M (n=3 for each growing and regressing tumours of $1x10^5$ cells/0.1 ml PBS (1 flank) group, n=6 for each growing and regressing tumours of $2x10^6$ cells/0.2 ml PBS (1 flank) group, n=6 for each growing and regressing tumours of $2x10^6$ cells/0.2 ml PBS (both flanks)*).* for $p<0.05$ compared to growing tumours.*

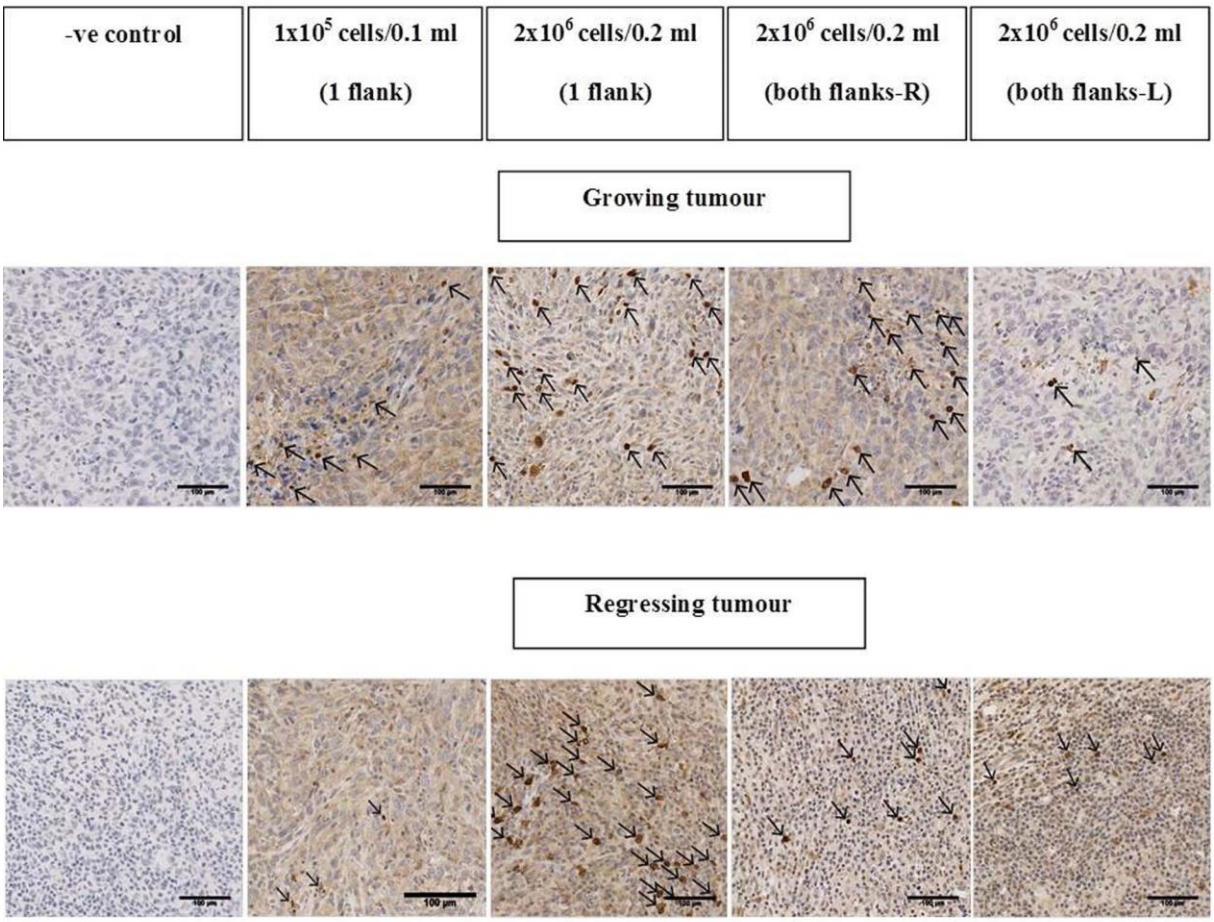

Figure 4.15. Caspase-3 immunohistochemistry staining in the tumours of rats injected with different concentration of Walker 256 tumour cells. Photomicrographs are of x200 original magnification (Scale bar: 100 µm). Negative control (-ve control) presents slides stained with secondary antibody only. Arrows indicate apoptotic cells positively stained for caspase-3. R:right flank tumour, L: left flank tumour. Images are representatives of each group.

To assess epithelial proliferation in the jejunum and colon, Ki-67 positively-stained crypt cells were counted. Figure 4.16 shows that there was no significant difference in cell proliferation between jejunum of control non-tumour rats and all rats from each tumour-bearing group ($p>0.05$). Additionally, no significant differences were seen within the colon ($p>0.05$). Figures 4.17i, ii and iii show the changes in cell proliferation in jejunum and colon of growing and regressing tumours from all tumour rat groups. No significant differences were seen in either jejunum or colon of all experimental groups ($p>0.05$). The photomicrographs of jejunum and colon are shown in Figures 4.18 and 4.19.

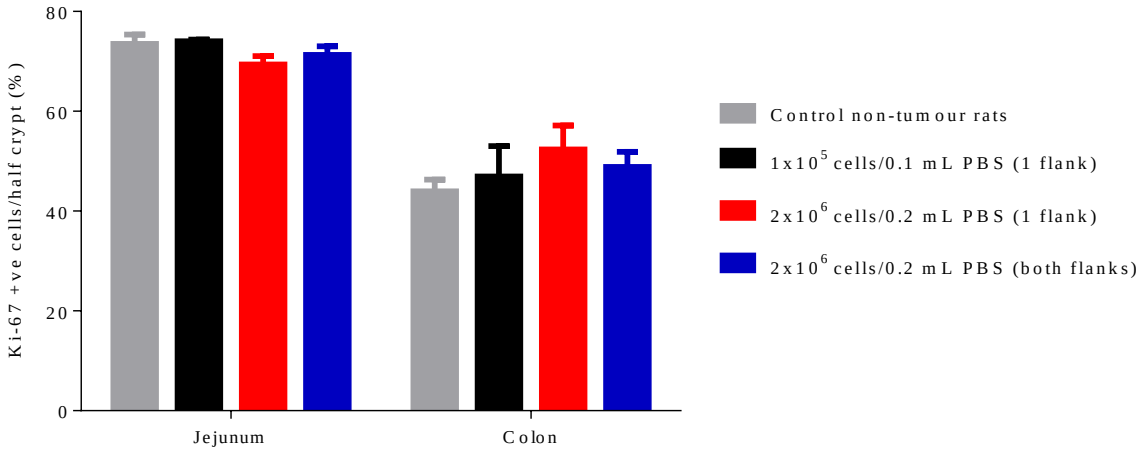

Figure 4.16. Changes in cell proliferation as identified by Ki-67 immunohistochemistry staining in jejunum and colon of Walker 256 tumour rats. Results presented as a percentage of positive cells/half crypt. Data presented as mean ± S.E.M (n=6 for control non-tumour, n=6 for $1x10^5$ cells/0.1 ml PBS (1 flank), n=12 for $2x10^6$ cells/0.2 ml PBS (1 flank) and n=12 for $2x10^6$ cells/0.2 ml PBS (both flanks)).

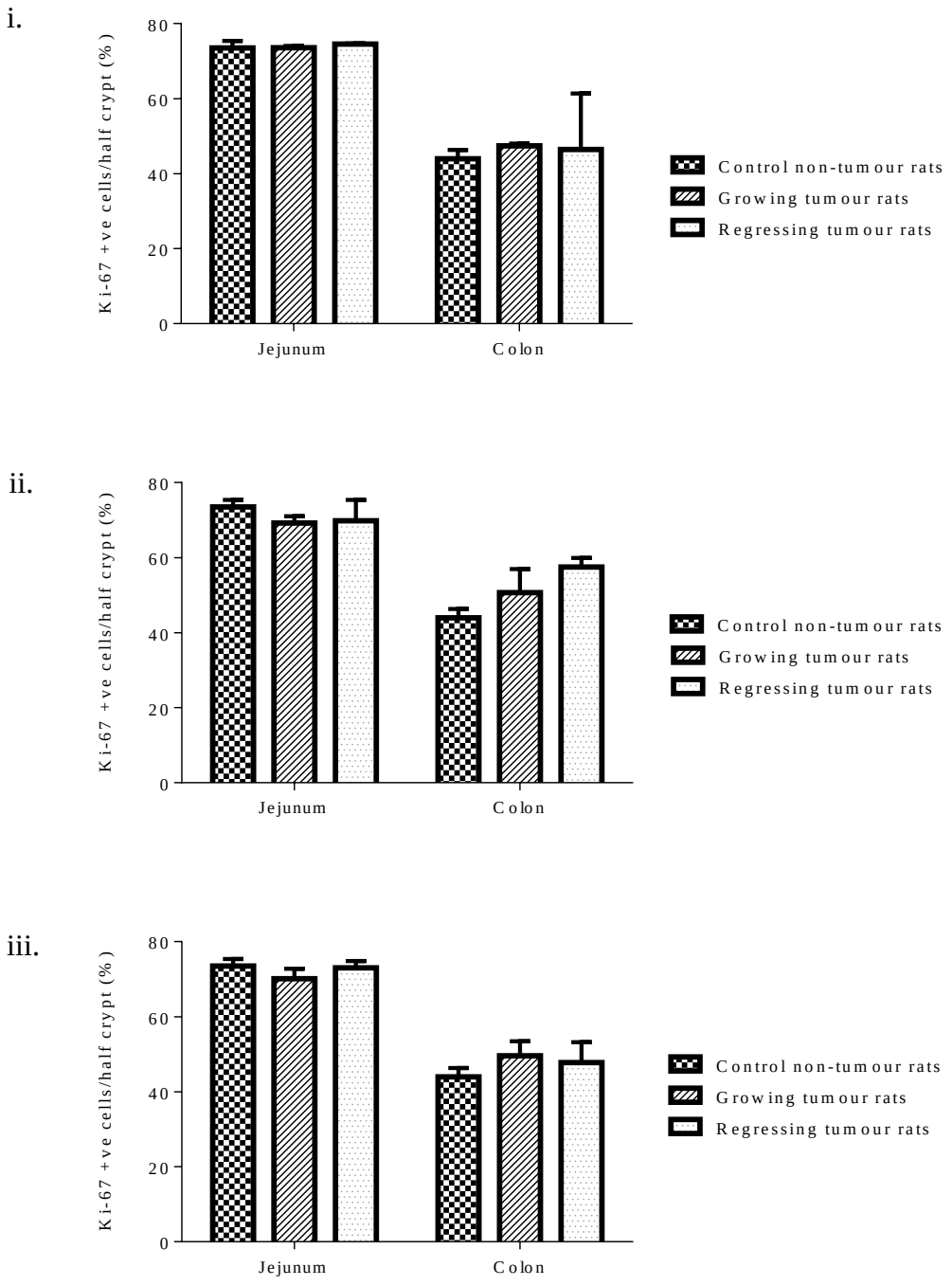

Figure 4.17. Changes in cell proliferation as identified by Ki-67 immunohistochemistry staining in jejunum and colon of rats injected with **i)** $1x10^5$ cells/0.1 ml (1 flank) **ii)** $2x10^6$ cells/0.2 ml (1 flank) **iii)** $2x10^6$ cells/0.2 ml (both flanks). Results presented as a percentage of positive cells/half crypt. Data presented as mean ± S.E.M (n=6 for control non-tumour group, n=3 for each growing and regressing tumours of $1x10^5$ cells/0.1 ml PBS (1 flank) group, n=6 for each growing and regressing tumours of $2x10^6$ cells/0.2 ml PBS (1 flank) group, n=6 for each growing and regressing tumours of $2x10^6$ cells/0.2 ml PBS (both flanks)).

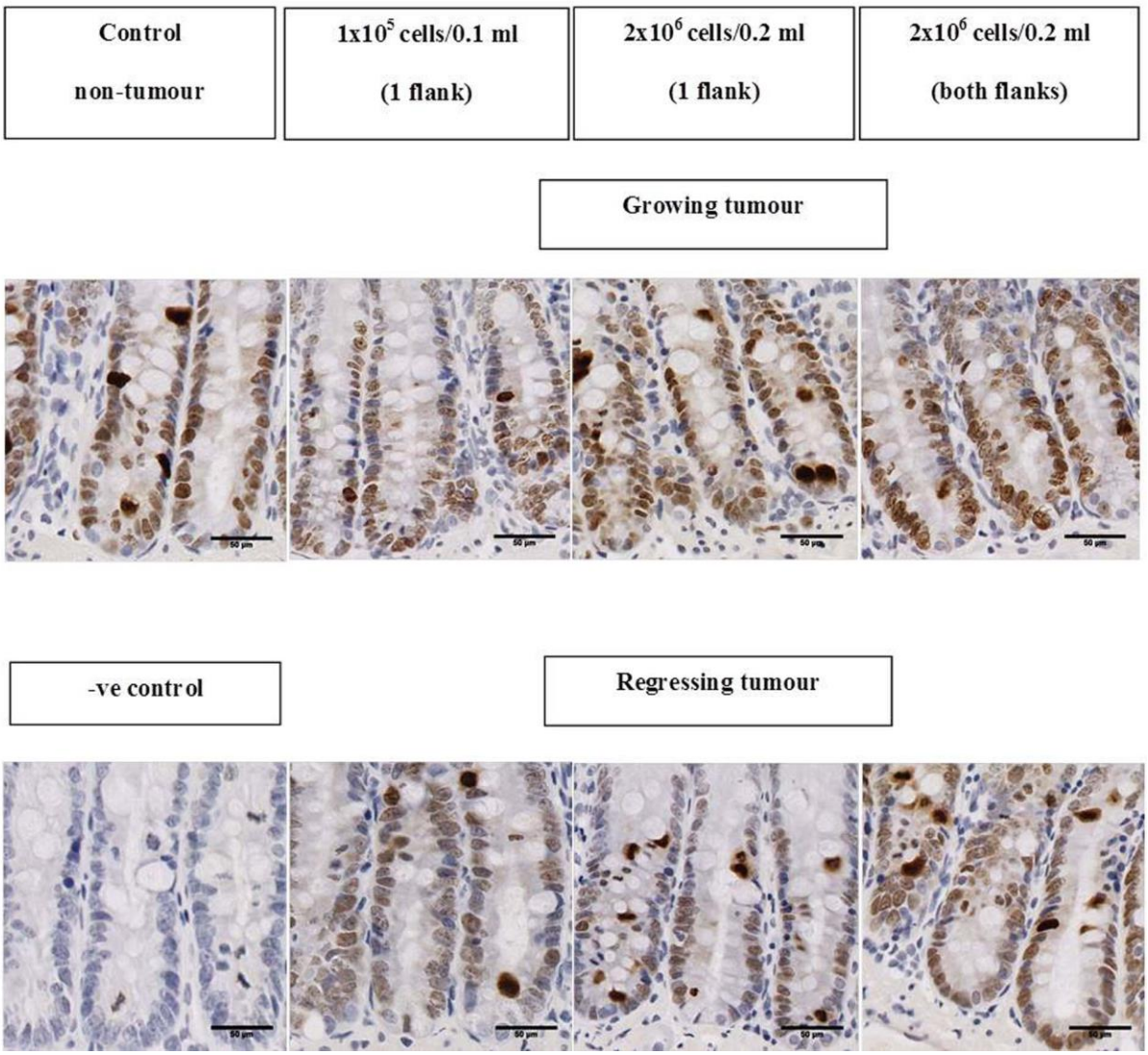

Figure 4.18. Ki-67 positively stained cells of jejunal crypts in control non-tumour rat andrats injected with different concentration of Walker 256 tumour cells. Photomicrographs are of x400 original magnification (Scale bar: 50 µm). Negative control (-ve control) presents slides stained with secondary antibody only. Images are representatives of each group.

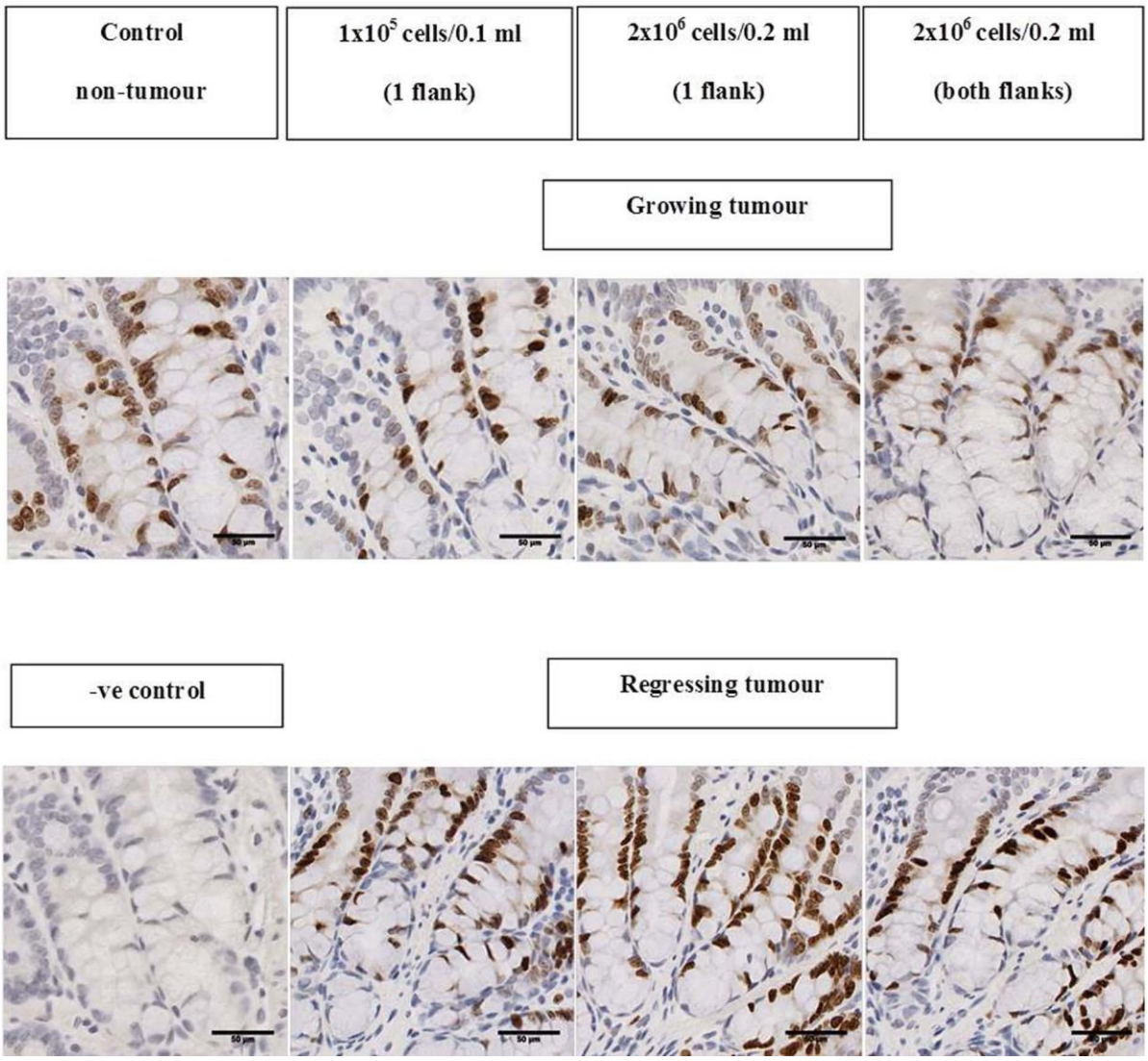

Figure 4.19. Ki-67 positively stained cells of colonic crypts in control non-tumour rat and rats injected with different concentration of Walker 256 tumour cells. Photomicrographs are of x400 original magnification (Scale bar: 50 µm). Negative control (-ve control) presents slides stained with secondary antibody only. Images are representatives of each group.

For Walker 256 tumour tissues, changes in the cell proliferation were also identified by Ki-67 staining. There was no significant difference in cell proliferation between any groups of tumour bearing rats (Figure 4.20). Figure 4.21i, ii and iii show the changes in cell proliferation in growing and regressing tumours from all tumour-bearing groups. Regressing tumours showed significantly decreased cell proliferation compared to growing tumours; $1x10^5$ cells/0.1 ml (1 flank); regressing tumours: 36.33 ± 2.38 % +ve cells/field versus growing tumours: 50.31 ± 1.16 % +ve cells/field, ($p<0.05$), $2x10^6$ cells/0.2 ml (1 flank); regressing tumours: 36.41 ± 0.54 % +ve cells/field versus growing tumours: 62.80 ± 3.81 % +ve cells/field, ($p<0.001$) and $2x10^6$ cells/0.2 ml (both flanks); regressing tumours: 44.08 ± 1.72 % +ve cells/field versus growing tumours: 63.18 ± 2.10 % +ve cells/field, ($p<0.01$), respectively. Figure 4.22 illustrates the results of Ki-67 immunohistochemistry staining in each tumour-bearing group including the growing and regressing tumours.

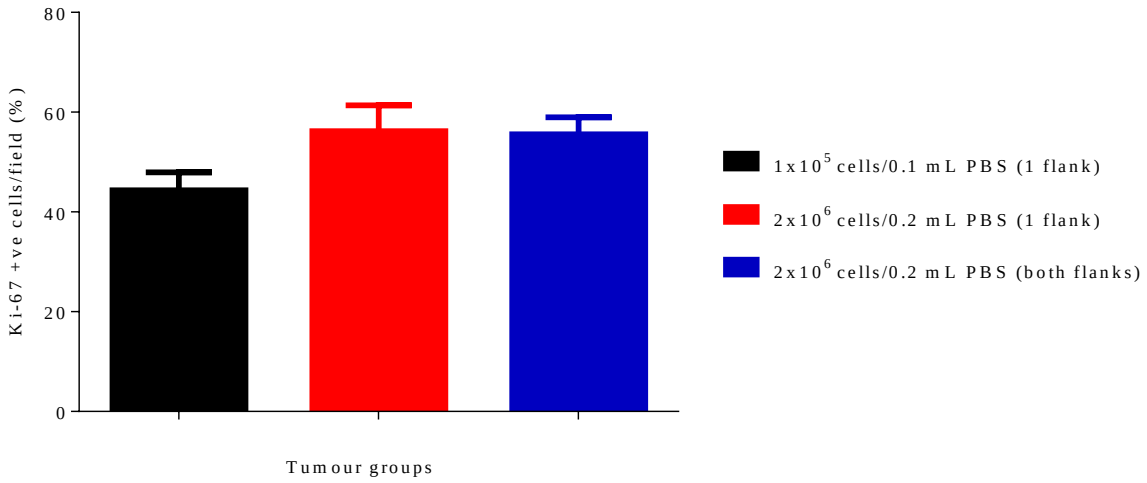

Figure 4.20. Changes in cell proliferation as identified by Ki-67 immunohistochemistry staining in tumour tissues of Walker 256 tumour rats. Results presented as a percentage of positive cells/40x field. Data presented as mean ± S.E.M (n=6 for $1x10^5$ cells/0.1 ml PBS (1 flank), n=12 for $2x10^6$ cells/0.2 ml PBS (1 flank) and n=12 for $2x10^6$ cells/0.2 ml PBS (both flanks)).

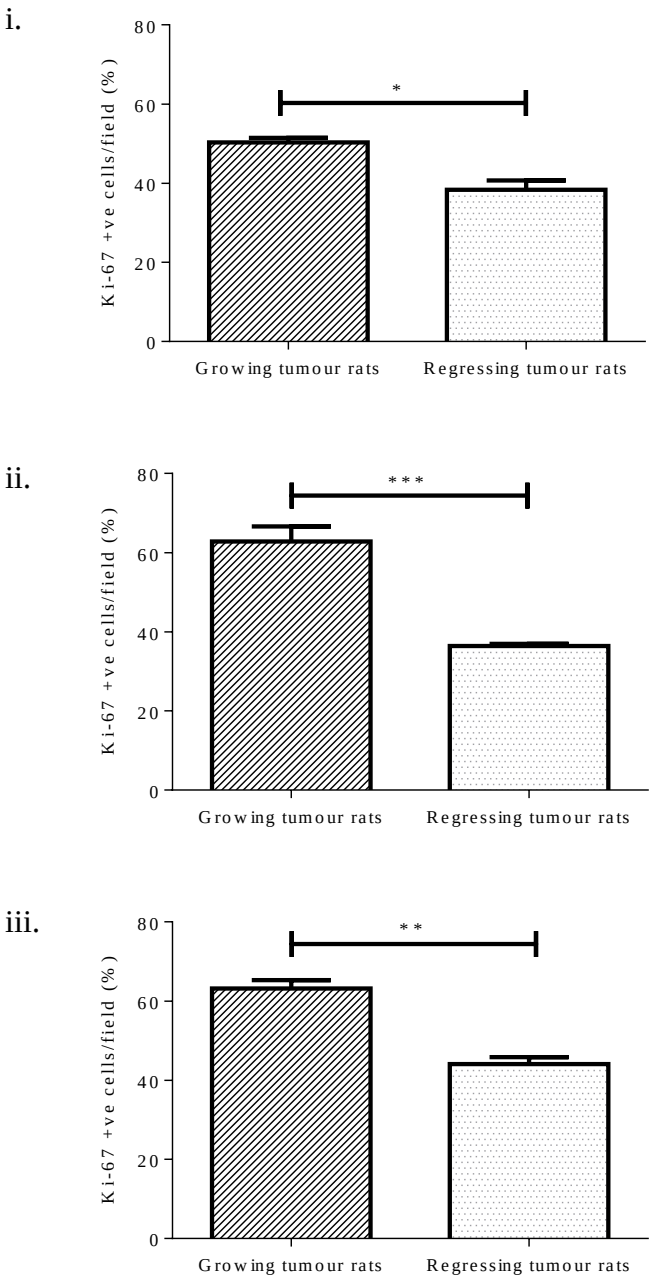

Figure 4.21. Changes in cell proliferation as identified by Ki-67 immunohistochemistry staining in tumour tissues of rats injected with **i)** $1x10^5$ cells/0.1 ml (1 flank) **ii)** $2x10^6$ cells/0.2 ml (1 flank) **iii)** $2x10^6$ cells/0.2 ml (both flanks). Results presented as a percentage of positive cells/ field. Data presented as mean ± S.E.M (n=3 for each growing and regressing tumours of $1x10^5$ cells/0.1 ml PBS (1 flank) group, n=6 for each growing and regressing tumours of $2x10^6$ cells/0.2 ml PBS (1 flank) group, n=6 for each growing and regressing tumours of $2x10^6$ cells/0.2 ml PBS (both flanks)). ** for p<0.05 compared to growing tumour rats, ** for p<0.01 compared to growing tumour rat and *** for p<0.001 compared to growing tumour rats.*

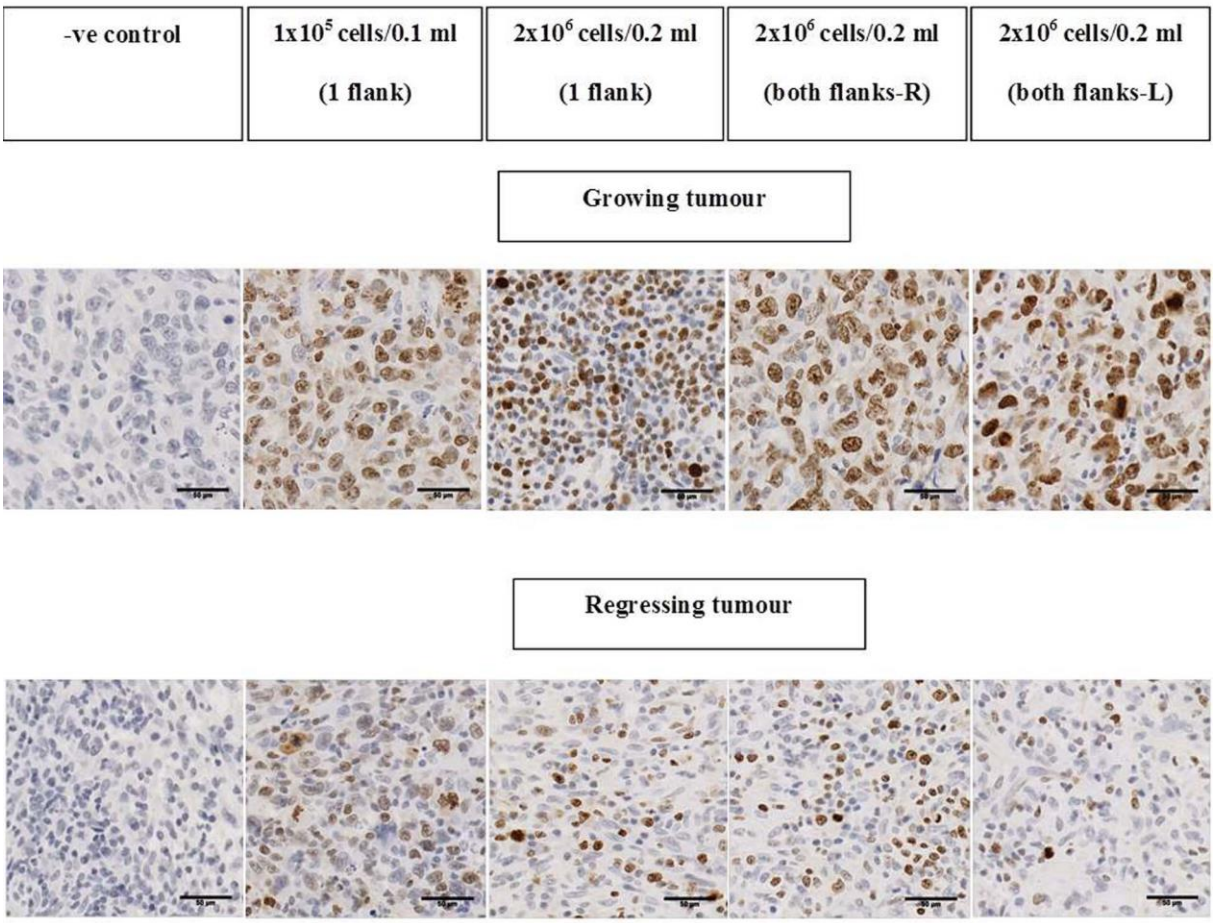

Figure 4.22. Ki-67 positively stained cells of tumours in rats injected with different concentration of Walker 256 tumour cells. Photomicrographs are of x400 original magnification (Scale bar: 50 µm). Negative control (-ve control) presents slides stained with secondary antibody only. Images are representatives of each group.

4.3.7 ErbB1 and ErbB2 mRNA expression in tumour tissue

Real-time PCR was carried out to determine *ErbB1* and *ErbB2* mRNA expression in Walker 256 tumour tissue. Experiments were only conducted on the growing tumours: the regressing tumours were excluded from this experiment. Results of *ErbB1* and *ErbB2* mRNA expression are presented in Figure 4.21. Rat stomach was used as positive control for calibration. Results were normalised by two housekeeping genes (*UBC* and *B2M*). For rats inoculated with Walker 256 tumour cells in both flanks, *ErbB1* and *ErbB2* mRNA expressions were detected in the tumours from each flank. There was no significant difference in *ErbB1* and *ErbB2* mRNA expression between each flank ($p>0.05$). No significant difference was found between any tumour-bearing groups. There were also no significant differences in the expression of both genes between all groups ($p>0.05$).

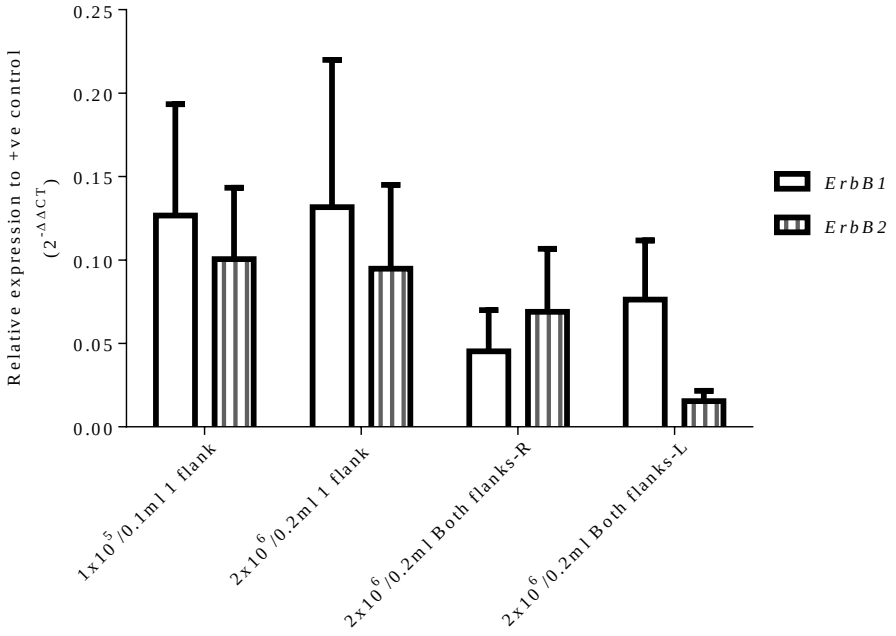

Figure 4.23. *ErbB1* and *ErbB2* mRNA expression in Walker 256 tumour tissues. Rat stomach was used as positive control for calibration. Results were normalised by 2 housekeeping genes: *UBC* and *B2M*. Data presented as mean ± S.E.M with n=3 for $1x10^5$ cells/0.1 ml (1 flank), n=6 for $2x10^6$ cells/0.2 ml (1 flank) and $2x10^6$ cells/0.2 ml (both flanks); R: right, L: left.

4.4 Discussion

This study aimed to develop an appropriate tumour-bearing rat model to study the mechanisms of lapatinib-induced diarrhoea. Throughout this study, rats had been assessed for any clinical signs or stress-related behaviour, body weight change and tumour growth throughout this study. All rats from each group were found to tolerate the tumours and did not show any symptoms of distress. There were rats that were killed earlier either due to necrotised tumours or the tumour burden reaching 10% of body weight; the premature removal of these animals caused a decrease in the total average weight as seen in the body weight graph. There were also differences in body weight range among rats in each group due to the experiments being carried out in three separate parts.

The optimum concentration of Walker 256 tumour cells to develop an appropriate tumour model to study lapatinib-induced diarrhoea is 2 million cells in 0.2 ml PBS and injected into 1 flank only. This is based on the tumour growth rate in which the concentration has given a consistent tumour growth, with tumours measurable by day 4 and reaching a maximum of 10% total body weight by 25 days post-inoculation. There were no visible tumours in any other site. Previous studies have shown that this tumour does not metastasise to other site (Takasuna, Hagiwara et al. 2006, Lewis, Harford-Wright et al. 2013). More importantly, the tumour was found not to cause any adverse effects or distress to the rats. This concentration allows tumour growth for 21 days which is preferable and appropriate to study lapatinib-induced diarrhoea. Clinically, patients treated with lapatinib monotherapy or combination therapy experienced a first diarrhoea event within 6 days of treatment initiation, with a median duration of 7 to 9 days (Di Leo, Gomez et al. 2008), while from previous animal study, it was shown that lapatinib-induced diarrhoea developed 14 days post-initial treatment (Bowen, Mayo et al. 2012). Thus, 21 days will allow time for lapatinib-induced diarrhoea to develop. Injecting the same concentration of cells into both

flanks causes the tumour burden to increase too rapidly in the rats and the experiment was required to be completed at day 15 (as tumour burden had already reached 10% of body weight); thus, injection of $2x10^6$ cells/0.2 ml into both flanks is not deemed an appropriate model to study lapatinib-induced diarrhoea. The lower concentration of Walker 256 cells ($1x10^5$ cells/0.1 ml) was found to be inadequate to develop an appropriate tumour-bearing model. This is in contrast with the results obtained from a previous study by Takasuna and colleagues (Takasuna, Hagiwara et al. 2006), which used this low concentration of Walker 256 tumour cells to develop a tumour-bearing rat model. However, it may be due to sex differences as in this study female albino Wistar rats were used, while in the study by Takasuna male albino Wistar rats were used which may have contributed to the different outcome (Takasuna, Hagiwara et al. 2006). It has been reported that several factors such as sex hormones, genetic differences and environmental causes may contribute to the development of gender disparity in cancer susceptibility (Dorak and Karpuzoglu 2012). Walker 256 cells are derived from female Wistar rat breast carcinoma, thus female Wistar rats were used in this study as to best mimic the original source.

Tumour regression was seen in the rats injected with Walker 256 tumour cells in this model, which was slightly unexpected. Nevertheless, previous studies also observed spontaneous Walker 256 tumour regression (Jensen and Muntzing 1970, Cavalcanti, Gregorini et al. 2003, Fernando Guimarães 2010) and found that the spontaneous regression has been associated with rat strain; spontaneous regression was higher in Wistar rats compared to Sprague-Dawley rats (Jensen and Muntzing 1970, Jaganjac, Poljak-Blazi et al. 2008). Previous studies reported tumour regression on day 12-14 (also observed in the current study) and suggested involvement of an adaptive immune response (Fernando Guimarães 2010). Studies by Jaganjac described the involvement of granulocytes in Walker 256 tumour regression, in which neutrophils plays an important role in the host defense

mechanisms against malignant cells (Jaganjac, Poljak-Blazi et al. 2008, Jaganjac, Poljak-Blazi et al. 2010). In the current study, complete blood counts were carried out, which included white blood cell counts. However, no changes were observed in white blood cell counts or in the individual white blood cell types, between non tumour-bearing versus tumour-bearing rats, and growing tumours versus regressing tumours. On the other hand, a significant increase in platelet levels in the blood of tumour-bearing rats compared to the non-tumour-bearing rats was observed and it was higher in the rats with growing tumours compared to the rats with regressing tumours. Platelets are known to play a crucial role in the maintenance of haemostasis. Besides their central role in haemostasis, platelets also assist and modulate inflammatory reactions and immune responses (Weyrich, Lindemann et al. 2003, Semple, Italiano et al. 2011). Thus, the higher platelet counts in the tumour rats are expected as platelet counts increase during conditions such as inflammation and tumorigenesis. Higher platelet levels in growing tumour rats compared to regressing tumour rats are also expected as progression of tumours will influence platelet activation (Karshovska, Weber et al. 2013). In the current study, a significant decrease in serum lactate dehydrogenase in both growing and regressing tumour rats was observed. Serum lactate dehydrogenase is elevated during tumour growth as lactate formation is upregulated in tumour cells by lactate dehydrogenase for tumour progression (Chen, Zhu et al. 2016). This may explain low serum lactate dehydrogenase in rats with regressing tumours. However, low level of serum lactate dehydrogenase was also observed in rats with growing tumours. Further studies are required to further clarify the mechanism underlying this regression progression, thus, tumour regression shall be taken into consideration in lapatinib-induced diarrhoea in tumour-bearing rats study.

As this study is concerned with the development of a tumour-bearing rat model to study lapatinib-induced diarrhoea, the changes in electrolytes such as sodium and chloride

from the blood biochemical analysis were also taken into consideration, as sodium and chloride play an important role in water reabsorption. The presence of chloride in the lumen provides the electrochemical driving force for paracellular movement of sodium. The resulting accumulation of sodium chloride in the lumen provides the osmotic gradient for water to flow to the lumen (Barrett and Keely 2000). The secretion of chloride ions is important in controlling fluid flow across various epithelial surfaces, including the intestine, helping to keep the fluidity (Barrett and Keely 2000). An increase in solutes in the intestinal lumen would result in the osmotic movement of water into the lumen, which may lead to diarrhoea (Stringer, Gibson et al. 2007). Therefore, it is thought that any significant changes in sodium and chloride may coincide with diarrhoea. In the current study, rats injected with $2x10^6$ cells/0.2 ml (1 flank) and $1x10^5$ cells/0.1 ml (1 flank) had a significant increase of sodium and chloride levels in serum, respectively, compared to control non-tumour rats; however none of the rats experienced diarrhoea. Thus, a direct connection between changes in sodium and chloride serum levels and diarrhoea requires further investigation. In human, the normal serum chloride level is 98-106 mmol/L (Ahmad, Wahid et al. 2016), while the normal serum sodium level is 135-145 mmol/L (Braun, Barstow et al. 2015). Both serum chloride and sodium levels in the tumour rats were increased compared to non-tumour rats. However, in comparison to human, the results obtained in this study for serum chloride and sodium levels were within the normal range. Thus, might support the outcome that all rats did not experience diarrhoea.

The histological analysis showed jejunal villi of rats injected with $1x10^5$ cells/0.1 ml in 1 flank were significantly shorter compared to control non-tumour rats and tumour-bearing rats injected with $2x10^6$ cells/0.2 ml in both 1 flank and 2 flanks. Healthy and extended jejunal villi in a tumour-bearing rat is important as the purpose of this study is to develop a tumour-bearing rat model to study lapatinib-induced diarrhoea. Shorter jejunal villi caused by

tumour growth would complicate any results relating to diarrhoea induced by lapatinib as atrophy of intestinal mucosa may lead to a secretory-type diarrhoea due to inability to control absorption and secretion through decreased surface area (Gibson and Keefe 2006). This further supports that $2x10^6$ cells/0.2 ml is the optimum concentration to develop a tumour-bearing rat to study lapatinib-induced diarrhoea. The shorter jejunal villi in rats with regressing tumours will also be taken into consideration in the lapatinib-induced diarrhoea study. However, no significant difference was found in jejunal and colonic crypt length among all the experimental groups including rats with growing and regressing tumours, thus showing no effect of Walker 256 tumour on jejunum and colon, further supporting that the tumour will not influence development of any damage to the jejunum and colon in the lapatinib-induced diarrhoea study.

Walker 256 tumour growth was found not to promote apoptosis in the crypt cells of jejunum and colon of all tumour-bearing rats from each group. Jejunal and colonic crypt cell proliferation was also unchanged during tumour development. This indicates that the tumour does not promote cell death or abnormal cell proliferation in jejunum and colon. Apoptotic and proliferating cells in tumour tissues from all tumour rat groups were also evaluated. Increased apoptotic tumour cells were observed in regressing tumours of rats injected with $2x10^6$ cells/0.2 ml in both flanks. This is expected, as one of the factors associated with spontaneous tumour regression (as seen in this study) is apoptosis. Other factors include the immune system and conditions in the tumour microenvironment, particularly the presence of inhibitors of metalloproteinases and angiogenesis (Ricci and Cerchiari 2010) and the absence or insufficiency of specific proteins such as epithelial cadherin (Munshi and Stack 2006), integrin (Hood and Cheresh 2002) and adenosine (Hoskin, Mader et al. 2008) could inhibit the tumour growth and metastases (Ricci and Cerchiari 2010). Lower tumour cell proliferation in regressing tumours compared to growing tumours of all groups are also

expected as regressing tumours display reduced tumourigenesis, hence a decrease in proliferating tumour cells. The findings above shall be taken into consideration in lapatinib-induced diarrhoea study as they may assist in elucidating the effect of lapatinib on the intestines as well as on the tumours.

Lapatinib is an oral small-molecule reversible dual inhibitor of ErbB1 and ErbB2 tyrosine kinases (Rusnak, Lackey et al. 2001). Lapatinib blocks downstream mitogen-activated protein kinase (MAPK) and phosphatidylinositol-3-kinase (PI3K) proliferation and survival signalling pathways in ErbB2 expressing breast cancer cell lines, tumor xenografts and patients with ErbB2-positive breast cancers (Spector, Xia et al. 2005, Rusnak, Alligood et al. 2007). Thus, apart from optimising Walker 256 tumour cell concentration and defining the tumour effect on the intestines to support lapatinib-induced diarrhoea in a tumour-bearing rat model study, it is also essential to determine *ErbB1* and *ErbB2* mRNA expression in Walker 256 tumour tissues. This will allow any future intervention studies to simultaneously assess the effect on gut protection as well as ensuring lapatinib's tumouricidal effect is not compromised. Results revealed the mRNA expression of *ErbB1* and *ErbB2* in the tumour tissue; therefore it is suitable to develop lapatinib-induced diarrhoea in this tumour-bearing rat model. Previous studies to observe the effect of ErbB1/ErbB2 targeted drugs also have been carried out in *ErbB1* and/or *ErbB2* mRNA expressing tumour tissues (Fujimoto-Ouchi, Sekiguchi et al. 2007, Wang, An et al. 2014, Bahr, Toraih et al. 2015).

ErbB1 mRNA expression was undetectable in Walker 256 cell line due to its low expression (Chapter 3), however, it was detectable in Walker 256 tumour tissue. This is not surprising as a study has demonstrated higher mRNA expression in tumours than in cell lines. The study which was conducted to determine mRNA expression in cell lines and tumours for estrogen receptor-positive and estrogen receptor-negative also found that the differences are due to the absence of stromal and immune components in the cell line

(Vincent, Findlay et al. 2015). ErbB1 protein expression was not confirmed in the current study. This limitation could be overcome by conducting experiments such as Western blotting or immunohistochemistry.

4.5 Conclusion

Walker 256 tumour does not cause any changes in jejunum and colon, thus there will be no interference of tumour on the intestines in the study of lapatinib-induced diarrhoea. The tumour concentration of 2 million cells in 0.2 ml PBS in one flank is the optimum concentration to develop an appropriate tumour-bearing rat model to study lapatinib-induced diarrhoea. As tumour regression was seen, this matter shall be taken into consideration in the future study in which the tumour growth shall be observed intently. However, it is important to clarify that the main purpose of this study is not to look at the effect of lapatinib on tumour growth in which this study aims to develop an appropriate rat tumour model to study TKI-induced gut damage. An in-depth study is required to study the underlying mechanisms of the tumour regression.

Chapter 5

Investigating lapatinib-induced diarrhoea in a tumour-bearing rat model

5.1 Introduction

Lapatinib is a targeted drug and dual inhibitor of ErbB1/ErbB2. It is used to treat ErbB2-positive breast cancer (Medina and Goodin 2008). Formation of ErbB1/ErbB2 or ErbB2/ErbB3 heterodimers enhances ligand binding, receptor tyrosine phosphorylation and cell proliferation compared with ErbB1 homodimers (Johnston and Leary 2006), hence, lapatinib has superior potency compared to single inhibitors of ErbB1 in inhibiting signal transduction of tumour proliferation and survival (Kaufman, Trudeau et al. 2009).

Targeted drugs are known to be effective in cancer treatment, but their use is limited by adverse effects (Loriot, Perlemuter et al. 2008). Diarrhoea has been reported in patients administered with targeted drugs. A large percentage of patients administered lapatinib experience diarrhoea (Burris, Taylor et al. 2009). Two factors might contribute to this toxicity. Firstly, the low aqueous solubility of lapatinib results in incomplete and unstable absorption, hence low bioavailability after oral administration (Burris, Taylor et al. 2009). In addition, the elimination half-life of lapatinib between single-dose and repeated doses shows great variation, and long-term administration of lapatinib can cause accumulation, which may intensify its toxicity (Bence, Anderson et al. 2005). All of these are the disadvantages of clinical use of lapatinib and may in part account for the large discrepancies in patient outcomes on this agent (Zhang, Fan et al. 2013).

Another factor that might contribute to the toxicity is ErbB1 inhibition by lapatinib. It is speculated that ErbB1 inhibition by lapatinib may interfere with the normal functioning in

the intestines leading to diarrhoea (Loriot, Perlemuter et al. 2008). Diarrhoea has also been reported in other cases of patients administered with targeted drugs, particularly ErbB1 tyrosine kinase inhibitor (Cohen, Williams et al. 2003, Cohen, Johnson et al. 2005, Johnson, Cohen et al. 2005, Dungo and Keating 2013). The mechanism of diarrhoea associated with ErbB1 tyrosine kinase inhibitors is poorly understood, which makes it extremely difficult to develop interventions and guidelines.

Thus, the purpose of this study was to gain new information about the mechanism behind the development of diarrhoea in targeted cancer therapy using the small molecule, ErbB1/ErbB2 tyrosine kinase inhibitor, lapatinib. To date, no study has looked specifically at the mechanisms behind its main adverse event, diarrhoea, using a clinically relevant tumour-bearing model. This study provides the first information regarding lapatinib-induced diarrhoea in rats with tumours. The outcome from this study will increase understanding of the mechanisms of lapatinib-induced diarrhoea.

In the previous study, the concentration of Walker 256 tumour cells required to develop an appropriate tumour-bearing rat model to study lapatinib-induced diarrhoea was established (Chapter 4). In this study, the established model has been used to investigate lapatinib-induced diarrhoea in tumour-bearing rats.

5.2 Materials and Methods

5.2.1 Animals

16 female albino Wistar rats were used in this study and weighed between 170-200g. All experimental procedures were approved by the Animal Ethics Committees of SA Pathology and the University of Adelaide. Due to the nature of the diarrhoea that can be induced by lapatinib, animals were monitored up to four times daily and if any animal showed

certain criteria (as defined by the Animal Ethics Committee) they were humanely killed. These criteria included a dull or ruffled coat, change in temperament, reluctance to move, weight loss and diarrhoea.

5.2.2 Drug

Lapatinib 250 mg/tablet (Tykerb®), Glaxo Smith-Kline) was supplied by Royal Adelaide Hospital. Preparation of the drug is described in Chapter 2 Section 2.1.

5.2.3 Lapatinib-induced diarrhoea in a tumour-bearing rat model

On arrival, rats were housed in groups for a week to acclimatise at the Animal Care Facility, Hanson Institute, SA Pathology.

The experiment was begun by inoculating Walker 256 rat breast tumour cells into the right flanks of all rats. Walker 256 cells were cultured as described in Chapter 2 (Sections 2.2 and 2.9). Each flank was inoculated with 0.2 ml of cell suspension containing $2x10^6$ Walker 256 cells as described in Chapter 4.

After 5 days, the tumours were measurable with digital calipers (and represented approximately 0.01% of bodyweight) and the rats were divided into 3 groups to prepare the rats for drug administration. The rats were divided into groups based on tumour size, to ensure consistency across groups, as follows:

- Group 1: saline vehicle rats (control; n=6)
- Group 2: lapatinib administered at 240 mg/kg once daily (L240 1x; n=6)
- Group 3: lapatinib 200 mg/kg twice daily (L200 2x; n=4).

Lapatinib was administered by oral gavage using a soft feeding tube starting on day 5. Control and L240 1x rats received the vehicle or lapatinib every morning while L200 2x rats

were administered with lapatinib every morning and afternoon, until the end of the study (day 21 or when the tumour reached 10% bodyweight). An experimental flow chart is included (Figure 5.1).

The rats were weighed every day and checked for responses to treatment including diarrhoea, weight loss, changes in temperament, changes in coat appearance, reluctance to move, and reduced food and water intake up to four times daily. The size of the tumour was measured by digital calipers every day to assess growth and to enable an estimation of the tumour as a % of bodyweight. The same formula as described in Chapter 4 Section 4.2.2 was used to measure the tumour burden. In the previous study (Chapter 4), it had been found that the tumour caused no distress to the animal. At the end of the experiment, all animals were killed by deep anaesthesia before cardiac puncture and cervical dislocation. Upon necropsy, tumour, jejunum and colon were collected for analysis. Organs and tumours were also weighed to determine any weight difference between groups.

Figure 5.1. Experimental flow chart.

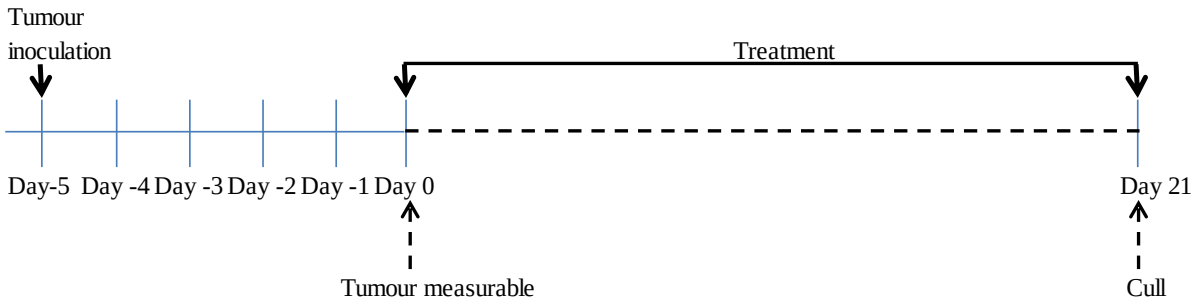

5.2.4 Diarrhoea assessment

The animals were assessed up to four times daily to check for the severity of diarrhoea. Mild diarrhoea was defined as soft stools, moderate diarrhoea as loose stools with perianal staining of fur and severe diarrhoea as watery stools +/- mucus with fur staining incorporating hind legs (Bowen, Mayo et al. 2012). Clinically in patients, grade 1 diarrhoea is defined as increase of 4 stools per day over baseline, mild increase in ostomy output

compared with baseline. Grade 2 is increase of 4–6 stools per day over baseline, intravenous fluid for 24 hours and moderate increase in ostomy output compared with baseline but not interfering with daily living. Grade 3 is increase of 7 stools per day over baseline, incontinence, intravenous fluids and severe increase in ostomy output compared with baseline and interfering with daily living activities. Grade 4 is defined as life-threatening consequences and grade 5 is death (Benson, Ajani et al. 2004).

5.2.5 Histological assessment

This method was carried out to evaluate the histopathological changes in jejunum, colon and tumour. The detailed procedures are described in Chapter 2 Section 2.10.

5.2.6 Measurement of villus height and crypt depth

This method was carried out to determine any morphological changes in jejunum and colon mucosa. The methods are described in Chapter 2 Section 2.11.

5.2.7 Immunohistochemistry staining

5.2.7.1 Caspase-3 and Ki-67 detection

Markers of apoptosis (caspase-3) and proliferation (Ki-67) in jejunum and colon were detected via immunohistochemistry. The detailed procedures are described in Chapter 2 Section 2.12. Details of caspase-3 and Ki-67 antibodies are described in Table 5.1.

5.2.7.2 Total and phosphorylated ErbB1 and ErbB2

Immunohistochemistry was used to demonstrate the presence and location of ErbB1 and ErbB2 in formalin fixed, paraffin embedded tissue sections. The same procedure as described for detection of caspase-3 and Ki-67 (Chapter 2, Section 2.12) was repeated until blocking with endogeneous peroxidase, in which after that non-specific binding was blocked by incubating slides in Covance blocking serum (Level 2 USA~Ultra Streptavidin Detection System, Signet Laboratories, Dedham MA, USA) for 30 minutes at room temperature.

Endogenous avidin and biotin was blocked using the Avidin-Biotin Blocking Kit (Vector Laboratories, Burlingame, CA), 15 minutes each. Following washing in PBS, sections were then incubated overnight for 16 hours with a rabbit primary antibody (ErbB1- 1:100, ErbB2- 1:100, pErbB1- 1:50, pErbB2- 1:100) (Abcam, UK) diluted in 50% Covance blocking serum in PBS at 4^{o}C in a humidified chamber. Details of the antibodies used in this study were described in Table 5.1. The concentration of each antibody was optimised using a specific positive control (ErbB1: rat skin, ErbB2: ErbB2-positive human breast carcinoma, pErbB1: rat skin, pErbB2: rat heart) prior to experiment.

Slides were washed in PBS (3x) following incubation with primary antibody and were incubated with Covance linking reagent for 20 minutes at room temperature. Then, Covance labelling reagent was applied to the sections and incubated for 20 minutes at room temperature. Slides were rinsed in PBS prior to the application of DAB solution from Covance kit for antibody visualisation. The same subsequent steps after incubation with DAB solution were carried out as described in Chapter 2, Section 2.12. Slides were examined using a light microscope (Olympus) prior digital analysed using NanoZoomer and confirmed by expertise in Mucositis Research Group. Qualitative analysis was performed using NDP software and staining intensity was scored as 0: no staining, 1: weak staining, 2: moderate staining, 3: strong staining and 4: intense staining. This qualitative grading system has been published extensively (Bowen, Gibson et al. 2005, Yeoh, Bowen et al. 2005, Bowen, Mayo et al. 2014) and has been used routinely in our laboratory (Yeoh, Bowen et al. 2005, Al-Dasooqi, Gibson et al. 2010). All assessments were done in both jejunum (villi and crypts) and colon (apical and basal region) and blinded to treatment.

Table 5.1. Description of the antibodies used in immunohistochemistry staining.

Primary antibody (µg/ml)	Clone	Concentration used (µg/ml)	Secondary antibody	Manufacturer)
Anti-caspase-3 (100 µg/ml)	Rabbit polyclonal	1	Goat anti-rabbit IgG	Abcam
Anti-Ki-67 (100 µg/ml)	Rabbit polyclonal	1	Goat anti-rabbit IgG	Abcam
Anti-ErbB1 (200 µg/ml)	Rabbit polyclonal	2	Multispecies Linking Reagent	Abcam
Anti-pErbB1 (Tyr 1173) (100 µg/ml)	Rabbit polyclonal	2	Multispecies Linking Reagent	Santa Cruz
Anti-ErbB2 (200 µg/ml)	Rabbit polyclonal	2	Multispecies Linking Reagent	Abcam
Anti-pErbB2 (phospho Y1248) (1000 µg/ml)	Rabbit polyclonal	10	Multispecies Linking Reagent	Abcam

5.2.8 Tumour mitotic index

Mitotic index is used to describe the proportion of cells of a tissue which are in mitosis at a particular point in time. It can be crudely estimated by counting the number of mitotic figures per high power field and is employed in pathology as a measure of the rate of cellular proliferation in certain malignant tumours (Burkitt, Young et al. 1993). In this study, mitotic index of tumours from all rats was determined by counting the number of mitotic figures in 10 randomly selected x40 fields using haematoxylin and eosin (H&E) slides from histological assessment experiment.

5.2.9 Statistical analysis

Body and organ weight, villus height and crypt depth measurement, apoptosis (caspase-3) and proliferation (Ki-67), immunohistochemistry staining intensity as well as tumour growth results were statistically analysed using two-way ANOVA with Tukey's multiple comparison test to compare means of each group. Means of body weight and tumour growth data were compared between each experimental day of all groups. Results for tumour weight and tumour mitotic index were analysed via one-way ANOVA with Tukey's multiple comparison test to compare means between all groups. Statistical significance was accepted as $p<0.05$.

5.3 Results

5.3.1 Body weight

There were no difference observed between rats' body weight and adjusted body weight to percentage of tumour (Figure 5.2 A and B), or the percentage weight changes for both graphs (Figure 5.3 A and B). Body weight increased in all rats from day 5 until day 1

pre-treatment except for L200 2x that showed a fluctuating weight, however there were no significant differences between all groups ($p>0.05$) (Figure 5.2 A).

Once daily lapatinib treatment (L240 1x) was associated with a decrease in weight gain compared to controls. This was statistically significant at days 3 (0.80 % vs 6.19 %, $p<0.01$), 4 (0.88 % vs 7.14 %, $p<0.001$), 5 (0.39 % vs 8.27 %, $p<0.0001$), 6 (1.69 % vs 9.41 %, $p<0.0001$), 7 (2.67 % vs 8.93 %, $p<0.001$), 8 (3.25 % vs 11.17 %, $p<0.0001$), 9 (4.36 % vs 12.20 %, $p<0.05$), 10 (5.30 % vs 12.97 %, $p<0.05$), 11 (6.23 % vs 14.68 %, $p<0.01$), 12 (6.65 % vs 15.00 %, $p<0.01$) and 13 (8.10 % vs 14.97 %, $p<0.05$) (Figure 5.3 A).

Twice daily lapatinib treatment rats (L200 2x) lost 1.38 ± 1.55 % of body weight on day 2, 2.80 ± 1.64 % on day 3, 5.17 ± 1.51 % on day 4, 7.15 ± 1.32 % on day 5, 9.54 ± 1.43 % on day 6, 11.34 ± 1.42 % on day 7 and 13.16 ± 1.75 % on day 8. These were statistically significant compared to controls (day 2: $p<0.001$, days 3 to 8: $p<0.0001$) (Figure 5.3 A).

L200 2x also showed a significant weight loss compared to L240 1x at days 4 ($p<0.01$), 5 ($p<0.001$) and 6 to 8 ($p<0.0001$) (Figure 5.3 A). L200 2x rats were killed on day 8 due to severe weight loss. Rats from other groups which were supposed to be killed on day 21 were killed on day 18 due to some rats displaying necrotised tumours.

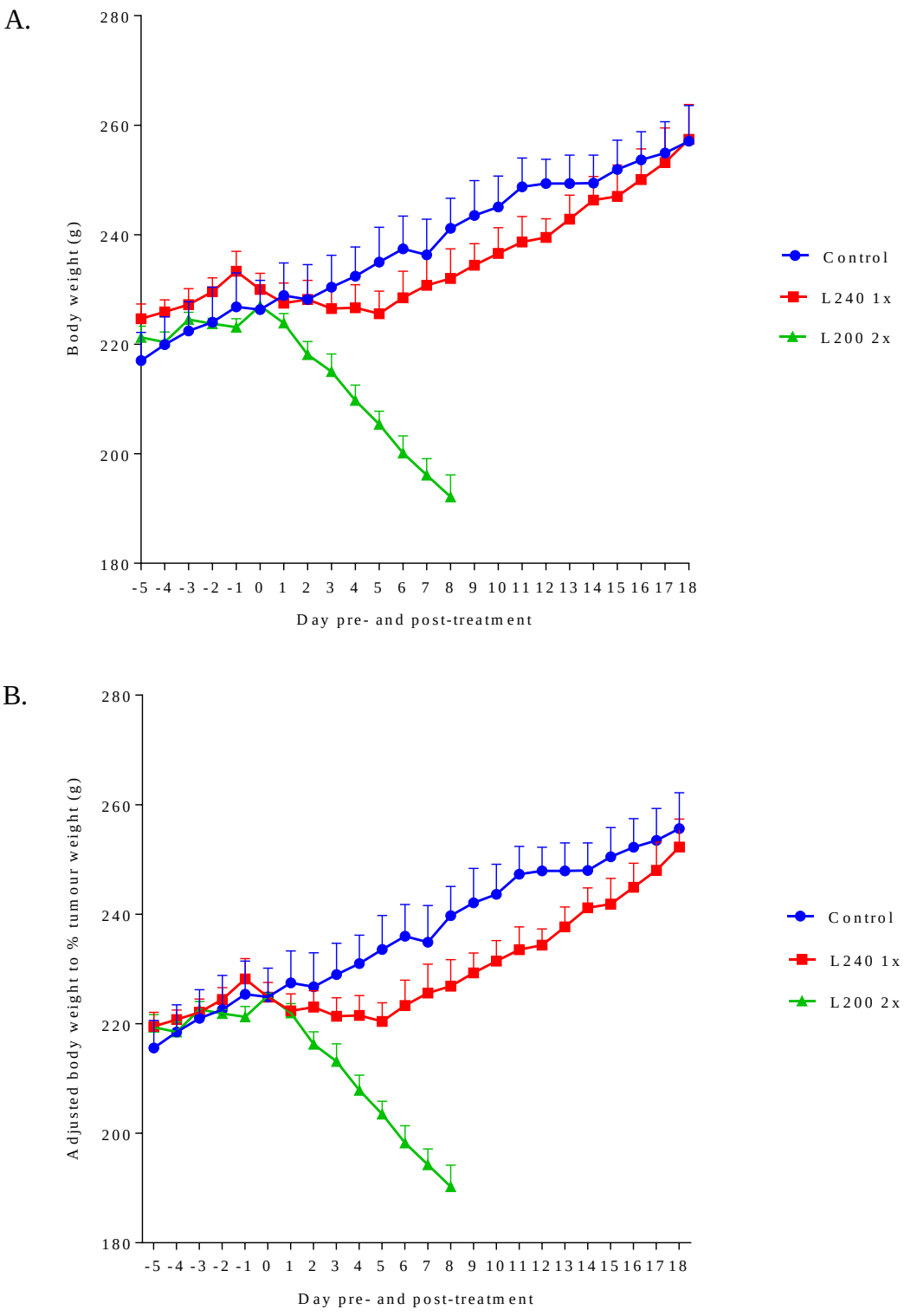

Figure 5.2. **(A)** Body weight and **(B)** Adjusted body weight to percentage tumour weight for all groups. Control: vehicle-treated control rats, L240 1x: lapatinib 240mg/kg once daily administration, L200 2x: lapatinib 200 mg/kg twice daily administration. Data are presented as mean ± S.E.M (n=6 for Control, n=6 for L240 1x and n=4 for L200 2x).

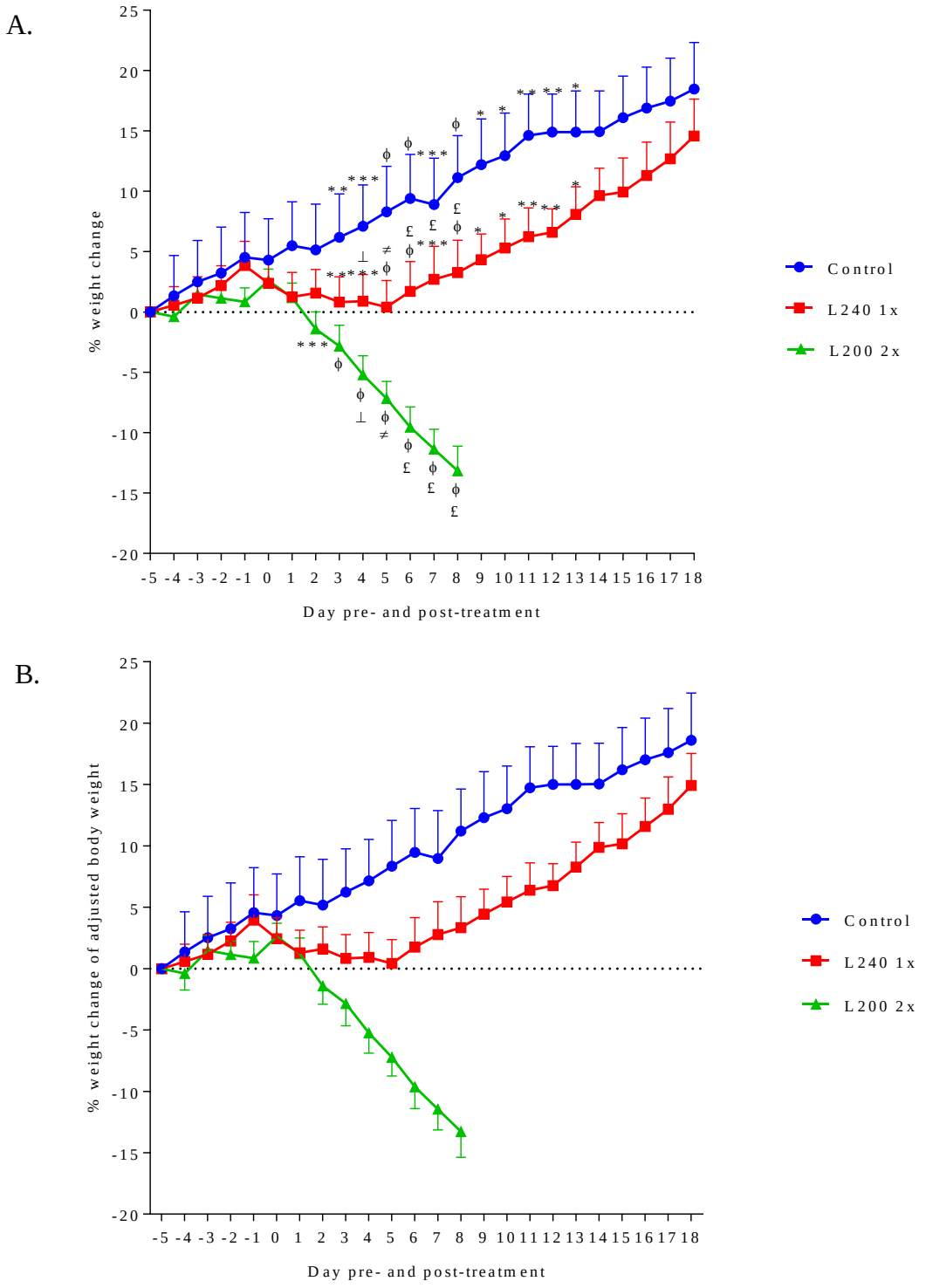

Figure 5.3. (A) Percentage weight change and **(B)** percentage weight change of adjusted weight compared to the starting weight on day 5 pre-initial treatment for all groups. Control: vehicle-treated control rats, L240 1x: lapatinib 240mg/kg once daily administration, L200 2x: lapatinib 200 mg/kg twice daily administration. Data are presented as mean ± S.E.M (n=6 for Control, n=6 for L240 1x and n=4 for L200 2x). ** for p<0.05 compared to controls, ** for p<0.01 compared to controls, *** for p<0.001 compared to controls, ϕ for p<0.0001 compared to controls, ⊥ for p<0.01 compared to L240 1x, ≠ for p<0.001 compared to L240 1x and £ for p<0.0001 compared to L240 1x.*

5.3.2 Tumour growth

Tumour burden in the experimental groups was measured to evaluate any effect of lapatinib on tumour growth. However, the results indicated that both L240 1x and L200 2x rats did not show any decrease in tumour growth after lapatinib administration (Figure 5.4). The unexpected results were also seen in vehicle-treated control rats that showed a decrease in tumour burden. No significant difference was found in the tumour growth among all groups from day 0 until day 8 post-initial treatment. There were no significant differences between controls and L240 1x until day 16. However, the tumour burden in L240 1x rats was significantly higher than control rats at days 17 (4.51 ± 1.39 % vs 1.92 ± 0.62 %) ($p<0.05$) and 18 (4.89 ± 1.52 % vs 1.68 ± 0.69 %) ($p<0.01$).

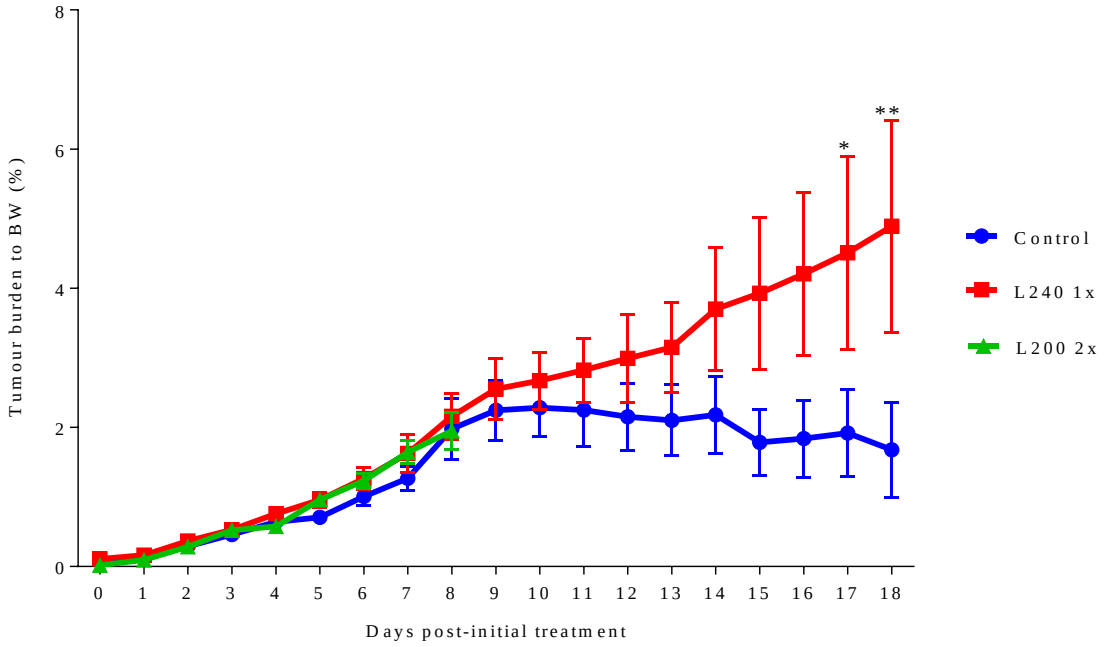

Figure 5.4. Percentage of tumour burden over body weight for all groups after treatment. Control: vehicle-treated control rats, L240 1x: lapatinib 240mg/kg once daily administration, L200 2x: lapatinib 200 mg/kg twice daily administration. Data are presented as mean ± S.E.M (n=6 for Control, n=6 for L240 1x and n=4 for L200 2x). * *for $p<0.05$ compared to controls and ** for $p<0.01$ compared to controls.*

5.3.3 Tumour weight

Tumours from the experimental groups were also weighed upon necropsy. A graph of tumour weight and percentage of tumour weight over body weight are shown below in Figures 5.5 A and B. As mentioned earlier, rats from L200 2x group were killed on day 8, thus the tumours were weighed upon necropsy on day 8 compared to the rats from other groups in which the tumours were weighed upon necropsy on day 18. Therefore, the lower tumour weight and tumour weight percentage over body weight in L200 2x was expected. No significant differences were found in tumour weight between all groups.

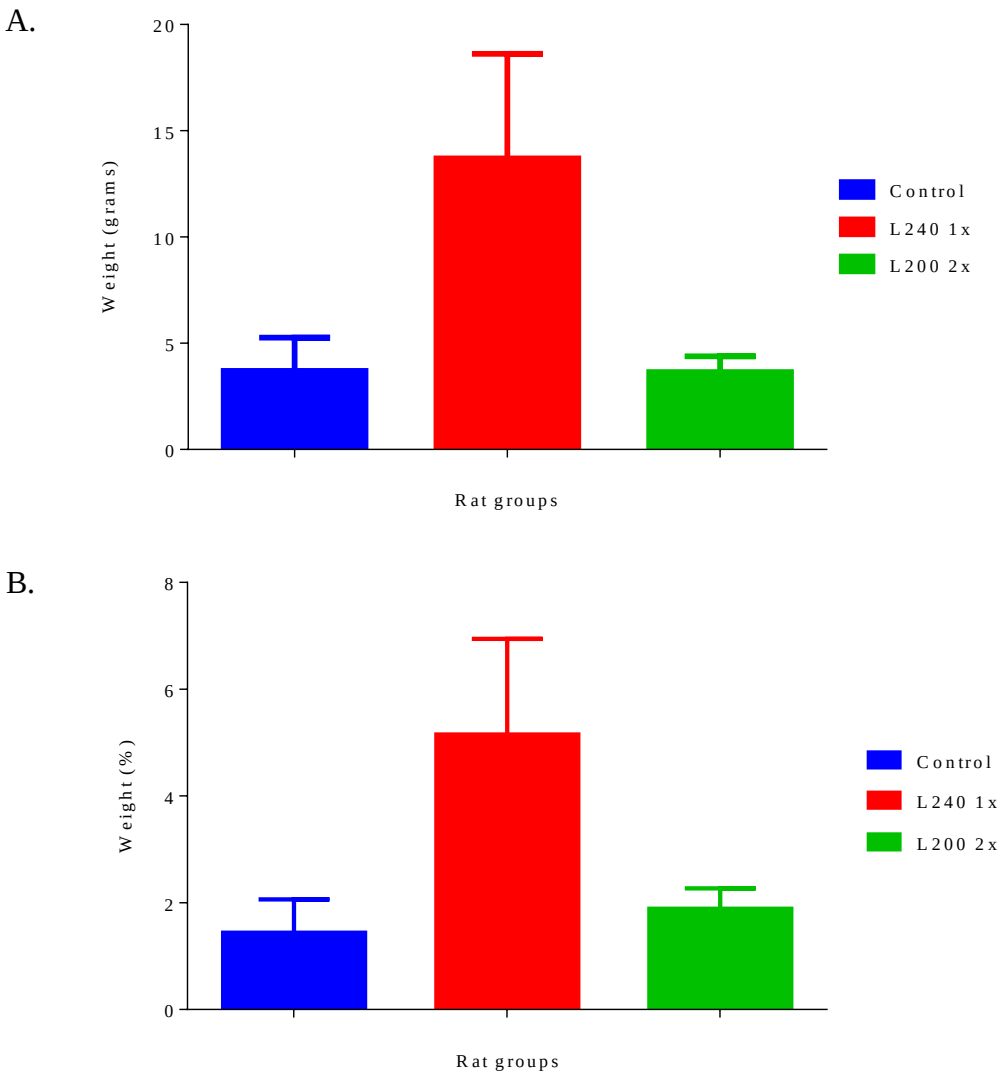

Figure 5.5. (A) Tumour weight and **(B)** percentage tumour weight over body weight of all experimental groups. Control: vehicle-treated control rats, L240 1x: lapatinib 240mg/kg once daily administration, L200 2x: lapatinib 200 mg/kg twice daily administration. Data are

presented as mean ± S.E.M (n=6 for Control, n=6 for L240 1x and n=4 for L200 2x).

5.3.4 Tumour mitotic index

Tumour mitotic index for each group was determined by counting the number of mitotic figures in 10 randomly selected x40 fields (Figure 5.6). However, there were no significant differences in the mitotic cell counts between all groups. The photomicrographs are shown in Figure 5.7.

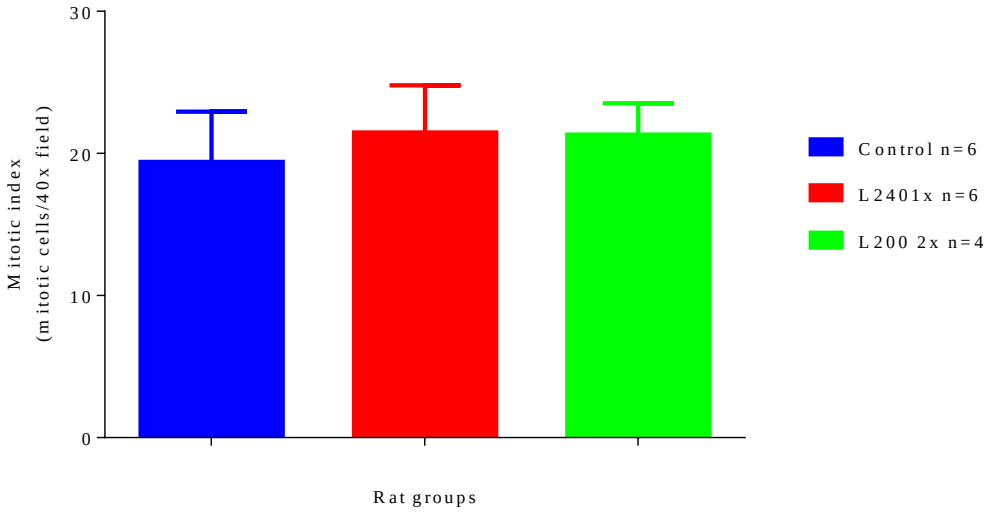

Figure 5.6. Tumour mitotic index for all groups after treatment. Control: vehicle-treated control rats, L240 1x: lapatinib 240mg/kg once daily administration, L200 2x: lapatinib 200 mg/kg twice daily administration. Data are presented as mean ± S.E.M (n=6 for Control, n=6 for L240 1x and n=4 for L200 2x).

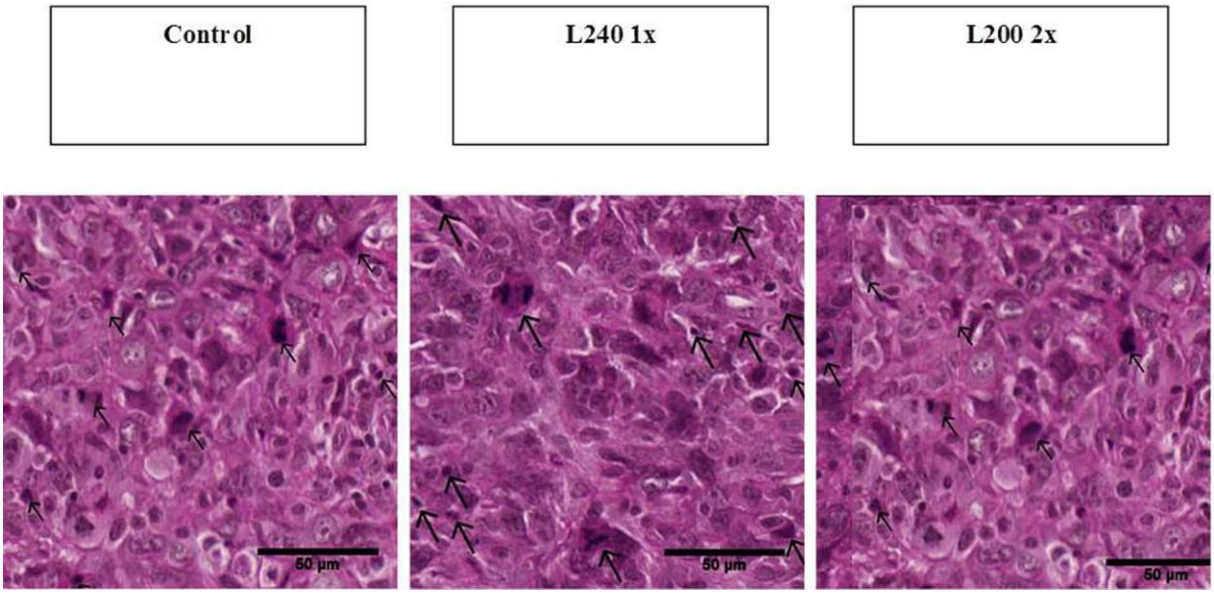

Figure 5.7. Mitotic cells of tumour rats treated with saline/vehicle: Control, lapatinib 240 mg/kg once daily: L240 1x and lapatinib 200 mg/kg twice daily: L200 2x. Arrows indicate mitotic cells. Images are representatives of each group (Photomicrographs are of x400 original magnification, scale bar: 50 µm).

5.3.5 Organ weight

Total organ weight is shown in Figure 5.8 A. No significant differences between controls, L240 1x and L200 2x rats were observed in kidney, spleen, stomach and large intestine weight as a percentage of body weight (Figure 5.8 B). However, there was a significant difference in liver weight as a percentage of body weight, in which L240 1x (5.27 ± 0.20 %) and L200 2x (5.14 ± 0.30 %) were heavier than controls (3.82 ± 0.10%) ($p<0.0001$). L240 1x small intestines (3.41 ± 0.24 %) showed a significant increase in weight percentage compared to controls (2.98 ± 0.14 %) ($p<0.05$) and L200 2x rats (2.34 ± 0.07 %) ($p<0.0001$). Small intestines of L200 2x rats were also significantly lighter than controls ($p<0.01$) (Figure 5.8 B). Upon necropsy, it was observed that lapatinib-treated rats had yellow or pale liver. The other parts of the body such as ears and skin, mesentery lymph nodes, thymus, Payer's patches, stomach content and others were also yellow.

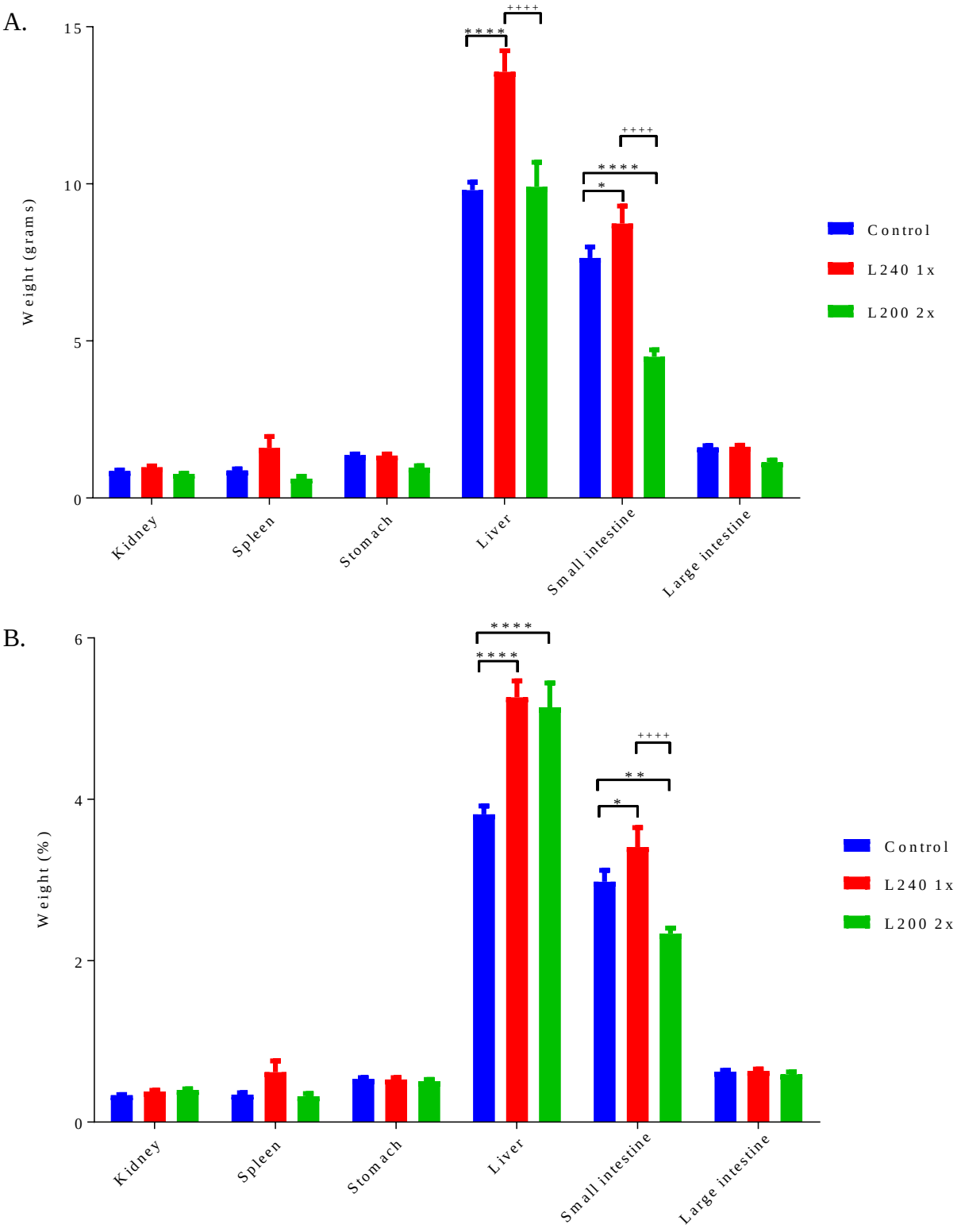

Figure 5.8. A. Total organ weight **B.** Organ weight as a percentage of body weight. Control: vehicle-treated control rats, L240 1x: lapatinib 240mg/kg once daily administration, L200 2x: lapatinib 200 mg/kg twice daily administration. Data are presented as mean ± S.E.M and were compared between groups (n=6 for Control, n=6 for L240 1x and n=4 for L200 2x. ** for p<0.05 compared to controls, ** for p<0.01 compared to controls, **** for p<0.0001 compared to controls and $^{++++}$ for p<0.0001 compared to L240 1x.*

5.3.6 Diarrhoea assessment

Diarrhoea was graded as 0 (no diarrhoea), grade 1 (mild diarrhoea defined as soft stools), grade 2 (moderate diarrhoea defined as loose stools with perianal staining of fur) and grade 3 (severe diarrhoea defined as watery stools +/- mucus with fur staining incorporating hind legs). No control or L240 1x rats experienced diarrhoea. However, 80% of L200 2x rats experienced diarrhoea. Overall incidence of grade 1 diarrhoea in L200 2x rats was 25% on days 1-4, 75% on day 5, 50% on days 6 and 7, and 25% on day 8. On day 4, an additional 25% of animals experienced grade 2 diarrhoea. No grade 3 diarrhoea was observed. Results are presented in Figure 5.9.

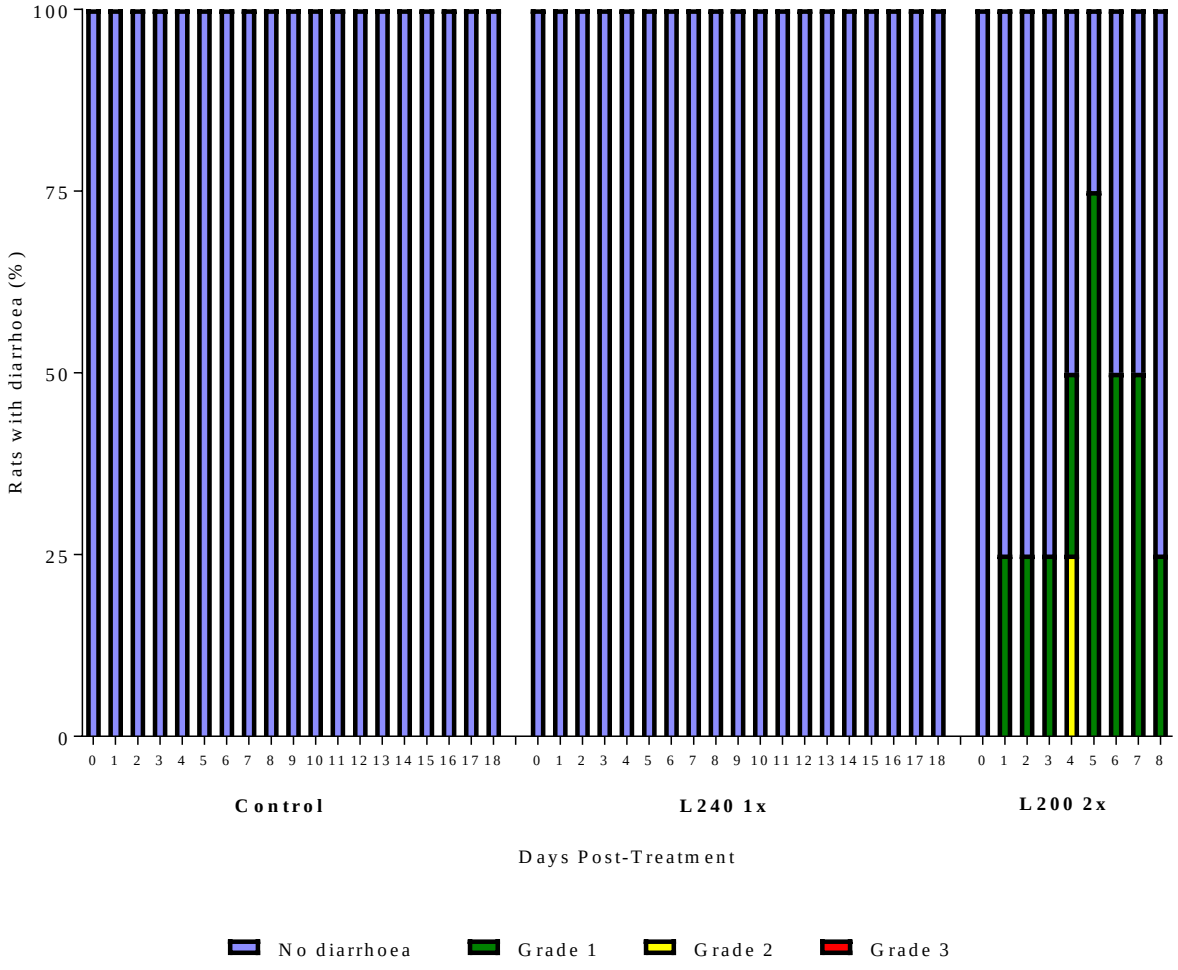

Figure 5.9. Incidence of diarrhoea in rats administered with saline/vehicle (Control) n=6, lapatinib 240 mg/kg once daily (L240 1x) n=6 and lapatinib 200mg/kg twice daily (L200 2x) n=4.

5.3.7 Histological analysis

5.3.7.1 Jejunum and colon

No histological changes were evident in control or L240 1x rats. Marked damage evident as villus atrophy and blunting was observed in the jejunum of L200 2x rats. No marked changes were seen in the jejunal crypts between groups. Histological damage was not observed in the colon of any groups (Figure 5.10).

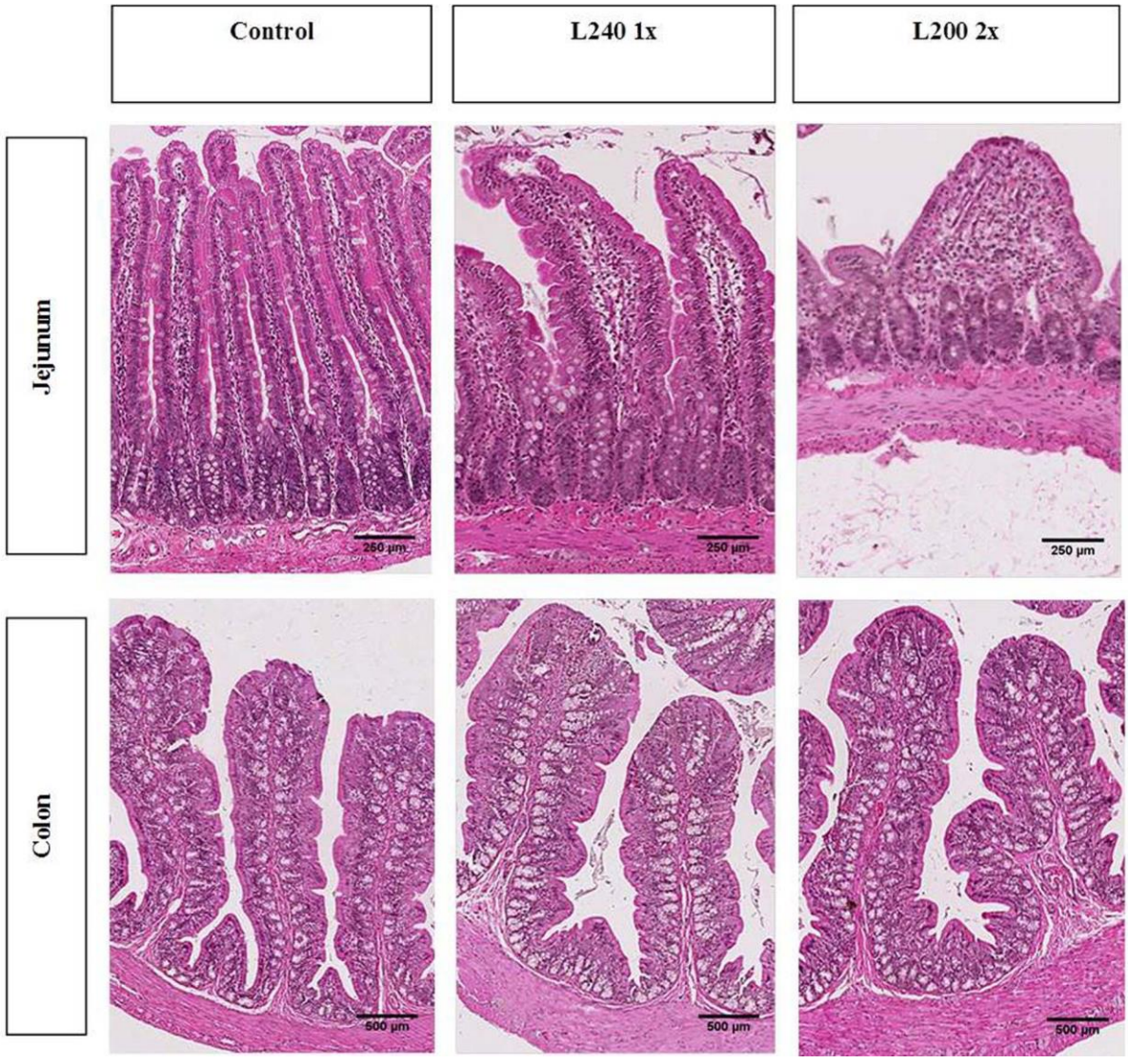

Figure 5.10. Histological images of jejunum (Photomicrographs are of x50 original magnification, scale bar: 250 µm) and colon (Photomicrographs are of x25 original magnification, scale bar: 500 µm) from tumour rats treated with saline/vehicle (Control), lapatinib 240 mg/kg once daily (L240 1x) and lapatinib 200 mg/kg twice daily (L200 2x). Images are representatives of each group.

5.3.8 Measurement of villus height and crypt depth in jejunum and colon

The histological changes in jejunum and colon were also clarified from the measurement of villus height and crypt depth. From Figure 5.11, it was shown that among the jejunal villi, jejunal crypts and colonic crypts, only jejunal villi showed significant differences between experimental groups. The jejunal villi of L240 1x (440.46 ± 16.06 µm) and L200 2x rats (284.49 ± 42.34 µm) were significantly shorter than control rats (537.26 ± 35.41 µm); $p<0.01$ and $p<0.0001$ respectively. L200 2x rats also possessed significantly shorter jejunal villi compared to L240 1x rats ($p<0.0001$).

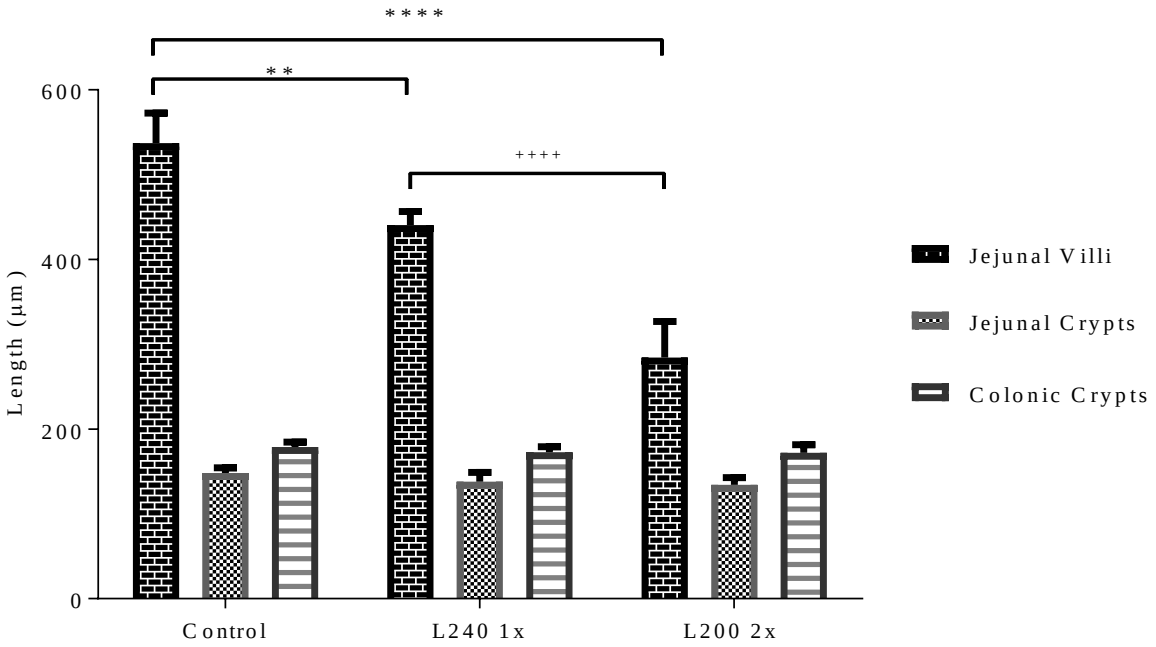

Figure 5.11. Villus height and crypt depth of jejunum and colon in tumour rats treated with saline/vehicle (Control), lapatinib 240 mg/kg once daily (L240 1x) and lapatinib 200 mg/kg twice daily (L200 2x). Data are presented as mean ± S.E.M (n=6 for Control, n=6 for L240 1x and n=4 for L200 2x). *** for $p<0.01$ compared to controls, **** for $p<0.0001$ compared to controls and $^{++++}$ for $p<0.0001$ compared to L240 1x.*

5.3.9 Caspase-3 and Ki-67 protein detection in jejunum and colon

5.3.9.1 Caspase-3 (apoptosis)

To assess epithelial apoptosis in the jejunum and colon, caspase-3 positively stained crypt cells were counted. It was shown (Figure 5.12) that there were no significant differences in crypt cell apoptosis between jejunum of saline/vehicle-treated control (Control) and rats administered with lapatinib 240 mg/kg once daily (L240 1x) as well as rats administered with lapatinib 200 mg/kg twice daily (L200 1x). However, there were significant differences of crypt cell apoptosis in the colon. It was shown that numbers of apoptotic cells in the colonic crypts of L240 1x (0.24 ± 0.06) were significantly higher than in controls (0.07 ± 0.02) ($p<0.01$). Apoptotic cell numbers were also significantly higher in colonic crypts of L200 2x (0.29 ± 0.07) compared to controls ($p<0.001$). No significant difference was found in colonic crypt cell apoptosis between L240 1x and L200 2x. The photomicrographs of caspase-3 staining are shown in Figure 5.13.

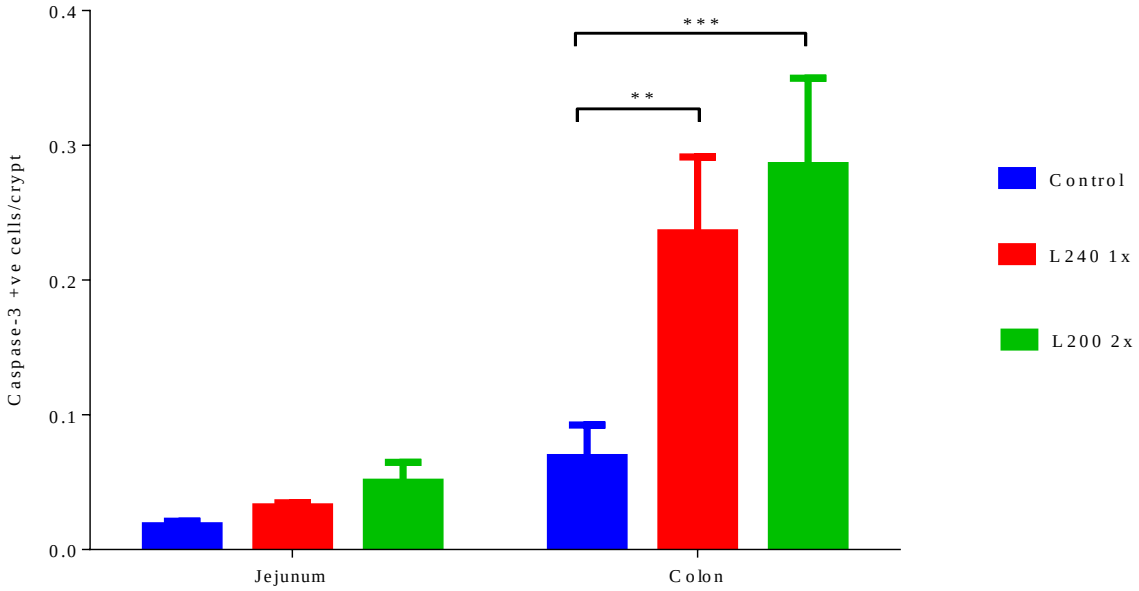

Figure 5.12. Changes in cell apoptosis as identified by caspase-3 immunohistochemistry staining in jejunum and colon of tumour rats treated with saline/vehicle (Control), lapatinib 240 mg/kg once daily (L240 1x) and lapatinib 200 mg/kg twice daily (L200 2x). Data are presented as mean ± S.E.M (n=6 for Control, n=6 for L240 1x and n=4 for L200 2x). *** for $p<0.01$ compared to controls and *** for $p<0.001$ compared to controls.*

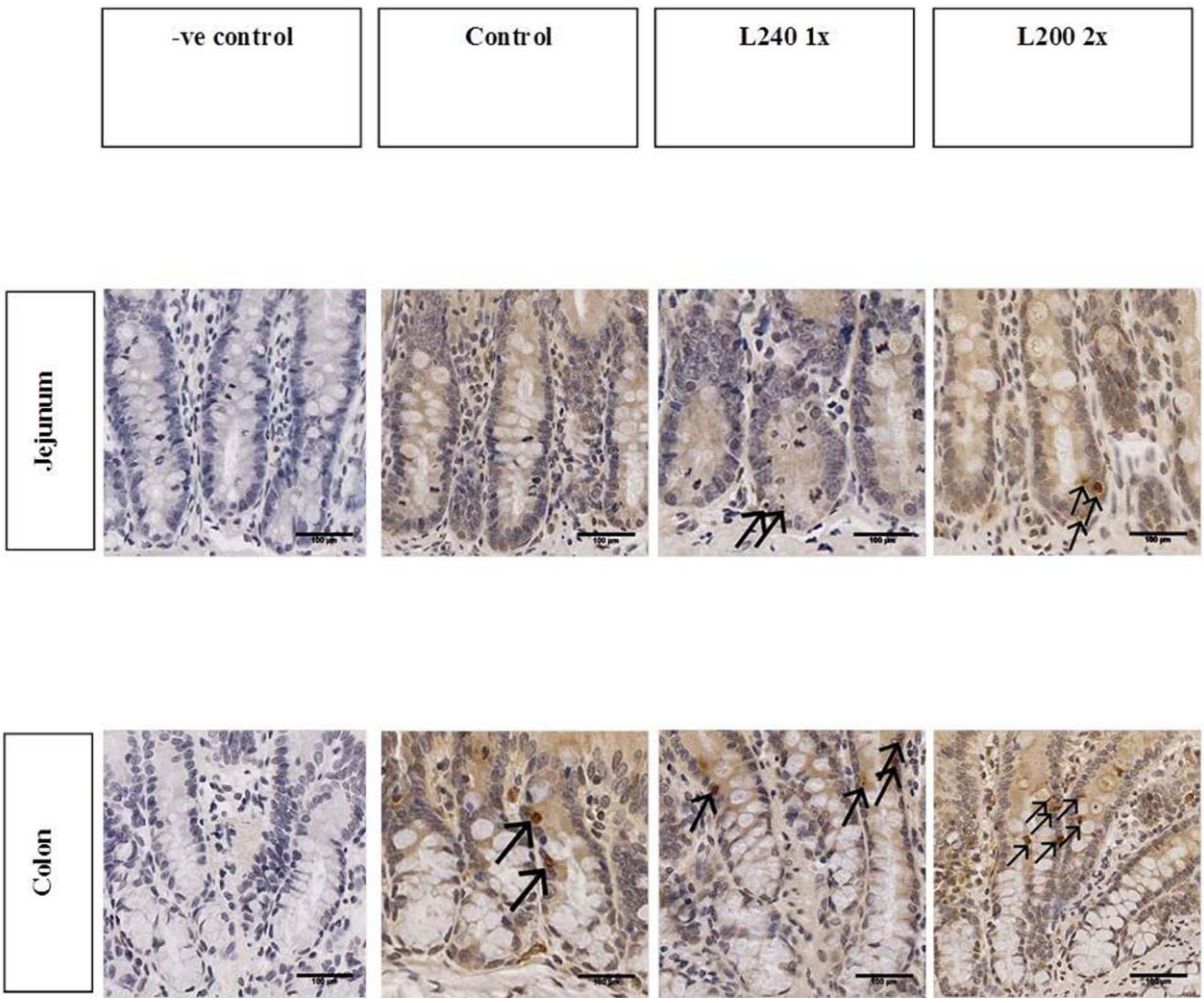

Figure 5.13. Caspase-3 immunohistochemistry staining in the jejunum and colon of tumour rats treated with saline/vehicle (Control), lapatinib 240 mg/kg once daily (L240 1x) and lapatinib 200 mg/kg twice daily (L200 2x). Negative control (-ve control) presents slides stained with secondary antibody only. Arrows indicate apoptotic cells positively stained for caspase-3. Images are representatives of each group (Photomicrographs are of x200 original magnification, scale bar: 100 µm).

5.3.9.2 Ki-67 (proliferation)

To assess cell proliferation in the jejunum and colon, Ki-67 positively-stained crypt cells were counted. There were no significant differences in crypt cell proliferation between jejunum of control and L240 1x rats, or L200 1x rats (Figure 5.14). There were also no significant differences in colonic crypt cell proliferation between all experimental groups. The photomicrographs of Ki-67 staining are shown in Figure 5.15.

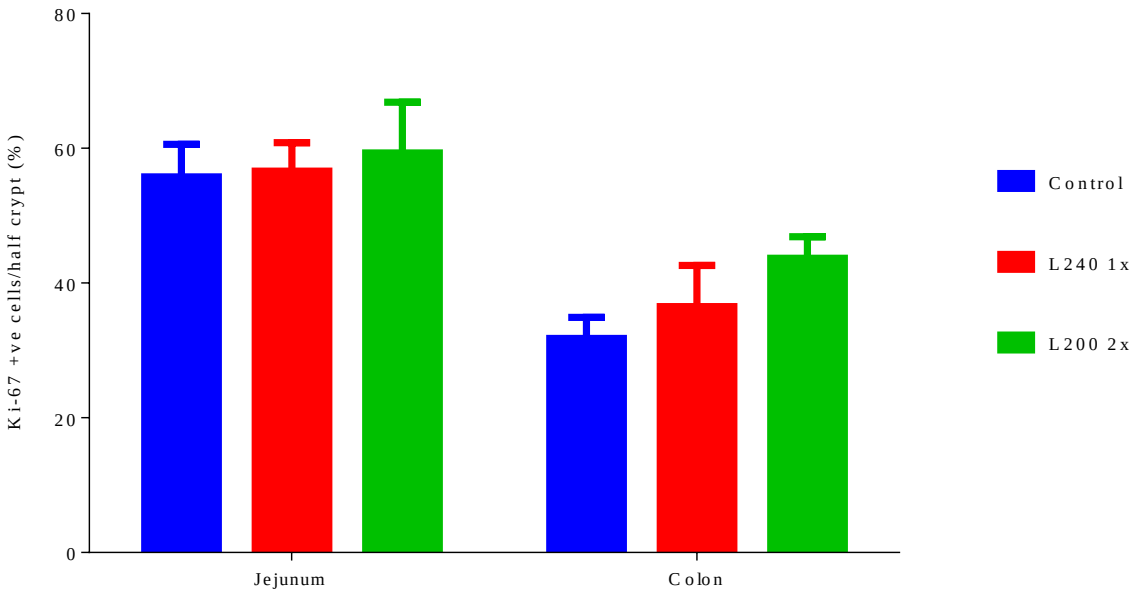

Figure 5.14. Changes in cell proliferation as identified by Ki-67 immunohistochemistry staining in jejunum and colon of tumour rats treated with saline/vehicle (Control), lapatinib 240 mg/kg once daily (L240 1x) and lapatinib 200 mg/kg twice daily (L200 2x). Results presented as a percentage of positive cells/half crypt. Data are presented as mean ±S.E.M (n=6 for Control, n=6 for L240 1x and n=4 for L200 2x).

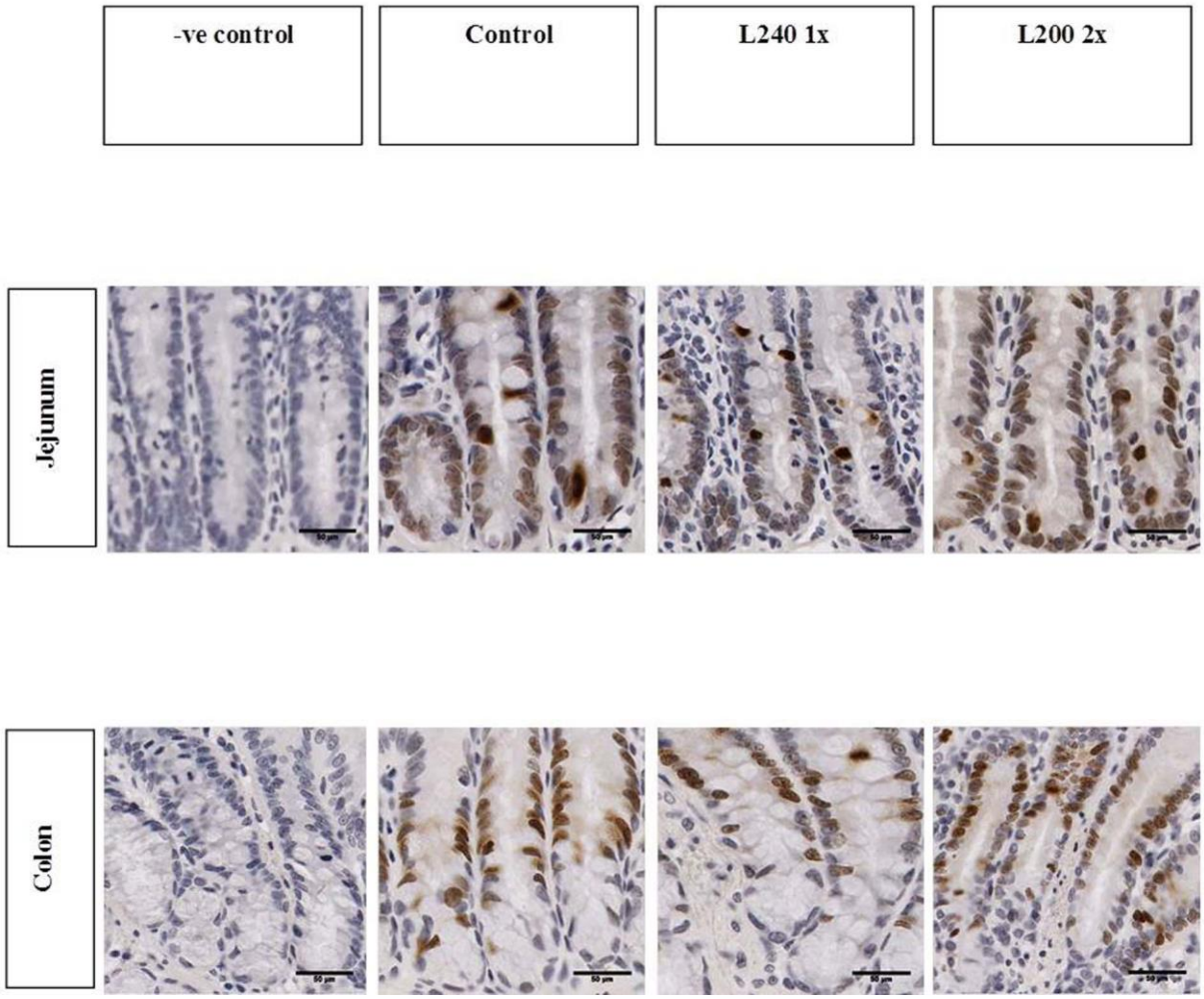

Figure 5.15. Ki-67 immunohistochemistry staining in the jejunum and colon of tumour rats treated with saline/vehicle (Control), lapatinib 240 mg/kg once daily (L240 1x) and lapatinib 200 mg/kg twice daily (L200 2x). Negative control (-ve control) presents slides stained with secondary antibody only. Images are representatives of each group (Photomicrographs are of x400 original magnification, scale bar: 50 µm).

5.3.10 Total and phosphorylated ErbB1 and ErbB2 protein detection in jejunum and colon

The protein expression of ErbB1, ErbB2, pErbB1 and pErbb2 in the jejunum and colon of control, L240 1x and L200 2x rats were evaluated based on the staining intensity. The staining intensities were considered at both jejunal crypts and villi as well as colonic apical and basal layers and were scored as described in the method (Section 5.2.7.2).

Results presented in Figure 5.16A show that only ErbB2 expression in jejunal crypts was associated with a significant difference between the experimental groups. ErbB2 protein expression was significantly lower in L240 1x and L200 2x compared to the controls ($p<0.05$). However, there were no significant differences in ErbB2 expression in the jejunal villi of all experimental groups. No significant differences were seen in ErbB1, pErbB1 and pErbB2 expression in the jejunal crypts and villi of control, L240 1x and L200 2x.

There were no significant differences in ErbB1, ErbB2, pErbB1 and pErbB2 expression in the colonic apical or basal regions of all experimental groups (Figure 5.16B). The photomicrographs of the immunostaining in jejunum and colon are shown in Figures 5.17 and 5.18.

A. Jejunum

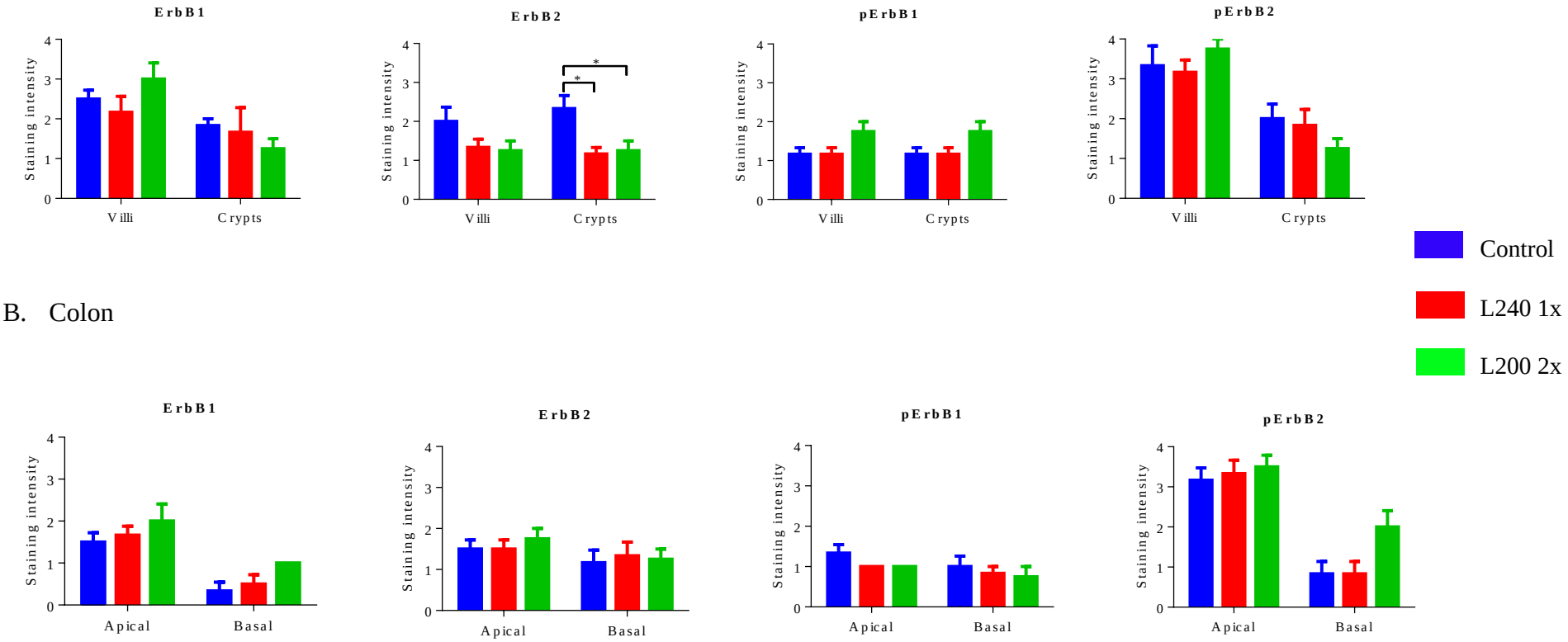

B. Colon

Figure 5.16. Changes in Erbb1, ErbB2, pErbB1 and pErbB2 staining in the (A) Jejunum: crypts and villi (B) Colon: apical and basal regions of tumour rats treated with saline/vehicle (Control), lapatinib 240 mg/kg once daily (L240 1x) and lapatinib 200 mg/kg twice daily (L200 2x). Data are presented as mean±S.E.M (n=6 for Control, n=6 for L240 1x and n=4 for L200 2x). ** for p<0.05 compared to controls.*

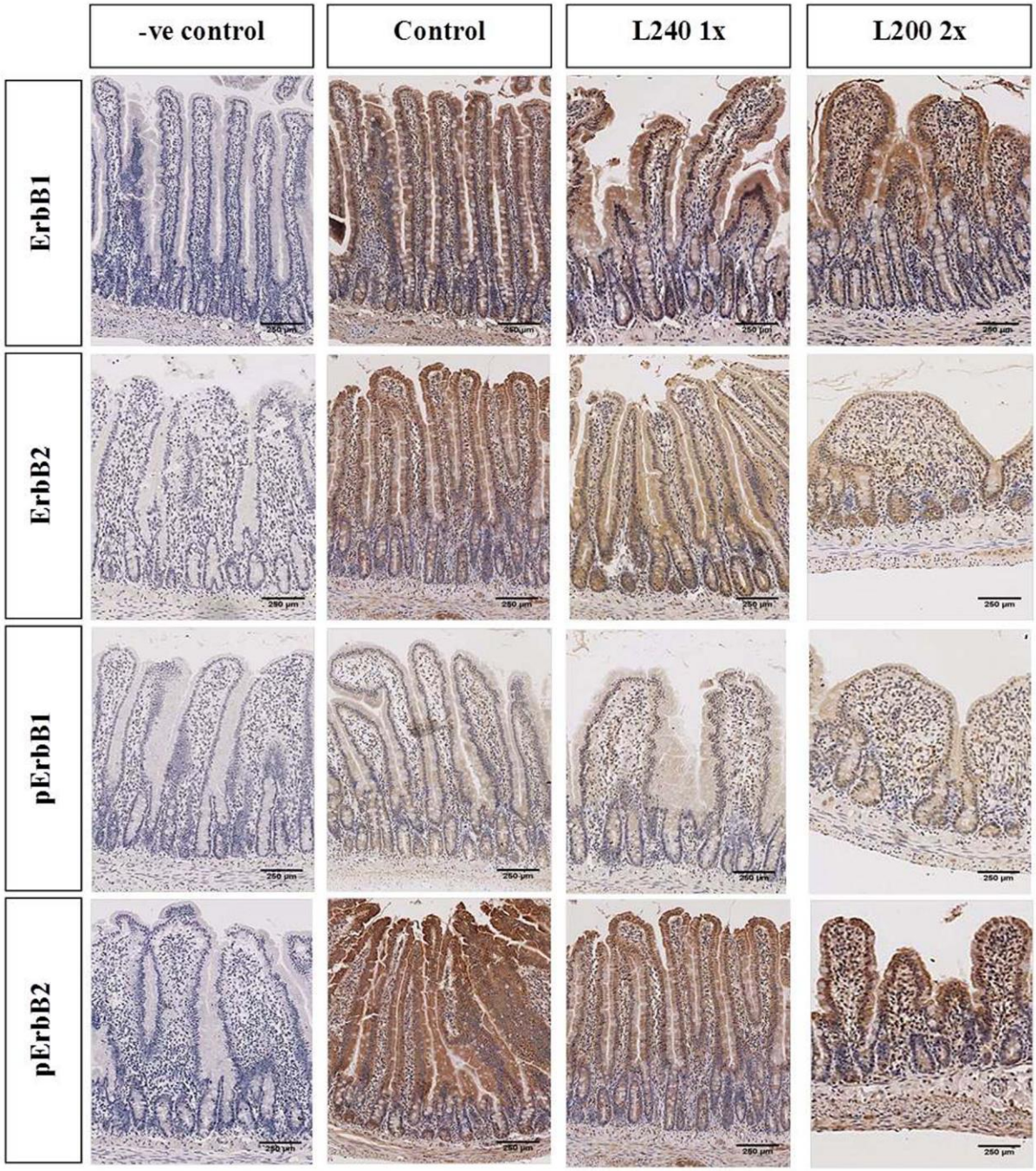

Figure 5.17. ErbB1, ErbB2, pErbB1 and pErbB2 immunohistochemistry staining in the jejunum of tumour rats treated with saline/vehicle (Control), lapatinib 240 mg/kg once daily (L240 1x) and lapatinib 200 mg/kg twice daily (L200 2x). Negative control (-ve control) presents slides stained with secondary antibody only. Images are representatives of each group (Photomicrographs are of x50 original magnification, scale bar: 250 µm).

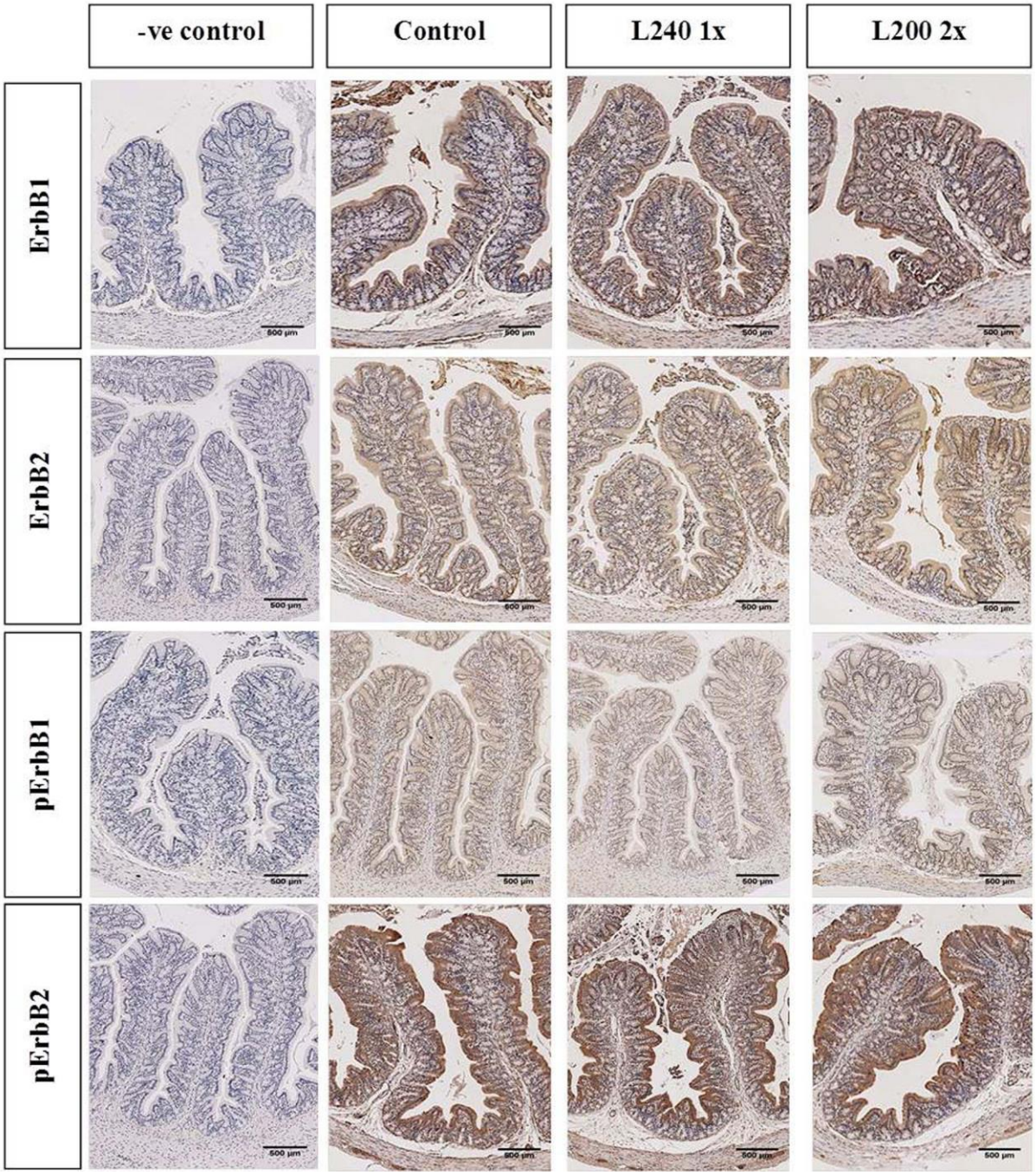

Figure 5.18. ErbB1, ErbB2, pErbB1 and pErbB2 immunohistochemistry staining in the colon of tumour rats treated with saline/vehicle (Control), lapatinib 240 mg/kg once daily (L240 1x) and lapatinib 200 mg/kg twice daily (L200 2x). Negative control (-ve control) presents slides stained with secondary antibody only. Images are representatives of each group (Photomicrographs are of x25 original magnification, scale bar: 500 µm).

5.4 Discussion

The purpose of this experiment was to use a tumour-bearing rat model to interrogate mechanisms of lapatinib-induced gastrointestinal mucosal injury. This study compared once daily lapatinib administration (240 mg/kg q.d.) with a regimen of twice daily lapatinib administration (200 mg/kg b.i.d.) to indicate the optimum dosage of lapatinib required to induce diarrhoea in tumour-bearing rats (as opposed to tumour-naïve animals). The experiment reflected a previous clinical study by Burris III et al (Burris, Taylor et al. 2009) which found that twice daily administration of lapatinib caused severe diarrhoea compared to once daily dosing. However, in this present study, although 240 mg/kg q.d. lapatinib was similar to the clinical dose and has also has been shown to induce diarrhoea in male rats (Bowen, Mayo et al. 2012), it did not cause diarrhoea in this study. In addition, there were no changes in tissue architecture at this dose, indicating that 240 mg/kg q.d. is insufficient to cause gastrointestinal changes necessary to induce diarrhoea. In comparison, 200 mg/kg b.i.d. lapatinib was associated with diarrhoea and intestinal histopathology. The rats experienced grade 1/2 diarrhoea; which was similar with grade 1/2 diarrhoea events in patients (Crown, Burris et al. 2008). Diarrhoea was also observed on day 1 which was very early onset compared to clinical situation in which patients who were administered with twice daily dosing of lapatinib experienced diarrhoea on day 6-7 of treatment (Burris, Taylor et al. 2009) . However, due to profound weight loss, the 200mg/kg b.i.d. rats had to be removed early from the study.

It should also be noted that the current study was conducted in tumour-bearing rats in which the diarrhoea incidence was expected to be higher. However, the rats did not experience diarrhoea as was expected. Results obtained from Chapter 4 showed Walker 256 tumour does not cause any changes in jejunum and colon, thus there were no interference of tumour on the intestines in the current study.

There are few factors that could be taken into consideration which contributed to the lack of diarrhoea seen in the group treated with once daily lapatinib. Firstly, rats were not fasted before treatment with lapatinib. Previous pharmacokinetic studies of lapatinib found that lapatinib exposure varies considerably in patients (Koch, Reddy et al. 2009) and was also noted in the previous study conducted by our research group (Bowen, Mayo et al. 2012). The causes for this are currently unknown, but may be influenced by the presence of food in the stomach which has been shown to increase bioavailability of lapatinib. As such, lapatinib is directed to be taken at least 1 hour before or after food (Koch, Reddy et al. 2009). A limitation in this current study was that pharmacokinetic studies were not carried out to determine serum lapatinib concentration in order to evaluate lapatinib absorption in the rats treated with different regimens. As such, no comparisons could be made between males and females, and between tumour naïve versus tumour burdened rats in terms of lapatinib exposure.

Secondly, the compound and vehicle used in this study was different to previous work. Previously lapatinib ditosylate was sourced directly from GSK and dissolved in 0.5% hydroxypropylmethylcellulose with 0.1% Tween 80 (Bowen, Mayo et al. 2012) while in the current study lapatinib tablets were crushed and dissolved in normal saline based on the doses required which were 240 and 200 mg/kg. The tablet has been observed to dissolve better in normal saline than in 0.5% hydroxypropylmethylcellulose with 0.1% Tween 80. Lapatinib tablet, TYKERB® (GSK, Australia) contains the active ingredient lapatinib ditosylate monohydrate. Each film-coated tablet contains 250 mg of lapatinib and also contains microcrystalline cellulose, povidone, sodium starch glycolate, magnesium stearate, hypromellose titanium dioxide, macrogol/PEG400, polysorbate, iron oxide yellow and iron oxide red. However, since lapatinib is a delayed release tablet which is orally administered, there could be differences in its efficacy when administered orally as a suspension as was

applied in the current study. The efficacy of delayed release tablet versus oral suspension formulation has been compared which showed that the oral suspension limits the drug's efficacy while the delayed release tablet formulation demonstrated an improved pharmacokinetic (Durani, Tosh et al. 2015). However, no difference in diarrhoea side effect was demonstrated between delayed release tablet and oral suspension formulation.

Although oral suspension of lapatinib was administered to the rats, the normal absorption process of the drug might not be altered. Lapatinib; a yellow solid with its solubility of 0.007 mg/ml in water and 0.001 mg/ml in 0.1 N hydrochloric acid is known as a weak base (Scheffler, Di Gion et al. 2011). Given its p*K*a of 6.63, in which the p*K*a is the pH at which half of the drug is in its ionised form (Nadanaciva, Lu et al. 2011), lapatinib remains in an ionised/charged form in the acidic environment of stomach (pH 1.5-3.5). However, soon after it enters the small intestine (pH 6.6-7.4), a substantial proportion of lapatinib becomes unionised/uncharged, which is when the drug is available for absorption across the mucosal membrane of small intestine (Siepmann, Siepmann et al. 2016). Assuming due to its low solubility, low bioavailability and weak acid p*K*a, a proportion of the drug may not be absorbed, thus 'escapes' absorption and enters colon. Continuous dosing may also lead to accumulation of the drug in the intestine which explains diarrhoea incidence (Bence, Anderson et al. 2005, Scheffler, Di Gion et al. 2011), that was not observed in the current study in the group treated with once daily lapatinib.

Based on the tumour burden (as % bodyweight), tumour weight and tumour mitotic index results, tumour growth was not inhibited in rats treated with lapatinib. This finding was unexpected since previous tumour-bearing preclinical models have shown tumour control by lapatinib (Chu, Blackwell et al. 2005, Zhou, Li et al. 2006, Scaltriti, Verma et al. 2009) in which lapatinib shows sensitivity towards ErbB1 and ErbB2 expressing tumours. As the

expression of ErbB1 and ErbB2 has been shown in Walker 256 tumour tissue (Chapter 4), thus sensitivity to lapatinib is expected.

In the current study, control rats showed tumour regression (5 out of 6 rats) while in lapatinib-treated rats (240 mg/kg), tumours grew until the end of the study. Tumour regression was not surprising given that 50% of rats showed tumour loss when establishing the tumour model (Chapter 4). What was unexpected was that only control rats had regression. This may be due to an immune response against the tumour in control rats which was not present in lapatinib-treated rats. Further studies will need to focus on the tumour microenvironment and systemic immune responses to tumour burden.

Thirdly and finally, caked drug powder was observed in the rats' intestines upon necropsy. The caked drug powder could be the accumulation of the drug that was unable to be absorbed in the normal absorption of lapatinib as explained in the earlier paragraph. Further investigation is warranted to assess the changes in drug exposure as the accumulated, caked drug powder might also be associated with further reduction in absorption of oral drugs and hence interfere with their anticancer effect.

Rats administered with lapatinib 200 mg/kg b.i.d. suffered severe weight loss. This may be due to caking of the drug powder in stomach which was observed during necropsy. Caking of lapatinib powder was also observed in rats administered with lapatinib 240 mg/kg q.d. However, it was observed during necropsy that the caked powder did not cause any blockage of food.

Upon necropsy, it was also observed that both lapatinib-treated groups had yellow or pale liver with also yellow coloured area at sites distant to the administration route which could be due to drug metabolism. This condition was not observed in previous works conducted in male rats, thus supporting influence of sex in drug metabolism (Bowen, Mayo et

al. 2012). There is a known influence of sex in drug metabolism. Metabolism by the liver represents the most common biochemical means of drug elimination (Eichelbaum and Burk 2001). A superfamily of enzymes prominently involved in drug metabolism is the cytochrome P450 (P450s) family. Among the numerous isoforms, cytochrome P450 3A4 (CYP 3A4) is one of the most important, since it constitutes a major portion (30% on average) of total hepatic P450 content and is involved in the metabolism of >50% of drugs on the market (Thummel and Wilkinson 1998, Eichelbaum and Burk 2001). It has also been reported that CYP 3A4 is the major determinant of intestinal wall metabolism (von Richter, Greiner et al. 2001). Lapatinib is metabolised extensively by CYP 3A4 and 3A5 (Dhillon and Wagstaff 2007, EMEA 2008). Previous human studies have reported higher CYP 3A4 activity in females compared to males (Hulst, Fleishaker et al. 1994, Cummins, Wu et al. 2002, Mirghani, Sayi et al. 2006, Diczfalusy, Miura et al. 2008), which could theoretically account for increased elimination of lapatinib. Although plausible, the current study did not measure lapatinib serum concentrations and thus no comparison between male and female rats could be completed. However, this assumption is supported by preclinical toxicity studies carried out by GlaxoSmithKline during development of lapatinib indicating that female rats are more susceptible to drug toxicity due to higher exposures compared to males (EMEA 2008), although diarrhoea was not observed in group treated with once daily lapatinib.

This study found no significant tissue pathology in lapatinib-treated rats except for the significant reduction in jejunal villus height particularly in rats administered with lapatinib 200 mg/kg b.i.d. Reduced jejunal villus height and diarrhoea incidence in rats treated with lapatinib 200 mg/kg b.i.d. supports the theory of tyrosine kinase inhibitor-induced direct mucosal damage leading to diarrhoea (Loriot, Perlemuter et al. 2008). Atrophy of intestinal mucosa may lead to a secretory/osmotic-type diarrhoea due to inability to control absorption and secretion through decreased surface area (Gibson and Keefe 2006). However, villous

atrophy could also be associated with other factors such as food deprivation and severe weight loss (Genton, Cani et al. 2015) which was also seen in the rats administered with lapatinib 200 mg/kg b.i.d.

The only indirect suggestion of gut damage in the experiment was increased small intestinal weight in rats treated with lapatinib 240 mg/kg q.d. Increased small intestinal weight has been consistently observed with regenerative crypt hyperplasia following chemotherapy insult to the intestine in previous experiments (Gibson, Bowen et al. 2005, Gibson, Stringer et al. 2007). However, this is in contrast with the results obtained in this study that did not show a significant increase in jejunal crypt cell proliferation. Other causes such as oedema and muscle thickening could possibly increase small intestinal weight. Rats treated with lapatinib 200 mg/kg b.i.d. showed decreased small intestinal weight and no changes in jejunal crypt cell proliferation; in fact the small intestinal wall was very thin in rats administered with lapatinib 200 mg/kg b.i.d. upon necropsy. This decrease in small intestinal weight in rats treated with an ErbB1 inhibitor has also been seen in a previous study (Rasmussen, Viby et al. 2010).

Since no architectural changes were evident in the colon, this supports the hypothesis that lapatinib-induced diarrhoea is caused by alterations in the small intestine (Burris, Hurwitz et al. 2005), given that small intestine is the most likely site of absorption of lapatinib, with absorption and accumulation of drug more likely occurs within the jejunal mucosal cell, hence exposure of the mucosal surface to the accumulated drug is higher in that region. Supporting this is the observation that ErbB2 expression was decreased in the crypts of the jejunum but in no other region. Previous studies have shown the cytotoxicity effect of lapatinib is more related to ErbB2 inhibition than ErbB1 inhibition (Konecny, Pegram et al. 2006, Rusnak, Alligood et al. 2007). Lapatinib activity on ErbB2 protein as well as on ErbB2 dimers has been shown in previous study (Scaltriti, Verma et al. 2009). On the other hand, a significant

increase in apoptosis (caspase-3) was seen in the colon in both lapatinib-treated groups, whilst no change in apoptosis was noted in the jejunum. As mentioned in the earlier paragraph, the drug that is not absorbed in the small intestine might 'escape' which could then affect colon. Increase apoptosis in colon but not in jejunum could be due to longer transit time in colon. Previous study showed that no damage severity was observed in rats treated with interleukin-11 after methotrexate treatment although results indicated apoptosis (Gibson, Keefe et al. 2002). Pritchard et al (Pritchard, Potten et al. 1998) found that apoptosis was not directly associated with intestinal damage after chemotherapy. These findings may support the current study that lapatinib induces apoptosis in colon but with no damage severity.

5.5 Conclusion

The current study was unable to find a dose and a schedule of lapatinib that was able to induce diarrhoea with tolerable levels of systemic toxicity. As such, further research is required to test a number of different schedules to find an appropriate way to model lapatinib-induced diarrhoea in breast cancer-bearing rats. This will enable future work to focus on uncovering mechanisms of lapatinib-induced diarrhoea and to test interventions for diarrhoea management.

Chapter 6

Effect of lapatinib on T84 colonic epithelial monolayer integrity

6.1 Introduction

Lapatinib, an ErbB1/ErbB2 dual tyrosine kinase inhibitor, is known to be effective in treating ErbB2-positive advanced or metastatic breast cancer (Medina and Goodin 2008). Although lapatinib has been recognised for its effectiveness, diarrhoea has been associated with the drug's administration (Crown, Burris et al. 2008, Burris, Taylor et al. 2009) and the mechanism leading to diarrhoea remains to be fully elucidated. Unlike diarrhoea associated with the use of conventional chemotherapeutic agents (Gibson, Bowen et al. 2003, Logan, Stringer et al. 2009), the diarrhoeal side effects of lapatinib are associated with no apparent damage to the intestinal epithelium (Bowen, Mayo et al. 2012). It is well-established that treatment with conventional chemotherapy drugs causes atrophy of intestinal mucosa leading to mixed secretory/osmotic-type diarrhoea due to inability to control solute absorption and secretion through decreased surface area (Gibson and Keefe 2006), however, it seems that lapatinib-induced diarrhoea occurs through a different mechanism.

Activated chloride secretion from the intestinal crypt plays a major role in secretory diarrhoea (Field 2003). The generation of the electrochemical driving force required for chloride (Cl^-) secretion by crypt epithelial cells depends on their ability to accumulate intracellular Cl^- ions to concentrations greater than their electrochemical equilibrium (Barrett and Keely 2000, Kunzelmann and Mall 2002). Chloride enters the cell across the basolateral membrane through the activity of sodium-potassium-chloride (Na^+-K^+-$2Cl^-$) cotransporters. The cotransporter is, in turn, driven by a strong inwardly-directed electrochemical Na^+ gradient established by the basolaterally-located sodium-potassium-adenosine triphosphatase

(Na^+-K^+-ATPase). In order to maintain the membrane potential at rest and during Cl^- secretion, both Na^+ and K^+ must be recycled out of the cell through the basolateral membrane. The Na^+-K^+-ATPase serves to recycle Na^+, while basolateral K^+ channels recycle K^+ (Schultheiss and Diener 1998). The basolateral K^+ conductance in intestinal epithelial cells is formed by at least two different types of K^+ channels, one is activated by calcium (Ca^{2+})-mobilizing secretagogues and the other by cyclic adenosine monophosphate (cAMP)-dependent agonists (Heitzmann and Warth 2008).

Studies have revealed that ErbB1 is a critical regulator in intestinal ion transport (McCole, Rogler et al. 2005, McCole, Truong et al. 2007). ErbB1 is widely expressed in the gastrointestinal mucosa in which it regulates Cl^- secretion in order to maintain normal gut homeostasis (McCole and Barrett 2009). A study also found that during chronic inflammation, there is a potential effect of ErbB1 activation on epithelial electrogenic Na^+ that would be expected to ameliorate diarrhoeal symptoms associated with colitis (McCole, Rogler et al. 2005). The process of Cl^- secretion is under tight control, and regulatory breakdown can lead to various complications, such as diarrhoea (Barrett 2000). It has been suggested that inhibition of ErbB1 may cause dysregulation of the Cl^- secretory process, leading to diarrhoea; this has been suggested for lapatinib as well as with other ErbB1 tyrosine kinase inhibitors (Loriot, Perlemuter et al. 2008, Bowen 2014). However, studies by our group do not support that the inhibition of Cl^- leads to diarrhoea as blood biochemical analysis found that 240 mg/kg lapatinib had no significant effect on serum chloride (Bowen, Mayo et al. 2012). However, it has to be noted that terminal blood collection occurred 24 hours after lapatinib treatment in which not all rats had diarrhoea at time of death. Furthermore, there was no effect on serum chloride only at this particular concentration (240 mg/kg) (Bowen, Mayo et al. 2012, Bowen, Mayo et al. 2014). Thus, the role of chloride secretion in lapatinib-induced diarrhoea remains unclear.

In this study, both measurements of permeability via transepithelial electrical resistance (TEER), and paracellular ion movement using the Ussing chamber was carried out. TEER measured the movement of ions actively transported by epithelial cells from the passive movement of ions through paracellular or intercellular pathways, while Ussing chamber analysis is able to eliminate the passive transepithelial driving force created by the spontaneous electrical potential across the epithelium by clamping the potential to zero with an external current passed across the epithelium (Clarke 2009). This current which is known as the short-circuit current (I_{sc}), is equivalent to the algebraic sum of electrogenic ion movement by active transport (Clarke 2009). Previous study had shown that I_{sc} values in T84 monolayers are solely reflective of net chloride transport (Dharmsathaphorn and Pandol 1986). The T84 cell line was derived from a lung metastasis of human colon carcinoma. T84 cells are able to spontaneously differentiate into an enterocyte-like phenotype (Ou, Baranov et al. 2009). This cell type forms monolayers with well-developed tight junctions (McRoberts and Barrett 1989, Ou, Baranov et al. 2009) and has been proven to be a robust model for the study of molecular mechanisms of intestinal secretion since the early 1980s (Dharmsathaphorn, McRoberts et al. 1984, Barrett 1993).

It has also been shown in previous studies that lapatinib is effective either as a monotherapy or in combination with chemotherapy (Chu, Blackwell et al. 2005, Geyer, Forster et al. 2006, Johnston, Trudeau et al. 2008, Kaufman, Trudeau et al. 2009). Several studies have demonstrated the efficacy and safety of lapatinib when used in combination with paclitaxel (Di Leo, Gomez et al. 2008, Gomez, Doval et al. 2008, Jagiello-Gruszfeld, Tjulandin et al. 2010). However, diarrhoea is worsened during lapatinib and paclitaxel combination treatment which may be due to shared metabolic and drug efflux pathways between drugs (Medina and Goodin 2008, Bowen, Mayo et al. 2012).

Thus, the current study aimed to determine the cytotoxic effect of lapatinib and paclitaxel on T84 human colonic epithelial cells. The effect of lapatinib, paclitaxel as well as a combination of paclitaxel and lapatinib on T84 colonic epithelial monolayer integrity was also investigated.

6.2 Materials and methods

6.2.1 Cell culture

Description of the T84 cell line and details of the cell culture procedures are described in Chapter 2 (Section 2.1 and 2.2).

6.2.2 Chemicals

Chemicals were purchased from Sigma Chemical Co. (St Louis, MO, USA) unless otherwise stated. XTT kit was purchased from Roche Diagnostics GmbH (Germany), as mentioned in Chapter 2 (Section 2.1). Lapatinib was supplied by Glaxo SmithKline (GSK, Australia) as explained in Chapter 2 (Section 2.1). Paclitaxel Ebewe® (EBEWE Pharma, Austria) was purchased from the Royal Adelaide Hospital.

Lapatinib stock (10 mM) was prepared as described in Chapter 2 (Section 2.1). Paclitaxel was dissolved in 50% ethanol in sterile water to 7 mM.

Ringer's solution used for Ussing chambers (Section 6.2.6) consisted of 4 stock solutions. Stock A solution was made up of 2.3 M sodium chloride (NaCl) while Stock B was 48 mM potassium hydrogen phosphate (K_2HPO_4) and Stock C was 0.5 M sodium hydrogen carbonate ($NaHCO_3$). Stock D was prepared by combining 24 mM magnesium chloride hexahydrate ($MgCl_2.6H_2O$) with 24 mM calcium chloride dihydrate ($CaCl_2.2H_2O$). Prior to experiments using Ussing chambers, 300 ml of Milli-Q water (Milli-Q® Intergral Water Purification System, Merck Millipore, Australia) was added into a 500 ml volumetric flask.

Then, 25 ml of each stock solution was added into the volumetric flask, followed by MilliQ water to make up 500 ml of Ringer's solution. Prior to usage, 5 ml of 1 M glucose was added to the 500 ml of Ringer's solution composition.

6.2.3 XTT cell proliferation assay

This method has been described in Chapter 2 (Section 2.3). To determine any difference in the cytotoxic effect of lapatinib and paclitaxel on the cell line, lapatinib stock 10 mM and paclitaxel 7 mM were diluted with three different media; serum-free medium, 5% serum-supplemented medium and 10% serum-supplemented medium, which were prepared as a series of concentrations. Lapatinib was diluted to 1-20 µM (1, 2.5, 5, 7.5, 10, 12.5, 15, 17.5 and 20 µM) and 10-100 µM (10, 20, 30, 40, 50, 60, 70, 80, 90 and 100 µM) while paclitaxel was diluted to 1-10 µM (1, 2, 3, 4, 5, 6, 7, 8, 9 and 10 µM) and 10-100 µM (10, 20, 30, 40, 50, 60, 70, 80, 90 and 100 µM). The cells were then treated with lapatinib, which had been diluted with three different media, respectively, at the series of concentrations that were mentioned above. The treated cells were then incubated at 37^{o}C with CO_2 for 48 hour and the same procedure as described in Chapter 2 Section 2.3 was carried out. An equivalent serial dilution of DMSO and 50% ethanol was used as a control treatment. Inhibition of cell proliferation was calculated and a graph of percentage of cell viability versus concentration of lapatinib was then plotted and the IC_{50} (a dose that inhibited 50% cell growth) was determined from the graph. The experiment was performed in triplicates and was repeated 3 times.

6.2.4 Effect of lapatinib on cell permeability

Four hundred microliters of T84 cell suspension, consisting of $4x10^5$ cells, was seeded in Millicell-HA culture plate inserts (0.6 cm^2 membrane area, 0.45 µm pore diameter and 12 mm diameter) (Millicell®, Millipore, USA) in a 48-well plate (Becton Dickinson, USA), to which was added with 600 µl medium. The medium used was DMEM/ Nutrient F-12 Ham,

which was supplemented with 10% serum, 1% penicillin-gentamycin with fungizone and 2 mM L-glutamine (Chapter 2 Section 2.2). The cell density of T84 cells to form a monolayer was determined based on previous studies (Hoda, Scharl et al. 2010, Paul, Marchelletta et al. 2012). The cells were then incubated at 37ºC with 5% CO_2 for 48 hours to allow cell attachment prior to transepithelial electrical resistance (TEER) measurement. The culture plate insert in which the cells were seeded is termed as apical chamber while the 48-well plate in which the medium was added is termed as basolateral chamber.

After 48 hours incubation, the cell medium was refreshed prior to TEER measurement every 24 hours using a voltohmmeter (Millipore EVOM^2, World Precision Instruments, USA). The formation of a sealed monolayer was monitored by serial measurements of the TEER. Monolayer integrity was established once the TEER reached more than 800 ohms/cm^2. A higher TEER reflects stronger tight junctions between cells and decreased monolayer permeability (Forsythe, Xu et al. 2002). To calculate the resistance measurement of the cell monolayer, the mean resistance measurements of inserts without cells were subtracted from the monolayer measurements and corrected for the area of the filter (Xiao, Chen et al. 2011).

Lapatinib treatment began once the TEER of the seeded cells reached >800 ohms/cm^2. Lapatinib 10 mM was diluted to 10 and 100 µM while paclitaxel 7 mM was diluted to 2, 5, 10, 20 and 50 µM. Experiments were carried out using medium (DMEM/ Nutrient F-12 Ham) supplemented with 10% serum. Optimal concentrations of the drugs and serum were determined based on the results obtained from the XTT cell proliferation assay. As the main objective of this study is to determine the effect of lapatinib on cell permeability, Lapatinib was added either to the apical, basolateral or both apical and basolateral chambers of the monolayer system, while paclitaxel was added to the basolateral only. The apical chamber is considered as the luminal-side, while the basal chamber is analogous to the serosal side.

Paclitaxel was added to the basal chamber only as to reflect its normal administration in patients in which paclitaxel is administered intravenously. Then, TEER measurement was taken prior to incubation (0 hour). The TEER measurements were carried out subsequently at 0.5, 24 and 48 hours without changing the medium. DMSO, 50% ethanol (50% EtOH) and triton x-100 (TX-100) were used as control treatments. The experiment was performed in duplicate and was repeated 3 times.

6.2.5 Effect of lapatinib on Cl- secretion

T84 cell monolayers, prepared as described in Section 6.2.5, were pre-treated with lapatinib, paclitaxel and both lapatinib and paclitaxel for 48 hours. Concentrations of lapatinib and paclitaxel used in this experiment were determined based on the results obtained from the TEER experiment (effect of lapatinib on cell permeability).

Prior to each experiment, the Ussing chamber set up was calibrated according to manufacturer instructions (Physiologic instrument, USA). Salt bridges were adjusted for voltage, current and resistance using the manual (Physiologic instrument, USA). After the Ussing equipment had been set up, the Ringer's solution in the chamber was emptied in order to insert the monolayers which had been pre-treated with the drugs as mentioned in the first paragraph. Baseline TEER values of the pre-treated monolayers were measured according to the method described in Section 6.2.4. Then, the pre-treated monolayers were rinsed gently with PBS prior to mounting into the sliders. Subsequently, the sliders were inserted into Ussing chambers while ensuring not to change the distance between the electrodes. The left side of the chambers indicates the luminal surface of T84 cells while the right chamber indicates the basolateral surface of the cells. Both sides of the monolayer were bathed with 5 ml of Ringer's solution supplemented with 1 mM glucose. The monolayers in the Ussing chambers were then left to equilibrate for 5 minutes. After that, short-circuit current (I_{sc}) was applied continuously by voltage clamp apparatus to maintain the transepithelial voltage at

zero potential difference. Samples were allowed to equilibrate for 15 minutes before proceeding to stimulation with secretagogues. I_{sc} was recorded and analysed using a digital data acquisition system (Acquire & Analyze version 2.3). Change in I_{sc} (ΔI_{sc}) demonstrated changes in net electrogenic ion movement across the monolayer, where a positive value indicated ion secretion in the apical direction (Ohland, DeVinney et al. 2012).

Baseline measurement of TEER, I_{sc} and conductance were recorded prior to stimulation with the first secretagogue. As mentioned above, I_{sc} is a measure of ion movement across the monolayer, while conductance (G) and its reciprocal, resistance or TEER, are a useful measure of the integrity of the monolayer preparation, in relation to the paracellular pathway across the monolayer (Clarke 2009).

To assess secretion, the monolayers were first pre-incubated with 20 µM amiloride from the apical side for 15 minutes prior to stimulation of calcium (Ca^{2+})-dependent Cl^- secretion by the muscarinic agonist, carbachol (200 µM from the basolateral side), for 15 minutes. Lastly, cyclic adenosine monophosphate (cAMP)-dependent Cl^- secretion was induced by forskolin (10 µM from apical and basolateral sides), for 20 minutes. The secretagogue was induced once stable I_{sc} was attained and measurements were taken at baseline and peak secretion, respectively.

6.2.6 Statistical analysis

Results were statistically analysed using the Kruskal-Wallis test with Tukey's multiple comparisons test to compare means between all groups. Statistical significance was accepted as $p<0.05$.

6.3 Results

6.3.1 XTT assay

Cytotoxic effects of lapatinib and paclitaxel on the T84 human colonic epithelial cell line were studied via XTT assay. This experiment was carried out to determine any difference in the drugs' cytotoxic effect using media with three different serum conditions (serum-free medium, 5% serum-supplemented medium and 10% serum-supplemented medium). T84 cells were treated with lapatinib and paclitaxel.

It was shown that the experiment which was carried out using serum-free medium resulted in a lowest IC_{50} (a dose that inhibited 50% cell growth), followed by 5% serum-supplemented and 10% serum-supplemented. Lapatinib did not inhibit T84 cell proliferation at a lower concentration (Figure 6.1A). However, at higher concentrations, lapatinib, in all differently prepared media, showed 50% inhibition on T84 cell growth (serum-free-medium: 26.48 ± 1.64 µM, 5% serum-medium: 43.24 ± 2.73 µM, 10% serum-medium: 58.59 ± 1.37 µM) (Figure 6.1B). Significant differences in IC_{50} were seen between serum-free medium and 5% serum-supplemented ($p<0.0001$), and 10% serum-supplemented ($p<0.0001$).

At a lower concentration, paclitaxel in the experiment using serum-free-medium showed 50% cell inhibition at 4.78 ± 0.34 µM, while 50% cell inhibition was not seen in 5 and 10% serum-supplemented media (Figure 6.2A). However, at a higher concentration range, paclitaxel exhibited IC_{50} as follows; serum-free-medium: 7.52 ± 0.25 µM, 5% serum-medium: 12.58 ±1.13 µM, 10% serum-medium: 18.48 ± 0.77 µM) (Figure 6.2B). Significant difference in IC_{50} was observed between serum-free medium and 10% serum-supplemented ($p<0.001$).

In serum-free medium, paclitaxel 10-100 inhibited T84 cell proliferation significantly at 7.52 ± 0.25 µM compared to lapatinib 10-100 which inhibited T84 cells at 26.48 ± 1.64 µM

($p<0.0001$). While in 5% serum-medium, paclitaxel 10-100 was significantly toxic against T84 cells at 12.58 ± 1.13 µM than lapatinib 10-100 which was toxic to T84 cells at 43.24 ± 2.73 µM ($p<0.0001$). Paclitaxel 10-100 in 10% serum-medium was also significantly toxic against T84 cells at 18.48 ± 0.77 µM compared to lapatinib 10-100 which was cytotoxic at 58.59 ± 1.37 µM ($p<0.0001$) (Figures 6.1B and 6.2B). DMSO (Figures 6.3A and B) and 50% ethanol (EtOH) (Figures 6.4A and B) did not reduce T84 cell viability.

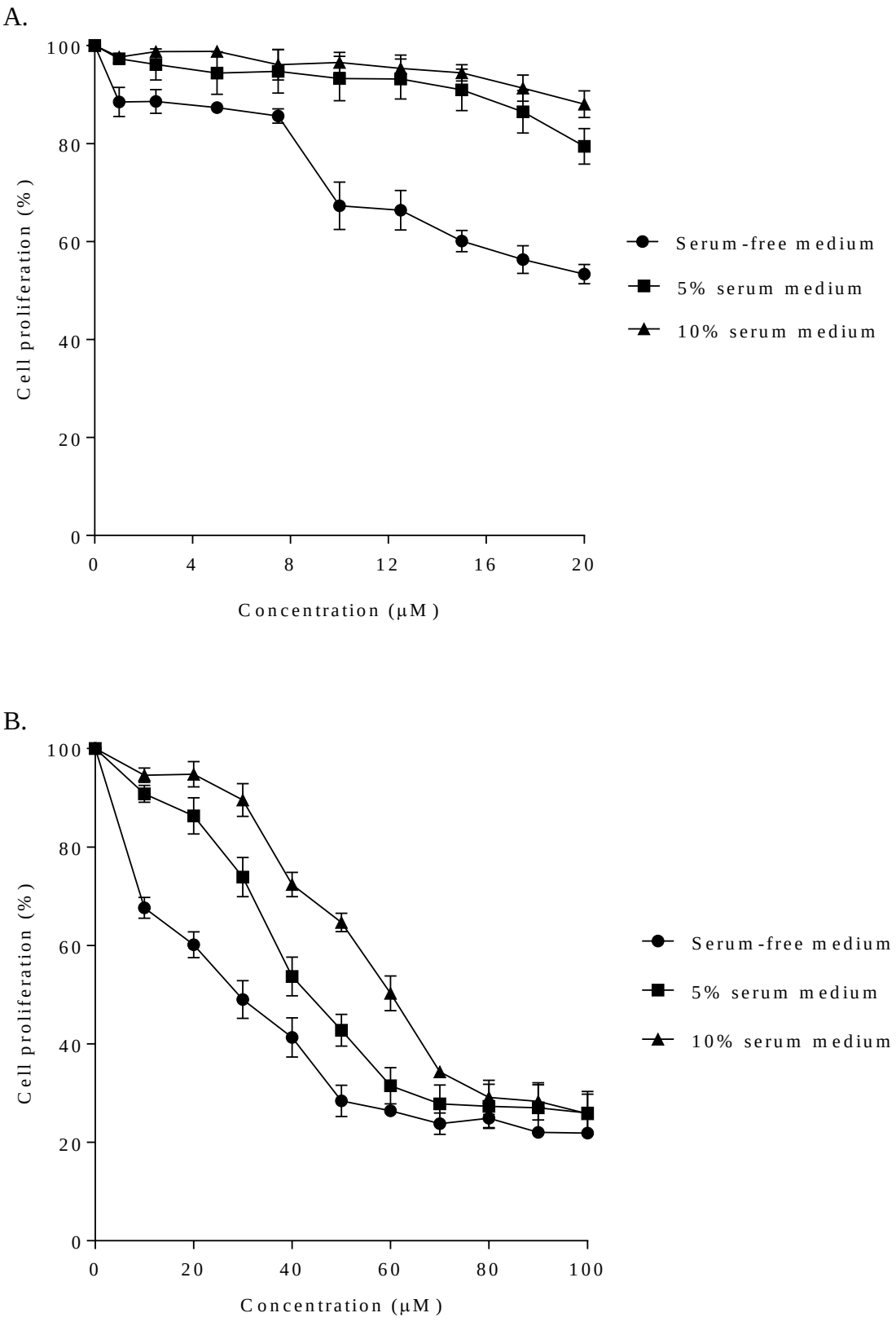

Figure 6.1. The effect of lapatinib 1-20 µM (A) and 10-100 µM (B) treatment on T84 cells as assessed by XTT assay. Each experiment was repeated 3 times with 3 replicates in each experiment (n=9). Data are presented as mean ± S.E.M.

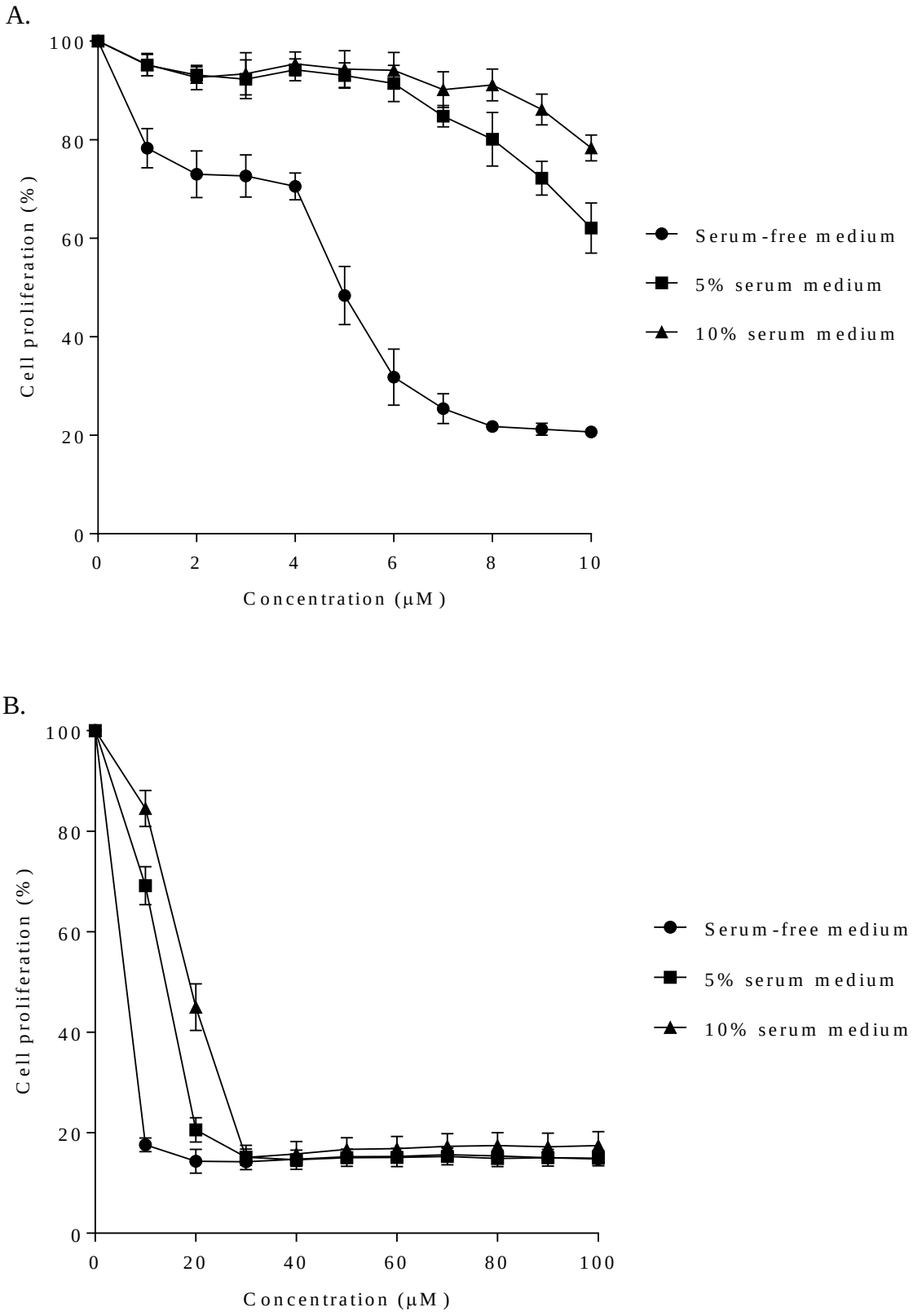

Figure 6.2. The effect of paclitaxel 1-10 μM (A) and 10-100 μM (B) treatment on T84 cells as assessed by XTT assay. Each experiment was repeated 3 times with 3 replicates in each experiment (n=9). Data are presented as mean ± S.E.M.

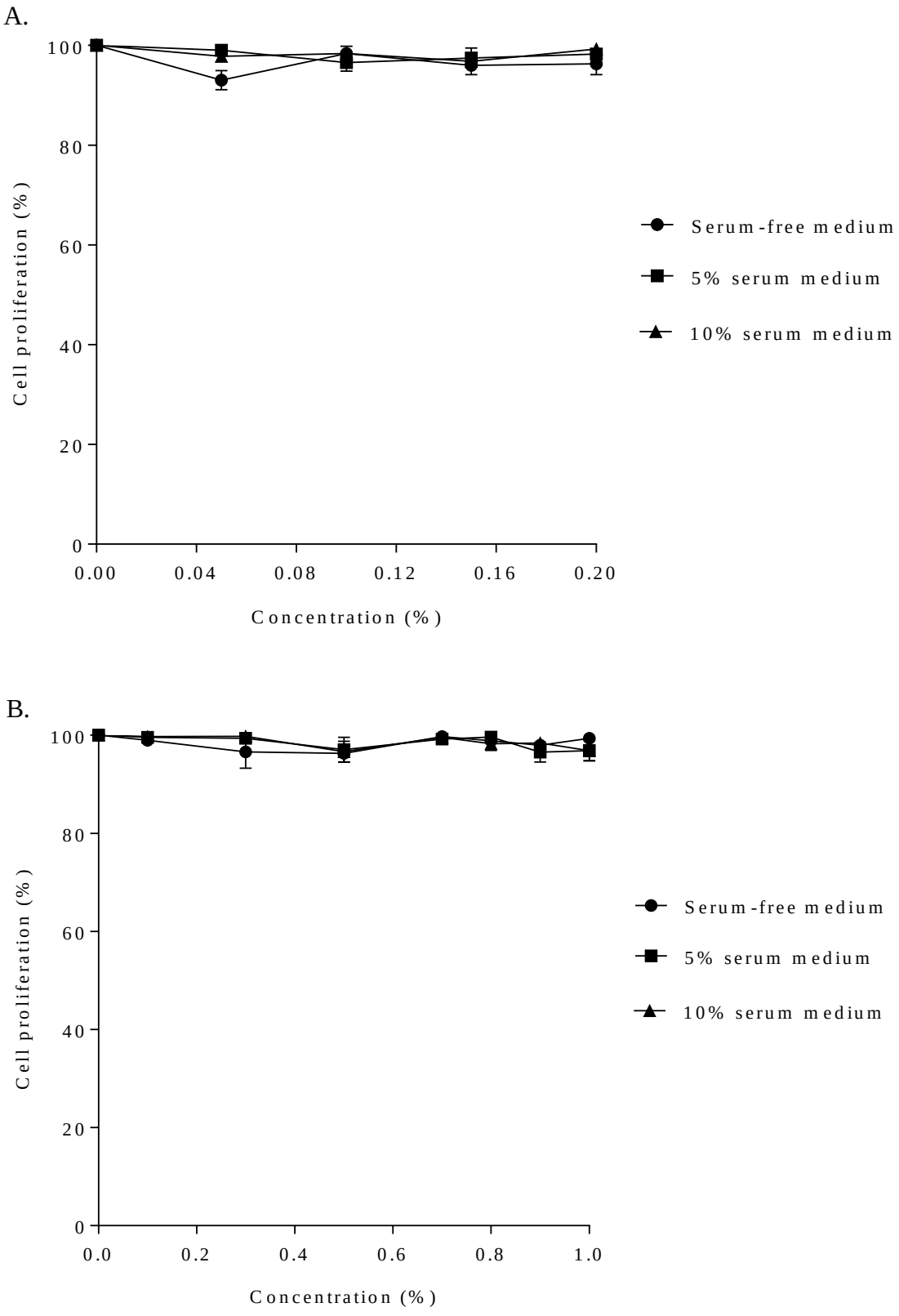

Figure 6.3. The effect of DMSO as a control treatment on T84 cells, as assessed by XTT assay. The concentrations were equivalent to the concentrations of lapatinib used. Each experiment was repeated 3 times with 3 replicates in each experiment (n=9). Data are presented as mean ± S.E.M.

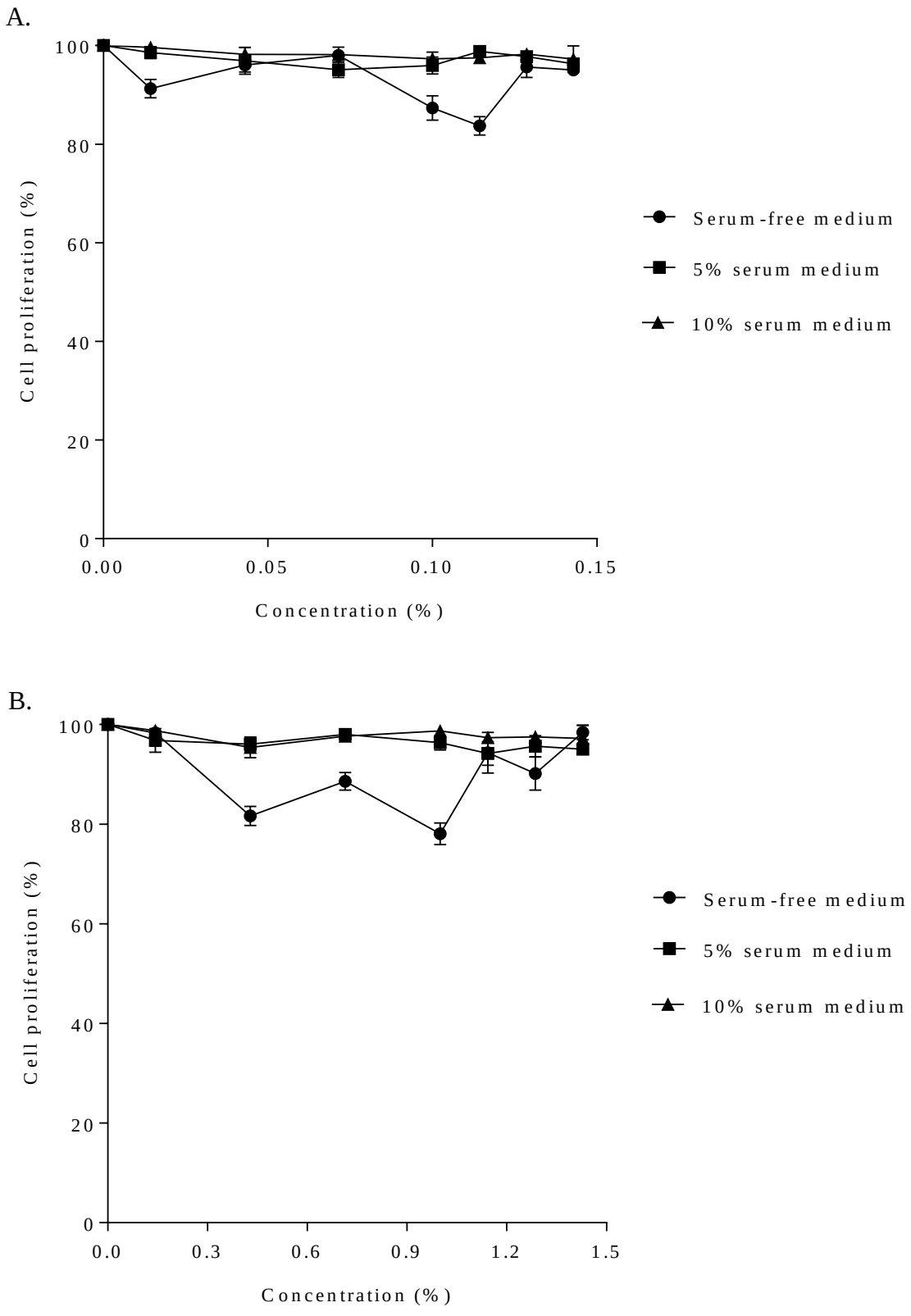

Figure 6.4. The effect of 50% EtOH as a control treatment on T84 cells as assessed by XTT assay. The concentrations were equivalent to the concentrations of paclitaxel used. Each experiment was repeated 3 times with 3 replicates in each experiment (n=9). Data are presented as mean ± S.E.M.

6.3.2 Effect of lapatinib on permeability

The T84 human colonic epithelial monolayers were exposed to lapatinib as well as paclitaxel to investigate the effect of the drugs on permeability. The cell permeability was measured via TEER at 0, 0.5, 24 and 48 hours incubation. Results were expressed as change of resistance from baseline. DMSO and 50% EtOH were used as negative controls while TX-100 was used as a positive control.

At 0.5, 24 and 48 hours, data show that the cell monolayers exhibited higher resistance associated with lapatinib 10 µM and 100 µM when treated on the apical (Figure 6.5A), basolateral (Figure 6.5B) and both apical and basolateral sides (Figure 6.5C) when compared to TX-100. The cell monolayer also showed a higher resistance against DMSO compared to TX-100. Results showed no significant differences in the cell resistance between lapatinib 10 µM and 100 µM at different incubation periods ($p>0.05$) (Figures 6.5A-C). Results also showed no significant differences between LAP 10 µM and LAP 100 µM treated apically, basolaterally or both apically and basolaterally ($p>0.05$) (Table 6.1).

It was observed that at lower concentrations (2, 5 and 10 µM), paclitaxel started to show a decrease in TEER at 48 hours incubation. The decrease in TEER was concentration-dependent, however, no significant difference was seen in the cell resistance between the lower concentrations of paclitaxel ($p>0.05$) (Figure 6.6A). The T84 cell monolayer showed a tremendous decrease in cell resistance when exposed to higher concentrations (20 and 50 µM) of paclitaxel. Significant differences between the higher concentrations (20 and 50 µM) was observed at 48 hours incubation, in which the T84 monolayer possessed higher resistance when exposed to paclitaxel 20 µM compared to when it was exposed to 50 µM ($p<0.05$) (Figure 6.6B). DMSO did not affect cell permeability while 50% EtOH was observed to slightly affect permeability which was shown by the decrease in TEER. TX-100 as a positive control proved to increase permeability significantly (Figure 6.6).

The effect of lapatinib in combination with paclitaxel on the colonic epithelial cell monolayer was also observed as shown in Figure 6.7. Results showed that paclitaxel at lower (2, 5 and 10 µM) and higher (20 and 50 µM) concentrations as well as in combination with lapatinib 10 or 100 µM decreased cell monolayer resistance (Figure 6.7A and B). However, there were no significant differences in resistance among the lower concentrations of paclitaxel in combination with lapatinib 10 µM or 100 µM ($p>0.05$). A similar situation was observed with higher concentrations of paclitaxel ($p>0.05$).

The resistance between paclitaxel in combination with lapatinib and single treatment of paclitaxel was compared, as shown in Table 6.2. At 24 hours incubation, paclitaxel 5 µM combined with lapatinib 100 µM showed significantly lower cell resistance (-34.21 ± 15.23 ohms/cm^2) than paclitaxel 5 µM only (13.09 ± 13.72 ohms/cm^2) ($p<0.05$) (Table 6.2). No significant difference was seen between paclitaxel 2 µM combined with lapatinib 100 and paclitaxel 2 µM only. Paclitaxel 10 µM combined with lapatinib 100 µM (-37.92 ± 13.47 ohms/cm^2) revealed no significant difference in resistance compared to single treatment of paclitaxel 10 µM (-2.04 ± 21.96 ohms/cm^2) ($p>0.05$) indicating no influence of lapatinib in the decrease of cell resistance (Table 6.2).

With 48 hours pre-incubation, paclitaxel 5 µM combined with lapatinib 100 µM showed significantly lower cell resistance (-53.06 ± 9.14 ohms/cm^2) than paclitaxel 5 µM only (-1.80 ± 13.36 ohms/cm^2) ($p<0.01$) (Table 6.2) showing influence of lapatinib in decreasing cellular resistance. However, paclitaxel 10 µM combined with lapatinib 100 µM (-59.45 ± 9.99 ohms/cm^2) exhibited no significant difference in resistance compared to single treatment of paclitaxel 10 µM (-22.75 ± 16.48 ohms/cm^2) ($p>0.05$) indicating no influence of lapatinib in the decrease of cell resistance at 48 hours incubation (Table 6.2).

Table 6.3 shows the comparative resistance between paclitaxel at a higher concentration combined with lapatinib and single treatment of paclitaxel at higher

concentrations T84 monolayers showed no significant difference in resistance when treated with paclitaxel at higher concentration in combination with lapatinib compared to when the monolayer was single-treated with the same concentration of paclitaxel, indicating no influence of lapatinib in decreasing the cellular resistance.

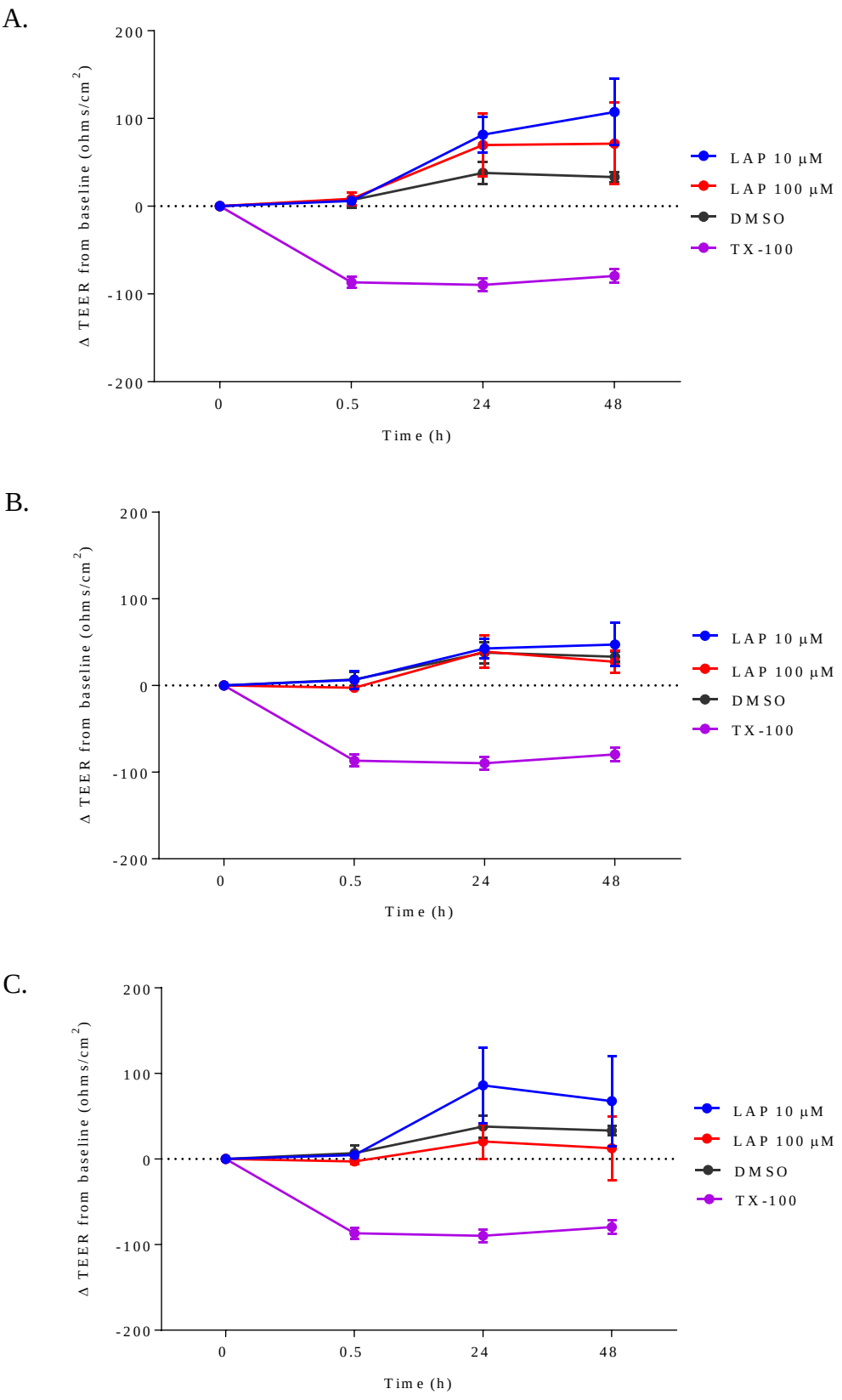

Figure 6.5. The effect of lapatinib at 10 and 100 µM on T84 colonic epithelial monolayer permeability as evaluated by TEER. **A.** Apical treatment. **B.** Basolateral treatment. **C.** Both apical and basolateral treatment. Each experiment was repeated 3 times with 2 replicates in each experiment (n=6). Data are presented as mean ± S.E.M. *LAP: lapatinib.*

Table 6.1. The effect of lapatinib (10 and 100 µM) on T84 colonic epithelial monolayer permeability as evaluated by TEER.

Sample	Δ TEER from baseline (ohms/cm^2)			
	0 h	0.5 h	24 h	48 h
LAP 10 µM A	0.00 ± 0.00	6.08 ± 3.01	81.53 ± 20.08	107.38 ± 37.62
LAP 100 µM A	0.00 ± 0.00	8.39 ± 7.55	69.65 ± 35.60	71.42 ± 46.57
LAP 10 µM B	0.00 ± 0.00	6.56 ± 10.28	42.84 ± 11.25	47.21 ± 25.00
LAP 100 µM B	0.00 ± 0.00	-2.69 ± 4.60	39.21 ± 19.03	27.25 ± 12.90
LAP 10 µM A + B	0.00 ± 0.00	4.66 ± 3.74	86.03 ± 43.88	67.68 ± 52.54
LAP 100 µM A + B	0.00 ± 0.00	-2.80 ± 2.86	20.45 ± 20.09	12.69 ± 37.23
DMSO	0.00 ± 0.00	6.92 ± 8.50	37.91 ± 12.53	33.27 ± 5.74
TX-100	0.00 ± 0.00	-86.64 ± 6.70	-89.58 ± 7.27	-79.48 ± 7.90

*Data presented as mean ± S.E.M (n=6). Results were compared between different concentration of lapatinib at different region of treatment. Results were significantly different at the level of $p<0.05$. LAP: lapatinib, A: apical region, B: basolateral region, A + B: apical and basolateral regions.

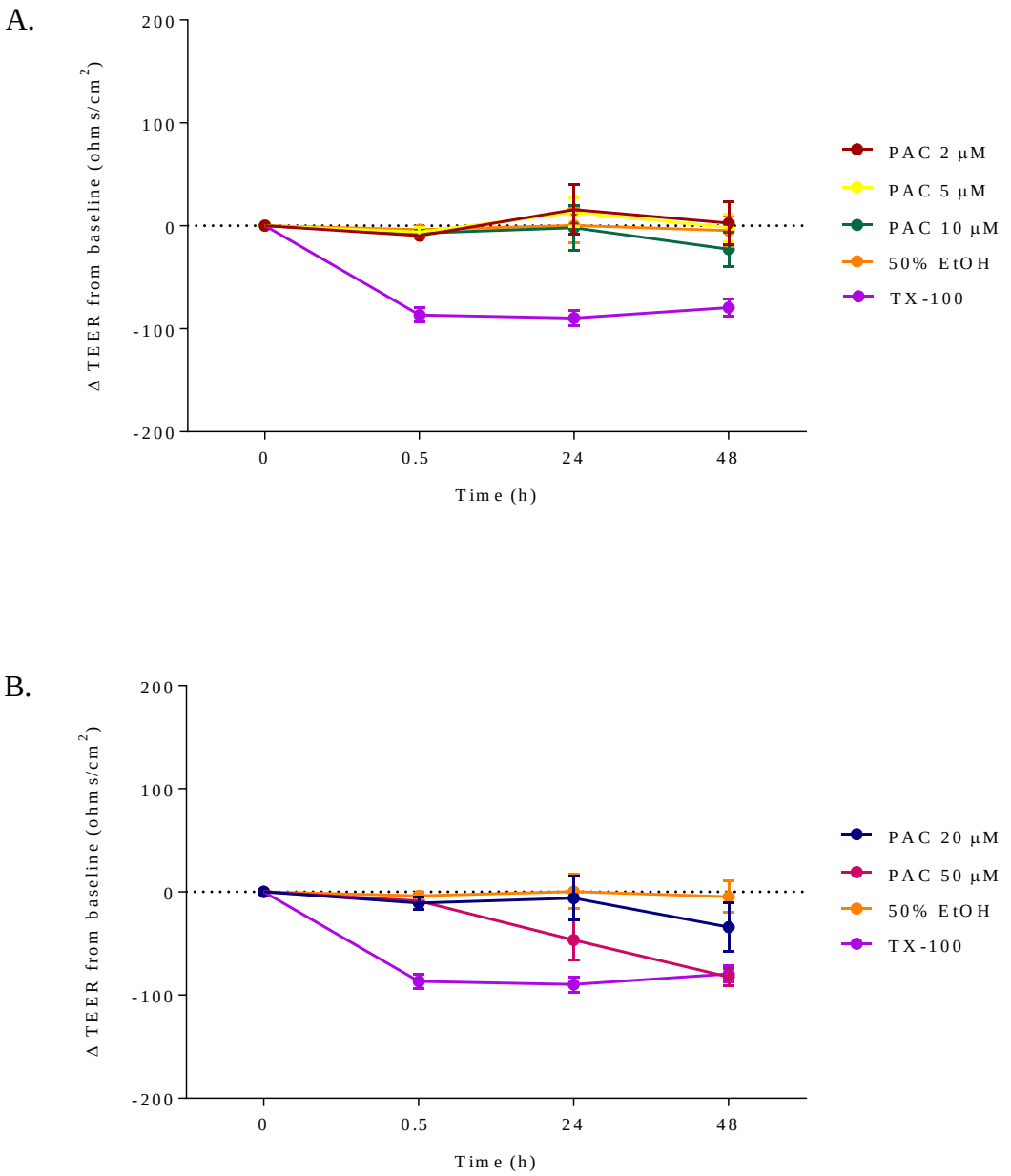

Figure 6.6. The effect of paclitaxel at **A.** lower concentrations (2, 5 and 10 µM), and **B.** higher concentrations (20 and 50 µM) on T84 colonic epithelial monolayer permeability as evaluated by TEER. Each experiment was repeated 3 times with 2 replicates in each experiment (n=6). Data are presented as mean ± S.E.M. *PAC: paclitaxel.*

A.

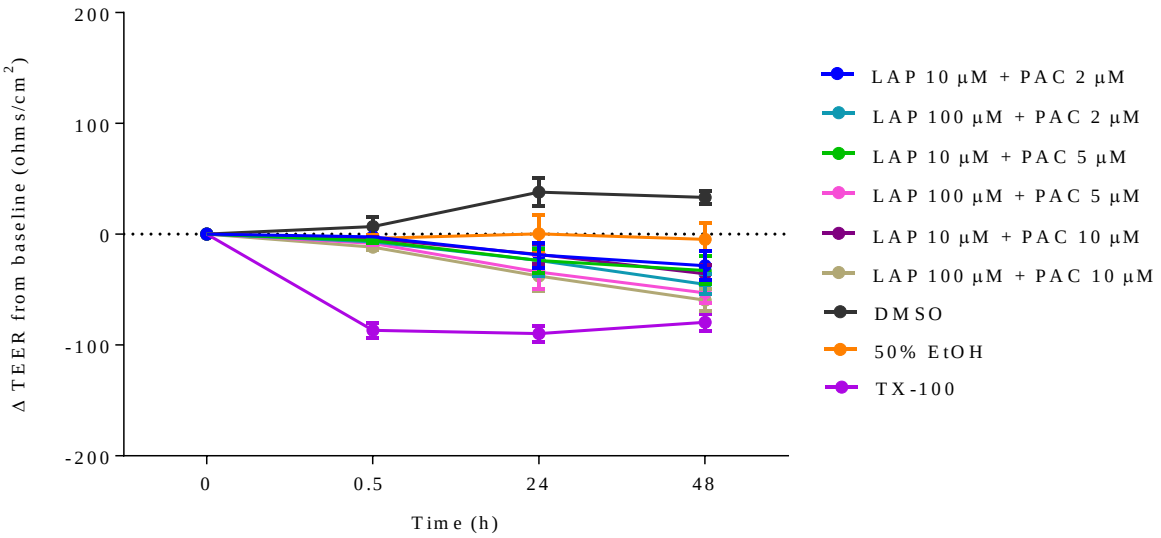

B.

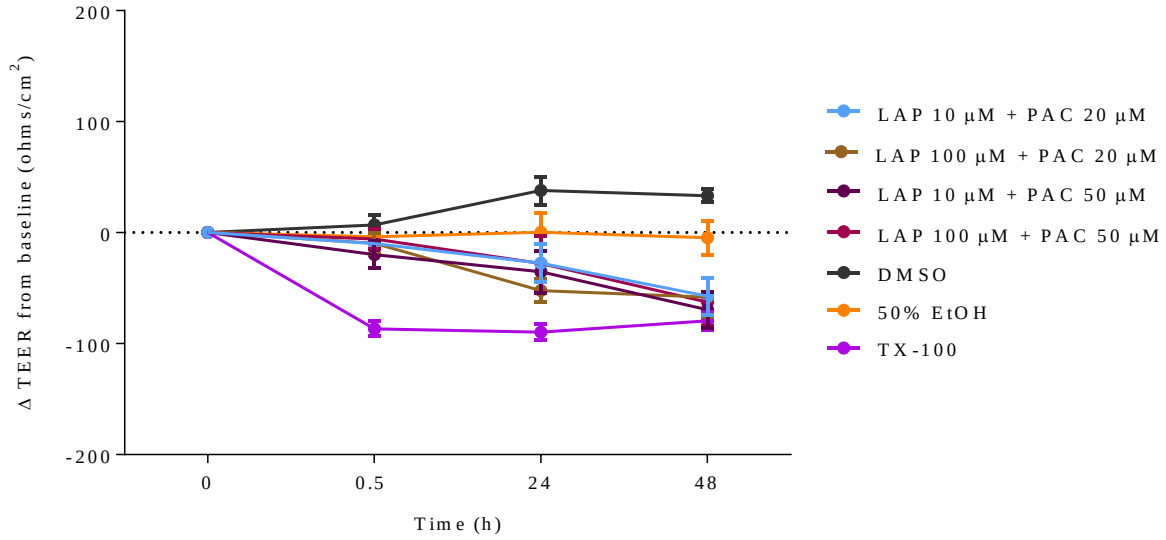

Figure 6.7. The effect of lapatinib in combination with paclitaxel at **A.** lower concentrations (2, 5 and 10 µM), and **B.** higher concentrations (20 and 50 µM) on T84 colonic epithelial monolayer permeability as evaluated by TEER. Each experiment was repeated 3 times with 2 replicates in each experiment (n=6). Data presented as mean ± S.E.M. *LAP: lapatinib, PAC: paclitaxel.*

Table 6.2. The effect of lapatinib (10 and 100 µM) in combination with paclitaxel (2, 5 and 10 µM) on T84 colonic epithelial monolayer permeability as evaluated by TEER.

Sample	Δ TEER frombaseline (ohms/cm^2)			
	0 h	0.5 h	24 h	48 h
PAC 2 µM + LAP 10 µM	0.00 ± 0.00	-2.47 ± 2.76	-18.77 ± 11.26	-28.39 ± 12.84
PAC 5 µM + LAP 10 µM	0.00 ± 0.00	-5.73 ± 2.19	-23.75 ± 10.80	-32.67 ± 12.66
PAC 10 µM + LAP 10 µM	0.00 ± 0.00	-3.90 ± 1.09	-18.17 ± 8.90	-35.61 ± 7.67
PAC 2 µM + LAP 100 µM	0.00 ± 0.00	-6.99 ± 1.30	-23.74 ± 13.92	-45.23 ± 9.10
PAC 5 µM + LAP 100 µM	0.00 ± 0.00	-8.36 ± 1.03	-34.21 ± 15.23 $_{+}$	-53.06 ± 9.14 $_{++}$
PAC 10 µM + LAP 100 µM	0.00 ± 0.00	-11.64 ± 2.67	-37.79 ± 13.47	-59.45 ± 9.99
PAC 2 µM	0.00 ± 0.00	-9.62 ± 1.34	15.81 ± 12.20	2.50 ± 20.61
PAC 5 µM	0.00 ± 0.00	-5.99 ± 4.44	13.09 ± 13.72	-1.80 ± 13.36
PAC 10 µM	0.00 ± 0.00	-7.12 ± 3.44	-2.04 ± 21.96	-22.75 ± 16.48
DMSO	0.00 ± 0.00	6.92 ± 8.50	37.91 ± 12.53	33.27 ± 5.74
TX-100	0.00 ± 0.00	-86.64 ± 6.70	-89.58 ± 7.27	-79.48 ± 7.90

*Data presented as mean ± S.E.M (n=6). Results were compared between combination of paclitaxel and lapatinib and paclitaxel only at the same concentration of paclitaxel within the same incubation time. Results were significantly different at the level of $p<0.05$. $_{+}$ for $p<0.05$ compared to PAC 5 µM at 24 h, $_{++}$ for $p<0.01$ compared to PAC 5 µM at 48 h. LAP: lapatinib, PAC: paclitaxel.

Table 6.3. The effect of lapatinib (10 and 100 µM) in combination with paclitaxel (20 and 50 µM) on T84 colonic epithelial monolayer permeability as evaluated by TEER.

Sample	Δ TEER from baseline (ohms/cm^2)			
	0 h	0.5 h	24 h	48 h
PAC 20 µM + LAP 10 µM	0.00 ± 0.00	-9.93 ± 5.19	-27.65 ± 17.05	-57.34 ± 16.85
PAC 50 µM + LAP 10 µM	0.00 ± 0.00	-19.93 ± 12.04	-35.16 ± 18.83	-69.50 ± 16.34
PAC 20 µM + LAP 100 µM	0.00 ± 0.00	-9.60 ± 9.35	-52.21 ± 10.08	-58.27 ± 17.52
PAC 50 µM + LAP 100 µM	0.00 ± 0.00	-5.83 ± 9.17	-27.82 ± 25.11	-62.77 ± 21.81
PAC 20 µM	0.00 ± 0.00	-10.84 ± 5.91	-6.00 ± 21.28	-34.05 ± 23.82
PAC 50 µM	0.00 ± 0.00	-8.71 ± 5.32	-46.70 ± 19.04	-82.51 ± 8.64
DMSO	0.00 ± 0.00	6.92 ± 8.50	37.91 ± 12.53	33.27 ± 5.74
TX-100	0.00 ± 0.00	-86.64 ± 6.70	-89.58 ± 7.27	-79.48 ± 7.90

*Data presented as mean ± S.E.M (n=6). Results were compared between combination of paclitaxel and lapatinib and paclitaxel only at the same concentration of paclitaxel within the same incubation time. Results were significantly different at the level of $p<0.05$. LAP: lapatinib, PAC: paclitaxel.

6.3.3 Effect of lapatinib on Cl- secretion

Monolayers of T84 colonic epithelial cells were pre-treated with lapatinib and paclitaxel and incubated for 48 hours and mounted into Ussing chambers. Concentrations of the drugs used in this experiment were determined based on results obtained from TEER experiment. Concentrations of the drugs used were lapatinib 100 µM treated from apical side (LAP 100 A) or basolateral side (LAP 100 B) or both apical and basolateral sides (LAP 100 A+B), LAP 100 µM treated from apical or basolateral side combined with PAC 5 µM (LAP 100 A + PAC 5, LAP 100 B + PAC 5) and LAP 100 µM treated from apical side combined with PAC 20 µM (LAP 100 A + PAC 20) as well as PAC 20 µM single treatment (PAC 20). As mentioned earlier in the methods, all concentrations of paclitaxel were treated from the basolateral side. The concentrations were also selected based on the assumption that they would be able to potentiate response to Cl^- secretion.

Experiments were conducted at established monolayer resistance and it was observed that pre-treatment of T84 cells with lapatinib or paclitaxel did not affect baseline $I_{sc.}$ Baseline resistances of all samples were recorded. Baseline I_{sc} compared to the untreated monolayers were also noted. As shown in Figure 6.8A, all of the samples showed TEER >1000 ohms/cm^2 which demonstrated established monolayer integrity. There were no significant differences in resistance between any samples ($p>0.05$). Pre-treatment of monolayers with lapatinib and/or paclitaxel for 48 hours also exhibited no significant differences in baseline I_{sc} between samples ($p>0.05$) (Figure 6.8B), while baseline conductance (G) showed significantly different results between control untreated monolayers (2.34 ± 0.44 mho) and PAC 20 (10.57 ± 2.98 mho) ($p<0.05$) (Figure 6.8C).

After 15 minutes equilibrium the pre-treated monolayers were stimulated apically for 15 minutes with amiloride which stops the Na^{2+} current by preventing Na^{2+} absorption via the

epithelium sodium channel. As such, any change in I_{sc} is not expected as Na^{2+} does not contribute to basal isogenic current in T84s.

The monolayers were then treated with the Ca^{2+}-dependent Cl^- secretagogue, carbachol, added to the basolateral sides. Readings were taken for 15 minutes following carbachol. There was a decreased response in chloride conductance in monolayers treated with lapatinib alone (Figure 6.9A) and lapatinib combined with paclitaxel as well as paclitaxel only (Figure 6.9B). However, no significant differences were seen in ΔI_{sc} between all samples ($p>0.05$) (Figure 6.9C).

Next the cAMP-dependent Cl^- secretagogue, forskolin was added to the apical and basolateral chambers and changes in Cl- conductance were measured for 20 minutes. Monolayers that were pre-treated with lapatinib only (Figure 6.10A), the lapatinib/paclitaxel combination and paclitaxel alone (Figure 6.10B) all had reduced response to forskolin compared to controls, but no significant differences in ΔI_{sc} were seen between any group ($p>0.05$) (Figure 6.10C).

As no significant differences in baseline I_{sc} or agonist-induced ΔI_{sc} were found, a secondary analysis was carried out in which some data were pooled. Specifically, the conditions where lapatinib was added to the apical, basal or both surfaces were combined and analysed again. Results are shown in Figure 6.11 and 6.12. Figure 6.11A shows lower baseline I_{sc} of monolayers pre-treated with LAP 100 A + PAC 20 and PAC 20 single treatment compared to other samples however results were not significantly different ($p>0.05$). Baseline conductances were increased in pre-treated samples in the order of PAC 20 B > LAP 100 A + PAC 20 > LAP 100 + PAC 5 > LAP 100 > control untreated monolayers, however the results were not significantly different ($p>0.05$) (Figure 6.11B).

The ΔI_{sc} of pre-treated samples was decreased when stimulated with the Ca^{2+}-dependent agonist: control untreated monolayers > LAP 100 > LAP 100 + PAC 5 > LAP 100 A + PAC 20 > PAC 20. PAC 20 single treatment (15.49 ± 1.42 μA/cm^2) exhibited significantly lower ΔI_{sc} compared to control untreated monolayers (38.09 ± 5.51 μA/cm^2) ($p<0.05$) (Figure 6.12A). The same decreasing order was also seen in ΔI_{sc} of pre-treated samples when stimulated with cAMP-dependent agonist, however, all samples showed no significant differences in ΔI_{sc} (Figure 6.12B).

It is noted that each group has different replicates. This was due to lower TEER (< 800 ohms/cm^2) in some of the pre-treated monolayers, thus Ussing experiments were not able to be carried out on the monolayers. Due to time constraint, the experiments were also not able to be repeated to obtain same sample size for each group.

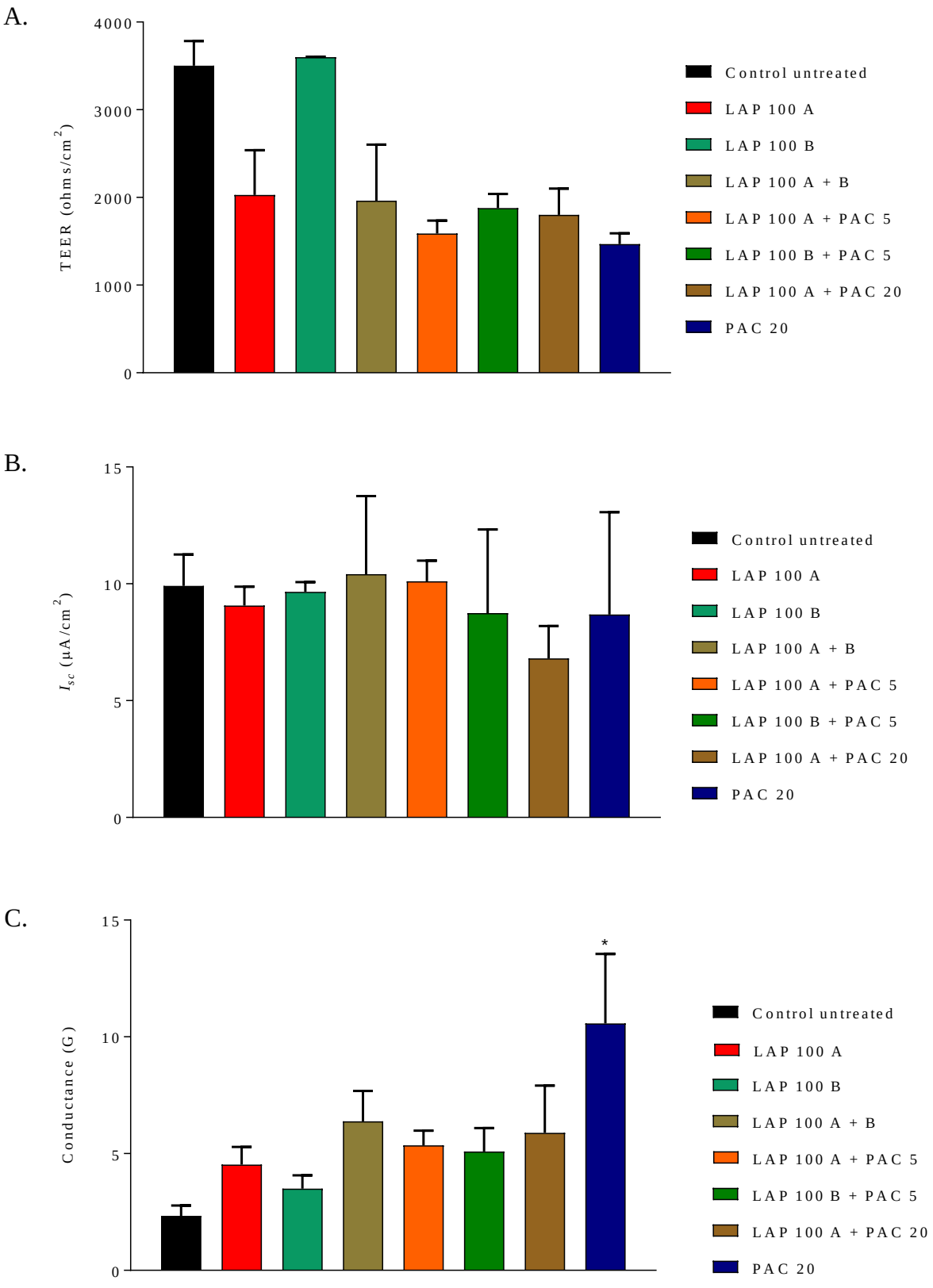

Figure 6.8. Baseline readings of T84 monolayer after 48 hours pre- treatment with LAP +/- PAC. **A.** TEER. **B.** I_{sc}. **C.** Conductance. Data are presented as mean ± S.E.M (n=5 for Control untreated, n=5 for LAP 100 A, n=2 for LAP 100 B, n=3 for LAP 100 A + B, n=5 for LAP 100 A + PAC 5, n=4 for LAP 100 B + PAC 5, n=2 for LAP 100 A + PAC 20 and n=3 for PAC 20). ** indicates $p<0.05$ compared to Control untreated. A: apical, B: basolateral.*

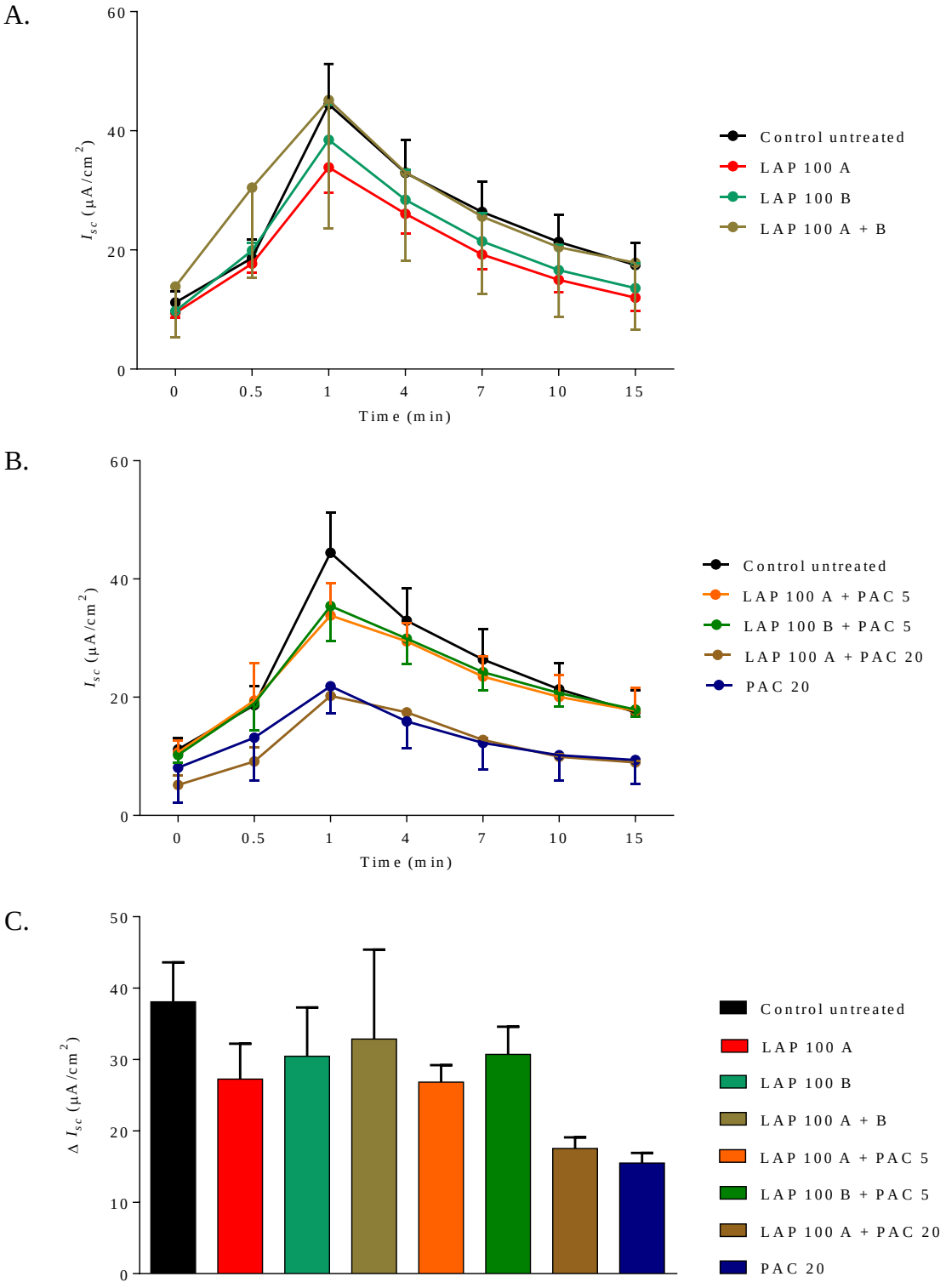

Figure 6.9. Effect of LAP +/- PAC after 48 hours pre-treatment on T84 cell monolayer on Cl^- secretion induced by carbachol as evaluated by I_{sc} measurement. **A.** I_{sc} for LAP only. **B.** I_{sc} for PAC +/- LAP. **C.** Changes in I_{sc} for all samples. Data are presented as mean ± S.E.M (n=5 for Control untreated, n=5 for LAP 100 A, n=2 for LAP 100 B, n=3 for LAP 100 A + B, n=5 for LAP 100 A + PAC 5, n=4 for LAP 100 B + PAC 5, n=2 for LAP 100 A + PAC 20 and n=3 for PAC 20). *A: apical and B: basolateral.*

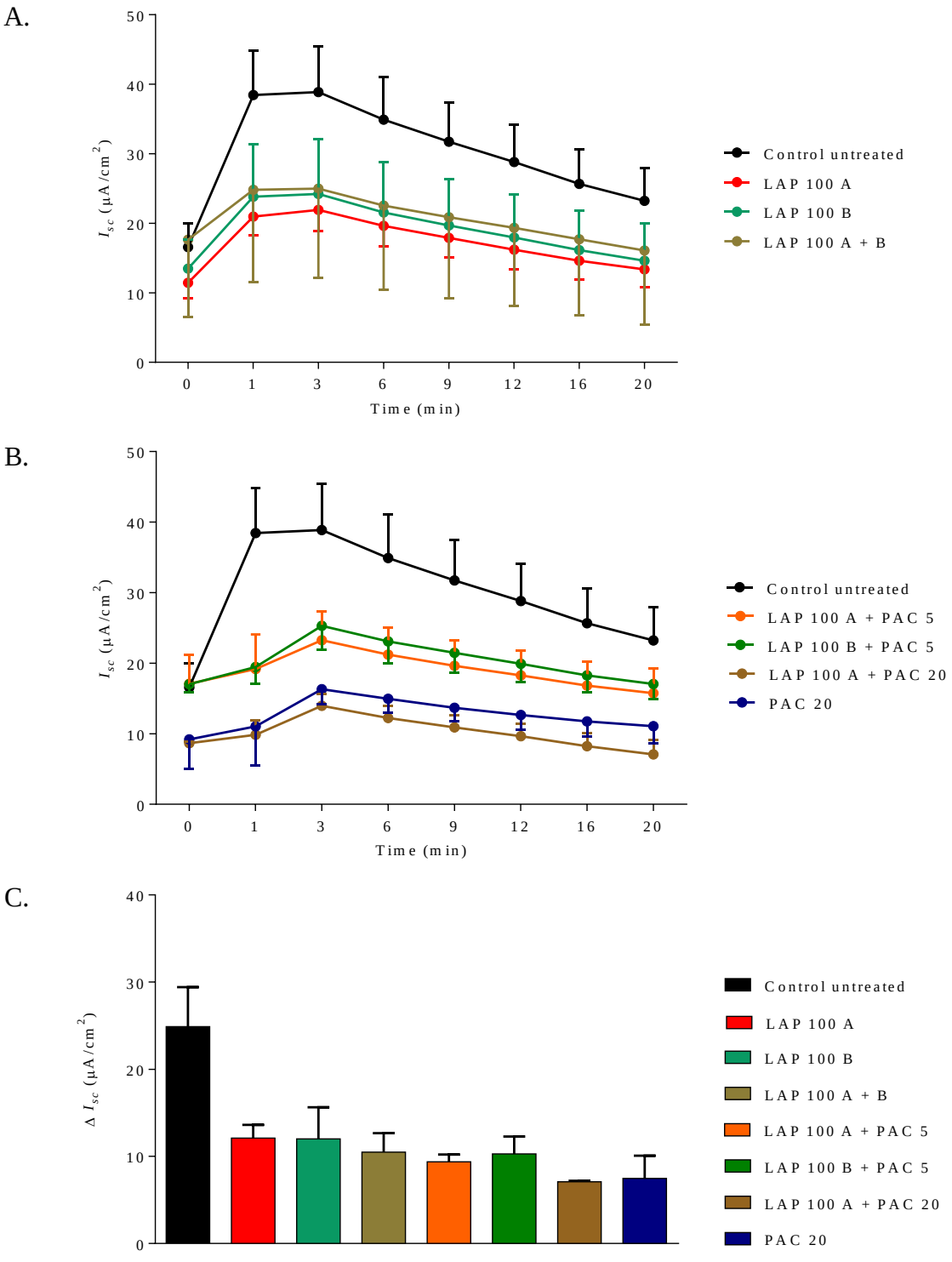

Figure 6.10. Effect of LAP +/- PAC after 48 hours pre-treatment on T84 cell monolayer on Cl^- secretion induced by forskolin as evaluated by *Isc* measurement. **A.** I_{sc} for LAP only. **B.** I_{sc} for PAC +/- LAP. **C.** Changes in I_{sc} for all samples. Data are presented as mean ± S.E.M (n=5 for Control untreated, n=5 for LAP 100 A, n=2 for LAP 100 B, n=3 for LAP 100 A + B, n=5 for LAP 100 A + PAC 5, n=4 for LAP 100 B + PAC 5, n=2 for LAP 100 A + PAC 20 and n=3 for PAC 20). *A: apical and B: basolateral.*

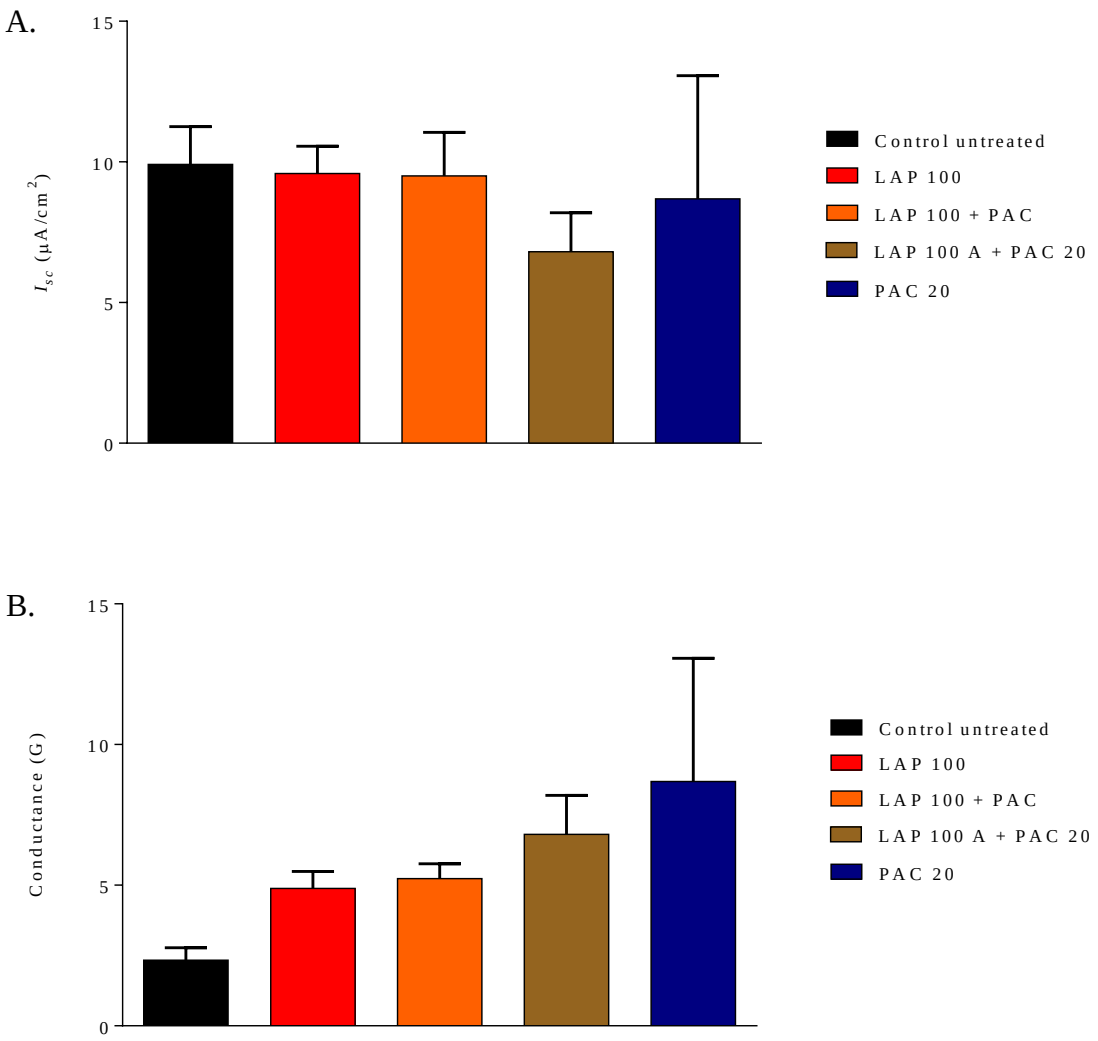

Figure 6.11. Secondary analysis on baseline readings of effect of LAP +/- PAC after 48 hours pre-treatment on T84 cell monolayer A. Baseline I_{sc}. B. Baseline conductance. Data are presented as mean ± S.E.M (n=5 for Control untreated, n=10 for LAP 100, n=9 for LAP 100 + PAC 5, n=2 for LAP 100 A + PAC 20 and n= 3 for PAC 20). A: apical and B: basolateral. LAP 100 (pooled data of LAP A, B and A+B), LAP 100 + PAC 5 (pooled data of LAP 100 A + PAC 5 and LAP 100 B + PAC 5).

A.

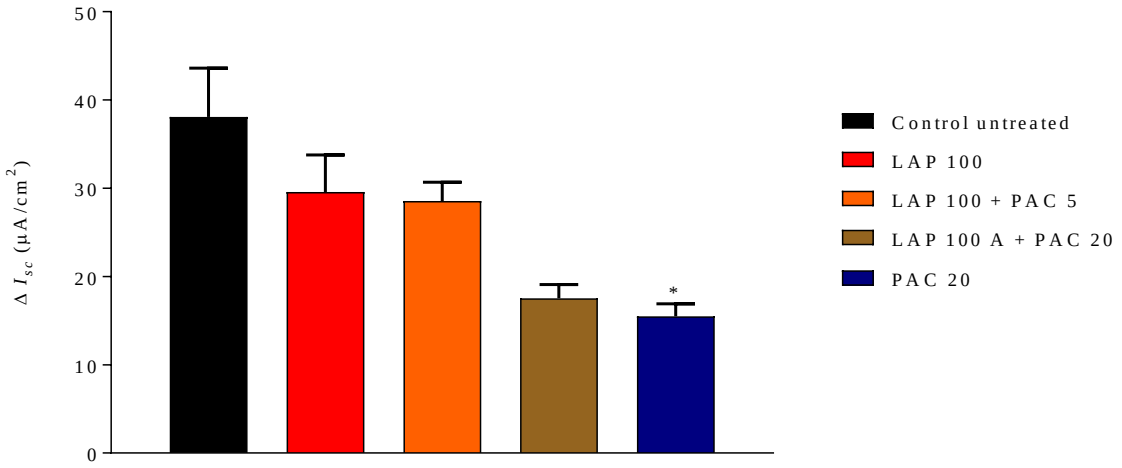

B.

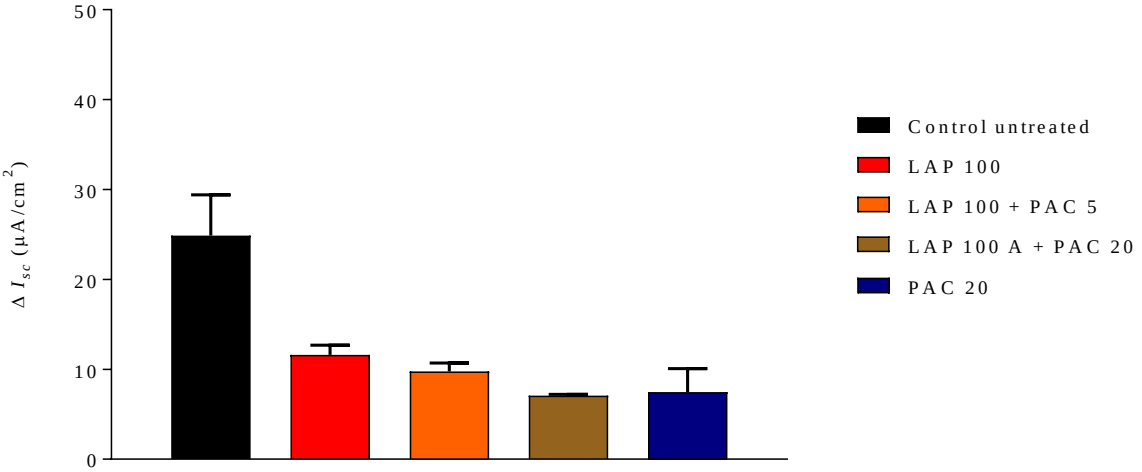

Figure 6.12. Secondary analysis on effect of LAP +/- PAC after 48 hours pre-treatment on T84 cell monolayer as evaluated by I_{sc} measurement. A. ΔI_{sc} carbachol. B. ΔI_{sc} forskolin. Data are presented as mean ± S.E.M (n=5 for Control untreated, n=10 for LAP 100, n=9 for LAP 100 + PAC 5, n=2 for LAP 100 A + PAC 20 and n= 3 for PAC 20). * *indicates $p<0.05$ compared to Control untreated. A: apical and B: basolateral. LAP 100 (pooled data of LAP A, B and A+B), LAP 100 + PAC 5 (pooled data of LAP 100 A + PAC 5 and LAP 100 B + PAC 5).*

6.4 Discussion

This is the first study to specifically investigate the effect of lapatinib and paclitaxel treatment on chloride secretion in the T84 model of colonic epithelium. Lapatinib and paclitaxel were first tested for their cytotoxic effect on proliferating cells. The experiments were conducted using serum-deprived, 5 % and 10% serum-supplemented medium in which to determine the appropriate medium condition to be used in the subsequent experiments. Both drugs showed a higher cytotoxic effect on serum-starved cells compared to cells maintained in serum-supplemented medium. It has been reported that starvation of nutrients leads to cell death as well as reducing cell viability (Jung, Li et al. 2015, Xu, Huang et al. 2015), however our data showed that all vehicle control cells maintained around 100% viability. As such, the duration of starvation was not sufficient to reduce viability per se. Thus, more subtle changes leading to drug sensitivity were at play, such as changes in expression of the Bcl-2 family of proteins (Diaz, Nguewa et al. 2010), that increases expression of cleaved caspase-3, caspase-7 and poly (adenosine diphosphate-ribose) polymerase (PARP) (Li, Zhu et al. 2013) that regulate apoptosis. Cytotoxicity results also revealed that T84 cells were relatively resistant to lapatinib with an IC_{50} of 26.48 ± 1.64 µM in serum-free-medium, 43.24 ± 2.73 µM in 5% serum-medium and 58.59 ± 1.37 µM in 10% serum-medium. In comparison, the effect of paclitaxel was more potent with an IC_{50} reached at 7.52 ± 0.25 µM in serum-free-medium, 12.58 ± 1.13 µM in 5% serum-medium and 18.48 ± 0.77 µM in 10% serum-medium. The lack of response of T84 cells to lapatinib is likely due to low target expression. Previous studies have shown that human tumour cell lines overexpressing ErbB1 and ErbB2 were more sensitive to growth inhibition by lapatinib and the expression of ErbB1 and ErbB2 was correlated with lapatinib IC_{50}, mainly for ErbB2 (Rusnak, Lackey et al. 2001, Konecny, Pegram et al. 2006, Rusnak, Alligood et al. 2007). A study by Rusnak also showed that based on tissue specificity, colon cell lines are less

sensitive towards lapatinib compared to breast cell lines (Rusnak, Alligood et al. 2007). Both ErbB1 and ErbB2 are expressed in T84 cell line (Keely and Barrett 1999), however, the relative expression of ErbB2 in this cell line is unknown. Thus, the lack of response of T84 cells to lapatinib might be due to lower ErbB2 expression as ErbB1 has been shown to be widely expressed in the colonic epithelial cells (McCole and Barrett 2009). The expression of ErbB1 and ErbB2 was not determined in the current study. As such, the mechanisms of lower sensitivity to lapatinib in the colon cell lines require further investigations.

On the other hand, paclitaxel, which was more potent than lapatinib in inhibiting T84 cell proliferation, is a microtubule-binding compound and is widely used in the treatment of cancers such as breast, ovarian and lung cancer (Gornstein and Schwarz 2014). Paclitaxel acts by binding along the length of cell microtubules and thus suppresses microtubule depolymerisation and repolymerisation, leading to mitotic arrest and apoptosis in dividing cells (Nogales, Wolf et al. 1995). Thus, a more potent activity of paclitaxel is expected when compared to lapatinib, as lapatinib targets specific receptor tyrosine kinases, in contrast with paclitaxel which is a typical chemotherapy agent that acts against all actively dividing cells (Widakowich, de Castro et al. 2007).

As it has been shown in the current study that lapatinib and paclitaxel have cytotoxic effects on the T84 human colonic epithelial cell line, TEER experiments were conducted to determine the effect of both drugs on cell permeability. Concentrations of lapatinib and paclitaxel that were used in permeability studies were estimated from the cytotoxicity assay. Medium supplemented with 10 % serum was used to grow T84 cells in order to form a cell monolayer with an established TEER prior to the subsequent experiments. The process of forming monolayer requires an extensive time and a well-nourished environment; therefore it is necessary for the medium to be supplemented with 10 % serum. However in Ussing experiment whereby the effect of lapatinib on Cl^- secretion was studied, medium

supplemented with serum was replaced with Ringers solution supplemented with glucose as nourishment to the monolayer. The experiment was carried out only in a short period of time.

Based on the TEER results obtained, it was observed that lapatinib at both higher and lower concentrations, treated either from apical, basal or both apical and basal sides, as well as at different incubation hours does not affect colonic epithelial cell permeability. This suggests that lapatinib does not damage cell-cell adhesion properties, and likely spares epithelial tight junctions. As such, the mechanism of diarrhoea is not related to overt changes in membrane barrier permeability.

In order to traverse the epithelium, two routes are available which are the transcellular and paracellular. Molecules with hydrophobic properties, or those able to interact with transport mechanisms, are absorbed primarily through the transcellular pathway. Passive diffusion of remaining molecules occurs through the paracellular pathway which is regulated by tight junctions (Wardill, Bowen et al. 2012). The permeability of the intestinal epithelium depends on the regulation of intercellular tight junctions. Tight junctions were originally conceptualised as secreted extracellular cement forming an absolute and unregulated barrier within the paracellular space (Fasano and Shea-Donohue 2005). The present study evaluated that lapatinib does not alter T84 paracellular permeability which means not affecting the cells' tight junctions. However, investigations are needed to further clarify effects of lapatinib on the tight junctions. On the other hand, paclitaxel which is a widely used chemotherapeutic agent to treat various tumours (Weaver 2014), was shown to increase permeability in a concentration-dependent manner. One of the adverse events of paclitaxel is gut toxicity manifesting as diarrhoea (Jones, Erban et al. 2005, Kaur Saharan, Das et al. 2015), thus diarrhoea incidence in paclitaxel administration might be associated with the alteration of tight junction proteins (Wardill, Bowen et al. 2012). Importantly, lapatinib is often given in conjunction with paclitaxel clinically (Crown, Burris et al. 2008), and this is associated with

increased frequency and severity of diarrhoea than with either agent alone (Crown, Burris et al. 2008). This study supported those observations with further increases in permeability seen when high dose lapatinib was combined with either lower or higher concentrations of paclitaxel. Combination of lapatinib and paclitaxel also worsens diarrhoea in rat models (Bowen, Mayo et al. 2012). The present study supports the hypothesis that worsened diarrhoea events with the drug combination of lapatinib and paclitaxel is due to altered colonic epithelial tight junctions (Wardill, Bowen et al. 2012).

Chloride secretion is the predominant driving force for fluid secretion in the intestine (Barrett and Keely 2000). To examine the effect of lapatinib as well as paclitaxel on intestinal chloride transport, T84 human colonic epithelial cell monolayers were mounted in Ussing chambers and the changes in short circuit current (I_{sc}) were measured. This experiment was conducted to examine the possibility that diarrhoeal side effects experienced by patients administered with lapatinib could be related to alterations in chloride secretion. In this experiment, the effect of lapatinib at suprapharmacological concentration was tested because it was shown in TEER results that lapatinib at lower concentrations did not affect cell permeability. Experiments were then conducted at established monolayer resistance and it was observed that pre-treatment of T84 cells with lapatinib or paclitaxel did not affect baseline $I_{sc.}$ Chloride secretion was measured as I_{sc} across the T84 cell monolayers that were mounted in Ussing chambers (Dharmsathaphorn and Pandol 1986), thus the findings reflected that pre-treatment with both drugs does not alter baseline chloride secretion.

Besides baseline I_{sc} of pre-treated monolayers, baseline conductance was also measured. Conductance acts as an electrophysiological indicator of barrier function in which tissue conductance can also be used as an indication of passive ion transfer that reflects the permeability (Penner, Aschenbach et al. 2014). The present study exhibited higher baseline conductance of cell monolayer pre-treated with a high concentration of paclitaxel which

reflected higher permeability, consequently lower barrier function/resistance, compared to control untreated monolayers. The finding is supported by the TEER results that showed that higher concentration of paclitaxel increased cell monolayer permeability.

Again, in opposition to our working hypothesis, lapatinib did not potentiate a significant response to known chloride secretagogues, such as carbachol or forskolin. As mentioned earlier, chloride secretion was measured as changes in I_{sc} in which decrease in I_{sc} indicates decrease in chloride secretion which could be related to the transactivation of ErbB1 and recruitment of downstream effectors such as the subsequent activation of extracellular signal-regulated kinase (ERK, also known as p 44/42 mitogen activated protein kinase or MAPK) activity (Chow, Carlstrom et al. 2003). Thus, indicating lapatinib-induced diarrhoea might be independent of ErbB1 transactivation.

A similar outcome was also observed in combination treatment of lapatinib with paclitaxel at a lower concentration. In contrast, high dose paclitaxel, with and without lapatinib, was associated with a decreased response to chloride agonists. But, as decreased chloride secretion would theoretically lead to less water movement into the lumen, paclitaxel-induced hyposecretion is somewhat questionable, especially when considering the combination of lapatinib and paclitaxel are known to worsen diarrhoea. As such, the mechanisms of paclitaxel-induced diarrhoea seem to be separate from epithelial chloride secretion. Another possibility is that high dose paclitaxel treated monolayers with 48 hours incubation were metabolically injured by the chemotherapy and could not mount a normal secretory response to either carbachol or forskolin. This is reflected by the timeframe of clinical onset of chemotherapy-induced diarrhoea which could be within 24 hours, after 24 hours or more than 24 hours (Stein, Voigt et al. 2009).

6.5 Conclusion

Lapatinib does not affect colonic epithelial monolayer permeability. However, lapatinib and paclitaxel combination treatment as well as paclitaxel single treatment affect permeability, possibly via inhibition of tight junction proteins, thus causing diarrhoea. Both drugs also do not affect chloride secretion, however, due to lapatinib being an ErbB1 inhibitor which could interfere with chloride secretion, further investigations are required. Effect of lapatinib on chloride secretion might occur via other mechanisms unrelated to calcium or cAMP regulated chloride secretion. The mechanism of lapatinib-induced diarrhoea may be mediated by other unknown mechanisms. The cytotoxic effect of lapatinib as well as paclitaxel on T84 colonic cell line was also shown not to contribute to its effect on T84 monolayer permeability and chloride secretion. Overall, further investigations are needed to clarify the possible mechanisms of lapatinib-induced diarrhoea.

Chapter 7

General discussion

7.1 Introduction

The studies contained within this thesis contributes to our knowledge on the effects of lapatinib on both tumour and intestine since each model was novel and provides the first documented evidence of lapatinib in this context. Firstly, I aimed to uncover the cytotoxic effects of lapatinib on rat tumour and intestinal cell lines and also to identify the candidate markers which are involved in these effects. A tumour-bearing rat model to study the effect of lapatinib on the intestine *in vivo* was then developed which allowed lapatinib-induced diarrhoea to be investigated in a situation that reflects the patient setting. Finally, permeability changes in colonic epithelial monolayers following lapatinib was determined, giving new insights into the functional changes on the intestine.

7.2 Mechanisms of lapatinib-induced diarrhoea in breast cancer therapy

Molecularly targeted therapies are one of the cancer treatments that have been widely developed; however, they are frequently associated with adverse events. The oral ErbB1/ErbB2 dual targeted tyrosine kinase inhibitor, lapatinib has been approved for the treatment of ErbB2 overexpressing breast cancer (Geyer, Forster et al. 2006). However, despite its advancements in cancer treatment, the mechanisms involved in its gut toxicity, particularly diarrhoea, are poorly characterised (Moy and Goss 2007). Diarrhoea is one of the most common adverse events recorded following treatments with tyrosine kinase inhibitors that block ErbB1 signalling and is a dose limiting toxicity (Keefe and Gibson 2007). ErbB1 inhibition within the intestine has been postulated as the mechanism underpinning diarrhoea-induced by ErbB1 tyrosine kinase inhibitors (Loriot, Perlemuter et al. 2008). Our preliminary

investigation in this thesis has proven that cells expressing relatively high levels of *ErbB1/ErbB2* are more sensitive to lapatinib, in which lapatinib exhibited higher cytotoxic effect on the IEC-6 jejunal cells that expressed higher levels of *ErbB1* and *ErbB2* mRNAs, compared to the Walker 256 tumour cells which the *ErbB1* mRNA was unable to be detected while *ErbB2* mRNA was relatively expressed (Chapter 3). This is not surprising as lapatinib is only indicated in *ErbB2* overexpressing breast cancer. Lapatinib-induced diarrhoea in patients might also be explained by this increased sensitivity of small intestinal cells to the drug, which induces late apoptosis in small intestinal cells, leading to barrier disruption and consequently diarrhoea. With these preliminary findings, we extended our investigation to mechanisms that might be related to lapatinib-induced diarrhoea.

The ErbB1 receptor, as well as its ligands, is vital for mucosal protection and the adaptive response to external injury (Schneider and Wolf 2009). Disruption of ErbB1 signalling produces major defects in gut epithelial homeostasis (Dvorak, Khailova et al. 2008, Yusta, Holland et al. 2009) suggesting the essential role of ErbB1 in gut mucosal growth (McCole and Barrett 2007, Fiske, Threadgill et al. 2009). Studies have shown that diarrhoea induced by ErbB1 tyrosine kinase inhibitor monotherapy is dose-dependent rather than associated with pharmacokinetics, suggesting that the toxicity is predominantly caused by luminal exposure to the drug (Keefe and Gibson 2007). ErbB1 is expressed by cells of epithelial origin, including the skin and gastrointestinal tract; thus it is not surprising that toxicities affect these systems. The prevailing hypothesis is that inhibition of ErbB1 signalling will lead to reduced growth and healing of the intestinal epithelium, leading to mucosal atrophy, due to the stimulatory effect of the ErbB1 pathway on enterocyte proliferation (Berlanga-Acosta, Playford et al. 2001) . The role of ErbB2 in the intestine is unclear at this stage. ErbB2 has been extensively studied in many types of cancers (Baselga and Swain 2009). Although no ligands have been identified for ErbB2, its activation can be induced by

heterodimerisation with ligand-occupied ErbB1, ErbB3 or ErbB4 (Jackson-Fisher, Bellinger et al. 2004). ErbB2 has been implicated in mediating myoblast cell survival and in inhibiting cancer cell apoptosis (Andrechek, Hardy et al. 2002, Lucs, Muller et al. 2010). ErbB2 is transactivated by tumour necrosis factor alpha (TNF-α), which in turn protects intestinal epithelial cells from TNF-α-induced apoptosis (Yamaoka, Yan et al. 2008). However, determination of its role in intestinal development and epithelial response to injury and inflammation has been hampered by the fact that ErbB2 deletion is embryonically lethal due to both cardiac and neural defects (Lee, Simon et al. 1995). Zhang et al conducted an experiment using intestinal epithelium-specific *ErbB2* and *ErbB3* knockout mice and reported that both receptors plays important cytoprotective and reparative roles in the colonic epithelium following injury, by promoting colon epithelial cell survival (Zhang, Dubé et al. 2012).

In Chapter 4 of this thesis, we found that inoculation of Walker 256 tumour does not affect the intestine in terms of morphometry or apoptosis. As such, we proceeded with the Walker 256 tumour rat model confident that any changes seen following lapatinib treatment were separate to the tumour burden. Lapatinib administration in the tumour rat model enabled us to further clarify the mechanisms that might be related to lapatinib-induced diarrhoea (Chapter 5). Lack of significant tissue pathology were observed in rats treated with both lower and higher dose of lapatinib which might be explained by the unaffected ErbB1 protein expression in the intestine as ErbB1 plays an important role in maintaining growth and healing of the intestinal epithelium (Berlanga-Acosta, Playford et al. 2001). However, other factors also play important roles in maintaining normal gut homeostasis such as toll-like receptors, prostaglandin and others (McCole and Barrett 2007) which were not tested in this thesis. Villus atrophy was observed in the rats treated with both lower and higher doses of lapatinib, but significant tissue pathology was only observed in the rats administered with the

higher dose in which the rats also experienced diarrhoea. Villus atrophy could also be associated with other factors such as decreased food intake and severe weight loss (Genton, Cani et al. 2015), which was also seen in the rats administered with the higher dose of lapatinib that experienced severe weight loss.

In Chapter 5 of this thesis, only ErbB2 protein in the jejunal crypts showed a decrease in expression when treated with lapatinib. This suggests that lapatinib may mediate some of its effects in the intestine by reducing ErbB2 protein expression, rather than ErbB1, particularly in the small intestine. No severe damage was observed in the colon, thus supporting the hypothesis that lapatinib-induced diarrhoea is caused by alterations in the small intestine (Burris, Hurwitz et al. 2005), given that exposure of the mucosal surface to the accumulated drug is higher in that region. Supporting this is the observation that ErbB2 expression was decreased in the crypts of the jejunum but in no other region. Accumulation of the drug in the jejunal mucosa could also be due to defects of drug uptake and efflux transporter as previous studies have reported polymorphism of the drug transporter *ABCG2* and also *CYP3A4* and *CYP3A5* genes modified the pharmacokinetics and therefore toxicities of the drug (Li, Cusatis et al. 2007). However, further investigation is required as no significant toxicity was observed with lapatinib-treated rats in the current study.

Lapatinib was found to be cytotoxic to the IEC-6 jejunal cell line compared to T84 colonic epithelial cell line as reported in Chapters 3 and 6. The cytotoxic effect of lapatinib on IEC-6 cells could be influenced by expression of ErbB1 and ErbB2 in which both receptors are expressed in the IEC-6 jejunal cells. ErbB1 and ErbB2 are expressed in T84 colonic epithelial cell line (Keely and Barrett 1999, Yan, Liu et al. 2013), in which ErbB1 is widely expressed in colonic epithelial cells (McCole and Barrett 2009). However, in the current work, we were not able to compare lapatinib sensitivity between jejunal cells (IEC-6) and colonic epithelial cells (T84) in the aspect of ErbB1 and/or ErbB2 expressions as both

receptors were not tested in the T84 cells. Nevertheless, previous studies have shown the cytotoxicity effect of lapatinib is more related to ErbB2 inhibition than ErbB1 inhibition (Konecny, Pegram et al. 2006, Rusnak, Alligood et al. 2007).

Additionally, a significant increase in apoptosis (caspase-3) was seen in the colon in both lapatinib-treated groups, whilst no change in apoptosis was noted in the jejunum (Chapter 5). Previous study showed that no severe damage was observed in rats treated with interleukin-11 after methotrexate treatment although results indicated apoptosis (Gibson, Keefe et al. 2002). Pritchard et al (Pritchard, Potten et al. 1998) found that apoptosis was not directly associated with intestinal damage after chemotherapy. These findings may support our current study that lapatinib induces apoptosis in colon but with no severe damage.

Although mucosal atrophy has been suggested to mediate ErbB-inhibitor induced diarrhoea (Rasmussen, Viby et al. 2010), an alternative theory implicates excess chloride secretion caused by altered ErbB1 signalling to downstream pathways and channels (Harandi, Zaidi et al. 2009). In the final experimental chapter of this thesis we hypothesised that lapatinib-induced diarrhoea is due to an inhibition of ErbB1 activity in colonocytes leading to increased chloride secretion, however, our findings did not show an effect of lapatinib on chloride secretion. Lapatinib also did not affect colonic epithelial permeability. However, as mentioned earlier, in this study, lapatinib is shown to inhibit small intestine via late apoptosis induction. As mentioned in the previous paragraph, only ErbB2 in the jejunum showed a decrease in expression when treated with lapatinib, which shows that lapatinib is more effective in decreasing ErbB2 expression than ErbB1. This could possibly explain no diarrhoea event in the rats. As what have been informed earlier, ErbB1 plays a vital role in the regulation of chloride secretion in normal gut homeostasis, thus no inhibition of ErbB1 may possibly explain no inhibition on regulation of chloride secretion, thus no diarrhoea. Nevertheless, rats that were administered with a higher dose of lapatinib experienced mild

diarrhoea which could possibly due to mucosal atrophy. Lapatinib is an ErbB1 inhibitor in which previous studies have shown various role of ErbB1 in gastrointestinal development thus required further investigation.

In summary, the work contained in this thesis has shown that:

- lapatinib cytotoxicity is related to the relative expression of *ErbB1* and *ErbB2* mRNA (Chapter 3)
- lapatinib induced late apoptosis in jejunal cells but preferentially induced necrosis in cancer cells (Chapter 3)
- Walker 256 tumour does not affect jejunal and colonic epithelium in rats inoculated with the tumour cells (Chapter 4)
- clinically relevant doses of lapatinib in female rats leads to caspase-3 mediated apoptosis in the colonic epithelium and villus atrophy (not due to caspase 3-dependent apoptosis) in the jejunum (Chapter 5)
- lapatinib inhibition on the intestine might be related to ErbB2 inhibition in the jejunal crypts (Chapter 5)
- lapatinib at clinically relevant doses does not increase electrogenic chloride secretion in the colon T84 monolayer, refuting the hypothesis of ErbB1 induced secretory responses as a mechanism of lapatinib-induced diarrhoea (Chapter 6)
- a link between ErbB1 expression and diarrhoea was not found by these studies. However, there may be downstream or other pathway effects related to diarrhoea (Chapters 5 and 6).

7.3 Future directions

Outcomes from this thesis have identified a number of points that need further clarification to improve our understanding in the mechanisms of lapatinib-induced diarrhoea. Limitations of current work for example lack of robust ErbB expression in a tumour model which could be due to the subcutaneous position of the tumour might be able to be overcome with orthotopic placement of the tumour which could increase expression of ErbB receptors. Orthotopic xenograft model has similar tumour microenvironment as the original tumour and are therefore expected to be more closely resemble the natural tumourigenesis in human. Experiments such as western blot and cell cycle analysis as well as detailed assessment of *ErbB1* and *ErbB2* mRNA expressions in the tumour and intestinal tissues of rats treated with lapatinib would be able to provide better understanding of the mechanisms of cytotoxicity induced by lapatinib.

Although lapatinib has been tested for its bioavailability, predicting lapatinib-induced diarrhoea might be possible with consideration of contributing factors including sex, immune status and age. A pharmacokinetic analysis on the rats' serum should also be a priority when investigating the mechanisms of ErbB1 tyrosine kinase inhibitor-induced diarrhoea in order to have a better understanding on the drug distribution, absorption, metabolism and excretion throughout the animal studies.

ErbB1 knockout mice or an isogenic or improved tumour-bearing model will allow evaluation of interventions for lapatinib-induced diarrhoea in rats that are not immunologically altered, whilst ensuring that there is no tumour protection. Works carried out in mice with genetic knock-out of intestinal *ErbB1* or *ErbB2* would dissect the role each receptor plays individually in lapatinib-induced diarrhoea. Based on the findings obtained from this thesis, interventions that target maintenance of expression of ErbB2 within jejunum may be effective at preventing lapatinib-induced diarrhoea.

7.4 Conclusion

Finally, our investigations managed to describe the minor impact of lapatinib on the gastrointestinal mucosa. Thus, much remains to be learned on the mechanisms related to lapatinib or ErbB1 targeted therapy-induced diarrhoea. Understanding the mechanism of damage will lead to an ability to target prevention or treatment as well as managing targeted therapy-induced diarrhoea appropriately.

References

Abdul Razak, A. R., D. Soulieres, S. A. Laurie, S. J. Hotte, S. Singh, E. Winquist, S. Chia, C. Le Tourneau, P. F. Nguyen-Tan, E. X. Chen, K. K. Chan, T. Wang, N. Giri, C. Mormont, S. Quinn and L. L. Siu (2012). "A phase II trial of dacomitinib, an oral pan-human EGF receptor (HER) inhibitor, as first-line treatment in recurrent and/or metastatic squamous-cell carcinoma of the head and neck." Annals of oncology : official journal of the European Society for Medical Oncology / ESMO.

Ahmad, M. S., A. Wahid, M. Ahmad, N. Mahboob and R. Mehmood (2016). "Prevalence of Electrolyte Disorders Among Cases of Diarrhea with Severe Dehydration and Correlation of Electrolyte Levels with Age of the Patients." Journal of the College of Physicians and Surgeons--Pakistan: JCPSP **26**(5): 394-398.

Al-Dasooqi, N., J. M. Bowen, R. J. Gibson, R. M. Logan, A. M. Stringer and D. M. Keefe (2011). "Selection of housekeeping genes for gene expression studies in a rat model of irinotecan-induced mucositis." Chemotherapy **57**(1): 43-53.

Al-Dasooqi, N., R. J. Gibson, J. M. Bowen, R. M. Logan, A. M. Stringer and D. M. Keefe (2010). "Matrix metalloproteinases are possible mediators for the development of alimentary tract mucositis in the dark agouti rat." Exp Biol Med (Maywood) **235**(10): 1244-1256.

Altman, S. A., L. Randers and G. Rao (1993). "Comparison of trypan blue dye exclusion and fluorometric assays for mammalian cell viability determinations." Biotechnology progress **9**(6): 671-674.

Amit, I., A. Citri, T. Shay, Y. Lu, M. Katz, F. Zhang, G. Tarcic, D. Siwak, J. Lahad, J. Jacob-Hirsch, N. Amariglio, N. Vaisman, E. Segal, G. Rechavi, U. Alon, G. B. Mills, E. Domany and Y. Yarden (2007). "A module of negative feedback regulators defines growth factor signaling." Nat Genet **39**(4): 503-512.

Andrechek, E. R., W. R. Hardy, A. A. Girgis-Gabardo, R. L. Perry, R. Butler, F. L. Graham, R. C. Kahn, M. A. Rudnicki and W. J. Muller (2002). "ErbB2 is required for muscle spindle and myoblast cell survival." Molecular and cellular biology **22**(13): 4714-4722.

Appert-Collin, A., P. Hubert, G. Cremel and A. Bennasroune (2015). "Role of ErbB Receptors in Cancer Cell Migration and Invasion." Front Pharmacol **6**: 283.

Aroldi, F., P. Bertocchi, F. Meriggi, C. Abeni, C. Ogliosi, L. Rota, C. Zambelli, C. Bna and A. Zaniboni (2014). "Tyrosine Kinase Inhibitors in EGFR-Mutated Large-Cell Neuroendocrine Carcinoma of the Lung? A Case Report." Case Rep Oncol **7**(2): 478-483.

Arteaga, C. L. (2003). "ErbB-targeted therapeutic approaches in human cancer." Experimental cell research **284**(1): 122-130.

Asnacios, A., S. Naveau and G. Perlemuter (2009). "Gastrointestinal toxicities of novel agents in cancer therapy." Eur J Cancer **45 Suppl 1**: 332-342.

Avraham, R., A. Sas-Chen, O. Manor, I. Steinfeld, R. Shalgi, G. Tarcic, N. Bossel, A. Zeisel, I. Amit, Y. Zwang, E. Enerly, H. G. Russnes, F. Biagioni, M. Mottolese, S. Strano, G. Blandino, A. L. Borresen-Dale, Y. Pilpel, Z. Yakhini, E. Segal and Y. Yarden (2010). "EGF

decreases the abundance of microRNAs that restrain oncogenic transcription factors." Sci Signal **3**(124): ra43.

Avraham, R. and Y. Yarden (2011). "Feedback regulation of EGFR signalling: decision making by early and delayed loops." Nat Rev Mol Cell Biol **12**(2): 104-117.

Awada, A. H., H. Dumez, A. Hendlisz, P. Wolter, T. Besse-Hammer, M. Uttenreuther-Fischer, P. Stopfer, F. Fleischer, M. Piccart and P. Schoffski (2012). "Phase I study of pulsatile 3-day administration of afatinib (BIBW 2992) in combination with docetaxel in advanced solid tumors." Investigational new drugs.

Awada, A. H., H. Dumez, A. Hendlisz, P. Wolter, T. Besse-Hammer, M. Uttenreuther-Fischer, P. Stopfer, F. Fleischer, M. Piccart and P. Schoffski (2013). "Phase I study of pulsatile 3-day administration of afatinib (BIBW 2992) in combination with docetaxel in advanced solid tumors." Investigational new drugs **31**(3): 734-741.

Bahr, H. I., E. A. Toraih, E. A. Mohammed, H. M. Mohammad, E. A. Ali and S. A. Zaitone (2015). "Chemopreventive effect of leflunomide against Ehrlich's solid tumor grown in mice: Effect on EGF and EGFR expression and tumor proliferation." Life sciences **141**: 193-201.

Baker, D. E. (2006). "Loperamide: a pharmacological review." Reviews in gastroenterological disorders **7**: S11-18.

Barrett, K. E. (1993). "Positive and negative regulation of chloride secretion in T84 cells." Am J Physiol **265**(4 Pt 1): C859-868.

Barrett, K. E. (2000). "New insights into the pathogenesis of intestinal dysfunction: secretory diarrhea and cystic fibrosis." World J Gastroenterol **6**(4): 470-474.

Barrett, K. E. and S. J. Keely (2000). "Chloride secretion by the intestinal epithelium: molecular basis and regulatory aspects." Annu Rev Physiol **62**: 535-572.

Baselga, J. and C. L. Arteaga (2005). "Critical update and emerging trends in epidermal growth factor receptor targeting in cancer." J Clin Oncol **23**(11): 2445-2459.

Baselga, J., D. Rischin, M. Ranson, H. Calvert, E. Raymond, D. G. Kieback, S. B. Kaye, L. Gianni, A. Harris, T. Bjork, S. D. Averbuch, A. Feyereislova, H. Swaisland, F. Rojo and J. Albanell (2002). "Phase I safety, pharmacokinetic, and pharmacodynamic trial of ZD1839, a selective oral epidermal growth factor receptor tyrosine kinase inhibitor, in patients with five selected solid tumor types." J Clin Oncol **20**(21): 4292-4302.

Baselga, J. and S. M. Swain (2009). "Novel anticancer targets: revisiting ERBB2 and discovering ERBB3." Nature Reviews Cancer **9**(7): 463-475.

Batra, S. K., S. Castelino-Prabhu, C. J. Wikstrand, X. Zhu, P. A. Humphrey, H. S. Friedman and D. D. Bigner (1995). "Epidermal growth factor ligand-independent, unregulated, cell-transforming potential of a naturally occurring human mutant EGFRvIII gene." Cell growth & differentiation : the molecular biology journal of the American Association for Cancer Research **6**(10): 1251-1259.

Baulida, J., M. H. Kraus, M. Alimandi, P. P. Di Fiore and G. Carpenter (1996). "All ErbB receptors other than the epidermal growth factor receptor are endocytosis impaired." The Journal of biological chemistry **271**(9): 5251-5257.

Beck, P., J. Wong, Y. Li, S. Swaminathan, R. Xavier, K. Devaney and D. K. Podolsky (2004). "Chemotherapy-and radiotherapy-induced intestinal damage is regulated by intestinal trefoil factor." Gastroenterology **126**(3): 796-808.

Bence, A. K., E. B. Anderson, M. A. Halepota, M. A. Doukas, P. A. DeSimone, G. A. Davis, D. A. Smith, K. M. Koch, A. G. Stead, S. Mangum, C. J. Bowen, N. L. Spector, S. Hsieh and V. R. Adams (2005). "Phase I pharmacokinetic studies evaluating single and multiple doses of oral GW572016, a dual EGFR-ErbB2 inhibitor, in healthy subjects." Invest New Drugs **23**(1): 39-49.

Bennani-Baiti, N. and D. Walsh (2011). "Animal models of the cancer anorexia-cachexia syndrome." Support Care Cancer **19**(9): 1451-1463.

Benson, A. B., 3rd, J. A. Ajani, R. B. Catalano, C. Engelking, S. M. Kornblau, J. A. Martenson, Jr., R. McCallum, E. P. Mitchell, T. M. O'Dorisio, E. E. Vokes and S. Wadler (2004). "Recommended guidelines for the treatment of cancer treatment-induced diarrhea." Journal of clinical oncology : official journal of the American Society of Clinical Oncology **22**(14): 2918-2926.

Berasain, C., E. R. Garcia-Trevijano, J. Castillo, E. Erroba, D. C. Lee, J. Prieto and M. A. Avila (2005). "Amphiregulin: an early trigger of liver regeneration in mice." Gastroenterology **128**(2): 424-432.

Berlanga-Acosta, J., R. Playford, N. Mandir and R. Goodlad (2001). "Gastrointestinal cell proliferation and crypt fission are separate but complementary means of increasing tissue mass following infusion of epidermal growth factor in rats." Gut **48**(6): 803-807.

Bertelsen, L. S., K. E. Barrett and S. J. Keely (2004). "Gs protein-coupled receptor agonists induce transactivation of the epidermal growth factor receptor in T84 cells: implications for epithelial secretory responses." J Biol Chem **279**(8): 6271-6279.

Biesalski, B., B. Yilmaz, H. G. Buchholz, N. Bausbacher, M. Schreckenberger and O. Thews (2012). "An allogenic site-specific rat model of bone metastases for nuclear medicine and experimental oncology." Nucl Med Biol **39**(4): 502-508.

Blick, S. K. and L. J. Scott (2007). "Cetuximab: a review of its use in squamous cell carcinoma of the head and neck and metastatic colorectal cancer." Drugs **67**(17): 2585-2607.

Bowen, J. M. (2014). "Development of the rat model of lapatinib-induced diarrhoea." Scientifica **2014**: 194185.

Bowen, J. M. (2014). "Development of the rat model of lapatinib-induced diarrhoea." Scientifica (Cairo) **2014**: 194185.

Bowen, J. M., R. J. Gibson and D. M. Keefe (2011). "Animal models of mucositis: implications for therapy." J Support Oncol **9**(5): 161-168.

Bowen, J. M., R. J. Gibson, D. M. Keefe and A. G. Cummins (2005). "Cytotoxic chemotherapy upregulates pro-apoptotic Bax and Bak in the small intestine of rats and humans." Pathology **37**(1): 56-62.

Bowen, J. M., B. J. Mayo, E. Plews, E. Bateman, A. M. Stringer, F. M. Boyle, J. W. Finnie and D. M. Keefe (2012). "Development of a rat model of oral small molecule receptor tyrosine kinase inhibitor-induced diarrhea." Cancer Biol Ther **13**(13): 1269-1275.

Bowen, J. M., B. J. Mayo, E. Plews, E. Bateman, A. Wignall, A. M. Stringer, F. M. Boyle and D. M. Keefe (2014). "Determining the mechanisms of lapatinib-induced diarrhoea using a rat model." Cancer Chemother Pharmacol **74**(3): 617-627.

Braun, M. M., C. H. Barstow and N. J. Pyzocha (2015). "Diagnosis and management of sodium disorders: hyponatremia and hypernatremia." Am. Fam. Physician **91**: 299-307.

Breen, C. M., P. J. Mannon and B. A. Benjamin (1998). "Peptide YY inhibits vasopressin-stimulated chloride secretion in inner medullary collecting duct cells." Am J Physiol **275**(3 Pt 2): F452-457.

Burkitt, H. G., B. Young and J. W. Heath (1993). Wheater's Functional Histology: A Text and Colour Atlas. Edinburgh, UK, Churchill Livingstone.

Burris, H. A., 3rd, H. I. Hurwitz, E. C. Dees, A. Dowlati, K. L. Blackwell, B. O'Neil, P. K. Marcom, M. J. Ellis, B. Overmoyer, S. F. Jones, J. L. Harris, D. A. Smith, K. M. Koch, A. Stead, S. Mangum and N. L. Spector (2005). "Phase I safety, pharmacokinetics, and clinical activity study of lapatinib (GW572016), a reversible dual inhibitor of epidermal growth factor

receptor tyrosine kinases, in heavily pretreated patients with metastatic carcinomas." J Clin Oncol **23**(23): 5305-5313.

Burris, H. A., 3rd, C. W. Taylor, S. F. Jones, K. M. Koch, M. J. Versola, N. Arya, R. A. Fleming, D. A. Smith, L. Pandite, N. Spector and G. Wilding (2009). "A phase I and pharmacokinetic study of oral lapatinib administered once or twice daily in patients with solid malignancies." Clinical cancer research : an official journal of the American Association for Cancer Research **15**(21): 6702-6708.

Calvo, E. and E. K. Rowinsky (2005). "Clinical experience with monoclonal antibodies to epidermal growth factor receptor." Current oncology reports **7**(2): 96-103.

Carpenter, C. D., H. A. Ingraham, C. Cochet, G. M. Walton, C. S. Lazar, J. M. Sowadski, M. G. Rosenfeld and G. N. Gill (1991). "Structural analysis of the transmembrane domain of the epidermal growth factor receptor." J Biol Chem **266**(9): 5750-5755.

Carpenter, G. (1987). "Receptors for epidermal growth factor and other polypeptide mitogens." Annual review of biochemistry **56**: 881-914.

Carpenter, G. (2000). "The EGF receptor: a nexus for trafficking and signaling." BioEssays : news and reviews in molecular, cellular and developmental biology **22**(8): 697-707.

Carpenter, G. and S. Cohen (1990). "Epidermal growth factor." The Journal of biological chemistry **265**(14): 7709-7712.

Cavalcanti, T. C., C. C. Gregorini, F. Guimaraes, O. Rettori and A. N. Vieira-Matos (2003). "Changes in red blood cell osmotic fragility induced by total plasma and plasma fractions obtained from rats bearing progressive and regressive variants of the Walker 256 tumor." Braz J Med Biol Res **36**(7): 887-895.

Chailler, P. and D. Menard (1999). "Ontogeny of EGF receptors in the human gut." Frontiers in bioscience : a journal and virtual library **4**: D87-101.

Chen, C., Y.-H. Zhu and J.-A. Huang (2016). "Clinical evaluation of potential usefulness of serum lactate dehydrogenase level in follow-up of small cell lung cancer."

Cherny, N. I. (2008). "Evaluation and management of treatment-related diarrhea in patients with advanced cancer: a review." Journal of pain and symptom management **36**(4): 413-423.

Chien, A. J., P. N. Munster, M. E. Melisko, H. S. Rugo, J. W. Park, A. Goga, G. Auerback, E. Khanafshar, K. Ordovas and K. M. Koch (2014). "Phase I Dose-Escalation Study of 5-Day Intermittent Oral Lapatinib Therapy in Patients With Human Epidermal Growth Factor Receptor 2–Overexpressing Breast Cancer." Journal of Clinical Oncology **32**(14): 1472-1479.

Chow, J. Y., K. Carlstrom and K. E. Barrett (2003). "Growth hormone reduces chloride secretion in human colonic epithelial cells via EGF receptor and extracellular regulated kinase." Gastroenterology **125**(4): 1114-1124.

Chow, J. Y., J. M. Uribe and K. E. Barrett (2000). "A role for protein kinase cepsilon in the inhibitory effect of epidermal growth factor on calcium-stimulated chloride secretion in human colonic epithelial cells." J Biol Chem **275**(28): 21169-21176.

Christofi, F. L., J. Wunderlich, J. G. Yu, Y. Z. Wang, J. Xue, J. Guzman, N. Javed and H. Cooke (2004). "Mechanically evoked reflex electrogenic chloride secretion in rat distal colon is triggered by endogenous nucleotides acting at P2Y1, P2Y2, and P2Y4 receptors." J Comp Neurol **469**(1): 16-36.

Chu, I., K. Blackwell, S. Chen and J. Slingerland (2005). "The dual ErbB1/ErbB2 inhibitor, lapatinib (GW572016), cooperates with tamoxifen to inhibit both cell proliferation- and estrogen-dependent gene expression in antiestrogen-resistant breast cancer." Cancer research **65**(1): 18-25.

Ciuleanu, T., L. Stelmakh, S. Cicenas, S. Miliauskas, A. C. Grigorescu, C. Hillenbach, H. K. Johannsdottir, B. Klughammer and E. E. Gonzalez (2012). "Efficacy and safety of erlotinib versus chemotherapy in second-line treatment of patients with advanced, non-small-cell lung cancer with poor prognosis (TITAN): a randomised multicentre, open-label, phase 3 study." Lancet Oncol **13**(3): 300-308.

Clarke, L. L. (2009). "A guide to Ussing chamber studies of mouse intestine." American Journal of Physiology-Gastrointestinal and Liver Physiology **296**(6): G1151-G1166.

Clarke, L. L. (2009). "A guide to Ussing chamber studies of mouse intestine." Am J Physiol Gastrointest Liver Physiol **296**(6): G1151-1166.

Cohen, M. H., H. Chen, S. Shord, C. Fuchs, K. He, H. Zhao, S. Sickafuse, P. Keegan and R. Pazdur (2013). "Approval summary: Cetuximab in combination with cisplatin or carboplatin and 5-fluorouracil for the first-line treatment of patients with recurrent locoregional or metastatic squamous cell head and neck cancer." Oncologist **18**(4): 460-466.

Cohen, M. H., J. R. Johnson, Y. F. Chen, R. Sridhara and R. Pazdur (2005). "FDA drug approval summary: erlotinib (Tarceva) tablets." The oncologist **10**(7): 461-466.

Cohen, M. H., G. A. Williams, R. Sridhara, G. Chen and R. Pazdur (2003). "FDA drug approval summary: gefitinib (ZD1839) (Iressa) tablets." The oncologist **8**(4): 303-306.

Cohen, S. and G. A. Elliott (1963). "The stimulation of epidermal keratinization by a protein isolated from the submaxillary gland of the mouse." The Journal of investigative dermatology **40**: 1-5.

Collin de L'hortet, A., H. Gilgenkrantz and J. E. Guidotti (2012). "EGFR: A Master Piece in G1/S Phase Transition of Liver Regeneration." International journal of hepatology **2012**: 476910.

Crown, J. P., H. A. Burris, 3rd, F. Boyle, S. Jones, M. Koehler, B. O. Newstat, R. Parikh, C. Oliva, A. Preston, J. Byrne and S. Chan (2008). "Pooled analysis of diarrhea events in patients with cancer treated with lapatinib." Breast Cancer Res Treat **112**(2): 317-325.

Cummins, C. L., C. Y. Wu and L. Z. Benet (2002). "Sex-related differences in the clearance of cytochrome P450 3A4 substrates may be caused by P-glycoprotein." Clin Pharmacol Ther **72**(5): 474-489.

Cusatis, G., V. Gregorc, J. Li, A. Spreafico, R. G. Ingersoll, J. Verweij, V. Ludovini, E. Villa, M. Hidalgo, A. Sparreboom and S. D. Baker (2006). "Pharmacogenetics of ABCG2 and adverse reactions to gefitinib." J Natl Cancer Inst **98**(23): 1739-1742.

Dahlhoff, M., M. Schafer, E. Wolf and M. R. Schneider (2012). "Genetic deletion of the EGFR ligand epigen does not affect mouse embryonic development and tissue homeostasis." Exp Cell Res.

Dai, C.-l., A. K. Tiwari, C.-P. Wu, X.-d. Su, S.-R. Wang, D.-g. Liu, C. R. Ashby, Y. Huang, R. W. Robey and Y.-j. Liang (2008). "Lapatinib (Tykerb, GW572016) reverses multidrug resistance in cancer cells by inhibiting the activity of ATP-binding cassette subfamily B member 1 and G member 2." Cancer research **68**(19): 7905-7914.

de Lima, T. M., M. M. Lima, D. C. Almeida, J. R. Mendonca and R. Curi (2005). "Cachexia induced by Walker 256 tumor growth causes rat lymphocyte death." Cancer Immunol Immunother **54**(2): 179-186.

Deachapunya, C. and S. Poonyachoti (2013). "Activation of chloride secretion by isoflavone genistein in endometrial epithelial cells." Cellular Physiology and Biochemistry **32**(5): 1473-1486.

DeHaan, A. M., N. M. Wolters, E. T. Keller and K. M. Ignatoski (2009). "EGFR ligand switch in late stage prostate cancer contributes to changes in cell signaling and bone remodeling." The Prostate **69**(5): 528-537.

Dharmsathaphorn, K., J. A. McRoberts, K. G. Mandel, L. D. Tisdale and H. Masui (1984). "A human colonic tumor cell line that maintains vectorial electrolyte transport." Am J Physiol **246**(2 Pt 1): G204-208.

Dharmsathaphorn, K. and S. J. Pandol (1986). "Mechanism of chloride secretion induced by carbachol in a colonic epithelial cell line." J Clin Invest **77**(2): 348-354.

Dhillon, S. and A. J. Wagstaff (2007). "Lapatinib." Drugs **67**(14): 2101-2108; discussion 2109-2110.

Di Leo, A., H. L. Gomez, Z. Aziz, Z. Zvirbule, J. Bines, M. C. Arbushites, S. F. Guerrera, M. Koehler, C. Oliva and S. H. Stein (2008). "Phase III, double-blind, randomized study comparing lapatinib plus paclitaxel with placebo plus paclitaxel as first-line treatment for metastatic breast cancer." Journal of Clinical Oncology **26**(34): 5544-5552.

Di Leo, A., H. L. Gomez, Z. Aziz, Z. Zvirbule, J. Bines, M. C. Arbushites, S. F. Guerrera, M. Koehler, C. Oliva, S. H. Stein, L. S. Williams, J. Dering, R. S. Finn and M. F. Press (2008). "Phase III, double-blind, randomized study comparing lapatinib plus paclitaxel with placebo plus paclitaxel as first-line treatment for metastatic breast cancer." J Clin Oncol **26**(34): 5544-5552.

Diaz, R., P. A. Nguewa, R. Parrondo, C. Perez-Stable, I. Manrique, M. Redrado, R. Catena, M. Collantes, I. Peñuelas and J. A. Díaz-González (2010). "Antitumor and antiangiogenic effect of the dual EGFR and HER-2 tyrosine kinase inhibitor lapatinib in a lung cancer model." BMC cancer **10**(1): 188.

Diczfalusy, U., J. Miura, H. K. Roh, R. A. Mirghani, J. Sayi, H. Larsson, K. G. Bodin, A. Allqvist, M. Jande, J. W. Kim, E. Aklillu, L. L. Gustafsson and L. Bertilsson (2008). "4Beta-hydroxycholesterol is a new endogenous CYP3A marker: relationship to CYP3A5 genotype,

quinine 3-hydroxylation and sex in Koreans, Swedes and Tanzanians." Pharmacogenet Genomics **18**(3): 201-208.

Dienstmann, R. and E. Felip (2011). "Necitumumab in the treatment of advanced non-small cell lung cancer: translation from preclinical to clinical development." Expert Opin Biol Ther **11**(9): 1223-1231.

DiGiulio, S. (2015). "FDA Approves New Targeted Drug Tagrisso (Osimertinib) for NSCLC." Oncology Times.

DiGiulio, S. (2015). "FDA Grants Priority Review to Rociletinib for NSCLC." Oncology Times.

Dignass, A. U. and D. K. Podolsky (1993). "Cytokine modulation of intestinal epithelial cell restitution: central role of transforming growth factor beta." Gastroenterology **105**(5): 1323-1332.

Doi, T., H. Takiuchi, A. Ohtsu, N. Fuse, M. Goto, M. Yoshida, N. Dote, Y. Kuze, F. Jinno, M. Fujimoto, T. Takubo, N. Nakayama and R. Tsutsumi (2012). "Phase I first-in-human study of TAK-285, a novel investigational dual HER2/EGFR inhibitor, in cancer patients." British journal of cancer **106**(4): 666-672.

Donowitz, M., J. L. Montgomery, M. S. Walker and M. E. Cohen (1994). "Brush-border tyrosine phosphorylation stimulates ileal neutral NaCl absorption and brush-border Na(+)-H+ exchange." The American journal of physiology **266**(4 Pt 1): G647-656.

Dorak, M. T. and E. Karpuzoglu (2012). "Gender differences in cancer susceptibility: an inadequately addressed issue." Front Genet **3**: 268.

Dungo, R. T. and G. M. Keating (2013). "Afatinib: first global approval." Drugs **73**(13): 1503-1515.

Durani, U., P. K. Tosh, J. N. Barreto, L. L. Estes, P. J. Jannetto and A. J. Tande (2015). "Retrospective comparison of posaconazole levels in patients taking the delayed-release tablet versus the oral suspension." Antimicrobial agents and chemotherapy **59**(8): 4914-4918.

Dvorak, B., M. D. Halpern, H. Holubec, C. S. Williams, D. L. McWilliam, J. A. Dominguez, R. Stepankova, C. M. Payne and R. S. McCuskey (2002). "Epidermal growth factor reduces the development of necrotizing enterocolitis in a neonatal rat model." American journal of physiology. Gastrointestinal and liver physiology **282**(1): G156-164.

Dvorak, B., L. Khailova, J. A. Clark, D. M. Hosseini, K. M. Arganbright, C. A. Reynolds and M. D. Halpern (2008). "Comparison of epidermal growth factor and heparin-binding epidermal growth factor-like growth factor for prevention of experimental necrotizing enterocolitis." Journal of pediatric gastroenterology and nutrition **47**(1): 11-18.

Eichelbaum, M. and O. Burk (2001). "CYP3A genetics in drug metabolism." Nat Med **7**(3): 285-287.

Elmore, S. (2007). "Apoptosis: a review of programmed cell death." Toxicol Pathol **35**(4): 495-516.

EMEA, E. M. A. (2008). Evaluation of Medicines for Human Use: Assessment report for Tyverb. Assessment report for Tyverb International Proprietary Name: Lapatinib. EMEA/CHMP. London, UK. **EMEA/H/C/795:** 1-58.

Erlichman, C., M. Hidalgo, J. P. Boni, P. Martins, S. E. Quinn, C. Zacharchuk, P. Amorusi, A. A. Adjei and E. K. Rowinsky (2006). "Phase I study of EKB-569, an irreversible inhibitor of the epidermal growth factor receptor, in patients with advanced solid tumors." Journal of clinical oncology : official journal of the American Society of Clinical Oncology **24**(15): 2252-2260.

Ethier, S. P. (2002). "Signal transduction pathways: the molecular basis for targeted therapies." Seminars in radiation oncology **12**(3 Suppl 2): 3-10.

Fasano, A. and T. Shea-Donohue (2005). "Mechanisms of disease: the role of intestinal barrier function in the pathogenesis of gastrointestinal autoimmune diseases." Nature clinical practice Gastroenterology & hepatology **2**(9): 416-422.

Fernando Guimarães, F., Schanoski, A.S., Cavalcanti, T.C.S., Juliano, P.B., Viera-Matos, A.N. and Rettori, O. (2010). "Tumor Growth Characteristics of the Walker 256 AR Tumor, a Regressive Variant of the Rat Walker 256 A tumor." BRAZILIAN ARCHIVES OF BIOLOGY AND TECHNOLOGY **Vol.53** (n. 5): pp. 1101-1108.

Field, M. (2003). "Intestinal ion transport and the pathophysiology of diarrhea." J Clin Invest **111**(7): 931-943.

Finnberg, N. K., P. Gokare, A. Navaraj, K. A. Lang Kuhs, G. Cerniglia, H. Yagita, K. Takeda, N. Motoyama and W. S. El-Deiry (2016). "Agonists of the TRAIL Death Receptor DR5 Sensitize Intestinal Stem Cells to Chemotherapy-Induced Cell Death and Trigger Gastrointestinal Toxicity." Cancer Res **76**(3): 700-712.

Fiske, W. H., D. Threadgill and R. J. Coffey (2009). "ERBBs in the gastrointestinal tract: recent progress and new perspectives." Experimental cell research **315**(4): 583-601.

Forsythe, R. M., D. Z. Xu, Q. Lu and E. A. Deitch (2002). "Lipopolysaccharide-induced enterocyte-derived nitric oxide induces intestinal monolayer permeability in an autocrine fashion." Shock **17**(3): 180-184.

Frederick, L., X. Y. Wang, G. Eley and C. D. James (2000). "Diversity and frequency of epidermal growth factor receptor mutations in human glioblastomas." Cancer Res **60**(5): 1383-1387.

Fujimoto-Ouchi, K., F. Sekiguchi, H. Yasuno, Y. Moriya, K. Mori and Y. Tanaka (2007). "Antitumor activity of trastuzumab in combination with chemotherapy in human gastric cancer xenograft models." Cancer chemotherapy and pharmacology **59**(6): 795-805.

Fukuoka, M., S. Yano, G. Giaccone, T. Tamura, K. Nakagawa, J. Y. Douillard, Y. Nishiwaki, J. Vansteenkiste, S. Kudoh, D. Rischin, R. Eek, T. Horai, K. Noda, I. Takata, E. Smit, S. Averbuch, A. Macleod, A. Feyereislova, R. P. Dong and J. Baselga (2003). "Multi-institutional randomized phase II trial of gefitinib for previously treated patients with advanced non-small-cell lung cancer (The IDEAL 1 Trial) [corrected]." J Clin Oncol **21**(12): 2237-2246.

Garcia de Palazzo, I. E., G. P. Adams, P. Sundareshan, A. J. Wong, J. R. Testa, D. D. Bigner and L. M. Weiner (1993). "Expression of mutated epidermal growth factor receptor by non-small cell lung carcinomas." Cancer Res **53**(14): 3217-3220.

Genton, L., P. D. Cani and J. Schrenzel (2015). "Alterations of gut barrier and gut microbiota in food restriction, food deprivation and protein-energy wasting." Clinical Nutrition **34**(3): 341-349.

Geyer, C. E., J. Forster, D. Lindquist, S. Chan, C. G. Romieu, T. Pienkowski, A. Jagiello-Gruszfeld, J. Crown, A. Chan, B. Kaufman, D. Skarlos, M. Campone, N. Davidson, M. Berger, C. Oliva, S. D. Rubin, S. Stein and D. Cameron (2006). "Lapatinib plus capecitabine for HER2-positive advanced breast cancer." N Engl J Med **355**(26): 2733-2743.

Ghizdavat, A., G. Raduly, Z. Pap, L. Denes and Z. Pavai (2015). "Comparative study of HER2, EGFR, p53 and PTEN expression in the human gastrointestinal tract during fetal period." Romanian journal of morphology and embryology= Revue roumaine de morphologie et embryologie **56**(2): 475.

Gibson, G. (2011). "Conference scene: biomarkers in the next decade." Pharmacogenomics **12**(2): 155-157.

Gibson, R. J., J. M. Bowen, A. G. Cummins and D. M. Keefe (2005). "Relationship between dose of methotrexate, apoptosis, p53/p21 expression and intestinal crypt proliferation in the rat." Clin Exp Med **4**(4): 188-195.

Gibson, R. J., J. M. Bowen, M. R. Inglis, A. G. Cummins and D. M. Keefe (2003). "Irinotecan causes severe small intestinal damage, as well as colonic damage, in the rat with implanted breast cancer." J Gastroenterol Hepatol **18**(9): 1095-1100.

Gibson, R. J., J. M. Bowen and D. M. Keefe (2005). "Palifermin reduces diarrhea and increases survival following irinotecan treatment in tumor-bearing DA rats." International journal of cancer. Journal international du cancer **116**(3): 464-470.

Gibson, R. J. and D. M. Keefe (2006). "Cancer chemotherapy-induced diarrhoea and constipation: mechanisms of damage and prevention strategies." Support Care Cancer **14**(9): 890-900.

Gibson, R. J., D. M. Keefe, F. M. Thompson, J. M. Clarke, G. J. Goland and A. G. Cummins (2002). "Effect of interleukin-11 on ameliorating intestinal damage after methotrexate treatment of breast cancer in rats." Dig Dis Sci **47**(12): 2751-2757.

Gibson, R. J., A. M. Stringer, J. M. Bowen, R. M. Logan, A. S. Yeoh, J. Burns, E. Alvarez and D. M. Keefe (2007). "Velafermin improves gastrointestinal mucositis following irinotecan treatment in tumor-bearing DA rats." Cancer Biol Ther **6**(4): 541-547.

Giusti, R. M., K. A. Shastri, M. H. Cohen, P. Keegan and R. Pazdur (2007). "FDA drug approval summary: panitumumab (Vectibix)." The oncologist **12**(5): 577-583.

Goldstein, N. I., M. Prewett, K. Zuklys, P. Rockwell and J. Mendelsohn (1995). "Biological efficacy of a chimeric antibody to the epidermal growth factor receptor in a human tumor

xenograft model." Clinical cancer research : an official journal of the American Association for Cancer Research **1**(11): 1311-1318.

Gomez, H. L., D. C. Doval, M. A. Chavez, P. C. Ang, Z. Aziz, S. Nag, C. Ng, S. X. Franco, L. W. Chow, M. C. Arbushites, M. A. Casey, M. S. Berger, S. H. Stein and G. W. Sledge (2008). "Efficacy and safety of lapatinib as first-line therapy for ErbB2-amplified locally advanced or metastatic breast cancer." J Clin Oncol **26**(18): 2999-3005.

Gornstein, E. and T. L. Schwarz (2014). "The paradox of paclitaxel neurotoxicity: Mechanisms and unanswered questions." Neuropharmacology **76 Pt A**: 175-183.

Graus-Porta, D., R. R. Beerli, J. M. Daly and N. E. Hynes (1997). "ErbB-2, the preferred heterodimerization partner of all ErbB receptors, is a mediator of lateral signaling." EMBO J **16**(7): 1647-1655.

Gregory, C. D. and A. Devitt (2004). "The macrophage and the apoptotic cell: an innate immune interaction viewed simplistically?" Immunology **113**(1): 1-14.

Hanna, N., R. Lilenbaum, R. Ansari, T. Lynch, R. Govindan, P. A. Janne and P. Bonomi (2006). "Phase II trial of cetuximab in patients with previously treated non-small-cell lung cancer." J Clin Oncol **24**(33): 5253-5258.

Harandi, A., A. S. Zaidi, A. M. Stocker and D. A. Laber (2009). "Clinical efficacy and toxicity of anti-EGFR therapy in common cancers." Journal of oncology **2009**.

Hare, K. J., B. Hartmann, H. Kissow, J. J. Holst and S. S. Poulsen (2007). "The intestinotrophic peptide, glp-2, counteracts intestinal atrophy in mice induced by the epidermal growth factor receptor inhibitor, gefitinib." Clin Cancer Res **13**(17): 5170-5175.

Hartmann, J. T., C. Kollmannsberger, I. Cascorbi, F. Mayer, M. M. Schittenhelm, S. Heeger and C. Bokemeyer (2013). "A phase I pharmacokinetic study of matuzumab in combination with paclitaxel in patients with EGFR-expressing advanced non-small cell lung cancer." Invest New Drugs **31**(3): 661-668.

He, Y. C., J. W. Chen, J. Cao, D. Y. Pan and J. G. Qiao (2003). "Toxicities and therapeutic effect of 5-fluorouracil controlled release implant on tumor-bearing rats." World J Gastroenterol **9**(8): 1795-1798.

Health, U. D. o. and H. Services (2009). "Common terminology criteria for adverse events (CTCAE) version 4.0." National Cancer Institute(09-5410).

Hedhli, N. and K. S. Russell (2011). "Cardiotoxicity of molecularly targeted agents." Current cardiology reviews **7**(4): 221-233.

Hegde, P. S., D. Rusnak, M. Bertiaux, K. Alligood, J. Strum, R. Gagnon and T. M. Gilmer (2007). "Delineation of molecular mechanisms of sensitivity to lapatinib in breast cancer cell lines using global gene expression profiles." Molecular cancer therapeutics **6**(5): 1629-1640.

Heitzmann, D. and R. Warth (2008). "Physiology and pathophysiology of potassium channels in gastrointestinal epithelia." Physiol Rev **88**(3): 1119-1182.

Herbst, R. S. and C. J. Langer (2002). "Epidermal growth factor receptors as a target for cancer treatment: the emerging role of IMC-C225 in the treatment of lung and head and neck cancers." Seminars in oncology **29**(1 Suppl 4): 27-36.

Herbst, R. S. and D. M. Shin (2002). "Monoclonal antibodies to target epidermal growth factor receptor-positive tumors: a new paradigm for cancer therapy." Cancer **94**(5): 1593-1611.

Heymach, J. V., M. Nilsson, G. Blumenschein, V. Papadimitrakopoulou and R. Herbst (2006). "Epidermal growth factor receptor inhibitors in development for the treatment of non-small cell lung cancer." Clinical cancer research : an official journal of the American Association for Cancer Research **12**(14 Pt 2): 4441s-4445s.

Hidalgo, M., L. L. Siu, J. Nemunaitis, J. Rizzo, L. A. Hammond, C. Takimoto, S. G. Eckhardt, A. Tolcher, C. D. Britten, L. Denis, K. Ferrante, D. D. Von Hoff, S. Silberman and E. K. Rowinsky (2001). "Phase I and pharmacologic study of OSI-774, an epidermal growth factor receptor tyrosine kinase inhibitor, in patients with advanced solid malignancies." J Clin Oncol **19**(13): 3267-3279.

Hirsh, V., N. Blais, R. Burkes, S. Verma and K. Croitoru (2014). "Management of diarrhea induced by epidermal growth factor receptor tyrosine kinase inhibitors." Current Oncology **21**(6): 329-336.

Hobbs, S. S., J. A. Goettel, D. Liang, F. Yan, K. L. Edelblum, M. R. Frey, M. T. Mullane and D. B. Polk "TNF transactivation of EGFR stimulates cytoprotective COX-2 expression in gastrointestinal epithelial cells." Am J Physiol Gastrointest Liver Physiol **301**(2): G220-229.

Hoda, M. R., M. Scharl, S. J. Keely, D. F. McCole and K. E. Barrett (2010). "Apical leptin induces chloride secretion by intestinal epithelial cells and in a rat model of acute chemotherapy-induced colitis." Am J Physiol Gastrointest Liver Physiol **298**(5): G714-721.

Holbro, T. and N. E. Hynes (2004). "ErbB receptors: directing key signaling networks throughout life." Annual review of pharmacology and toxicology **44**: 195-217.

Hood, J. D. and D. A. Cheresh (2002). "Role of integrins in cell invasion and migration." Nature Reviews Cancer **2**(2): 91-100.

Hoskin, D. W., J. S. Mader, S. J. Furlong, D. M. Conrad and J. Blay (2008). "Inhibition of T cell and natural killer cell function by adenosine and its contribution to immune evasion by tumor cells (Review)." International journal of oncology **32**(3): 527-535.

Hsu, J. M., C. T. Chen, C. K. Chou, H. P. Kuo, L. Y. Li, C. Y. Lin, H. J. Lee, Y. N. Wang, M. Liu, H. W. Liao, B. Shi, C. C. Lai, M. T. Bedford, C. H. Tsai and M. C. Hung (2011). "Crosstalk between Arg 1175 methylation and Tyr 1173 phosphorylation negatively modulates EGFR-mediated ERK activation." Nature cell biology **13**(2): 174-181.

Hu, X., B. Han, A. Gu, Y. Zhang, S. C. Jiao, C. L. Wang, J. He, X. Jia, L. Zhang, J. Peng, M. Wu, K. Ying, J. Wang, K. Ma, S. Zhang, C. You, F. Tan, Y. Wang, L. Ding and Y. Sun (2014). "A single-arm, multicenter, safety-monitoring, phase IV study of icotinib in treating advanced non-small cell lung cancer (NSCLC)." Lung Cancer.

Huang, C., C. C. Park, S. G. Hilsenbeck, R. Ward, M. F. Rimawi, Y. C. Wang, J. Shou, M. J. Bissell, C. K. Osborne and R. Schiff (2011). "beta1 integrin mediates an alternative survival

pathway in breast cancer cells resistant to lapatinib." Breast cancer research : BCR **13**(4): R84.

Huang, F. S., C. J. Kemp, J. L. Williams, C. R. Erwin and B. W. Warner (2002). "Role of epidermal growth factor and its receptor in chemotherapy-induced intestinal injury." American Journal of Physiology-Gastrointestinal and Liver Physiology **282**(3): G432-G442.

Huang, S., E. A. Armstrong, S. Benavente, P. Chinnaiyan and P. M. Harari (2004). "Dual-agent molecular targeting of the epidermal growth factor receptor (EGFR): combining anti-EGFR antibody with tyrosine kinase inhibitor." Cancer Res **64**(15): 5355-5362.

Huang, S. M. and P. M. Harari (1999). "Epidermal growth factor receptor inhibition in cancer therapy: biology, rationale and preliminary clinical results." Investigational new drugs **17**(3): 259-269.

Hulst, L. K., J. C. Fleishaker, G. R. Peters, J. D. Harry, D. M. Wright and P. Ward (1994). "Effect of age and gender on tirilazad pharmacokinetics in humans." Clin Pharmacol Ther **55**(4): 378-384.

Ichikawa, T., H. Endoh, K. Hotta and K. Ishihara (2000). "The mucin biosynthesis stimulated by epidermal growth factor occurs in surface mucus cells, but not in gland mucus cells, of rat stomach." Life sciences **67**(9): 1095-1101.

Inatomi, O., A. Andoh, Y. Yagi, S. Bamba, T. Tsujikawa and Y. Fujiyama (2006). "Regulation of amphiregulin and epiregulin expression in human colonic subepithelial myofibroblasts." International journal of molecular medicine **18**(3): 497-503.

Ishikawa, S., G. Cepinskas, R. D. Specian, M. Itoh and P. R. Kvietys (1994). "Epidermal growth factor attenuates jejunal mucosal injury induced by oleic acid: role of mucus." The American journal of physiology **267**(6 Pt 1): G1067-1077.

Iwahara A, T. T., Takagi S, Kamiguchi H, Yusa T, Ohta Y (2008). "*In vivo* antitumor efficacy of TAK-285, a novel ErbB1/ErbB2 dual kinase inhibitor." Eur J Cancer **6**(99): Abstract 311.

Jackson-Fisher, A. J., G. Bellinger, R. Ramabhadran, J. K. Morris, K.-F. Lee and D. F. Stern (2004). "ErbB2 is required for ductal morphogenesis of the mammary gland." Proceedings of the National Academy of Sciences of the United States of America **101**(49): 17138-17143.

Jaganjac, M., M. Poljak-Blazi, I. Kirac, S. Borovic, R. Joerg Schaur and N. Zarkovic (2010). "Granulocytes as effective anticancer agent in experimental solid tumor models." Immunobiology **215**(12): 1015-1020.

Jaganjac, M., M. Poljak-Blazi, K. Zarkovic, R. J. Schaur and N. Zarkovic (2008). "The involvement of granulocytes in spontaneous regression of Walker 256 carcinoma." Cancer Lett **260**(1-2): 180-186.

Jagiello-Gruszfeld, A., S. Tjulandin, N. Dobrovolskaya, A. Manikhas, T. Pienkowski, M. DeSilvio, M. Ridderheim and R. Abbey (2010). "A single-arm phase II trial of first-line paclitaxel in combination with lapatinib in HER2-overexpressing metastatic breast cancer." Oncology **79**(1-2): 129-135.

Jankowitz, R. C., J. Abraham, A. R. Tan, S. A. Limentani, M. B. Tierno, L. M. Adamson, M. Buyse, N. Wolmark and S. A. Jacobs (2013). "Safety and efficacy of neratinib in combination

with weekly paclitaxel and trastuzumab in women with metastatic HER2positive breast cancer: an NSABP Foundation Research Program phase I study." Cancer chemotherapy and pharmacology **72**(6): 1205-1212.

Jensen, G. and J. Muntzing (1970). "Differences in the growth of the Walker carcinoma in Sprague-Dawley and Wistar rats." Z Krebsforsch **74**(1): 55-58.

Johnson, J. R., M. Cohen, R. Sridhara, Y. F. Chen, G. M. Williams, J. Duan, J. Gobburu, B. Booth, K. Benson, J. Leighton, L. S. Hsieh, N. Chidambaram, P. Zimmerman and R. Pazdur (2005). "Approval summary for erlotinib for treatment of patients with locally advanced or metastatic non-small cell lung cancer after failure of at least one prior chemotherapy regimen." Clin Cancer Res **11**(18): 6414-6421.

Johnston, S., M. Trudeau, B. Kaufman, H. Boussen, K. Blackwell, P. LoRusso, D. P. Lombardi, S. Ben Ahmed, D. L. Citrin, M. L. DeSilvio, J. Harris, R. E. Westlund, V. Salazar, T. Z. Zaks and N. L. Spector (2008). "Phase II study of predictive biomarker profiles for response targeting human epidermal growth factor receptor 2 (HER-2) in advanced inflammatory breast cancer with lapatinib monotherapy." Journal of clinical oncology : official journal of the American Society of Clinical Oncology **26**(7): 1066-1072.

Johnston, S. R. and A. Leary (2006). "Lapatinib: a novel EGFR/HER2 tyrosine kinase inhibitor for cancer." Drugs Today (Barc) **42**(7): 441-453.

Jones, D. E., Jr., R. Tran-Patterson, D. M. Cui, D. Davin, K. P. Estell and D. M. Miller (1995). "Epidermal growth factor secreted from the salivary gland is necessary for liver regeneration." The American journal of physiology **268**(5 Pt 1): G872-878.

Jones, S., J. Erban, B. Overmoyer, G. Budd, L. Hutchins, E. Lower, L. Laufman, S. Sundaram, W. Urba and K. Pritchard (2005). "Randomized phase III study of docetaxel compared with paclitaxel in metastatic breast cancer." Journal of Clinical Oncology **23**(24): 5542-5551.

Jorissen, R. N., F. Walker, N. Pouliot, T. P. Garrett, C. W. Ward and A. W. Burgess (2003). "Epidermal growth factor receptor: mechanisms of activation and signalling." Experimental cell research **284**(1): 31-53.

Jost, M., C. Kari and U. Rodeck (2000). "The EGF receptor - an essential regulator of multiple epidermal functions." European journal of dermatology : EJD **10**(7): 505-510.

Jung, S., C. Li, J. Duan, S. Lee, K. Kim, Y. Park, Y. Yang, K. I. Kim, J. S. Lim, C. I. Cheon, Y. S. Kang and M. S. Lee (2015). "TRIP-Br1 oncoprotein inhibits autophagy, apoptosis, and necroptosis under nutrient/serum-deprived condition." Oncotarget **6**(30): 29060-29075.

Kamath, S. and J. K. Buolamwini (2006). "Targeting EGFR and HER-2 receptor tyrosine kinases for cancer drug discovery and development." Medicinal research reviews **26**(5): 569-594.

Kapitanovic, S., S. Radosevic, M. Kapitanovic, S. Andelinovic, Z. Ferencic, M. Tavassoli, D. Primorac, Z. Sonicki, S. Spaventi, K. Pavelic and R. Spaventi (1997). "The expression of p185(HER-2/neu) correlates with the stage of disease and survival in colorectal cancer." Gastroenterology **112**(4): 1103-1113.

Karshovska, E., C. Weber and P. von Hundelshausen (2013). "Platelet chemokines in health and disease." Thromb Haemost **110**(5): 894-902.

Karunagaran, D., E. Tzahar, R. R. Beerli, X. Chen, D. Graus-Porta, B. J. Ratzkin, R. Seger, N. E. Hynes and Y. Yarden (1996). "ErbB-2 is a common auxiliary subunit of NDF and EGF receptors: implications for breast cancer." EMBO J **15**(2): 254-264.

Kaufman, B., M. Trudeau, A. Awada, K. Blackwell, T. Bachelot, V. Salazar, M. DeSilvio, R. Westlund, T. Zaks, N. Spector and S. Johnston (2009). "Lapatinib monotherapy in patients with HER2-overexpressing relapsed or refractory inflammatory breast cancer: final results and survival of the expanded HER2+ cohort in EGF103009, a phase II study." Lancet Oncol **10**(6): 581-588.

Kaur Saharan, H., S. Das and P. Varshney (2015). "Safety profile of Paclitaxel." International Journal of Pharmacy & Life Sciences **6**(1).

Kavanaugh, W. M. and L. T. Williams (1994). "An alternative to SH2 domains for binding tyrosine-phosphorylated proteins." Science **266**(5192): 1862-1865.

Keefe, D. M. and R. J. Gibson (2007). "Mucosal injury from targeted anti-cancer therapy." Support Care Cancer **15**(5): 483-490.

Keely, S. J. and K. E. Barrett (1999). "ErbB2 and ErbB3 receptors mediate inhibition of calcium-dependent chloride secretion in colonic epithelial cells." J Biol Chem **274**(47): 33449-33454.

Keely, S. J. and K. E. Barrett (2000). "Regulation of chloride secretion. Novel pathways and messengers." Ann N Y Acad Sci **915**: 67-76.

Keely, S. J. and K. E. Barrett (2003). "p38 mitogen-activated protein kinase inhibits calcium-dependent chloride secretion in T84 colonic epithelial cells." Am J Physiol Cell Physiol **284**(2): C339-348.

Keely, S. J., S. O. Calandrella and K. E. Barrett (2000). "Carbachol-stimulated transactivation of epidermal growth factor receptor and mitogen-activated protein kinase in T(84) cells is mediated by intracellular ca(2+), PYK-2, and p60(src)." J Biol Chem **275**(17): 12619-12625.

Kelly, S. and J. Hunter (1990). "Epidermal growth factor stimulates synthesis and secretion of mucus glycoproteins in human gastric mucosa." Clin Sci **79**(5): 425-427.

Khattri, A., Z. Zuo, J. Brägelmann, M. K. Keck, M. El Dinali, C. D. Brown, T. Stricker, A. Munagala, E. E. Cohen and M. W. Lingen (2015). "Rare occurrence of EGFRvIII deletion in head and neck squamous cell carcinoma." Oral oncology **51**(1): 53-58.

King, C. R., I. Borrello, F. Bellot, P. Comoglio and J. Schlessinger (1988). "Egf binding to its receptor triggers a rapid tyrosine phosphorylation of the erbB-2 protein in the mammary tumor cell line SK-BR-3." EMBO J **7**(6): 1647-1651.

Koch, K. M., N. J. Reddy, R. B. Cohen, N. L. Lewis, B. Whitehead, K. Mackay, A. Stead, A. P. Beelen and L. D. Lewis (2009). "Effects of food on the relative bioavailability of lapatinib in cancer patients." J Clin Oncol **27**(8): 1191-1196.

Kokai, Y., J. N. Myers, T. Wada, V. I. Brown, C. M. LeVea, J. G. Davis, K. Dobashi and M. I. Greene (1989). "Synergistic interaction of p185c-neu and the EGF receptor leads to transformation of rodent fibroblasts." Cell **58**(2): 287-292.

Konecny, G. E., M. D. Pegram, N. Venkatesan, R. Finn, G. Yang, M. Rahmeh, M. Untch, D. W. Rusnak, G. Spehar, R. J. Mullin, B. R. Keith, T. M. Gilmer, M. Berger, K. C. Podratz and D. J. Slamon (2006). "Activity of the dual kinase inhibitor lapatinib (GW572016) against HER-2-overexpressing and trastuzumab-treated breast cancer cells." Cancer Res **66**(3): 1630-1639.

Konturek, P. C., T. Brzozowski, S. J. Konturek, H. Ernst, D. Drozdowicz, R. Pajdo and E. G. Hahn (1997). "Expression of epidermal growth factor and transforming growth factor alpha during ulcer healing. Time sequence study." Scand J Gastroenterol **32**(1): 6-15.

Kuan, C. T., C. J. Wikstrand and D. D. Bigner (2001). "EGF mutant receptor vIII as a molecular target in cancer therapy." Endocr Relat Cancer **8**(2): 83-96.

Kunzelmann, K. and M. Mall (2002). "Electrolyte transport in the mammalian colon: mechanisms and implications for disease." Physiol Rev **82**(1): 245-289.

Lackey, K. E. (2006). "Lessons from the drug discovery of lapatinib, a dual ErbB1/2 tyrosine kinase inhibitor." Curr Top Med Chem **6**(5): 435-460.

Lee, D., R. S. Pearsall, S. Das, S. K. Dey, V. L. Godfrey and D. W. Threadgill (2004). "Epiregulin is not essential for development of intestinal tumors but is required for protection from intestinal damage." Molecular and cellular biology **24**(20): 8907-8916.

Lee, K.-F., H. Simon, H. Chen, B. Bates, M.-C. Hung and C. Hauser (1995). "Requirement for neuregulin receptor erbB2 in neural and cardiac development."

Lemos, C., E. Giovannetti, P. A. Zucali, Y. G. Assaraf, G. L. Scheffer, T. van der Straaten, A. D'Incecco, A. Falcone, H. J. Guchelaar, R. Danesi, A. Santoro, G. Giaccone, C. Tibaldi and G. J. Peters (2011). "Impact of ABCG2 polymorphisms on the clinical outcome and toxicity of gefitinib in non-small-cell lung cancer patients." Pharmacogenomics **12**(2): 159-170.

Lenferink, A. E., R. Pinkas-Kramarski, M. L. van de Poll, M. J. van Vugt, L. N. Klapper, E. Tzahar, H. Waterman, M. Sela, E. J. van Zoelen and Y. Yarden (1998). "Differential endocytic routing of homo- and hetero-dimeric ErbB tyrosine kinases confers signaling superiority to receptor heterodimers." EMBO J **17**(12): 3385-3397.

Lenferink, A. E., J. F. Simpson, L. K. Shawver, R. J. Coffey, J. T. Forbes and C. L. Arteaga (2000). "Blockade of the epidermal growth factor receptor tyrosine kinase suppresses tumorigenesis in MMTV/Neu + MMTV/TGF-alpha bigenic mice." Proc Natl Acad Sci U S A **97**(17): 9609-9614.

Levitzki, A. and A. Gazit (1995). "Tyrosine kinase inhibition: an approach to drug development." Science **267**(5205): 1782-1788.

Lewis, K. M., E. Harford-Wright, R. Vink and M. N. Ghabriel (2013). "Characterisation of Walker 256 breast carcinoma cells from two tumour cell banks as assessed using two models of secondary brain tumours." Cancer Cell Int **13**(1): 5.

Li, D., L. Ambrogio, T. Shimamura, S. Kubo, M. Takahashi, L. R. Chirieac, R. F. Padera, G. I. Shapiro, A. Baum, F. Himmelsbach, W. J. Rettig, M. Meyerson, F. Solca, H. Greulich and K. K. Wong (2008). "BIBW2992, an irreversible EGFR/HER2 inhibitor highly effective in preclinical lung cancer models." Oncogene **27**(34): 4702-4711.

Li, J., G. Cusatis, J. Brahmer, A. Sparreboom, R. W. Robey, S. E. Bates, M. Hidalgo and S. D. Baker (2007). "Association of variant ABCG2 and the pharmacokinetics of epidermal growth factor receptor tyrosine kinase inhibitors in cancer patients." Cancer Biol Ther **6**(3): 432-438.

Li, J., F. Zhu, R. A. Lubet, A. De Luca, C. Grubbs, M. E. Ericson, A. D'Alessio, N. Normanno, Z. Dong and A. M. Bode (2013). "Quercetin-3-methyl ether inhibits lapatinib-sensitive and-resistant breast cancer cell growth by inducing G2/M arrest and apoptosis." Molecular carcinogenesis **52**(2): 134-143.

Lin, H., Y. Zhao, J. Yu, W. Jiang and X. Sun (2012). "Effects of Traditional Chinese Medicine Wei-Wei-Kang-Granule on the Expression of Egfr and Nf-Kb in Chronic Atrophic Gastritis Rats." African Journal of Traditional, Complementary and Alternative Medicines **9**(1): 1-7.

Lin, J. H. (2004). "How significant is the role of P-glycoprotein in drug absorption and brain uptake?" Drugs of today **40**(1): 5-22.

Lin, N. U., L. A. Carey, M. C. Liu, J. Younger, S. E. Come, M. Ewend, G. J. Harris, E. Bullitt, A. D. Van den Abbeele and J. W. Henson (2008). "Phase II trial of lapatinib for brain

metastases in patients with human epidermal growth factor receptor 2–positive breast cancer." Journal of Clinical Oncology **26**(12): 1993-1999.

Lin, N. U., V. Diéras, D. Paul, D. Lossignol, C. Christodoulou, H.-J. Stemmler, H. Roché, M. C. Liu, R. Greil and E. Ciruelos (2009). "Multicenter phase II study of lapatinib in patients with brain metastases from HER2-positive breast cancer." Clinical Cancer Research **15**(4): 1452-1459.

Linggi, B. and G. Carpenter (2006). "ErbB receptors: new insights on mechanisms and biology." Trends in cell biology **16**(12): 649-656.

Liu, S. and R. Kurzrock (2014). "Toxicity of targeted therapy: Implications for response and impact of genetic polymorphisms." Cancer Treat Rev **40**(7): 883-891.

Logan, R. M., A. M. Stringer, J. M. Bowen, R. J. Gibson, S. T. Sonis and D. M. Keefe (2009). "Is the pathobiology of chemotherapy-induced alimentary tract mucositis influenced by the type of mucotoxic drug administered?" Cancer Chemother Pharmacol **63**(2): 239-251.

Loriot, Y., G. Perlemuter, D. Malka, F. Penault-Llorca, V. Boige, E. Deutsch, C. Massard, J. P. Armand and J. C. Soria (2008). "Drug insight: gastrointestinal and hepatic adverse effects of molecular-targeted agents in cancer therapy." Nat Clin Pract Oncol **5**(5): 268-278.

LoRusso, P., K. Venkatakrishnan, E. G. Chiorean, D. Noe, J. T. Wu, S. Sankoh, M. Corvez and E. A. Sausville (2014). "Phase 1 dose-escalation, pharmacokinetic, and cerebrospinal fluid distribution study of TAK-285, an investigational inhibitor of EGFR and HER2." Invest New Drugs **32**(1): 160-170.

Lucs, A. V., W. J. Muller and S. K. Muthuswamy (2010). "Shc is required for ErbB2-induced inhibition of apoptosis but is dispensable for cell proliferation and disruption of cell polarity." Oncogene **29**(2): 174-187.

Mannon, P. J. and J. M. Mele (2000). "Peptide YY Y1 receptor activates mitogen-activated protein kinase and proliferation in gut epithelial cells via the epidermal growth factor receptor." Biochem J **350 Pt 3**: 655-661.

Marchelletta, R. R., M. G. Gareau, D. F. McCole, S. Okamoto, E. Roel, R. Klinkenberg, D. G. Guiney, J. Fierer and K. E. Barrett (2013). "Altered expression and localization of ion transporters contribute to diarrhea in mice with Salmonella-induced enteritis." Gastroenterology **145**(6): 1358-1368 e1351-1354.

Martin, A. P., A. Miller, L. Emad, M. Rahmani, T. Walker, C. Mitchell, M. P. Hagan, M. A. Park, A. Yacoub, P. B. Fisher, S. Grant and P. Dent (2008). "Lapatinib resistance in HCT116 cells is mediated by elevated MCL-1 expression and decreased BAK activation and not by ERBB receptor kinase mutation." Molecular pharmacology **74**(3): 807-822.

McCole, D. F. and K. E. Barrett (2007). "Varied role of the gut epithelium in mucosal homeostasis." Curr Opin Gastroenterol **23**(6): 647-654.

McCole, D. F. and K. E. Barrett (2009). "Decoding epithelial signals: critical role for the epidermal growth factor receptor in controlling intestinal transport function." Acta Physiol (Oxf) **195**(1): 149-159.

McCole, D. F., S. J. Keely, R. J. Coffey and K. E. Barrett (2002). "Transactivation of the epidermal growth factor receptor in colonic epithelial cells by carbachol requires extracellular release of transforming growth factor-alpha." J Biol Chem **277**(45): 42603-42612.

McCole, D. F., G. Rogler, N. Varki and K. E. Barrett (2005). "Epidermal growth factor partially restores colonic ion transport responses in mouse models of chronic colitis." Gastroenterology **129**(2): 591-608.

McCole, D. F., A. Truong, M. Bunz and K. E. Barrett (2007). "Consequences of direct versus indirect activation of epidermal growth factor receptor in intestinal epithelial cells are dictated by protein-tyrosine phosphatase 1B." J Biol Chem **282**(18): 13303-13315.

McElroy, S. J., S. Hobbs, M. Kallen, N. Tejera, M. J. Rosen, A. Grishin, P. Matta, C. Schneider, J. Upperman, H. Ford, D. B. Polk and J. H. Weitkamp (2012). "Transactivation of EGFR by LPS induces COX-2 expression in enterocytes." PLoS One **7**(5): e38373.

McRoberts, J. and K. Barrett (1989). Hormone-regulated ion transport in T84 colonic cells. Functional epithelial cells in culture, Alan R. Liss New York**:** 235-265.

Medina, P. J. and S. Goodin (2008). "Lapatinib: a dual inhibitor of human epidermal growth factor receptor tyrosine kinases." Clin Ther **30**(8): 1426-1447.

Melosky, B. (2012). "Supportive care treatments for toxicities of anti-egfr and other targeted agents." Curr Oncol **19**(Suppl 1): S59-63.

Meropol, N. J., J. Berlin and J. R. Hecht (2003). Multicenter study of ABX-EGF monotherapy in patients with metastatic colorectal cancer. American Society of Clinical Oncology.

Miettinen, P. J., J. E. Berger, J. Meneses, Y. Phung, R. A. Pedersen, Z. Werb and R. Derynck (1995). "Epithelial immaturity and multiorgan failure in mice lacking epidermal growth factor receptor." Nature **376**(6538): 337-341.

Miller, V. A., V. Hirsh, J. Cadranel, Y. M. Chen, K. Park, S. W. Kim, C. Zhou, W. C. Su, M. Wang, Y. Sun, D. S. Heo, L. Crino, E. H. Tan, T. Y. Chao, M. Shahidi, X. J. Cong, R. M. Lorence and J. C. Yang (2012). "Afatinib versus placebo for patients with advanced, metastatic non-small-cell lung cancer after failure of erlotinib, gefitinib, or both, and one or two lines of chemotherapy (LUX-Lung 1): a phase 2b/3 randomised trial." The lancet oncology **13**(5): 528-538.

Mirghani, R. A., J. Sayi, E. Aklillu, A. Allqvist, M. Jande, A. Wennerholm, J. Eriksen, V. M. Herben, B. C. Jones, L. L. Gustafsson and L. Bertilsson (2006). "CYP3A5 genotype has significant effect on quinine 3-hydroxylation in Tanzanians, who have lower total CYP3A activity than a Swedish population." Pharmacogenet Genomics **16**(9): 637-645.

Moasser, M. M., A. Basso, S. D. Averbuch and N. Rosen (2001). "The tyrosine kinase inhibitor ZD1839 ("Iressa") inhibits HER2-driven signaling and suppresses the growth of HER2-overexpressing tumor cells." Cancer Res **61**(19): 7184-7188.

Montaner, B. and R. Perez-Tomas (1999). "Epidermal growth factor receptor (EGF-R) localization in the apical membrane of the enterocytes of rat duodenum." Cell Biol Int **23**(7): 475-479.

Montrose MH, K. S., Barrett KE (2003). Electrolyte secretion and absorption:small intestine and colon. Textbook of Gastroenterology. Y. T. Philadelphia, Lippincott Williams and Wilkins**:** 308-339.

Moscatello, D. K., M. Holgado-Madruga, D. R. Emlet, R. B. Montgomery and A. J. Wong (1998). "Constitutive activation of phosphatidylinositol 3-kinase by a naturally occurring mutant epidermal growth factor receptor." The Journal of biological chemistry **273**(1): 200-206.

Mosesson, Y. and Y. Yarden (2004). "Oncogenic growth factor receptors: implications for signal transduction therapy." Semin Cancer Biol **14**(4): 262-270.

Moulder, S. L., F. M. Yakes, S. K. Muthuswamy, R. Bianco, J. F. Simpson and C. L. Arteaga (2001). "Epidermal growth factor receptor (HER1) tyrosine kinase inhibitor ZD1839 (Iressa) inhibits HER2/neu (erbB2)-overexpressing breast cancer cells in vitro and in vivo." Cancer Res **61**(24): 8887-8895.

Moy, B. and P. E. Goss (2007). "Lapatinib-associated toxicity and practical management recommendations." Oncologist **12**(7): 756-765.

Moyer, J. D., E. G. Barbacci, K. K. Iwata, L. Arnold, B. Boman, A. Cunningham, C. DiOrio, J. Doty, M. J. Morin, M. P. Moyer, M. Neveu, V. A. Pollack, L. R. Pustilnik, M. M. Reynolds, D. Sloan, A. Theleman and P. Miller (1997). "Induction of apoptosis and cell cycle arrest by CP-358,774, an inhibitor of epidermal growth factor receptor tyrosine kinase." Cancer research **57**(21): 4838-4848.

Munshi, H. and M. Stack (2006). "Reciprocal interactions between adhesion receptor signaling and MMP regulation." Cancer and Metastasis Reviews **25**(1): 45-56.

Murakami, H., T. Tamura, T. Takahashi, H. Nokihara, T. Naito, Y. Nakamura, K. Nishio, Y. Seki, A. Sarashina, M. Shahidi and N. Yamamoto (2012). "Phase I study of continuous afatinib (BIBW 2992) in patients with advanced non-small cell lung cancer after prior chemotherapy/erlotinib/gefitinib (LUX-Lung 4)." Cancer chemotherapy and pharmacology **69**(4): 891-899.

Nadanaciva, S., S. Lu, D. F. Gebhard, B. A. Jessen, W. D. Pennie and Y. Will (2011). "A high content screening assay for identifying lysosomotropic compounds." Toxicology in vitro **25**(3): 715-723.

Nagane, M., F. Coufal, H. Lin, O. Bogler, W. K. Cavenee and H. J. Huang (1996). "A common mutant epidermal growth factor receptor confers enhanced tumorigenicity on human glioblastoma cells by increasing proliferation and reducing apoptosis." Cancer research **56**(21): 5079-5086.

Nakamura, M. and T. Nishida (1999). "Differential effects of epidermal growth factor and interleukin 6 on corneal epithelial cells and vascular endothelial cells." Cornea **18**(4): 452-458.

Nakayama, A., S. Takagi, T. Yusa, M. Yaguchi, A. Hayashi, T. Tamura, Y. Kawakita, T. Ishikawa and Y. Ohta (2013). "Antitumor Activity of TAK-285, an Investigational, Non-Pgp Substrate HER2/EGFR Kinase Inhibitor, in Cultured Tumor Cells, Mouse and Rat Xenograft Tumors, and in an HER2-Positive Brain Metastasis Model." Journal of Cancer **4**(7): 557-565.

Nasrollahzadeh, J., F. Siassi, M. Doosti, M. R. Eshraghian, F. Shokri, M. H. Modarressi, J. Mohammadi-Asl, K. Abdi, A. Nikmanesh and S. M. Karimian (2008). "The influence of feeding linoleic, gamma-linolenic and docosahexaenoic acid rich oils on rat brain tumor fatty acids composition and fatty acid binding protein 7 mRNA expression." Lipids Health Dis **7**: 45.

Nogales, E., S. G. Wolf, I. A. Khan, R. F. Luduena and K. H. Downing (1995). "Structure of tubulin at 6.5 A and location of the taxol-binding site." Nature **375**(6530): 424-427.

Ohland, C. L., R. DeVinney and W. K. MacNaughton (2012). "Escherichia coli-induced epithelial hyporesponsiveness to secretagogues is associated with altered CFTR localization." Cell Microbiol **14**(4): 447-459.

Opleta-Madsen, K., J. Hardin and D. G. Gall (1991). "Epidermal growth factor upregulates intestinal electrolyte and nutrient transport." The American journal of physiology **260**(6 Pt 1): G807-814.

Ou, G., V. Baranov, E. Lundmark, S. Hammarström and M. L. Hammarström (2009). "Contribution of intestinal epithelial cells to innate immunity of the human gut–studies on polarized monolayers of colon carcinoma cells." Scandinavian journal of immunology **69**(2): 150-161.

Paik, W. K., D. C. Paik and S. Kim (2007). "Historical review: the field of protein methylation." Trends in biochemical sciences **32**(3): 146-152.

Park, J. Y., Y. Q. Su, M. Ariga, E. Law, S. L. Jin and M. Conti (2004). "EGF-like growth factors as mediators of LH action in the ovulatory follicle." Science **303**(5658): 682-684.

Paul, G., R. R. Marchelletta, D. F. McCole and K. E. Barrett (2012). "Interferon-gamma alters downstream signaling originating from epidermal growth factor receptor in intestinal epithelial cells: functional consequences for ion transport." J Biol Chem **287**(3): 2144-2155.

Penner, G., J. Aschenbach, K. Wood, M. Walpole, R. Kanafany-Guzman, S. Hendrick and J. Campbell (2014). "Characterising barrier function among regions of the gastrointestinal tract in Holstein steers." Animal Production Science **54**(9): 1282-1287.

Podolsky, D. K. (1993). "Regulation of intestinal epithelial proliferation: a few answers, many questions." Am J Physiol **264**(2 Pt 1): G179-186.

Pollack, V. A., D. M. Savage, D. A. Baker, K. E. Tsaparikos, D. E. Sloan, J. D. Moyer, E. G. Barbacci, L. R. Pustilnik, T. A. Smolarek, J. A. Davis, M. P. Vaidya, L. D. Arnold, J. L. Doty, K. K. Iwata and M. J. Morin (1999). "Inhibition of epidermal growth factor receptor-associated tyrosine phosphorylation in human carcinomas with CP-358,774: dynamics of receptor inhibition in situ and antitumor effects in athymic mice." The Journal of pharmacology and experimental therapeutics **291**(2): 739-748.

Polli, J. W., K. L. Olson, J. P. Chism, L. S. John-Williams, R. L. Yeager, S. M. Woodard, V. Otto, S. Castellino and V. E. Demby (2009). "An unexpected synergist role of P-glycoprotein and breast cancer resistance protein on the central nervous system penetration of the tyrosine kinase inhibitor lapatinib (N-{3-chloro-4-[(3-fluorobenzyl) oxy] phenyl}-6-[5-({[2-

(methylsulfonyl) ethyl] amino} methyl)-2-furyl]-4-quinazolinamine; GW572016)." Drug Metabolism and Disposition **37**(2): 439-442.

Pritchard, D. M., C. S. Potten and J. A. Hickman (1998). "The relationships between p53-dependent apoptosis, inhibition of proliferation, and 5-fluorouracil-induced histopathology in murine intestinal epithelia." Cancer research **58**(23): 5453-5465.

Rabindran, S. K., C. M. Discafani, E. C. Rosfjord, M. Baxter, M. B. Floyd, J. Golas, W. A. Hallett, B. D. Johnson, R. Nilakantan, E. Overbeek, M. F. Reich, R. Shen, X. Shi, H. R. Tsou, Y. F. Wang and A. Wissner (2004). "Antitumor activity of HKI-272, an orally active, irreversible inhibitor of the HER-2 tyrosine kinase." Cancer research **64**(11): 3958-3965.

Rall, L. B., J. Scott, G. I. Bell, R. J. Crawford, J. D. Penschow, H. D. Niall and J. P. Coghlan (1985). "Mouse prepro-epidermal growth factor synthesis by the kidney and other tissues." Nature **313**(5999): 228-231.

Rasmussen, A. R., N. E. Viby, K. J. Hare, B. Hartmann, L. Thim, J. J. Holst and S. S. Poulsen (2010). "The intestinotrophic peptide, GLP-2, counteracts the gastrointestinal atrophy in mice induced by the epidermal growth factor receptor inhibitor, erlotinib, and cisplatin." Dig Dis Sci **55**(10): 2785-2796.

Reardon, D. A., T. Cloughesy, J. Rich, W. K. Alfred Yung, L. Yung, C. DiLea, J. Huang, M. Dugan, W. Mietlowski, A. Maes and C. Conrad (2012). "Pharmacokinetic drug interaction between AEE788 and RAD001 causing thrombocytopenia in patients with glioblastoma." Cancer Chemother Pharmacol **69**(1): 281-287.

Rebeca, R., L. Bracht, G. R. Noleto, G. R. Martinez, S. M. Cadena, E. G. Carnieri, M. E. Rocha and M. B. de Oliveira (2008). "Production of cachexia mediators by Walker 256 cells from ascitic tumors." Cell Biochem Funct **26**(6): 731-738.

Redon, C. E., J. S. Dickey, A. J. Nakamura, I. G. Kareva, D. Naf, S. Nowsheen, T. B. Kryston, W. M. Bonner, A. G. Georgakilas and O. A. Sedelnikova (2010). "Tumors induce complex DNA damage in distant proliferative tissues in vivo." Proceedings of the National Academy of Sciences **107**(42): 17992-17997.

Renouf, D. J., J. P. Velazquez-Martin, R. Simpson, L. L. Siu and P. L. Bedard (2012). "Ocular toxicity of targeted therapies." J Clin Oncol **30**(26): 3277-3286.

Rhodes, J. A., J. P. Tam, U. Finke, M. Saunders, J. Bernanke, W. Silen and R. A. Murphy (1986). "Transforming growth factor alpha inhibits secretion of gastric acid." Proceedings of the National Academy of Sciences of the United States of America **83**(11): 3844-3846.

Ricci, S. B. and U. Cerchiari (2010). "Spontaneous regression of malignant tumors: Importance of the immune system and other factors (Review)." Oncol Lett **1**(6): 941-945.

Richardson, G. and R. Dobish (2007). "Chemotherapy induced diarrhea." J Oncol Pharm Pract **13**(4): 181-198.

Ritland, S. R., S. J. Gendler, L. J. Burgart, D. W. Fry, J. M. Nelson, A. J. Bridges, L. Andress and W. E. Karnes (2000). "Inhibition of epidermal growth factor receptor tyrosine kinase fails to suppress adenoma formation in ApcMin mice but induces duodenal injury." Cancer research **60**(17): 4678-4681.

Rixe, O., S. X. Franco, D. A. Yardley, S. R. Johnston, M. Martin, B. K. Arun, S. P. Letrent and H. S. Rugo (2009). "A randomized, phase II, dose-finding study of the pan-ErbB receptor tyrosine-kinase inhibitor CI-1033 in patients with pretreated metastatic breast cancer." Cancer Chemother Pharmacol **64**(6): 1139-1148.

Robert, C., V. Sibaud, C. Mateus and B. S. Cherpelis (2012). "Advances in the management of cutaneous toxicities of targeted therapies." Seminars in oncology **39**(2): 227-240.

Roberts, R. B., C. L. Arteaga and D. W. Threadgill (2004). "Modeling the cancer patient with genetically engineered mice: prediction of toxicity from molecule-targeted therapies." Cancer Cell **5**(2): 115-120.

Rodrigues, G. A., M. Falasca, Z. Zhang, S. H. Ong and J. Schlessinger (2000). "A novel positive feedback loop mediated by the docking protein Gab1 and phosphatidylinositol 3-kinase in epidermal growth factor receptor signaling." Molecular and cellular biology **20**(4): 1448-1459.

Rudin, C. M., W. Liu, A. Desai, T. Karrison, X. Jiang, L. Janisch, S. Das, J. Ramirez, B. Poonkuzhali, E. Schuetz, D. L. Fackenthal, P. Chen, D. K. Armstrong, J. R. Brahmer, G. F. Fleming, E. E. Vokes, M. A. Carducci and M. J. Ratain (2008). "Pharmacogenomic and pharmacokinetic determinants of erlotinib toxicity." J Clin Oncol **26**(7): 1119-1127.

Rudmann, D. G. (2012). "On-target and off-target-based toxicologic effects." Toxicologic pathology: 0192623312464311.

Rusnak, D. W., K. J. Alligood, R. J. Mullin, G. M. Spehar, C. Arenas-Elliott, A. M. Martin, Y. Degenhardt, S. K. Rudolph, T. F. Haws, Jr., B. L. Hudson-Curtis and T. M. Gilmer (2007). "Assessment of epidermal growth factor receptor (EGFR, ErbB1) and HER2 (ErbB2) protein expression levels and response to lapatinib (Tykerb, GW572016) in an expanded panel of human normal and tumour cell lines." Cell Prolif **40**(4): 580-594.

Rusnak, D. W., K. Lackey, K. Affleck, E. R. Wood, K. J. Alligood, N. Rhodes, B. R. Keith, D. M. Murray, W. B. Knight, R. J. Mullin and T. M. Gilmer (2001). "The effects of the novel, reversible epidermal growth factor receptor/ErbB-2 tyrosine kinase inhibitor, GW2016, on the growth of human normal and tumor-derived cell lines in vitro and in vivo." Mol Cancer Ther **1**(2): 85-94.

Salomon, D. S., R. Brandt, F. Ciardiello and N. Normanno (1995). "Epidermal growth factor-related peptides and their receptors in human malignancies." Critical reviews in oncology/hematology **19**(3): 183-232.

Satoh, T., K. H. Lee, S. Y. Rha, Y. Sasaki, S. H. Park, Y. Komatsu, H. Yasui, T. Y. Kim, K. Yamaguchi, N. Fuse, Y. Yamada, T. Ura, S. Y. Kim, M. Munakata, S. Saitoh, K. Nishio, S. Morita, E. Yamamoto, Q. Zhang, J. M. Kim, Y. H. Kim and Y. Sakata (2015). "Randomized phase II trial of nimotuzumab plus irinotecan versus irinotecan alone as second-line therapy for patients with advanced gastric cancer." Gastric Cancer **18**(4): 824-832.

Sawaoka, H., S. Tsuji, M. Tsujii, E. S. Gunawan, N. Kawai, Y. Sasaki, M. Hori and S. Kawano (1999). "Involvement of cyclooxygenase-2 in proliferation and morphogenesis induced by transforming growth factor alpha in gastric epithelial cells." Prostaglandins Leukot Essent Fatty Acids **61**(5): 315-322.

Scaltriti, M., C. Verma, M. Guzman, J. Jimenez, J. Parra, K. Pedersen, D. Smith, S. Landolfi, S. R. y Cajal and J. Arribas (2009). "Lapatinib, a HER2 tyrosine kinase inhibitor, induces stabilization and accumulation of HER2 and potentiates trastuzumab-dependent cell cytotoxicity." Oncogene **28**(6): 803-814.

Scheffler, M., P. Di Gion, O. Doroshyenko, J. Wolf and U. Fuhr (2011). "Clinical pharmacokinetics of tyrosine kinase inhibitors: focus on 4-anilinoquinazolines." Clinical pharmacokinetics **50**(6): 371-403.

Schlessinger, J. (2000). "Cell signaling by receptor tyrosine kinases." Cell **103**(2): 211-225.

Schneider, M. R. and E. Wolf (2009). "The epidermal growth factor receptor ligands at a glance." J Cell Physiol **218**(3): 460-466.

Schreiber, A. B., M. E. Winkler and R. Derynck (1986). "Transforming growth factor-alpha: a more potent angiogenic mediator than epidermal growth factor." Science **232**(4755): 1250-1253.

Schuler, M., A. Awada, P. Harter, J. L. Canon, K. Possinger, M. Schmidt, J. De Greve, P. Neven, L. Dirix, W. Jonat, M. W. Beckmann, J. Schutte, P. A. Fasching, N. Gottschalk, T. Besse-Hammer, F. Fleischer, S. Wind, M. Uttenreuther-Fischer, M. Piccart and N. Harbeck (2012). "A phase II trial to assess efficacy and safety of afatinib in extensively pretreated patients with HER2-negative metastatic breast cancer." Breast cancer research and treatment **134**(3): 1149-1159.

Schultheiss, G. and M. Diener (1998). "K+ and Cl- conductances in the distal colon of the rat." Gen Pharmacol **31**(3): 337-342.

Schultz, G. S., M. White, R. Mitchell, G. Brown, J. Lynch, D. R. Twardzik and G. J. Todaro (1987). "Epithelial wound healing enhanced by transforming growth factor-alpha and vaccinia growth factor." Science **235**(4786): 350-352.

Semple, J. W., J. E. Italiano, Jr. and J. Freedman (2011). "Platelets and the immune continuum." Nat Rev Immunol **11**(4): 264-274.

Sequist, L. V., B. Besse, T. J. Lynch, V. A. Miller, K. K. Wong, B. Gitlitz, K. Eaton, C. Zacharchuk, A. Freyman, C. Powell, R. Ananthakrishnan, S. Quinn and J. C. Soria (2010). "Neratinib, an irreversible pan-ErbB receptor tyrosine kinase inhibitor: results of a phase II trial in patients with advanced non-small-cell lung cancer." Journal of clinical oncology : official journal of the American Society of Clinical Oncology **28**(18): 3076-3083.

Sequist, L. V., J.-C. Soria, J. W. Goldman, H. A. Wakelee, S. M. Gadgeel, A. Varga, V. Papadimitrakopoulou, B. J. Solomon, G. R. Oxnard and R. Dziadziuszko (2015). "Rociletinib in EGFR-mutated non–small-cell lung cancer." New England Journal of Medicine **372**(18): 1700-1709.

Shah, D. R., R. R. Shah and J. Morganroth (2013). "Tyrosine kinase inhibitors: their on-target toxicities as potential indicators of efficacy." Drug Saf **36**(6): 413-426.

Shell, S. A., R. L. Wrappel, P. Trusk, Y. Ohta, W. Klohs and S. S. Bacus (2008). "Tyrosine kinase inhibitors, such as TAK-285, GW-572016 or SU11248, protect or damage the heart base on their ability to activate AMPK." Eur J Cancer **6**(27): Abstract 78.

Sherwood, L. (2007). Human Physiology: From Cells to Systems. Belmont, CA USA, Thomson Brooks/Cole.

Shi, Y., L. Zhang, X. Liu, C. Zhou, L. Zhang, S. Zhang, D. Wang, Q. Li, S. Qin, C. Hu, Y. Zhang, J. Chen, Y. Cheng, J. Feng, H. Zhang, Y. Song, Y. L. Wu, N. Xu, J. Zhou, R. Luo, C. Bai, Y. Jin, W. Liu, Z. Wei, F. Tan, Y. Wang, L. Ding, H. Dai, S. Jiao, J. Wang, L. Liang, W. Zhang and Y. Sun (2013). "Icotinib versus gefitinib in previously treated advanced non-small-cell lung cancer (ICOGEN): a randomised, double-blind phase 3 non-inferiority trial." Lancet Oncol **14**(10): 953-961.

Shi, Y., L. Zhang, X. Liu, C. Zhou, S. Zhang, D. Wang, Q. Li, S. Qin, C. Hu and Y. Zhang (2013). "Icotinib versus gefitinib in previously treated advanced non-small-cell lung cancer (ICOGEN): a randomised, double-blind phase 3 non-inferiority trial." The lancet oncology **14**(10): 953-961.

Shitara, K., Y. Kuwana, K. Nakamura, Y. Tokutake, S. Ohta, H. Miyaji, M. Hasegawa and N. Hanai (1993). "A mouse/human chimeric anti-(ganglioside GD3) antibody with enhanced antitumor activities." Cancer immunology, immunotherapy : CII **36**(6): 373-380.

Siepmann, J., F. Siepmann and A. T. Florence (2016). "Factors influencing oral drug absorption and drug availability." Modern Pharmaceutics, Two Volume Set: 117.

Sigismund, S., E. Argenzio, D. Tosoni, E. Cavallaro, S. Polo and P. P. Di Fiore (2008). "Clathrin-mediated internalization is essential for sustained EGFR signaling but dispensable for degradation." Developmental cell **15**(2): 209-219.

Sigismund, S., T. Woelk, C. Puri, E. Maspero, C. Tacchetti, P. Transidico, P. P. Di Fiore and S. Polo (2005). "Clathrin-independent endocytosis of ubiquitinated cargos." Proceedings of the National Academy of Sciences of the United States of America **102**(8): 2760-2765.

Singh, A. B. and R. C. Harris (2005). "Autocrine, paracrine and juxtacrine signaling by EGFR ligands." Cellular signalling **17**(10): 1183-1193.

Slamon, D. J., W. Godolphin, L. A. Jones, J. A. Holt, S. G. Wong, D. E. Keith, W. J. Levin, S. G. Stuart, J. Udove, A. Ullrich and et al. (1989). "Studies of the HER-2/neu proto-oncogene in human breast and ovarian cancer." Science **244**(4905): 707-712.

Slieker, L. J., T. M. Martensen and M. D. Lane (1986). "Synthesis of epidermal growth factor receptor in human A431 cells. Glycosylation-dependent acquisition of ligand binding activity occurs post-translationally in the endoplasmic reticulum." The Journal of biological chemistry **261**(32): 15233-15241.

Solca, F., G. Dahl, A. Zoephel, G. Bader, M. Sanderson, C. Klein, O. Kraemer, F. Himmelsbach, E. Haaksma and G. R. Adolf (2012). "Target binding properties and cellular activity of afatinib (BIBW 2992), an irreversible ErbB family blocker." The Journal of pharmacology and experimental therapeutics **343**(2): 342-350.

Sonis, S. T., J. W. Costa, S. M. Evitts, L. E. Lindquist and M. Nicolson (1992). "Effect of epidermal growth factor on ulcerative mucositis in hamsters that receive cancer chemotherapy." Oral surgery, oral medicine, oral pathology **74**(6): 749-755.

Soria, J. C., J. Cortes, C. Massard, J. P. Armand, D. De Andreis, S. Ropert, E. Lopez, A. Catteau, J. James, J. F. Marier, M. Beliveau, R. E. Martell and J. Baselga (2012). "Phase I safety, pharmacokinetic and pharmacodynamic trial of BMS-599626 (AC480), an oral pan-HER receptor tyrosine kinase inhibitor, in patients with advanced solid tumors." Annals of oncology : official journal of the European Society for Medical Oncology / ESMO **23**(2): 463-471.

Soria, J. C., E. Felip, M. Cobo, S. Lu, K. Syrigos, K. H. Lee, E. Goker, V. Georgoulias, W. Li, D. Isla, S. Z. Guclu, A. Morabito, Y. J. Min, A. Ardizzoni, S. M. Gadgeel, B. Wang, V. K. Chand and G. D. Goss (2015). "Afatinib versus erlotinib as second-line treatment of patients with advanced squamous cell carcinoma of the lung (LUX-Lung 8): an open-label randomised controlled phase 3 trial." Lancet Oncol **16**(8): 897-907.

Spector, N. L., W. Xia, H. Burris, 3rd, H. Hurwitz, E. C. Dees, A. Dowlati, B. O'Neil, B. Overmoyer, P. K. Marcom, K. L. Blackwell, D. A. Smith, K. M. Koch, A. Stead, S. Mangum, M. J. Ellis, L. Liu, A. K. Man, T. M. Bremer, J. Harris and S. Bacus (2005). "Study of the biologic effects of lapatinib, a reversible inhibitor of ErbB1 and ErbB2 tyrosine kinases, on tumor growth and survival pathways in patients with advanced malignancies." J Clin Oncol **23**(11): 2502-2512.

Stein, A., W. Voigt and K. Jordan (2009). "Chemotherapy-induced diarrhea: pathophysiology, frequency and guideline-based management." Therapeutic advances in medical oncology.

Strachan, L., J. G. Murison, R. L. Prestidge, M. A. Sleeman, J. D. Watson and K. D. Kumble (2001). "Cloning and biological activity of epigen, a novel member of the epidermal growth factor superfamily." The Journal of biological chemistry **276**(21): 18265-18271.

Stringer, A. M., R. J. Gibson, J. M. Bowen, R. M. Logan, A. S. Yeoh and D. M. Keefe (2007). "Chemotherapy-induced mucositis: the role of gastrointestinal microflora and mucins in the luminal environment." J Support Oncol **5**(6): 259-267.

Stringer, A. M., R. J. Gibson, R. M. Logan, J. M. Bowen, A. S. Yeoh, J. Laurence and D. M. Keefe (2009). "Irinotecan-induced mucositis is associated with changes in intestinal mucins." Cancer chemotherapy and pharmacology **64**(1): 123-132.

Sukhotnik, I., D. Shteinberg, S. Ben Lulu, Y. Bashenko, J. G. Mogilner, B. M. Ure, R. Shaoul and A. G. Coran (2008). "Effect of transforming growth factor-alpha on enterocyte apoptosis is correlated with EGF receptor expression along the villus-crypt axis during methotrexate-induced intestinal mucositis in a rat." Apoptosis **13**(11): 1344-1355.

Sun, H., H. Dai, N. Shaik and W. F. Elmquist (2003). "Drug efflux transporters in the CNS." Advanced drug delivery reviews **55**(1): 83-105.

Takahashi, Y., J. Lee, C. Pickering, D. Bell, T. W. Jiffar, J. N. Myers, E. Y. Hanna and M. E. Kupferman (2016). "Human epidermal growth factor receptor 2/neu as a novel therapeutic target in sinonasal undifferentiated carcinoma." Head & neck.

Takasuna, K., T. Hagiwara, K. Watanabe, S. Onose, S. Yoshida, E. Kumazawa, E. Nagai and T. Kamataki (2006). "Optimal antidiarrhea treatment for antitumor agent irinotecan hydrochloride (CPT-11)-induced delayed diarrhea." Cancer Chemother Pharmacol **58**(4): 494-503.

Tan, C.-S., D. Gilligan and S. Pacey (2015). "Treatment approaches for EGFR-inhibitor-resistant patients with non-small-cell lung cancer." The Lancet Oncology **16**(9): e447-e459.

Taniguchi, K., S. Yamamoto, S. Aoki, S. Toda, K. Izuhara and Y. Hamasaki (2011). "Epigen is induced during the interleukin-13-stimulated cell proliferation in murine primary airway epithelial cells." Experimental lung research **37**(8): 461-470.

Taskar, K. S., V. Rudraraju, R. K. Mittapalli, R. Samala, H. R. Thorsheim, J. Lockman, B. Gril, E. Hua, D. Palmieri and J. W. Polli (2012). "Lapatinib distribution in HER2 overexpressing experimental brain metastases of breast cancer." Pharmaceutical research **29**(3): 770-781.

Thomas, S. K., F. V. Fossella, D. Liu, R. Schaerer, A. S. Tsao, M. S. Kies, K. M. Pisters, G. R. Blumenschein, Jr., B. S. Glisson, J. J. Lee, R. S. Herbst and R. G. Zinner (2006). "Asian ethnicity as a predictor of response in patients with non-small-cell lung cancer treated with gefitinib on an expanded access program." Clin Lung Cancer **7**(5): 326-331.

Thummel, K. E. and G. R. Wilkinson (1998). "In vitro and in vivo drug interactions involving human CYP3A." Annu Rev Pharmacol Toxicol **38**: 389-430.

Tjulandin, S., V. Moiseyenko, V. Semiglazov, G. Manikhas, M. Learoyd, A. Saunders, M. Stuart and U. Keilholz (2014). "Phase I, dose-finding study of AZD8931, an inhibitor of EGFR (erbB1), HER2 (erbB2) and HER3 (erbB3) signaling, in patients with advanced solid tumors." Invest New Drugs **32**(1): 145-153.

Ullrich, A., L. Coussens, J. S. Hayflick, T. J. Dull, A. Gray, A. W. Tam, J. Lee, Y. Yarden, T. A. Libermann, J. Schlessinger and et al. (1984). "Human epidermal growth factor receptor cDNA sequence and aberrant expression of the amplified gene in A431 epidermoid carcinoma cells." Nature **309**(5967): 418-425.

Ullrich, A. and J. Schlessinger (1990). "Signal transduction by receptors with tyrosine kinase activity." Cell **61**(2): 203-212.

Untergasser, A., I. Cutcutache, T. Koressaar, J. Ye, B. C. Faircloth, M. Remm and S. G. Rozen (2012). "Primer3--new capabilities and interfaces." Nucleic Acids Res **40**(15): e115.

Uribe, J. M. and K. E. Barrett (1997). "Nonmitogenic actions of growth factors: an integrated view of their role in intestinal physiology and pathophysiology." Gastroenterology **112**(1): 255-268.

Uribe, J. M., C. M. Gelbmann, A. E. Traynor-Kaplan and K. E. Barrett (1996). "Epidermal growth factor inhibits Ca(2+)-dependent Cl- transport in T84 human colonic epithelial cells." Am J Physiol **271**(3 Pt 1): C914-922.

Uribe, J. M., S. J. Keely, A. E. Traynor-Kaplan and K. E. Barrett (1996). "Phosphatidylinositol 3-kinase mediates the inhibitory effect of epidermal growth factor on calcium-dependent chloride secretion." J Biol Chem **271**(43): 26588-26595.

Van Cutsem, E., M. Peeters, S. Siena, Y. Humblet, A. Hendlisz, B. Neyns, J. L. Canon, J. L. Van Laethem, J. Maurel, G. Richardson, M. Wolf and R. G. Amado (2007). "Open-label phase III trial of panitumumab plus best supportive care compared with best supportive care

alone in patients with chemotherapy-refractory metastatic colorectal cancer." Journal of clinical oncology : official journal of the American Society of Clinical Oncology **25**(13): 1658-1664.

Van Sebille, Y. Z., R. J. Gibson, H. R. Wardill and J. M. Bowen (2015). "ErbB small molecule tyrosine kinase inhibitor (TKI) induced diarrhoea: Chloride secretion as a mechanistic hypothesis." Cancer Treat Rev **41**(7): 646-652.

Viele, C. S. (2003). "Overview of chemotherapy-induced diarrhea." Seminars in oncology nursing **19**(4 Suppl 3): 2-5.

Vincent, K. M., S. D. Findlay and L. M. Postovit (2015). "Assessing breast cancer cell lines as tumour models by comparison of mRNA expression profiles." Breast Cancer Research **17**(1): 1.

von Richter, O., B. Greiner, M. F. Fromm, R. Fraser, T. Omari, M. L. Barclay, J. Dent, A. A. Somogyi and M. Eichelbaum (2001). "Determination of in vivo absorption, metabolism, and transport of drugs by the human intestinal wall and liver with a novel perfusion technique." Clin Pharmacol Ther **70**(3): 217-227.

Wada, T., X. L. Qian and M. I. Greene (1990). "Intermolecular association of the p185neu protein and EGF receptor modulates EGF receptor function." Cell **61**(7): 1339-1347.

Wadler, S., M. Atkins, D. Karp, D. Neuberg, H. Haynes and J. P. Dutcher (1998). "Clinical trial of weekly intensive therapy with 5-fluorouracil on two different schedules combined with interferon alpha-2a and filgrastim in patients with advanced solid tumors: Eastern

Cooperative Oncology Group Study P-Z991." The cancer journal from Scientific American **4**(4): 261-268.

Wadler, S., A. B. Benson, 3rd, C. Engelking, R. Catalano, M. Field, S. M. Kornblau, E. Mitchell, J. Rubin, P. Trotta and E. Vokes (1998). "Recommended guidelines for the treatment of chemotherapy-induced diarrhea." Journal of clinical oncology : official journal of the American Society of Clinical Oncology **16**(9): 3169-3178.

Wang, P., F. An, X. Zhuang, J. Liu, L. Zhao, B. Zhang, L. Liu, P. Lin and M. Li (2014). "Chronopharmacology and mechanism of antitumor effect of erlotinib in Lewis tumor-bearing mice." PloS one **9**(7): e101720.

Wang, P., P. Fredlin, C. G. Davis and X. D. Yang (2003). Human anti-EGF receptor monoclonal antibody ABX-EGF: a potential monotherapy for the treatment of prostate cancer. American Society of Clinical Oncology.

Wang, Y. F., X. Xiang, X. Pei, S. Li, C. Tang, L. Wang and Z. F. Ke (2014). "Lung adenocarcinoma harboring L858R and T790M mutations in epidermal growth factor receptor, with poor response to gefitinib: A case report." Oncol Lett **8**(3): 1039-1042.

Wapnir, R. A. and S. Teichberg (2002). "Regulation mechanisms of intestinal secretion: implications in nutrient absorption." The Journal of nutritional biochemistry **13**(4): 190-199.

Wardill, H. R., J. M. Bowen and R. J. Gibson (2012). "Chemotherapy-induced gut toxicity: are alterations to intestinal tight junctions pivotal?" Cancer chemotherapy and pharmacology **70**(5): 627-635.

Weaver, B. A. (2014). "How Taxol/paclitaxel kills cancer cells." Molecular biology of the cell **25**(18): 2677-2681.

Weyrich, A. S., S. Lindemann and G. A. Zimmerman (2003). "The evolving role of platelets in inflammation." J Thromb Haemost **1**(9): 1897-1905.

Widakowich, C., G. de Castro, Jr., E. de Azambuja, P. Dinh and A. Awada (2007). "Review: side effects of approved molecular targeted therapies in solid cancers." The oncologist **12**(12): 1443-1455.

Wikstrand, C. J., L. P. Hale, S. K. Batra, M. L. Hill, P. A. Humphrey, S. N. Kurpad, R. E. McLendon, D. Moscatello, C. N. Pegram, C. J. Reist and et al. (1995). "Monoclonal antibodies against EGFRvIII are tumor specific and react with breast and lung carcinomas and malignant gliomas." Cancer research **55**(14): 3140-3148.

Wikstrand, C. J., C. J. Reist, G. E. Archer, M. R. Zalutsky and D. D. Bigner (1998). "The class III variant of the epidermal growth factor receptor (EGFRvIII): characterization and utilization as an immunotherapeutic target." J Neurovirol **4**(2): 148-158.

Wiley, H. S., J. J. Herbst, B. J. Walsh, D. A. Lauffenburger, M. G. Rosenfeld and G. N. Gill (1991). "The role of tyrosine kinase activity in endocytosis, compartmentation, and down-regulation of the epidermal growth factor receptor." J Biol Chem **266**(17): 11083-11094.

Wilkinson, G. R. (2005). "Drug metabolism and variability among patients in drug response." New England Journal of Medicine **352**(21): 2211-2221.

Wilson, A. J. a. G., P.R. (1999). "Role of Epidermal Growth Factor Receptor in Basal and Stimulated Colonic Epithelial Cell Migration In Vitro." Experimental Cell Research **250**(1): 187–196.

Wood, E. R., A. T. Truesdale, O. B. McDonald, D. Yuan, A. Hassell, S. H. Dickerson, B. Ellis, C. Pennisi, E. Horne, K. Lackey, K. J. Alligood, D. W. Rusnak, T. M. Gilmer and L. Shewchuk (2004). "A unique structure for epidermal growth factor receptor bound to GW572016 (Lapatinib): relationships among protein conformation, inhibitor off-rate, and receptor activity in tumor cells." Cancer research **64**(18): 6652-6659.

Wood, E. R., A. T. Truesdale, O. B. McDonald, D. Yuan, A. Hassell, S. H. Dickerson, B. Ellis, C. Pennisi, E. Horne, K. Lackey, K. J. Alligood, D. W. Rusnak, T. M. Gilmer and L. Shewchuk (2004). "A unique structure for epidermal growth factor receptor bound to GW572016 (Lapatinib): relationships among protein conformation, inhibitor off-rate, and receptor activity in tumor cells." Cancer Res **64**(18): 6652-6659.

Wood, S. R., Q. Zhao, L. H. Smith and C. K. Daniels (2003). "Altered morphology in cultured rat intestinal epithelial IEC-6 cells is associated with alkaline phosphatase expression." Tissue Cell **35**(1): 47-58.

Worthylake, R., L. K. Opresko and H. S. Wiley (1999). "ErbB-2 amplification inhibits down-regulation and induces constitutive activation of both ErbB-2 and epidermal growth factor receptors." J Biol Chem **274**(13): 8865-8874.

Xia, W., S. Bacus, P. Hegde, I. Husain, J. Strum, L. Liu, G. Paulazzo, L. Lyass, P. Trusk, J. Hill, J. Harris and N. L. Spector (2006). "A model of acquired autoresistance to a potent ErbB2 tyrosine kinase inhibitor and a therapeutic strategy to prevent its onset in breast cancer." Proceedings of the National Academy of Sciences of the United States of America **103**(20): 7795-7800.

Xia, W., C. M. Gerard, L. Liu, N. M. Baudson, T. L. Ory and N. L. Spector (2005). "Combining lapatinib (GW572016), a small molecule inhibitor of ErbB1 and ErbB2 tyrosine kinases, with therapeutic anti-ErbB2 antibodies enhances apoptosis of ErbB2-overexpressing breast cancer cells." Oncogene **24**(41): 6213-6221.

Xia, W., R. J. Mullin, B. R. Keith, L. H. Liu, H. Ma, D. W. Rusnak, G. Owens, K. J. Alligood and N. L. Spector (2002). "Anti-tumor activity of GW572016: a dual tyrosine kinase inhibitor blocks EGF activation of EGFR/erbB2 and downstream Erk1/2 and AKT pathways." Oncogene **21**(41): 6255-6263.

Xia, W., E. F. Petricoin, 3rd, S. Zhao, L. Liu, T. Osada, Q. Cheng, J. D. Wulfkuhle, W. R. Gwin, X. Yang, R. I. Gallagher, S. Bacus, H. K. Lyerly and N. L. Spector (2013). "An heregulin-EGFR-HER3 autocrine signaling axis can mediate acquired lapatinib resistance in HER2+ breast cancer models." Breast cancer research : BCR **15**(5): R85.

Xiao, W. D., W. Chen, L. H. Sun, W. S. Wang, S. W. Zhou and H. Yang (2011). "The protective effect of enteric glial cells on intestinal epithelial barrier function is enhanced by inhibiting inducible nitric oxide synthase activity under lipopolysaccharide stimulation." Mol Cell Neurosci **46**(2): 527-534.

Xu, J., G. Huang, Z. Zhang, J. Zhao, M. Zhang, Y. Wang, Z. Liu and J. Lu (2015). "Up-Regulation of Glioma-Associated Oncogene Homolog 1 Expression by Serum Starvation Promotes Cell Survival in ER-Positive Breast Cancer Cells." Cell Physiol Biochem **36**(5): 1862-1876.

Yamaoka, T., F. Yan, H. Cao, S. S. Hobbs, R. S. Dise, W. Tong and D. B. Polk (2008). "Transactivation of EGF receptor and ErbB2 protects intestinal epithelial cells from TNF-induced apoptosis." Proceedings of the National Academy of Sciences **105**(33): 11772-11777.

Yan, F., L. Liu, P. J. Dempsey, Y.-H. Tsai, E. W. Raines, C. L. Wilson, H. Cao, Z. Cao, L. Liu and D. B. Polk (2013). "A Lactobacillus rhamnosus GG-derived soluble protein, p40, stimulates ligand release from intestinal epithelial cells to transactivate epidermal growth factor receptor." Journal of Biological Chemistry **288**(42): 30742-30751.

Yang, J. C.-H., S. Popat, P. Georgiou, E. Miyamoto, J. D. Isaacson and H. A. Wakelee (2015). TIGER-3: A phase 3, open-label, randomized study of rociletinib vs cytotoxic chemotherapy in patients (pts) with mutant EGFR non-small cell lung cancer (NSCLC) progressing on prior EGFR TKI therapy and doublet chemotherapy. ASCO Annual Meeting Proceedings.

Yano, S., K. Kondo, M. Yamaguchi, G. Richmond, M. Hutchison, A. Wakeling, S. Averbuch and P. Wadsworth (2003). "Distribution and function of EGFR in human tissue and the effect of EGFR tyrosine kinase inhibition." Anticancer research **23**(5A): 3639-3650.

Yarden, Y. and M. X. Sliwkowski (2001). "Untangling the ErbB signalling network." Nature reviews. Molecular cell biology **2**(2): 127-137.

Yarden, Y. and A. Ullrich (1988). "Growth factor receptor tyrosine kinases." Annual review of biochemistry **57**: 443-478.

Yeoh, A. S., J. M. Bowen, R. J. Gibson and D. M. Keefe (2005). "Nuclear factor kappaB (NFkappaB) and cyclooxygenase-2 (Cox-2) expression in the irradiated colorectum is associated with subsequent histopathological changes." Int J Radiat Oncol Biol Phys **63**(5): 1295-1303.

Yusta, B., D. Holland, J. A. Koehler, M. Maziarz, J. L. Estall, R. Higgins and D. J. Drucker (2009). "ErbB signaling is required for the proliferative actions of GLP-2 in the murine gut." Gastroenterology **137**(3): 986-996.

Zhang, L., C. Fan, Z. Guo, Y. Li, S. Zhao, S. Yang, Y. Yang, J. Zhu and D. Lin (2013). "Discovery of a potent dual EGFR/HER-2 inhibitor L-2 (selatinib) for the treatment of cancer." Eur J Med Chem **69**: 833-841.

Zhang, Y., P. E. Dubé, M. K. Washington, F. Yan and D. B. Polk (2012). "ErbB2 and ErbB3 regulate recovery from dextran sulfate sodium-induced colitis by promoting mouse colon epithelial cell survival." Laboratory Investigation **92**(3): 437-450.

Zhou, Y., S. Li, Y. P. Hu, J. Wang, J. Hauser, A. N. Conway, M. A. Vinci, L. Humphrey, E. Zborowska, J. K. Willson and M. G. Brattain (2006). "Blockade of EGFR and ErbB2 by the novel dual EGFR and ErbB2 tyrosine kinase inhibitor GW572016 sensitizes human colon carcinoma GEO cells to apoptosis." Cancer Res **66**(1): 404-411.

Zhu, J., X. Jia, G. Xiao, Y. Kang, N. C. Partridge and L. Qin (2007). "EGF-like ligands stimulate osteoclastogenesis by regulating expression of osteoclast regulatory factors by osteoblasts: implications for osteolytic bone metastases." J Biol Chem **282**(37): 26656-26664.

Appendix

Fluorescence activated cell sorting analysis (FACS)

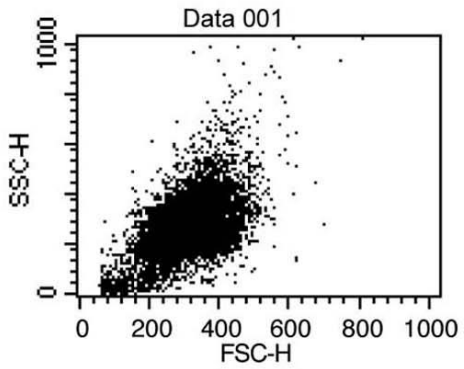

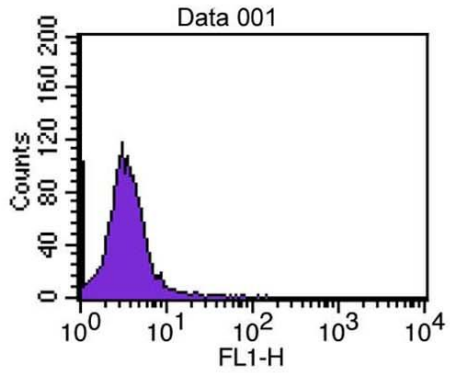

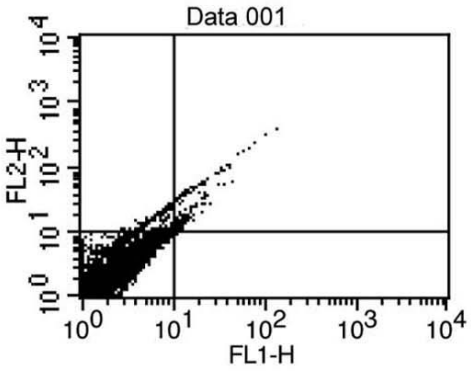

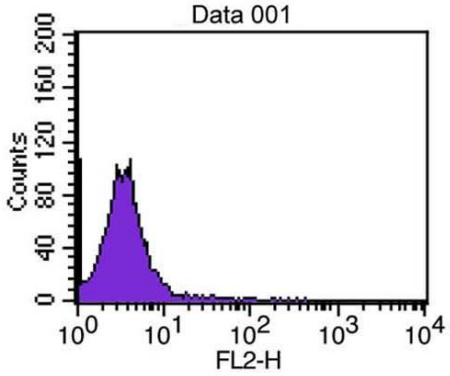

Quadrant Statistics

File: Data 001
Sample ID:
Tube: Untitled
Acquisition Date: 26-Apr-13
Gated Events: 10000
X Parameter: FL1-H (Log)
Quad Location: 10, 10

Log Data Units: Linear Values
Patient ID:
Panel: Untitled Acquisition Tube List
Gate: No Gate
Total Events: 10000
Y Parameter: FL2-H (Log)

Quad	Events	% Gated	% Total	X Mean	X Geo Mean	Y Mean	Y Geo Mean
UL	165	1.65	1.65	7.27	6.93	14.20	13.54
UR	150	1.50	1.50	19.50	16.63	40.40	27.91
LL	9684	96.84	96.84	3.38	3.10	3.52	3.15
LR	1	0.01	0.01	11.04	11.04	9.06	9.06

Histogram plot of negative control without staining for **Walker 256** control untreated cells (results are representative of each group)

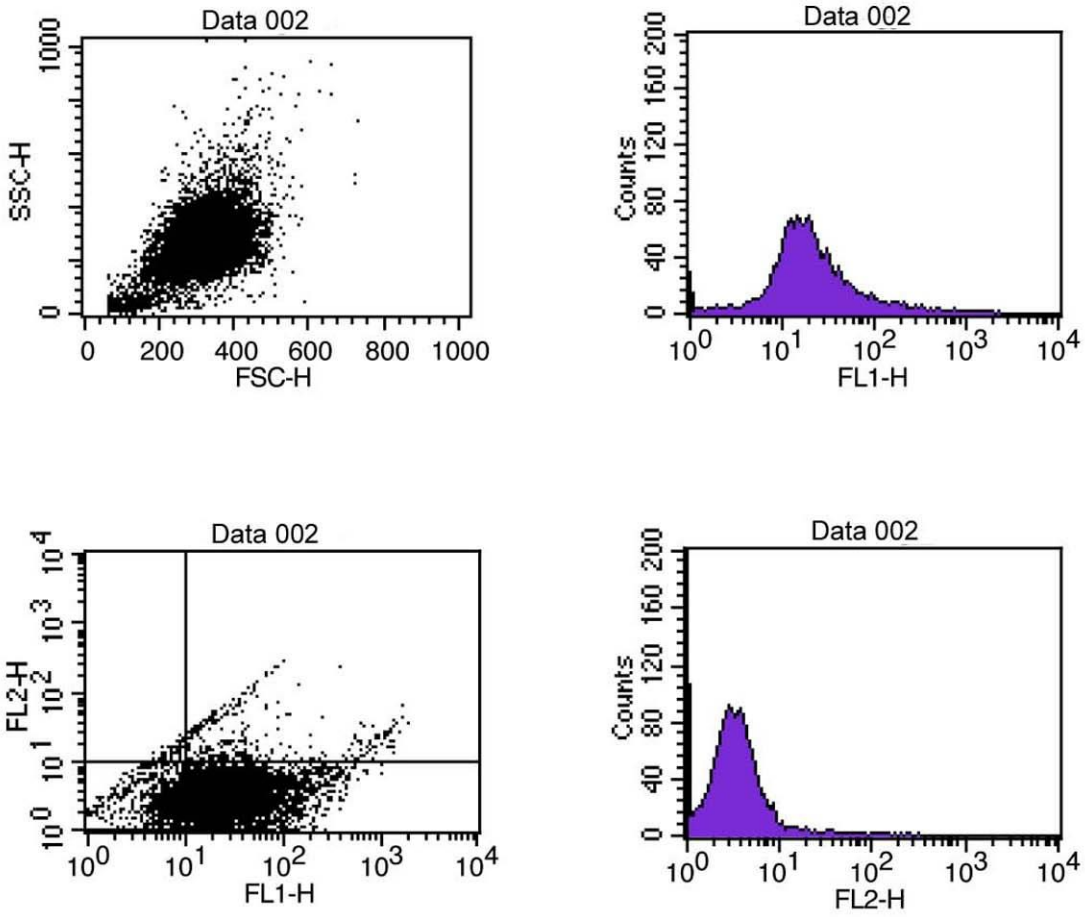

Quadrant Statistics

File: Data 002
Sample ID:
Tube: Untitled
Acquisition Date: 26-Apr-13
Gated Events: 10000
X Parameter: FL1-H (Log)
Quad Location: 10, 10

Log Data Units: Linear Values
Patient ID:
Panel: Untitled Acquisition Tube List
Gate: No Gate
Total Events: 10000
Y Parameter: FL2-H (Log)

Quad	Events	% Gated	% Total	X Mean	X Geo Mean	Y Mean	Y Geo Mean
UL	49	0.49	0.49	7.50	7.34	14.09	13.76
UR	307	3.07	3.07	232.17	63.52	32.06	22.46
LL	1769	17.69	17.69	7.09	6.37	2.75	2.41
LR	7875	78.75	78.75	35.64	24.39	3.55	3.20

Histogram plot of negative control with FITC staining for **Walker 256** control untreated cells (results are representative of each group)

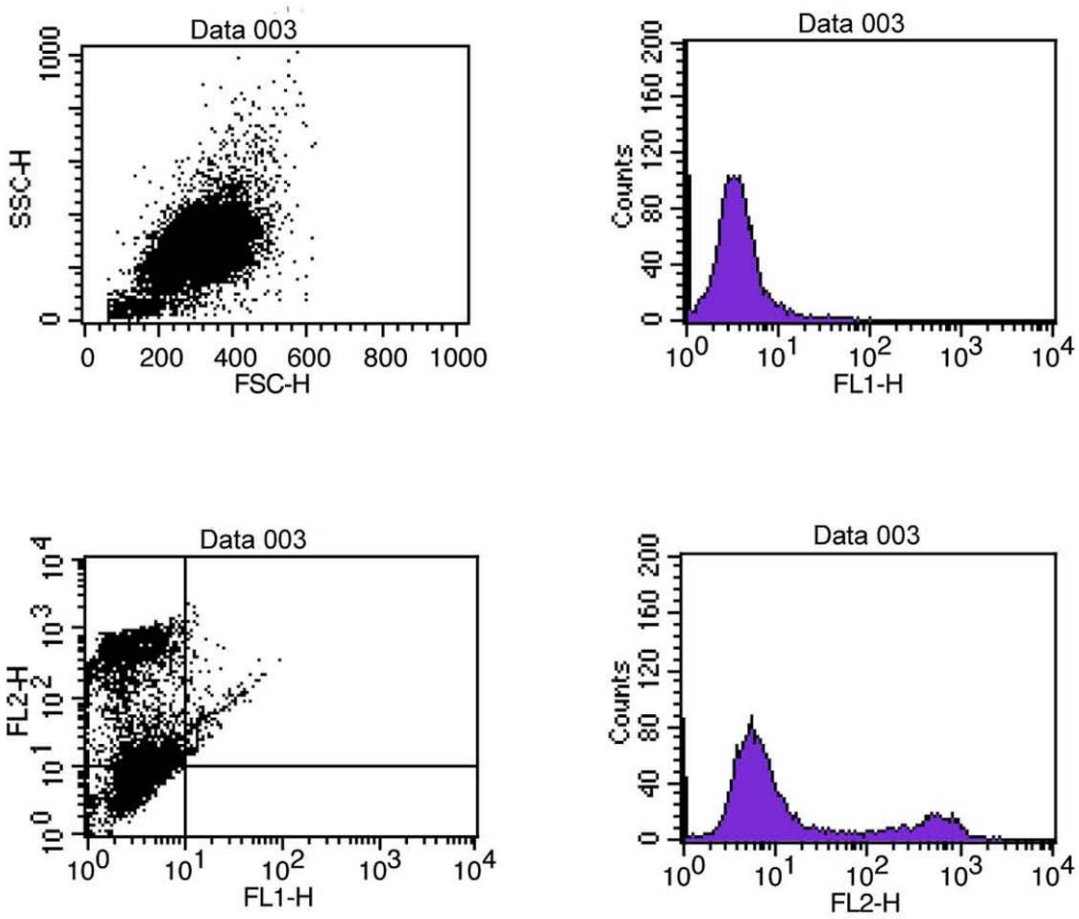

Quadrant Statistics

File: Data 003
Log Data Units: Linear Values
Sample ID:
Patient ID:
Tube: Untitled
Panel: Untitled Acquisition Tube List
Acquisition Date: 26-Apr-13
Gate: No Gate
Gated Events: 10000
Total Events: 10000
X Parameter: FL1-H (Log)
Y Parameter: FL2-H (Log)
Quad Location: 10, 10

Quad	Events	% Gated	% Total	X Mean	X Geo Mean	Y Mean	Y Geo Mean
UL	2982	29.82	29.82	3.81	3.24	258.12	92.80
UR	199	1.99	1.99	19.56	17.22	163.67	70.27
LL	6819	68.19	68.19	3.39	3.20	5.44	5.08
LR	0	0.00	0.00	***	***	***	***

Histogram plot of negative control with propidium iodide staining for **Walker 256** control untreated cells (results are representative of each group)

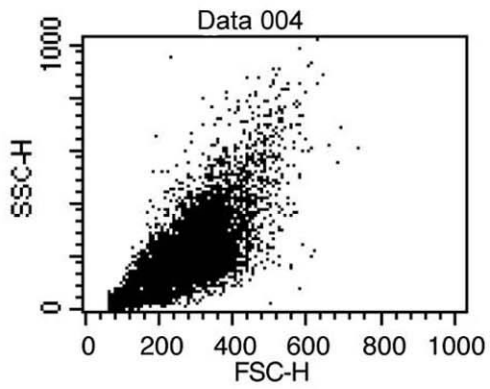

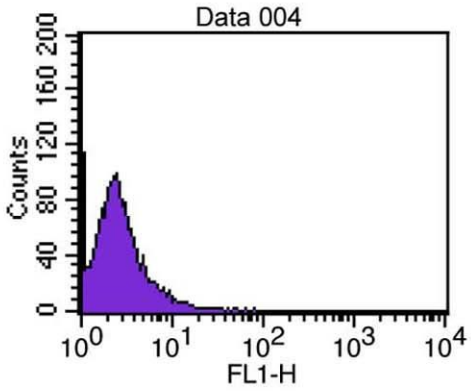

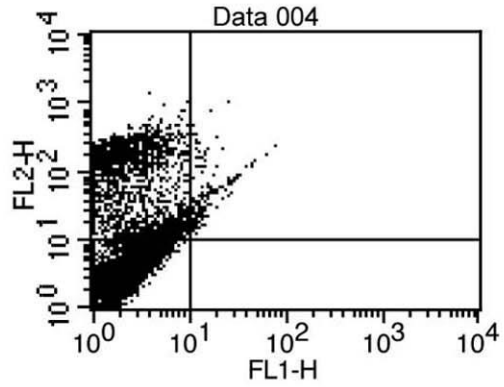

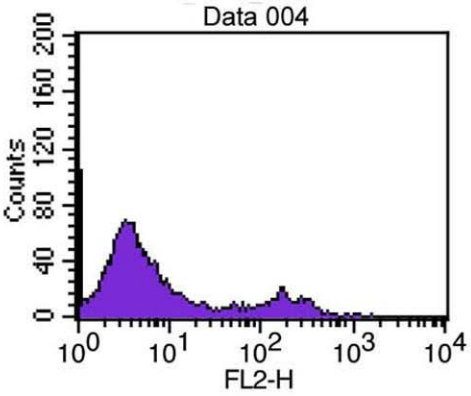

Quadrant Statistics

File: Data 004
Sample ID:
Tube: Untitled
Acquisition Date: 26-Apr-13
Gated Events: 10000
X Parameter: FL1-H (Log)
Quad Location: 10, 10

Log Data Units: Linear Values
Patient ID:
Panel: Untitled Acquisition Tube List
Gate: No Gate
Total Events: 10000
Y Parameter: FL2-H (Log)

Quad	Events	% Gated	% Total	X Mean	X Geo Mean	Y Mean	Y Geo Mean
UL	2145	21.45	21.45	3.48	2.72	109.45	59.46
UR	169	1.69	1.69	16.57	15.09	78.45	46.85
LL	7686	76.86	76.86	2.42	2.20	3.73	3.21
LR	0	0.00	0.00	***	***	***	***

Histogram plot of **Walker 256** control untreated cells at 6 hours incubation (results are representative of each group)

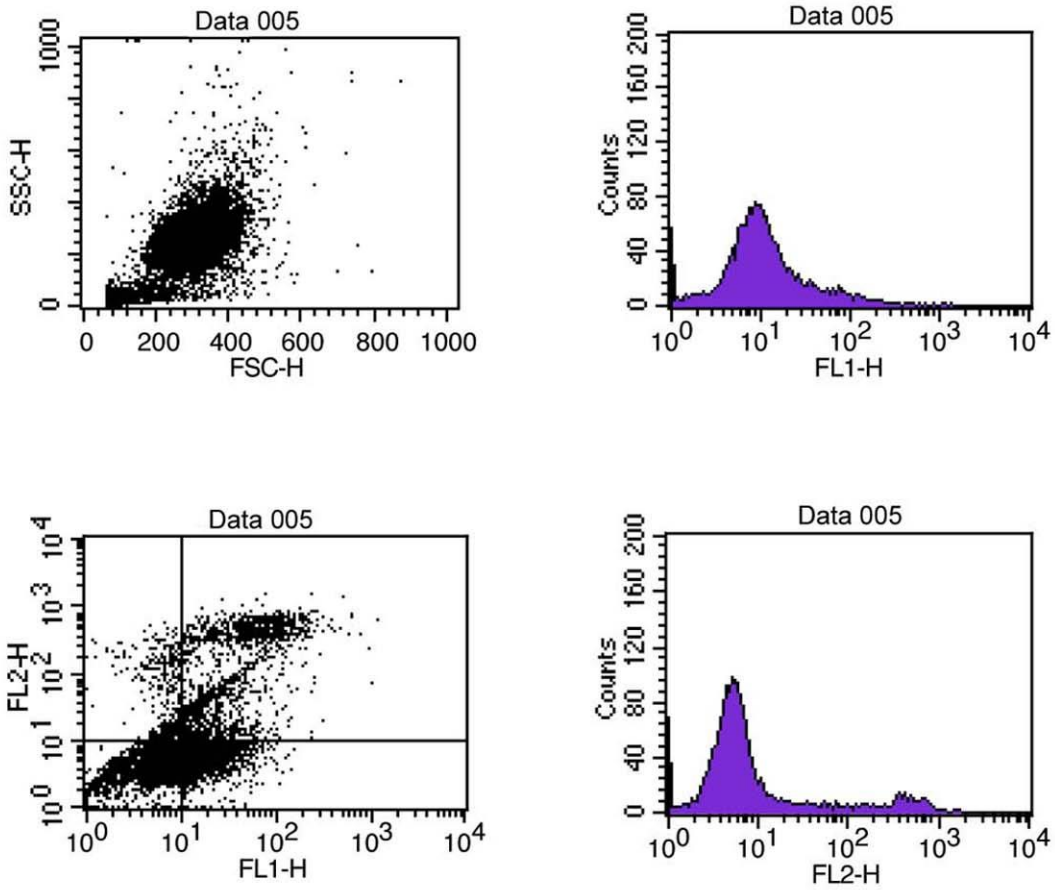

Quadrant Statistics

File: Data 005
Log Data Units: Linear Values
Sample ID:
Patient ID:
Tube: Untitled
Panel: Untitled Acquisition Tube List
Acquisition Date: 26-Apr-13
Gate: No Gate
Gated Events: 10000
Total Events: 10000
X Parameter: FL1-H (Log)
Y Parameter: FL2-H (Log)
Quad Location: 10, 10

Quad	Events	% Gated	% Total	X Mean	X Geo Mean	Y Mean	Y Geo Mean
UL	472	4.72	4.72	7.03	6.60	82.76	38.75
UR	1542	15.42	15.42	57.26	36.91	233.33	97.50
LL	5111	51.11	51.11	6.40	5.83	4.53	4.23
LR	2875	28.75	28.75	18.06	16.05	5.68	5.39

Histogram plot of **Walker 256** lapatinib-treated cells at 6 hours incubation (results are representative of each group)

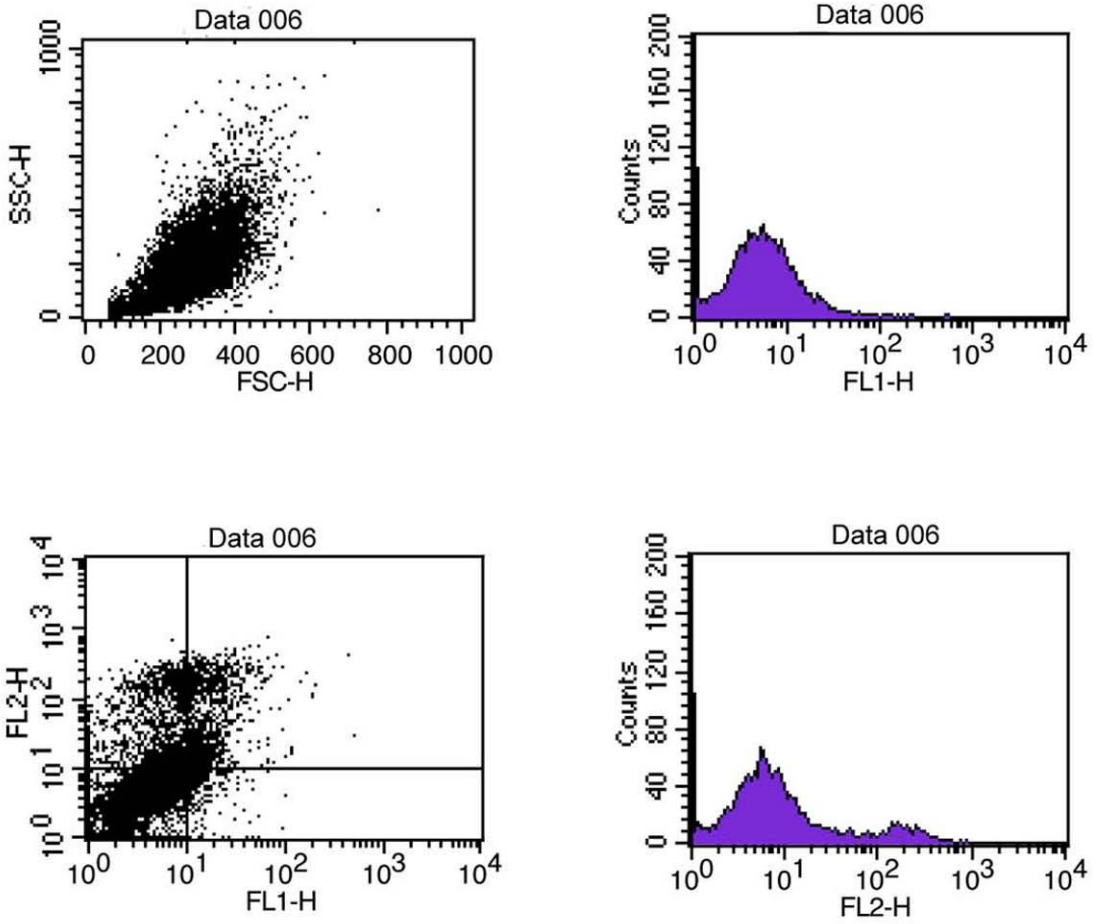

Quadrant Statistics

File: Data 006
Sample ID:
Tube: Untitled
Acquisition Date: 26-Apr-13
Gated Events: 10000
X Parameter: FL1-H (Log)
Quad Location: 10, 10

Log Data Units: Linear Values
Patient ID:
Panel: Untitled Acquisition Tube List
Gate: No Gate
Total Events: 10000
Y Parameter: FL2-H (Log)

Quad	Events	% Gated	% Total	X Mean	X Geo Mean	Y Mean	Y Geo Mean
UL	1637	16.37	16.37	6.12	5.39	60.50	30.69
UR	1221	12.21	12.21	20.23	16.93	89.34	44.41
LL	6813	68.13	68.13	4.24	3.59	4.58	3.78
LR	329	3.29	3.29	15.77	14.20	6.49	5.80

Histogram plot of **Walker 256** control untreated cells at 24 hours incubation (results are representative of each group)

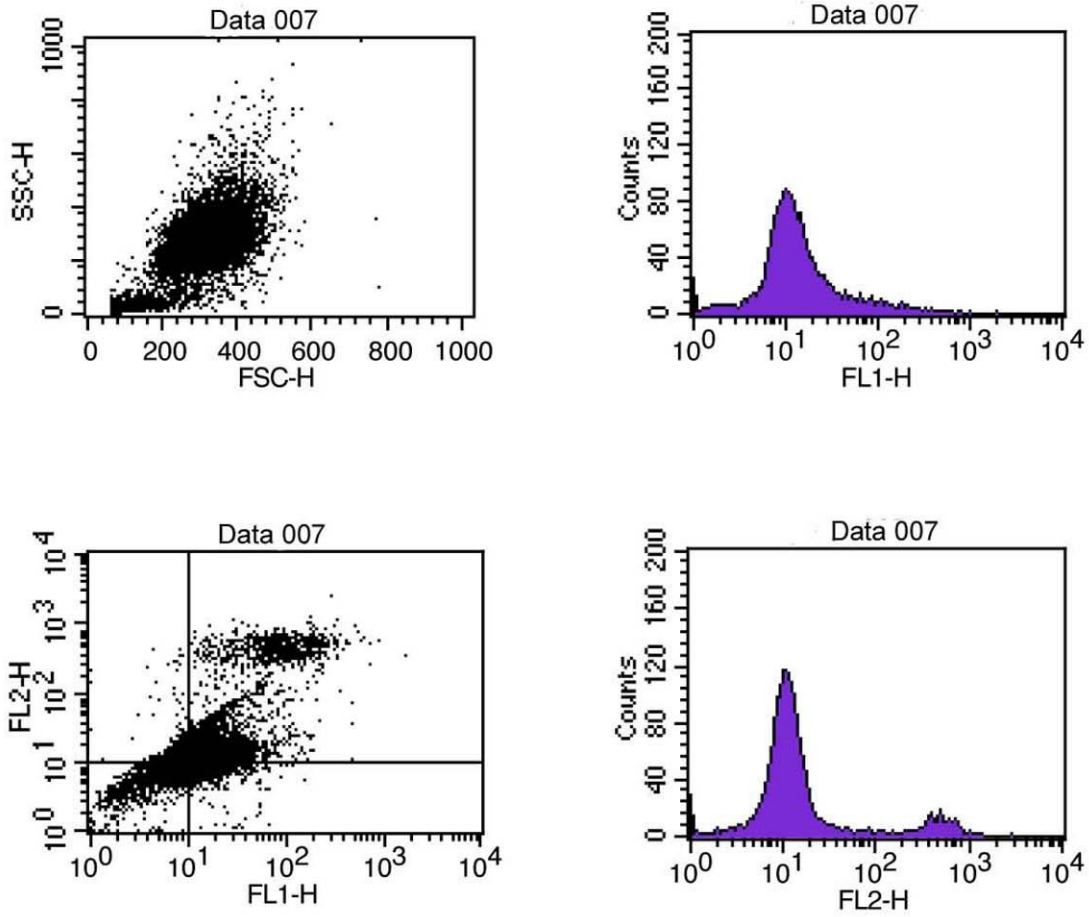

Quadrant Statistics

File: Data 007
Sample ID:
Tube: Untitled
Acquisition Date: 26-Apr-13
Gated Events: 10000
X Parameter: FL1-H (Log)
Quad Location: 10, 10

Log Data Units: Linear Values
Patient ID:
Panel: Untitled Acquisition Tube List
Gate: No Gate
Total Events: 10000
Y Parameter: FL2-H (Log)

Quad	Events	% Gated	% Total	X Mean	X Geo Mean	Y Mean	Y Geo Mean
UL	1621	16.21	16.21	8.38	8.24	15.15	12.54
UR	4472	44.72	44.72	35.58	22.35	93.12	27.25
LL	2566	25.66	25.66	6.60	6.01	7.11	6.66
LR	1341	13.41	13.41	17.53	15.80	8.05	7.84

Histogram plot of **Walker 256** lapatinib-treated cells at 24 hours incubation (results are representative of each group)

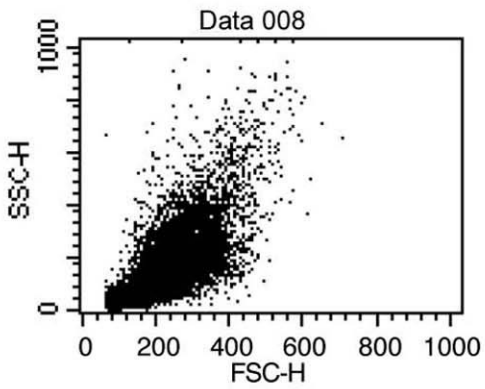

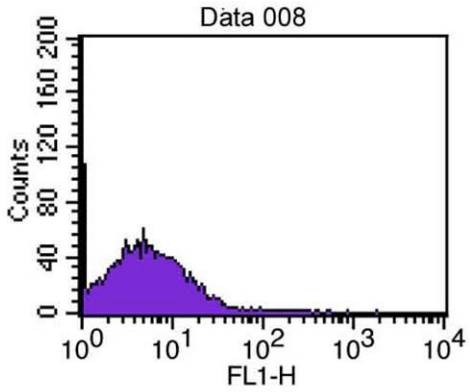

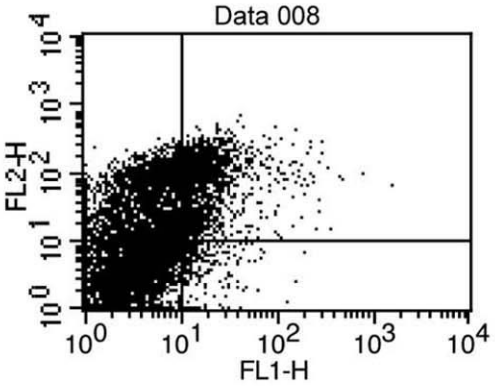

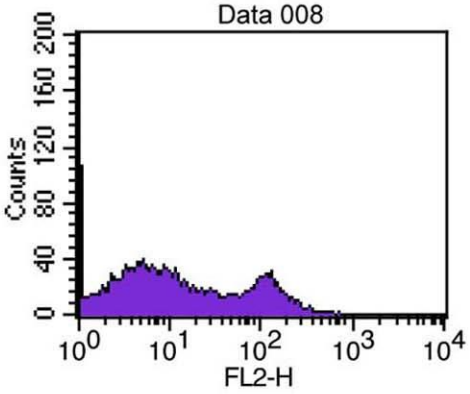

Quadrant Statistics

File: Data 008
Log Data Units: Linear Values
Sample ID:
Patient ID:
Tube: Untitled
Panel: Untitled Acquisition Tube List
Acquisition Date: 26-Apr-13
Gate: No Gate
Gated Events: 10000
Total Events: 10000
X Parameter: FL1-H (Log)
Y Parameter: FL2-H (Log)
Quad Location: 10, 10

Quad	Events	% Gated	% Total	X Mean	X Geo Mean	Y Mean	Y Geo Mean
UL	2770	27.70	27.70	5.32	4.48	54.40	36.50
UR	1732	17.32	17.32	25.25	18.24	98.39	69.04
LL	5254	52.54	52.54	3.43	2.80	3.86	3.00
LR	244	2.44	2.44	20.30	16.83	5.42	4.62

Histogram plot of **Walker 256** control untreated cells at 48 hours incubation (results are representative of each group)

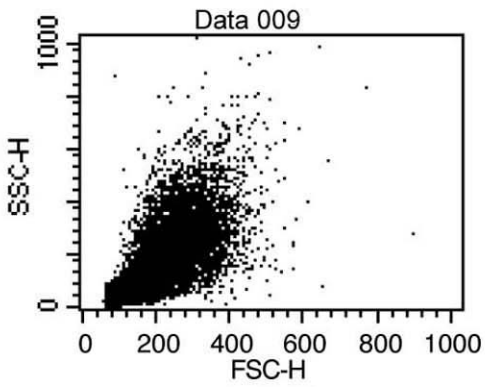

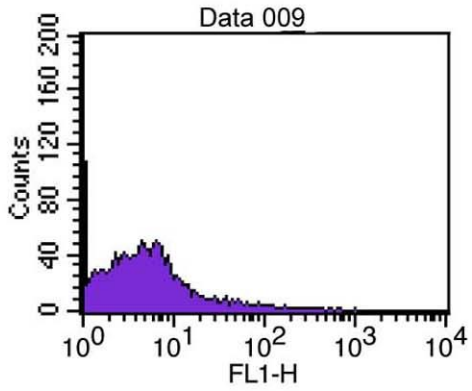

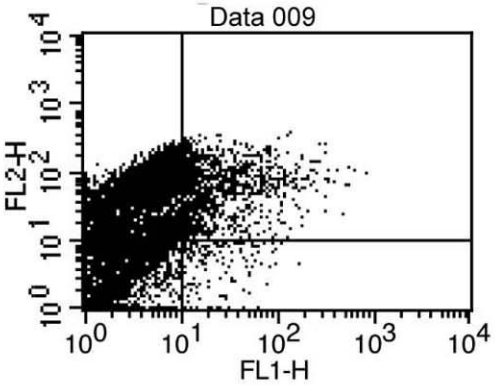

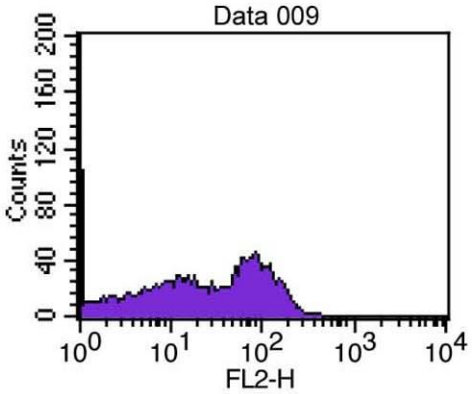

Quadrant Statistics

File: Data 009
Sample ID:
Tube: Untitled
Acquisition Date: 26-Apr-13
Gated Events: 10000
X Parameter: FL1-H (Log)
Quad Location: 10, 10

Log Data Units: Linear Values
Patient ID:
Panel: Untitled Acquisition Tube List
Gate: No Gate
Total Events: 10000
Y Parameter: FL2-H (Log)

Quad	Events	% Gated	% Total	X Mean	X Geo Mean	Y Mean	Y Geo Mean
UL	5393	53.93	53.93	4.63	3.87	60.52	44.99
UR	1308	13.08	13.08	37.78	23.56	78.73	57.40
LL	3139	31.39	31.39	2.51	1.98	3.94	2.93
LR	160	1.60	1.60	28.17	22.42	5.64	4.67

Histogram plot of **Walker 256** lapatinib-treated cells at 48 hours incubation (results are representative of each group)

Quadrant Statistics

File: Data.001
Sample ID:
Tube: Untitled
Acquisition Date: 30-Apr-13
Gated Events: 10000
X Parameter: FL1-H (Log)
Quad Location: 10, 11

Log Data Units: Linear Values
Patient ID:
Panel: Untitled Acquisition Tube Lis
Gate: No Gate
Total Events: 10000
Y Parameter: FL2-H (Log)

Quad	Events	% Gated	% Tota	X Mean	X Geo Mean	Y Mean	Y Geo Mear
UL	127	1.27	1.27	8.31	7.91	14.01	12.85
UR	319	3.19	3.19	24.19	18.16	38.05	25.29
LL	9545	95.45	95.45	3.20	2.86	3.53	3.04
LR	9	0.09	0.09	10.46	10.46	10.27	10.25

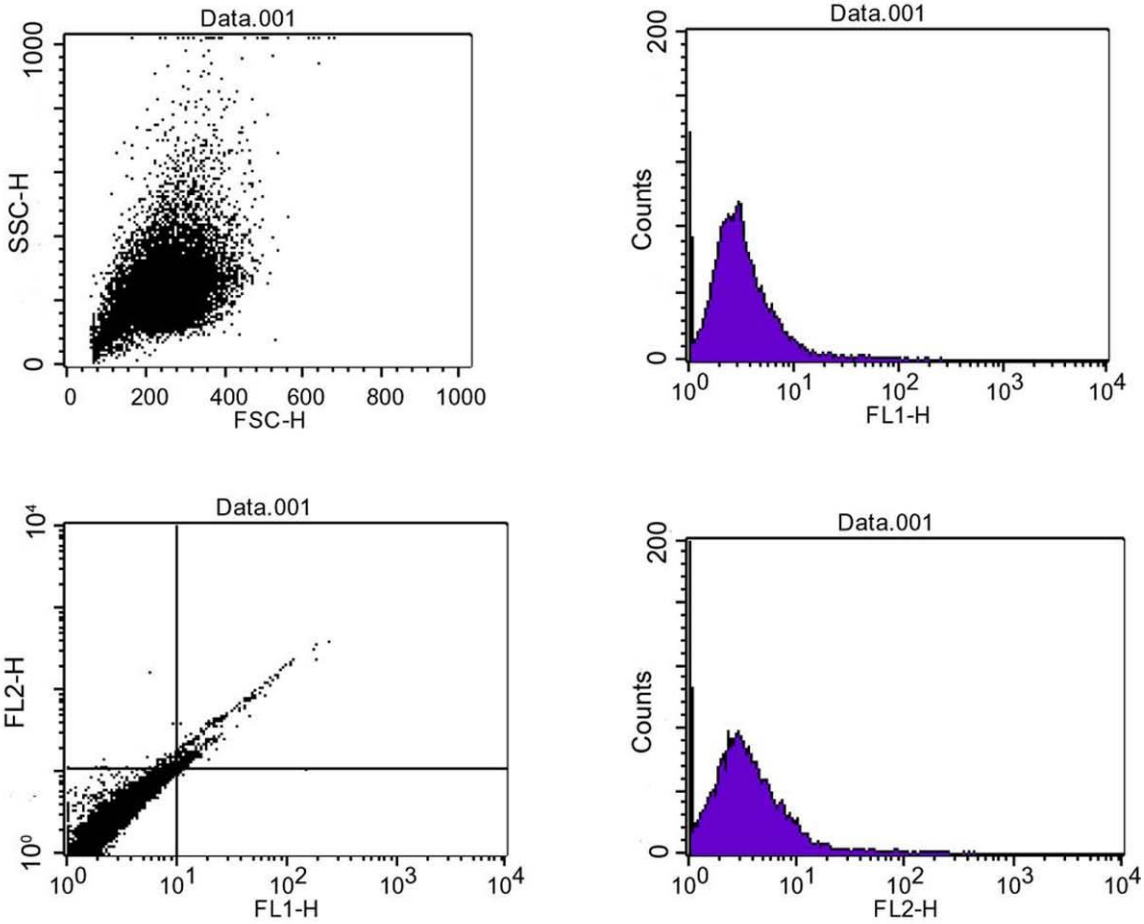

Histogram plot of negative control without staining for **IEC-6** control untreated cells (results are representative of each group)

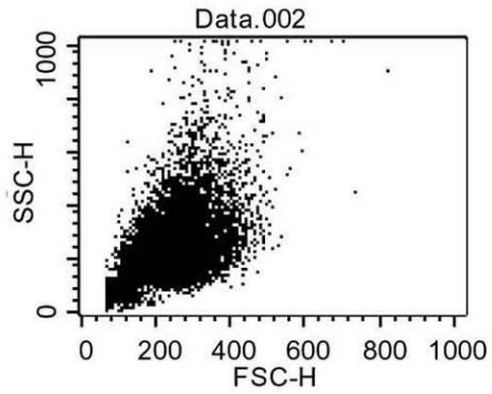

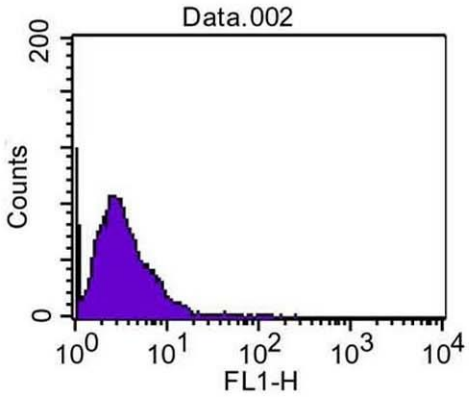

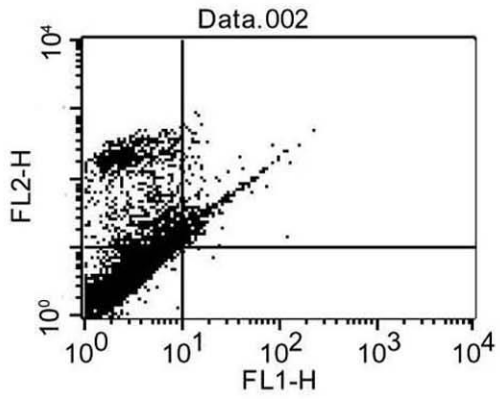

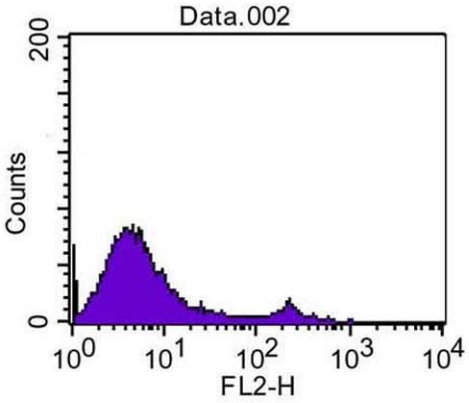

Quadrant Statistics

File: Data.002
Log Data Units: Linear Values
Sample ID:
Patient ID:
Tube: Untitled
Panel: Untitled Acquisition Tube Lis
Acquisition Date: 30-Apr-13
Gate: No Gate
Gated Events: 10000
Total Events: 10000
X Parameter: FL1-H (Log)
Y Parameter: FL2-H (Log)
Quad Location: 10, 10

Quad	Events	% Gated	% Tota	X Mean	X Geo Mean	Y Mean	Y Geo Mean
UL	1627	16.27	16.27	5.29	4.54	86.30	37.73
UR	365	3.65	3.65	21.10	16.94	66.54	37.79
LL	8004	80.04	80.04	3.01	2.75	4.29	3.82
LR	4	0.04	0.04	13.61	13.10	8.65	8.58

Histogram plot of negative control with FITC staining for **IEC-6** control untreated cells (results are representative of each group)

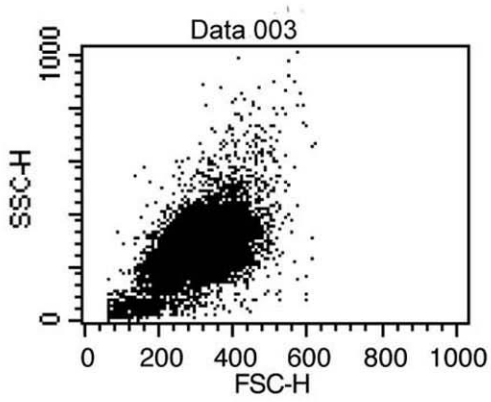

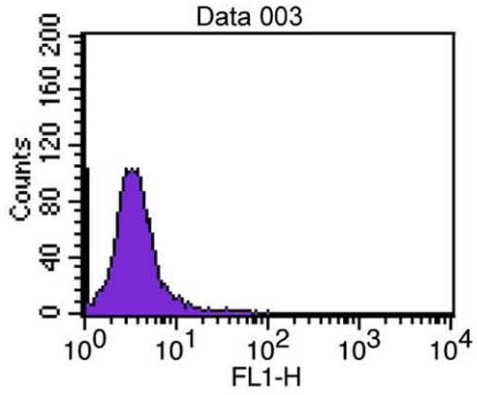

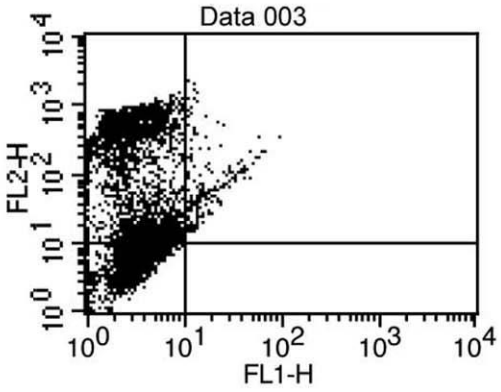

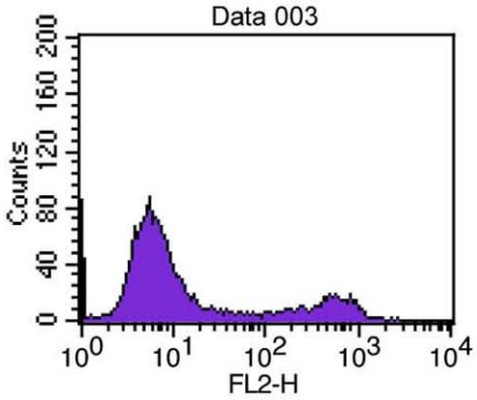

Quadrant Statistics

File: Data 003
Sample ID:
Tube: Untitled
Acquisition Date: 26-Apr-13
Gated Events: 10000
X Parameter: FL1-H (Log)
Quad Location: 10, 10

Log Data Units: Linear Values
Patient ID:
Panel: Untitled Acquisition Tube List
Gate: No Gate
Total Events: 10000
Y Parameter: FL2-H (Log)

Quad	Events	% Gated	% Total	X Mean	X Geo Mean	Y Mean	Y Geo Mean
UL	2982	29.82	29.82	3.81	3.24	258.12	92.80
UR	199	1.99	1.99	19.56	17.22	163.67	70.27
LL	6819	68.19	68.19	3.39	3.20	5.44	5.08
LR	0	0.00	0.00	***	***	***	***

Histogram plot of negative control with propidium iodide staining for **IEC-6** control untreated cells (results are representative of each group)

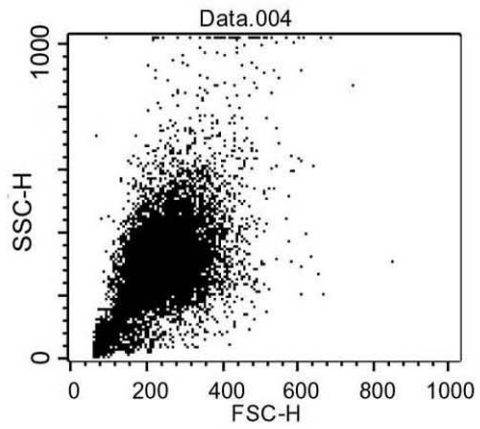

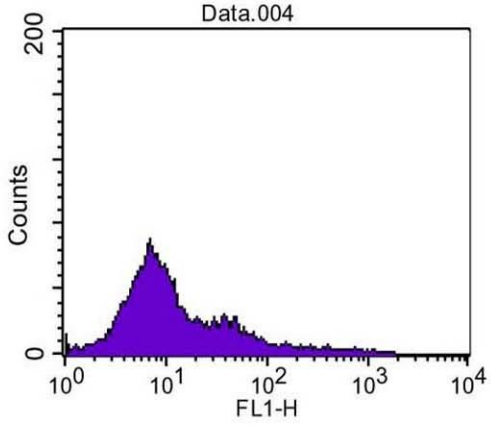

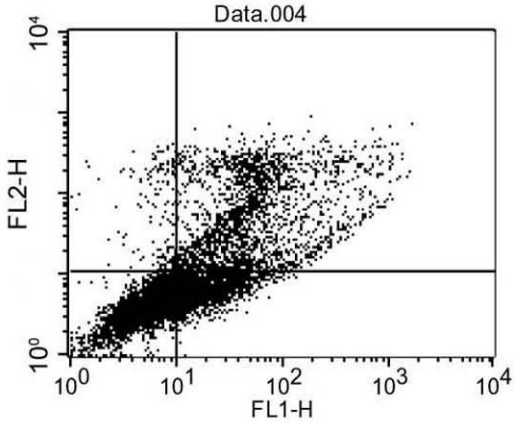

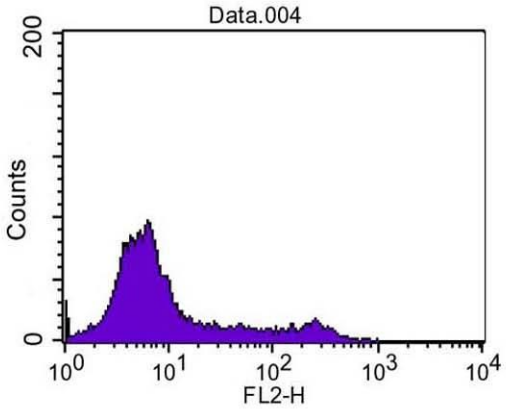

Quadrant Statistics

File: Data.004
Sample ID:
Tube: Untitled
Acquisition Date: 30-Apr-13
Gated Events: 10000
X Parameter: FL1-H (Log)
Quad Location: 10, 11

Log Data Units: Linear Values
Patient ID:
Panel: Untitled Acquisition Tube Lis
Gate: No Gate
Total Events: 10000
Y Parameter: FL2-H (Log)

Quad	Events	% Gated	% Tota	X Mean	X Geo Mean	Y Mean	Y Geo Mear
UL	202	2.02	2.02	7.39	6.90	95.20	46.49
UR	2227	22.27	22.27	100.20	51.47	98.98	54.01
LL	5592	55.92	55.92	5.93	5.49	4.74	4.38
LR	1979	19.79	19.79	20.49	17.63	6.87	6.54

Histogram plot of **IEC-6** control untreated cells at 6 hours incubation (results are representative of each group)

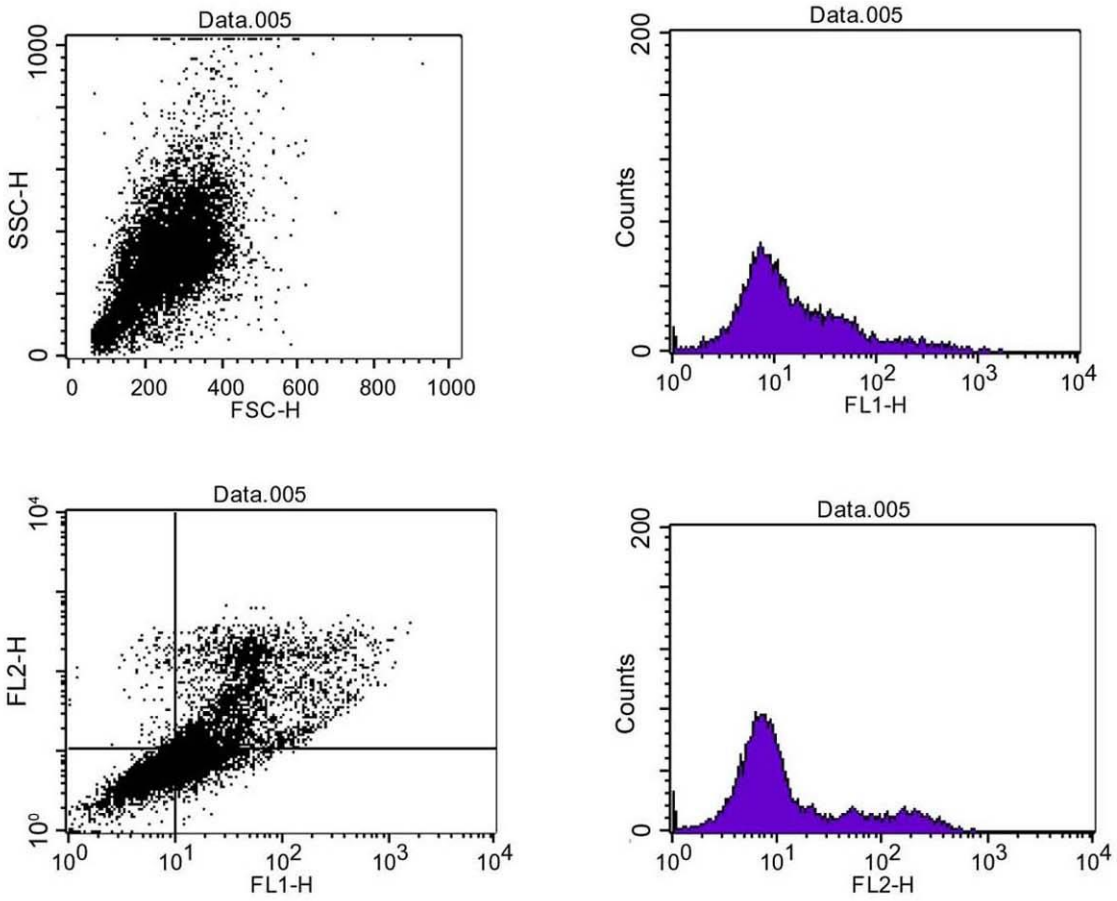

Quadrant Statistics

File: Data.005
Sample ID:
Tube: Untitled
Acquisition Date: 30-Apr-13
Gated Events: 10000
X Parameter: FL1-H (Log)
Quad Location: 10, 11

Log Data Units: Linear Values
Patient ID:
Panel: Untitled Acquisition Tube Lis
Gate: No Gate
Total Events: 10000
Y Parameter: FL2-H (Log)

Quad	Events	% Gated	% Tota	X Mean	X Geo Mean	Y Mean	Y Geo Mear
UL	194	1.94	1.94	7.72	7.30	66.82	31.00
UR	3064	30.64	30.64	80.37	43.96	80.32	45.21
LL	4763	47.63	47.63	6.37	5.97	5.79	5.39
LR	1979	19.79	19.79	18.51	16.47	7.67	7.40

Histogram plot of **IEC-6** lapatinib-treated cells at 6 hours incubation (results are representative of each group)

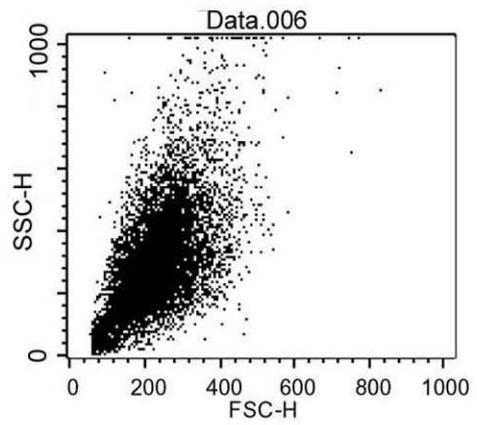

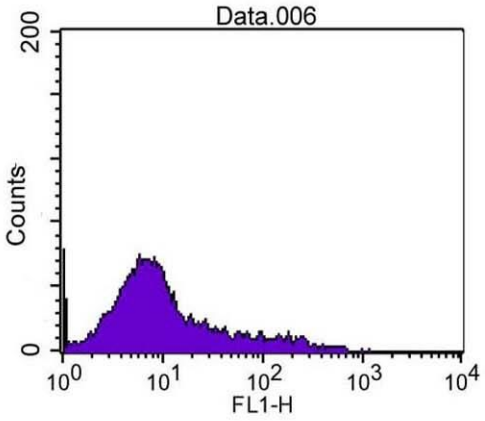

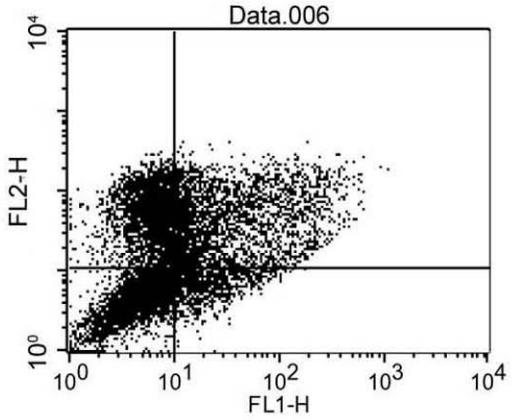

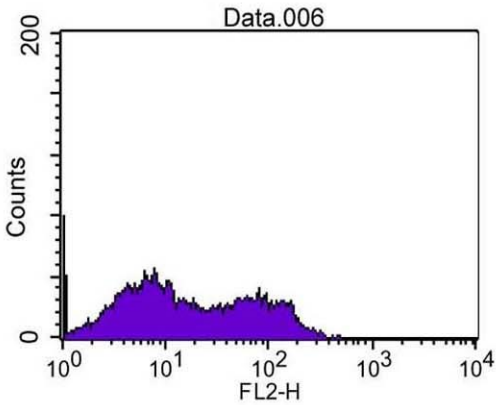

Quadrant Statistics

File: Data.006
Sample ID:
Tube: Untitled
Acquisition Date: 30-Apr-13
Gated Events: 10000
X Parameter: FL1-H (Log)
Quad Location: 10, 11

Log Data Units: Linear Values
Patient ID:
Panel: Untitled Acquisition Tube Lis
Gate: No Gate
Total Events: 10000
Y Parameter: FL2-H (Log)

Quad	Events	% Gated	% Tota	X Mean	X Geo Mean	Y Mean	Y Geo Mear
UL	2670	26.70	26.70	6.31	5.87	64.69	48.88
UR	2664	26.64	26.64	64.97	34.83	63.27	43.74
LL	3792	37.92	37.92	5.04	4.47	5.03	4.42
LR	874	8.74	8.74	26.12	21.26	7.22	6.76

Histogram plot of **IEC-6** control untreated cells at 24 hours incubation (results are representative of each group)

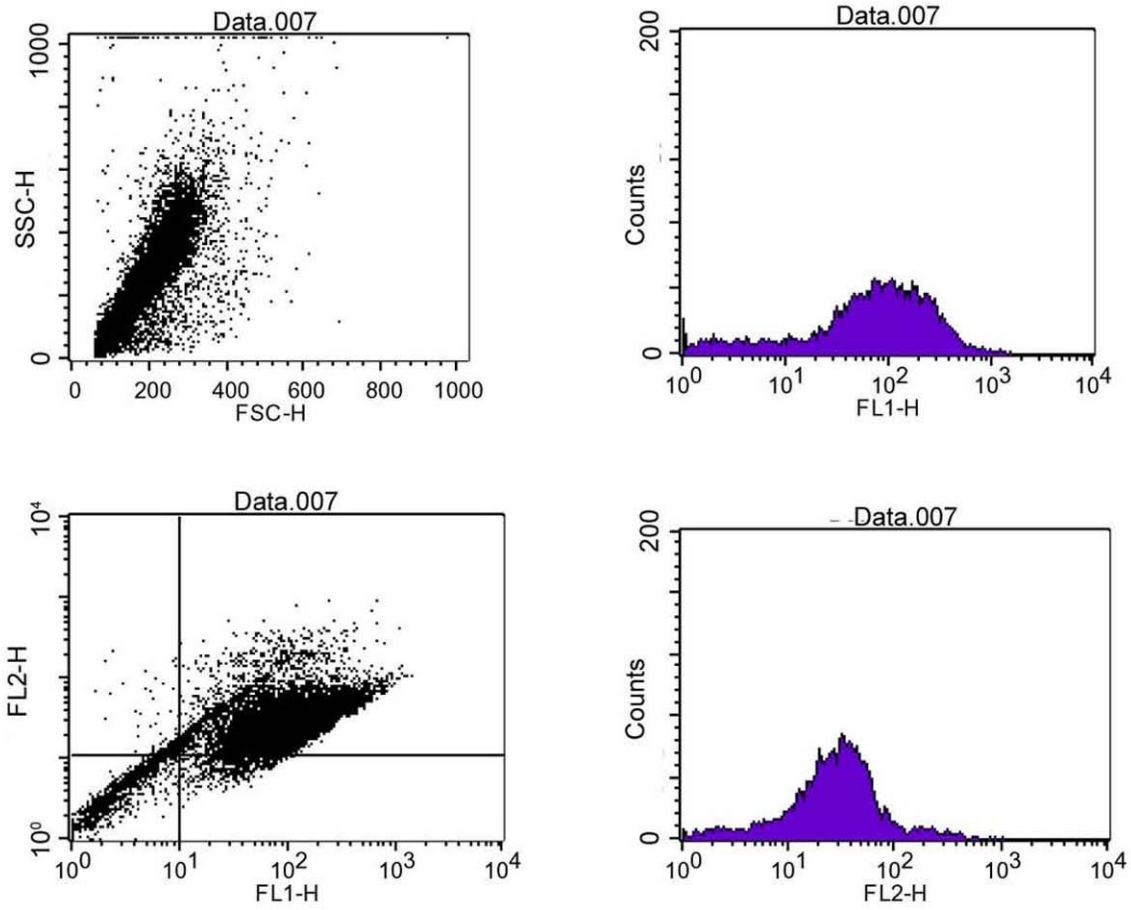

Quadrant Statistics

File: Data.007
Sample ID:
Tube: Untitled
Acquisition Date: 30-Apr-13
Gated Events: 10000
X Parameter: FL1-H (Log)
Quad Location: 10, 11

Log Data Units: Linear Values
Patient ID:
Panel: Untitled Acquisition Tube Lis
Gate: No Gate
Total Events: 10000
Y Parameter: FL2-H (Log)

Quad	Events	% Gated	% Tota	X Mean	X Geo Mean	Y Mean	Y Geo Mear
UL	195	1.95	1.95	7.73	7.46	22.60	16.67
UR	8409	84.09	84.09	137.23	98.02	41.99	32.85
LL	913	9.13	9.13	3.32	2.85	4.63	3.91
LR	483	4.83	4.83	37.99	33.20	8.30	8.07

Histogram plot of **IEC-6** lapatinib-treated cells at 24 hours incubation (results are representative of each group)

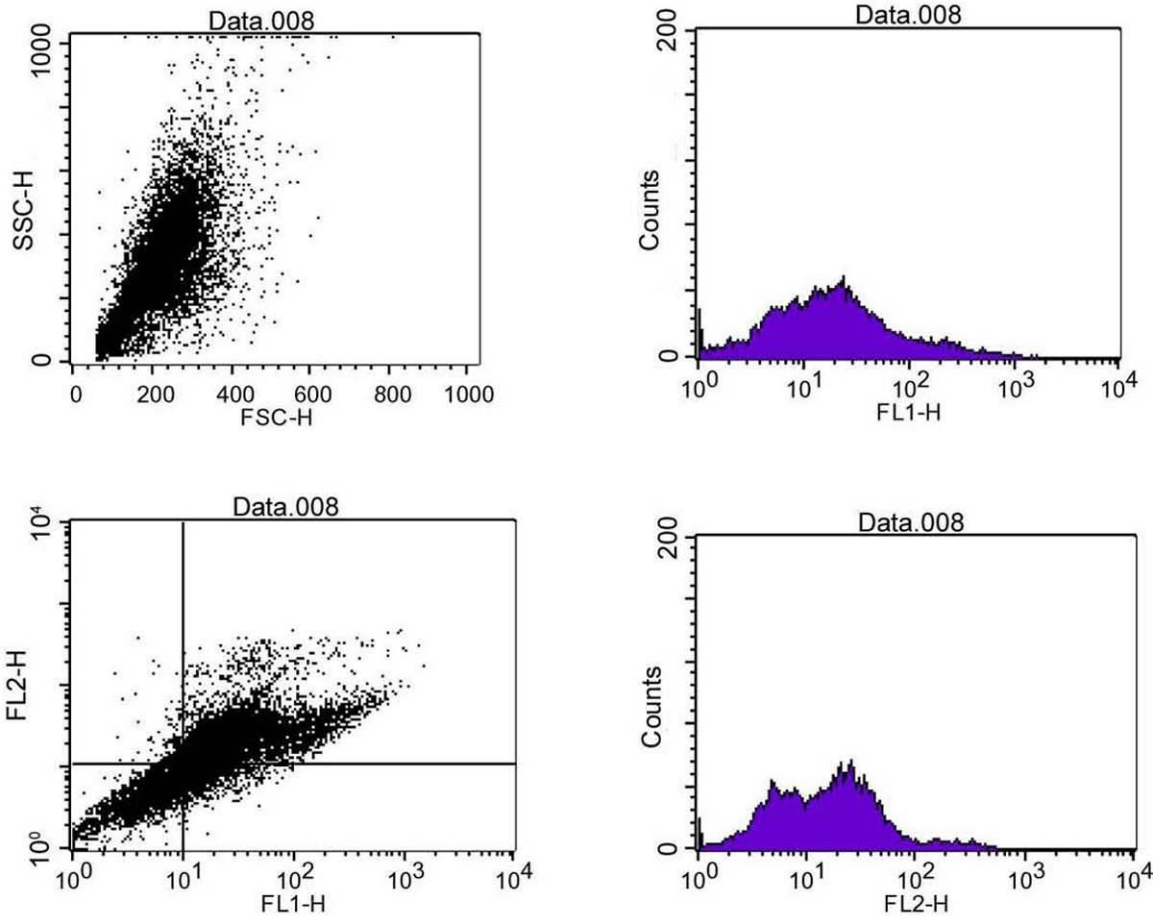

Quadrant Statistics

File: Data.008
Sample ID:
Tube: Untitled
Acquisition Date: 30-Apr-13
Gated Events: 10000
X Parameter: FL1-H (Log)
Quad Location: 10, 11

Log Data Units: Linear Values
Patient ID:
Panel: Untitled Acquisition Tube Lis
Gate: No Gate
Total Events: 10000
Y Parameter: FL2-H (Log)

Quad	Events	% Gated	% Tota	X Mean	X Geo Mean	Y Mean	Y Geo Mear
UL	344	3.44	3.44	8.19	8.02	21.64	16.76
UR	5728	57.28	57.28	60.28	35.68	36.13	27.36
LL	3025	30.25	30.25	5.36	4.77	5.13	4.66
LR	903	9.03	9.03	19.35	17.01	7.82	7.53

Histogram plot of **IEC-6** control untreated cells at 48 hours incubation (results are representative of each group)

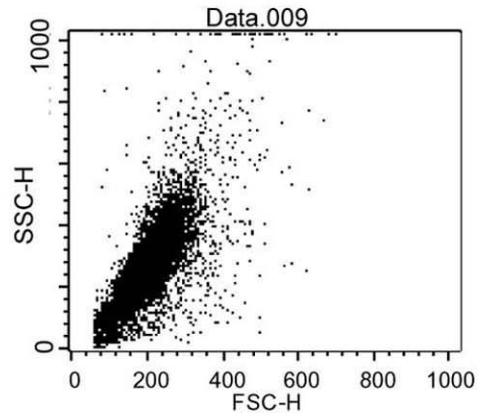

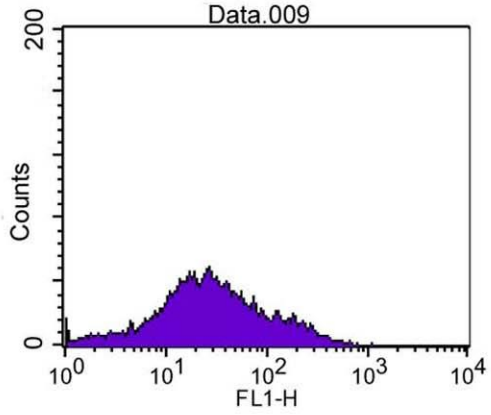

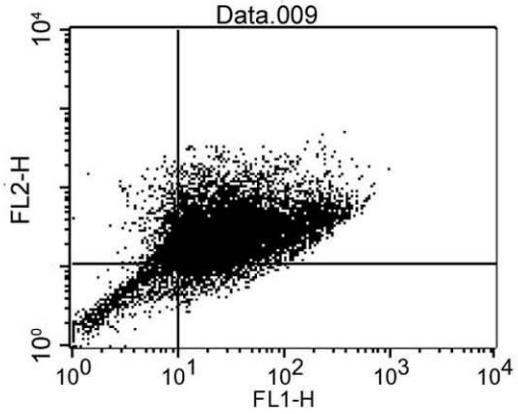

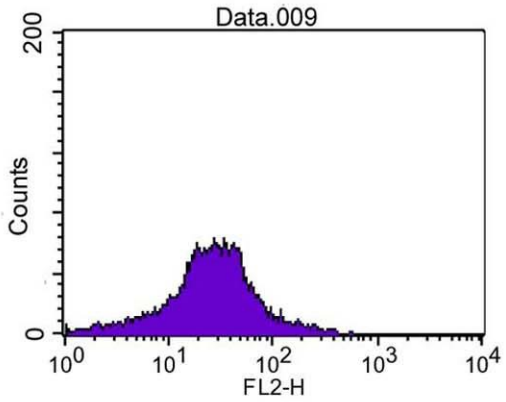

Quadrant Statistics

File: Data.009
Sample ID:
Tube: Untitled
Acquisition Date: 30-Apr-13
Gated Events: 10000
X Parameter: FL1-H (Log)
Quad Location: 10, 11

Log Data Units: Linear Values
Patient ID:
Panel: Untitled Acquisition Tube Lis
Gate: No Gate
Total Events: 10000
Y Parameter: FL2-H (Log)

Quad	Events	% Gated	% Tota	X Mean	X Geo Mean	Y Mean	Y Geo Mear
UL	779	7.79	7.79	7.78	7.53	33.45	24.72
UR	7776	77.76	77.76	61.26	38.93	39.96	31.98
LL	879	8.79	8.79	4.28	3.57	5.35	4.63
LR	566	5.66	5.66	22.98	20.22	8.12	7.87

Histogram plot of **IEC-6** lapatinib-treated cells at 48 hours incubation (results are representative of each group)

Real-time Polymerase Chain Reaction (Real-time PCR)

Melt curve graph analysis of UBC (housekeeping gene)

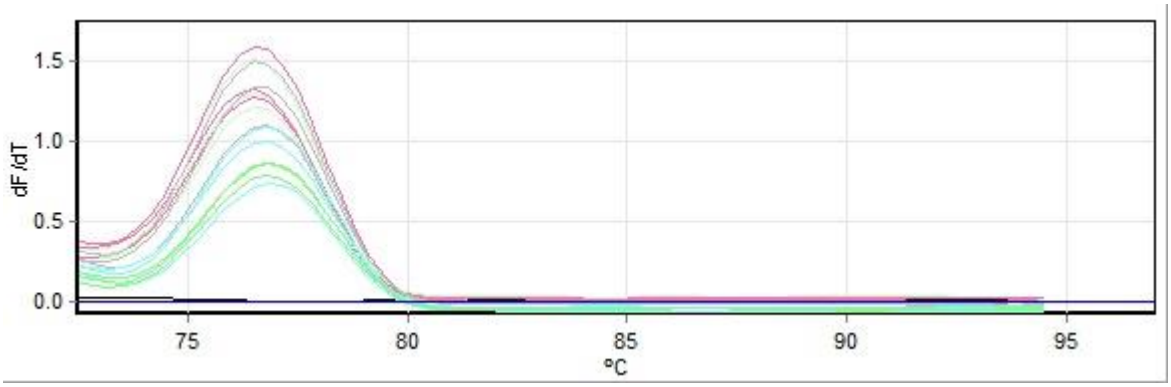

Melt curve graph analysis of B2M (housekeeping gene)

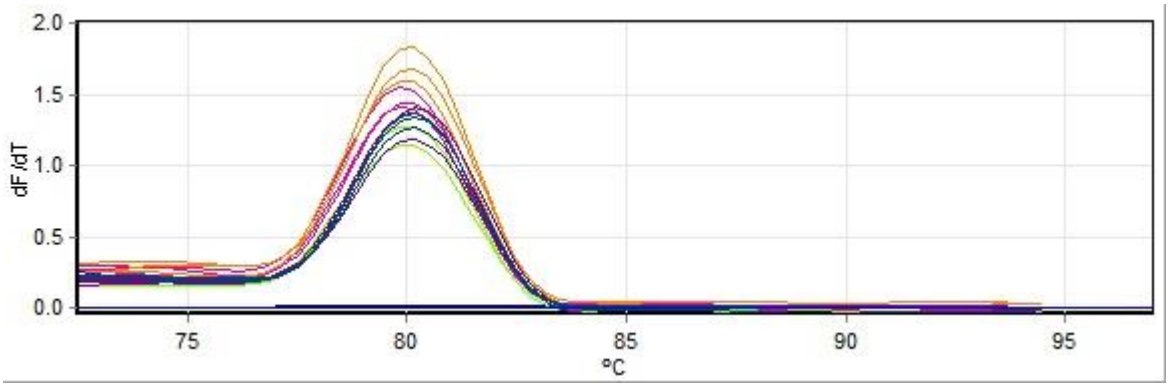

Melt curve graph analysis of ErbB1

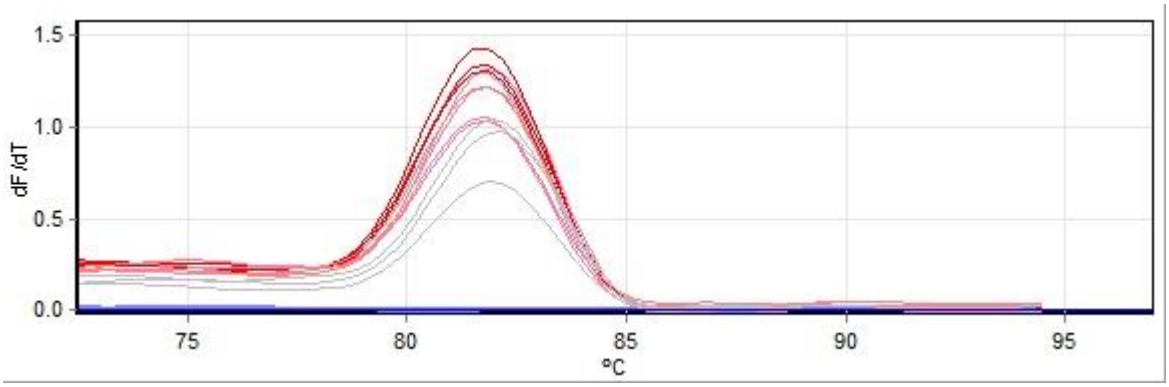

Melt curve graph analysis of ErbB2

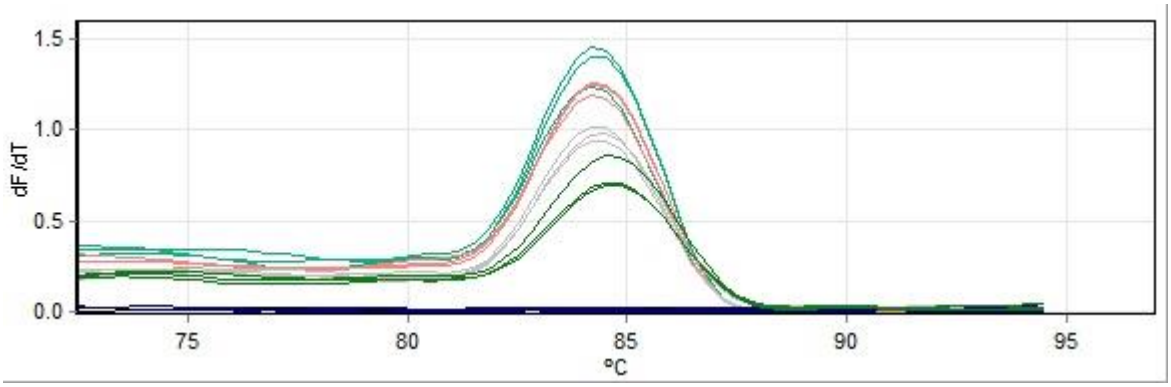

Immunohistochemistry staining of positive controls

Image below showing ErbB1 staining (2 µg/ml) in rat skin at x100 magnification

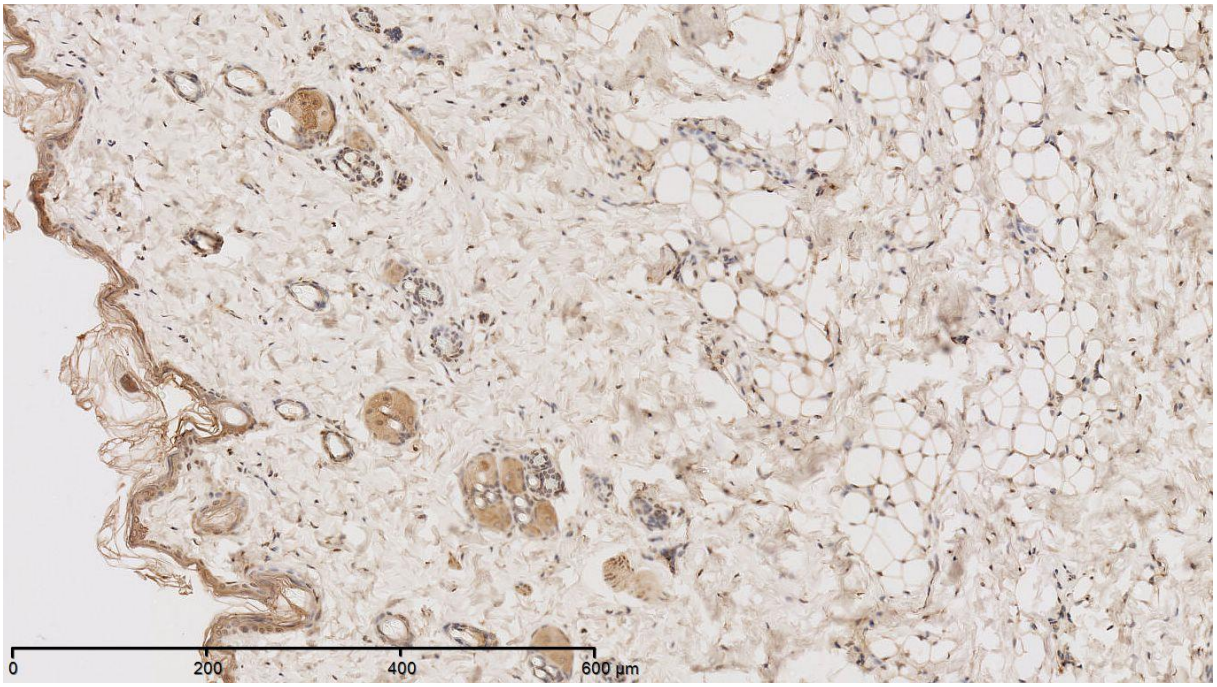

Image below showing ErbB2 staining (2 µg/ml) in ErbB2-positive human breast carcinoma at x100 magnification

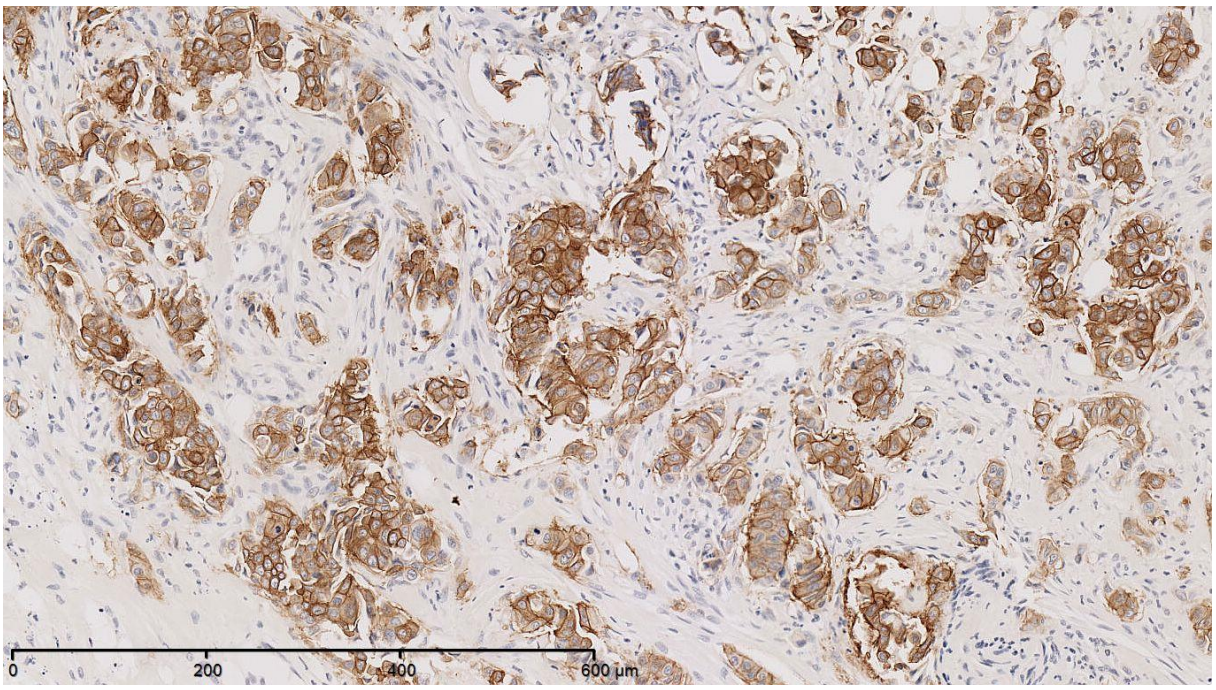

Image below showing pErbB1 staining (2 µg/ml) in rat skin at x100 magnification

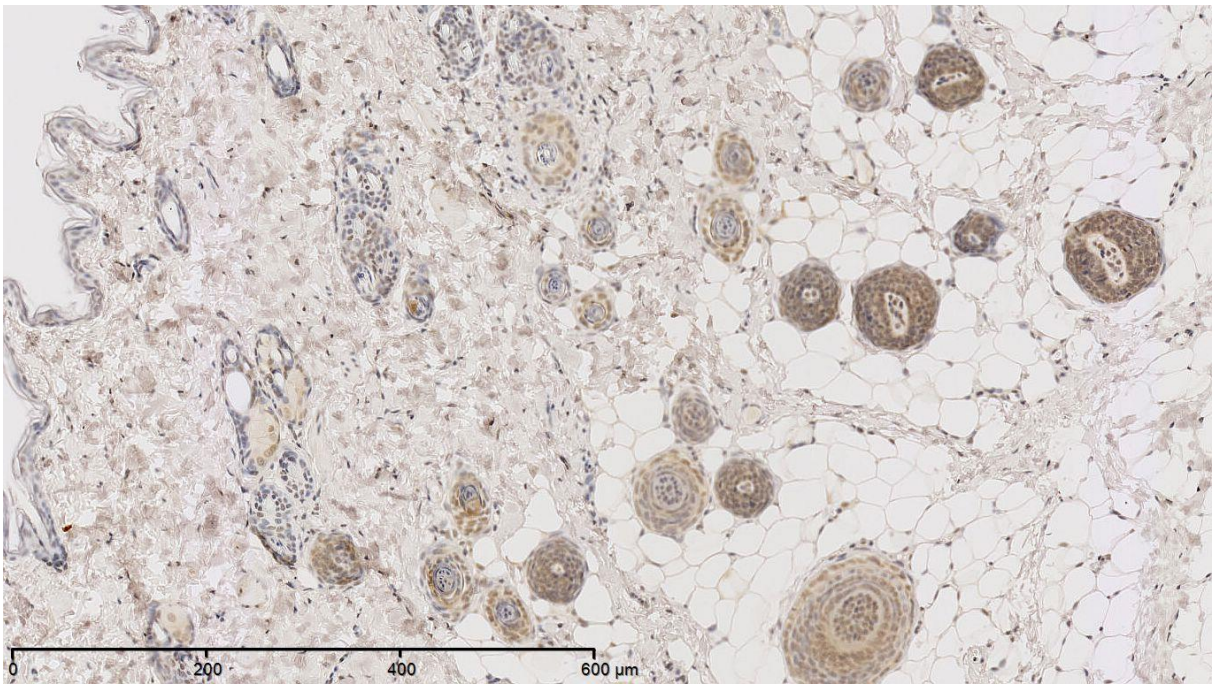

Image below showing pErbB2 staining (10 µg/ml) in rat heart at x100 magnification